

Let's be adaptable

The background features three overlapping watercolor-style circles. The top circle is yellow, the middle-left one is red, and the bottom-right one is beige. A thin black line starts at the top right, loops around the circles, and ends at the bottom left.

Tissue T cell adaptation in
homeostasis and inflammation

Lisanne Lutter

Let's be adaptable

Tissue T cell adaptation in homeostasis and
inflammation

Lisanne Lutter

Let's be adaptable

Tissue T cell adaptation in homeostasis and inflammation

© Lisanne Lutter, 2022

ISBN: 978-90-393-7512-9

DOI: <https://doi.org/10.33540/1160>

Printing by Print Service Ede - proefschriftprinten.nl

About the cover: adaptation in this thesis refers to how cells, while sharing a core profile, can acquire a different phenotype depending on the environment and circumstances. Similarly, the front and back cover are built from the same elements, similar in their core, but with a different appearance.

Printing of this thesis was kindly supported by Stichting Fonds Ebe Brander, Nederlandse Vereniging voor Gastroenterologie, Ferring B.V. and Infection & Immunity Utrecht.

All rights reserved. No part of this thesis may be reproduced, stored in a retrieval system or transmitted in any form or by any means without prior admission in writing of the author.

Let's be adaptable

Tissue T cell adaptation in homeostasis and inflammation

Laten we flexibel zijn
Weefsel T cel adaptatie in homeostase en ontsteking
(met een samenvatting in het Nederlands)

Proefschrift

ter verkrijging van de graad van doctor
aan de Universiteit Utrecht
op gezag van de rector magnificus,
prof. dr. H.R.B.M. Kummeling,
ingevolge het besluit van het college voor promoties
in het openbaar te verdedigen op
dinsdag 29 november 2022
des ochtends te 10.15 uur

door

Lisanne Lutter

geboren op 26 juli 1990
te Haarlem

Promotoren:

Prof. dr. F. van Wijk

Prof. dr. B. Oldenburg

Beoordelingscommissie:

Prof. dr. J.A.M. Borghans

Prof. dr. P.J. Coffe

Prof. dr. L. Koenderman

Dr. J.N. Samsom

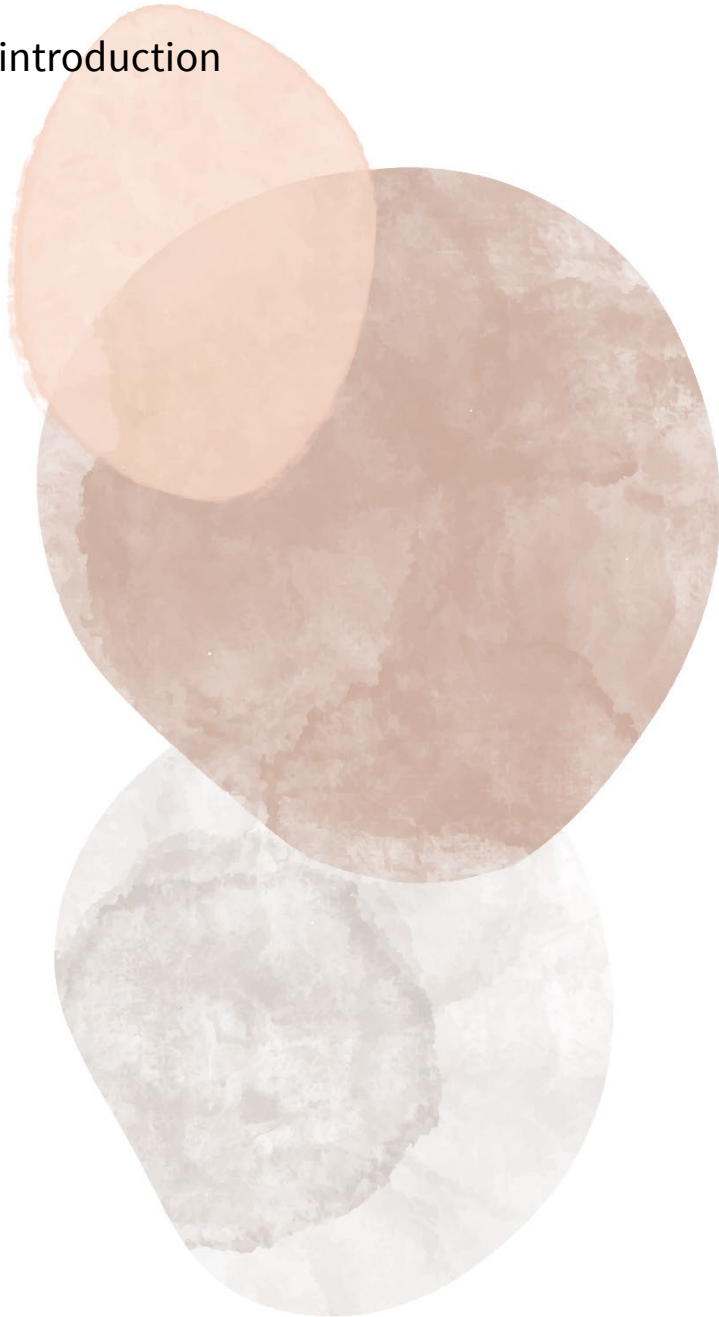
Prof. dr. G. Bouma

TABLE OF CONTENTS

Chapter 1	General introduction	7
Chapter 2	Conserved human effector Treg cell transcriptomic and epigenetic signature in arthritic joint inflammation	17
Chapter 3	Human regulatory T cells locally differentiate and are functionally heterogeneous within the inflamed arthritic joint	57
Chapter 4	Regulation of human regulatory T cell differentiation and functional adaptation in tissue and disease	85
Chapter 5	The elusive case of human intraepithelial T cells in gut homeostasis and inflammation	103
Chapter 6	Compartment-driven imprinting of intestinal CD4 (regulatory) T cells in inflammatory bowel disease and homeostasis	133
Chapter 7	Homeostatic function and inflammatory activation of ileal CD8 ⁺ tissue-resident T cells is dependent on mucosal location	161
Chapter 8	General discussion	183
Addendum	Nederlandse samenvatting	213
	Dankwoord	221
	Curriculum Vitae	227
	List of publications	228

Chapter 1

General introduction



INTRODUCTION

Homeostasis

Our bodies are continuously exposed to external particles through ingestion (e.g. food, medication), and physical contact (e.g. microbiota, viruses, crème, microplastics, injuries) but also by metabolic activity of cells within the body. During all these 'disturbances' the body maintains a stable internal environment within narrow ranges while adjusting to the changing environment.¹ In 1900 Richet termed this homeostasis.

“The living system is stable...it must be in order not to be destroyed, dissolved or disintegrated by colossal forces, often adverse, which surround it. By an apparent contradiction, it maintains its stability only if it is excitable and capable of modifying itself according to external stimuli and adjusting its response to the stimulation. In a sense, it is stable because it is modifiable – the slight instability is the necessary condition for the true stability of the organism.” (Richet, 1900)²

But what happens when these homeostatic mechanisms are disrupted? Inflammation is a physiological response to harmful stimuli (endogenous or exogenous). It is generally initiated to eliminate the threat and simultaneously minimize damage in the respective tissues. Inflammation is thus vital for healing and regaining homeostasis. Acute inflammation is self-limiting and will be resolved after elimination of the harmful stimulus, but persistent presence of a pathogen, allergen, or a self-protein recognized as foreign can result in chronic inflammation.³ The immune cells involved in inflammatory responses belong to the innate and the adaptive immune systems. The innate immune system is part of the first line of defense. This system is activated quickly (within minutes to hours) and reacts in an unspecific manner, i.e. the response is similar irrespective of the stimulus. Cells of the innate system include macrophages, mast cells, neutrophils and eosinophils. On the other hand, the adaptive immune system takes longer (at least 72 hours) to be activated but is specific. This system consists of B and T lymphocytes. T cells are one of the key drivers and mediators of chronic inflammation.³ In this thesis, we study T cells at sites where homeostasis has been disrupted resulting in (relapsing-remitting) chronic inflammation.

T cells

Most components our body is exposed to are processed into smaller molecules that can be presented to adaptive immune cells and may elicit a (subclinical) immune response. These presented molecules (antigens) can be recognized by T cells via their T cell receptor (TCR) which is unique for every T cell. For a minority of cells, primarily found in barrier tissues/epithelium, the TCR consists of a γ and δ chain (TCR $\gamma\delta$). Most T cells, however, bear a heterodimer consisting of an α and β chain (TCR $\alpha\beta$). The chains are formed by somatic recombination of the V, D, J gene segments; V(D)J recombination. Together, somatic recombination, the variety in V, D and J gene segments and the combination of a TCR α and

TCR β chain results in a unique TCR for every T cell in our body. TCR recombination takes place in the thymus where T cells mature.^{3,4}

TCR $\alpha\beta$ T cells are subdivided in two main subsets based on the surface markers, and TCR co-receptors, CD8 and CD4. CD8 T cells are cytotoxic T cells, whereas CD4 T cells are further subdivided in several T helper (Th) subsets and regulatory T cellT cells (Treg) characterized by expression of specific cytokines, transcription factors and chemokine receptors.³ Th cells are effector cells that aid in immune responses by regulating other cells and secretion of characteristic Th cell subset effector molecules. Th1 cells are known to regulate macrophages and monocytes, and express IL2, TNF α , and IFN γ as primary effector molecules. Each Th cells transcriptional program is regulated by a set of transcription factors (TF's), and for Th1 cells these constitute T-bet and STAT4. Th2 cells, programmed by GATA3 and STAT6, are known to regulate eosinophils, mast cells and basophils and expressors of IL-4, IL-5 and IL-13. Th17 cells are steered by the TF's ROR γ t and STAT3, primarily involved in regulating neutrophils with the main effector cytokines being IL-17, IL-21 and GM-CSF.^{3,5} On the other hand, Tregs are known for their role in limiting immune responses and maintaining self-tolerance via inhibition of T cell proliferation and effector responses (direct and indirect). They are considered as the major immunosuppressive lineage. Their function is governed by FOXP3 and STAT3, and exerted via IL-10, TGF β , and ICOS amongst others.^{3,6,7} More subsets are continuously being described and it has become increasingly clear that Th cell phenotypes are present on a gradual scale.⁸

Before a T cell differentiates towards an effector profile a T cell is considered naïve and has of yet to encounter its cognate antigen. Upon antigen recognition by the TCR a T cell differentiates and becomes a memory cell. Memory T cells can be distinguished in central memory (Tcm) cells that recirculate through lymphoid organs, whereas effector memory (Tem) cells are predominantly found in tissues. Finally, Temra's are terminally differentiated effector memory T cells. Upon stimulation, naïve cells can produce IL-2, whereas Tem, Tcm and Temra can secrete effector cytokines such as IFN γ and TNF α thereby exerting effector functions in immune responses.^{3,9} Also for this subdivision of T cells studies continuously expand our knowledge, including the discovery of a long term tissue resident T cell (Trm) population found in tissues first recognized in the mouse intestines in 1999.¹⁰

Tissue T cells

Most T cells in our body reside in tissues, especially at border tissues where many antigens are encountered such as the lungs, intestines and skin. Upon migration to a tissue compartment cells will adapt to the local environment to ensure their survival, which has been deemed crucial in enabling their local survival and functioning. For example, in mice it has been shown that Tregs can adapt to the local environment by acquiring a transcriptional program that resembles that of the dominant Th cell phenotype present.⁷ In **chapter 5** an extensive review on T cells residing in the mucosal barrier of the intestines is provided giving insight in the adaptation and regulation of the T cell compartment in a mucosal border tissue with

continuous antigen exposure, and potential consequences when homeostasis cannot be preserved.

Many of these T cells are considered (permanent) nonrecirculating residents of the tissue. Normally, antigens that the body encounters are presented in lymphoid follicles to initiate T cell differentiation and their migration to the site of antigen encounter. This takes approximately 72 hours, and therefore, if the antigen is derived from a harmful stimulus there is ample time for that stimulus to elicit local (tissue) damage. Trm cells, however, perform local surveillance and are able to respond to encountered antigens since they are antigen-experienced cells. This enables them to immediately react to potential threats to the body acting as a first line of specific defense. Trm cells are often distinguished from recirculating and infiltrating T cells by expression of the surface markers CD69 and CD103.^{11,12} A core transcriptional program further differentiates Trm from other memory T cells including upregulation of NOTCH, RUNX3, CXCR6, CD49a, PD-1, and CD101 with downregulation of CD62L, S1PR1, and KLF2.¹² Their presence at, primarily, border tissues can also be harmful if a rapid response is initiated or perpetuated since these cells have rapid effector function. Therefore, in addition to protective functions several studies have suggested Trm might be involved in the relapsing-remitting course of chronic inflammatory disorders.^{13,14} This seems to be further supported by the fact that many chronic relapsing-remitting disorders are characterized by recurrent inflammation at the same location. For example, patients with ileal Crohn's disease that underwent a ileocecal resection are often faced with disease recurrence at the anastomosis.¹⁵

Studying tissue T cells in humans remains challenging due to the difficulty in acquiring (sufficient) tissue and sampling for longitudinal profiling. However, studies have shown that differences between mouse and human tissue T cells exist.^{12,16} In contrast to laboratory mice, humans have a far longer life span and are exposed to more diverse antigens. This potentially limiting translation of findings from mice to humans emphasizes the necessity of human studies to this respect. A key open question remains the transcriptional programming of human tissue T cells in both homeostatic and inflammatory settings, as well as differences and commonalities of tissue T cells in different tissue compartments. Exploiting the knowledge derived from human studies will enable us to more precisely develop and apply therapeutic strategies for chronic inflammatory disorders. Studies have indicated that (tissue) T cells play an important role in the inflammatory process of Juvenile Idiopathic Arthritis (JIA) and Inflammatory Bowel Diseases (IBD),¹⁷⁻²⁰ which have been the focus in this thesis.

Juvenile Idiopathic Arthritis and Inflammatory Bowel Diseases

JIA encompasses all forms of arthritis with an onset before the age of 16, a duration for more than 6 weeks and an unclear origin.¹⁷ Subclassification is performed according to the revised criteria for JIA²⁸, and based on the clinical symptoms, number of affected joints, presence of rheumatoid factor or anti-nuclear autoantibodies amongst others. It is the most common autoimmune disease in children with an incidence of 2-20/100.000 children.¹⁷ Children with JIA

have a decreased health-related quality of life compared to their unaffected peers which is both physical, e.g. pain, disability, fatigue, and psychosocial, e.g. self-esteem, depression.²⁹ The pathogenesis of JIA is considered to be multifactorial with a genetic susceptibility, environmental triggers, an epigenetic and an immune cell component (both innate and adaptive).^{17,18} JIA is a predominant Th1/Th17-associated disease³⁰ with an intrinsic resistance of effector cells to regulation by Tregs.³¹ Treatment strategies include nonsteroidal anti-inflammatory drugs (NSAIDs), disease-modifying antirheumatic drugs (DMARDs; e.g. methotrexate), biologicals (e.g. tumor necrosis factor (TNF), interleukin (IL)-6 receptor or IL-1 blockers), and corticosteroids. Treatment of an inflamed joint in JIA patients often involves intra-articular corticosteroid injection following aspiration of synovial fluid (SF).³² We can employ SF to study the immune cells involved in the inflammatory process. In homeostatic conditions, the volume of SF is minimal acting as a lubricant to minimize friction of the cartilage and providing nutrients for surrounding structures.³³ Since immune cells are normally not present within SF this aspirate provides us with a clean population of infiltrating immune cells to study the local immunodynamics.

IBD, comprising Crohn's disease and ulcerative colitis, is a chronic relapsing-remitting inflammatory disease of the gastro-intestinal tract with an overall incidence of approximately 20/100.000 persons. Whereas ulcerative colitis is characterized by inflammation restricted to the colon, Crohn's disease encompasses inflammation of the whole gastro-intestinal tract and extra-intestinal manifestations including arthritis, erythema nodosum and anal fissures. Another distinction is that inflammation in ulcerative colitis is restricted to the mucosa while in Crohn's disease inflammation can be transmural.^{19,20} Subclassification of both diseases is performed according to the Montreal classification and includes the extent and severity of inflammation.³⁴ Treatment options are similar to other inflammatory disorders and include aminosalicylates, thiopurines, methotrexate, corticosteroids, and a growing arsenal of biologicals (e.g. TNF, integrin $\alpha 4\beta 7$, IL-12/IL-23, and JAK-STAT blockade).^{19,20} Due to its chronic nature patients experience a reduced quality of life, and 20% of patients with ulcerative colitis and 80% of patients with Crohn's disease require surgery.³⁵ Similar to JIA, IBD is a multifactorial disease with genetic susceptibility, microbial changes, lifestyle influences, immune cell infiltrates, epithelial cell alterations which have all been associated with disease onset and progression.^{19,20} The mucosa of the gastro-intestinal tract consists of an epithelial layer and the lamina propria separated by a basal membrane. This mucosal barrier separates the inner and outer world and is in constant contact with ingested particles (e.g. food, medication) and microbiota to which responses are regulated and transferred within the mucosa and throughout the body.³⁶ A colonoscopy enables us to visually assess the intestines with respect to occurrence of inflammation. During colonoscopies pinch biopsies can be taken which allow us to extract and study the inflammatory environment to understand the local situation in IBD.

Even though the first clinical descriptions for both JIA and IBD were published in the 18th and 19th century,^{37,38} it was not until the late 20th century for basic understanding of these diseases and development of therapeutic strategies. Despite the myriad of studies and enormous progress made over the past decades towards deciphering the pathogenesis of and treatment for both diseases we still lack an understanding especially in the human setting. Further fundamental insight in the differentiation and adaptation of immune cells to their respective sites of function will improve our understanding of the pathogenesis and relapsing-remitting course of these inflammatory diseases, and may lead to identification of new therapeutic targets and the fine-tuning of therapeutic strategies.

SCOPE AND OUTLINE OF THIS THESIS

The scope of this thesis is to explore the programming and adaptation of T cells at (tissue) sites in homeostasis and in inflammatory conditions, and decipher tissue commonalities as well as tissue specificity in these processes.

In **chapter 2** the molecular and epigenetic programming of SF Tregs is unraveled and compared to tumor-infiltrating Tregs to gain in-depth knowledge about Treg-programming in a human inflammatory environment. We extend on this in **chapter 3** by exploring phenotypical and functional heterogeneity within this SF Treg compartment. **Chapter 4** extends our focus on differentiation and adaptation of Tregs to a broad set of tissues in both homeostatic and inflammatory (autoimmune/inflammatory and cancer) conditions. In **chapter 5** the T cells residing at the mucosal barrier, the epithelium and lamina propria, of the intestines are reviewed. Subsequently, in **chapter 6** we describe how different CD4 T cell subsets adapt to this mucosal barrier in the human ileum of unaffected controls and patients with Crohn's disease. In **chapter 7** our focus is on the adaptation of CD8 tissue resident memory cells in the ileal mucosal barrier of patients with Crohn's disease. In the final chapter (**chapter 8**) the findings in this thesis together with unpublished data are discussed and put in a broader perspective.


REFERENCES

1. Silverthorn, D. U. *Human physiology: an integrated approach*. (Pearson International Edition).
2. Richet, C. R. *Dictionnaire de physiologie*. vol. 4 (Alcan, 1900).
3. Murphy, K., Travers, T. & Walport, M. *Janeway's Immunobiology*. (Garland Science, 2008).
4. Gaud, G., Lesourne, R. & Love, P. E. Regulatory mechanisms in T cell receptor signalling. *Nat. Rev. Immunol.* **18**, 485–497 (2018).
5. Wan, Y. Y. Multi-tasking of helper T cells. *Immunology* **130**, 166–171 (2010).
6. Stephens, L. A., Mottet, C., Mason, D. & Powrie, F. Human CD4(+)CD25(+) thymocytes and peripheral T cells have immune suppressive activity in vitro. *Eur. J. Immunol.* **31**, 1247–1254 (2001).
7. Liston, A. & Gray, D. H. D. Homeostatic control of regulatory T cell diversity. *Nat. Rev. Immunol.* **14**, 154–65 (2014).
8. Oestreich, K. J. & Weinmann, A. S. Master regulators or lineage-specifying? Changing views on CD4(+) T cell transcription factors. *Nat. Rev.* **12**, 799–804 (2012).
9. Sallusto, F., Lenig, D., Förster, R., Lipp, M. & Lanzavecchia, A. Two subsets of memory T lymphocytes with distinct homing potentials and effector functions. *Nature* **401**, 708–712 (1999).
10. Kim, S. K., Schluns, K. S. & Lefrançois, L. Induction and visualization of mucosal memory CD8 T cells following systemic virus infection. *J. Immunol.* **163**, 4125–4132 (1999).
11. Masopust, D. & Soerens, A. G. Tissue-Resident T Cells and Other Resident Leukocytes. *Annu. Rev. Immunol.* **37**, 521–546 (2019).
12. Kumar, B. V *et al.* Human Tissue-Resident Memory T Cells Are Defined by Core Transcriptional and Functional Signatures in Lymphoid and Mucosal Sites. *Cell Rep.* **20**, 2921–2934 (2017).
13. Clark, R. A. Resident memory T cells in human health and disease. *Sci. Transl. Med.* **7**, 269rv1-269rv1 (2015).
14. Park, C. O. & Kupper, T. S. The emerging role of resident memory T cells in protective immunity and inflammatory disease. *Nat. Med.* **21**, 688–697 (2015).
15. Ikeuchi, H. *et al.* Localization of recurrent lesions following ileocolic resection for Crohn's disease. *BMC Surg.* **21**, 145 (2021).
16. Szabo, P. A., Miron, M. & Farber, D. L. Location, location, location: Tissue resident memory T cells in mice and humans. *Sci. Immunol.* **4**, (2019).
17. Prakken, B., Albani, S. & Martini, A. Juvenile idiopathic arthritis. *Lancet (London, England)* **377**, 2138–2149 (2011).
18. van Loosdregt, J., van Wijk, F., Prakken, B. & Vastert, B. Update on research and clinical translation on specific clinical areas from biology to bedside: Unpacking the mysteries of juvenile idiopathic arthritis pathogenesis. *Best Pract. Res. Clin. Rheumatol.* **31**, 460–475 (2017).
19. Ungaro, R., Mehandru, S., Allen, P. B., Peyrin-biroulet, L. & Colombel, J. Ulcerative colitis. (2017).
20. Torres, J., Mehandru, S., Colombel, J. & Peyrin-biroulet, L. Seminar Crohn ' s disease. **389**, 1741–1755 (2017).
21. Mahata, S. K. & Corti, A. Chromogranin A and its fragments in cardiovascular, immunometabolic, and cancer regulation. *Ann. N. Y. Acad. Sci.* **1455**, 34–58 (2019).
22. Muntjewerff, E. M., Dunkel, G., Nicolassen, M. J. T., Mahata, S. K. & van den Bogaart, G. Catestatin as a Target for Treatment of Inflammatory Diseases. *Front. Immunol.* **9**, 2199 (2018).
23. Zhernakova, A. *et al.* Population-based metagenomics analysis reveals markers for gut microbiome composition and diversity. *Science* **352**, 565–569 (2016).
24. Zivkovic, P. M. *et al.* Serum Catestatin Levels and Arterial Stiffness Parameters Are Increased in Patients with Inflammatory Bowel Disease. *J. Clin. Med.* **9**, (2020).
25. Zissimopoulos, A. *et al.* Chromogranin A as a biomarker of disease activity and biologic therapy in inflammatory bowel disease: a prospective observational study. *Scand. J. Gastroenterol.* **49**, 942–949 (2014).
26. Wagner, M. *et al.* Increased fecal levels of chromogranin A, chromogranin B, and secretoneurin in collagenous colitis. *Inflammation* **36**, 855–861 (2013).
27. Sciola, V. *et al.* Plasma chromogranin a in patients with inflammatory bowel disease. *Inflamm. Bowel Dis.* **15**, 867–871 (2009).
28. Petty, R. E. *et al.* Revision of the proposed classification criteria for juvenile idiopathic arthritis: Durban, 1997. *J. Rheumatol.* **25**, 1991–1994 (1998).
29. Gutiérrez-Suárez, R. *et al.* Health-related quality of life of patients with juvenile idiopathic arthritis

- coming from 3 different geographic areas. The PRINTO multinational quality of life cohort study. *Rheumatology* **46**, 314–320 (2007).
30. Maggi, L. *et al.* Th17 and Th1 Lymphocytes in Oligoarticular Juvenile Idiopathic Arthritis. *Front. Immunol.* **10**, 450 (2019).
 31. Wehrens, E. J. *et al.* Functional human regulatory T cells fail to control autoimmune inflammation due to PKB/c-akt hyperactivation in effector cells. *Blood* **118**, 3538–48 (2011).
 32. Ringold, S. *et al.* 2019 American College of Rheumatology/Arthritis Foundation Guideline for the Treatment of Juvenile Idiopathic Arthritis: Therapeutic Approaches for Non-Systemic Polyarthritis, Sacroiliitis, and Enthesitis. *Arthritis Rheumatol. (Hoboken, N.J.)* **71**, 846–863 (2019).
 33. Kumar, P. & Clark, M. *Kumar & Clark's clinical medicine.* (Saunders Elsevier, 2009).
 34. Silverberg, M. S. *et al.* Toward an Integrated Clinical, Molecular and Serological Classification of Inflammatory Bowel Disease: Report of a Working Party of the 2005 Montreal World Congress of Gastroenterology. *Can. J. Gastroenterol.* **19**, 269076 (2005).
 35. Sica, G. S. & Biancone, L. Surgery for inflammatory bowel disease in the era of laparoscopy. *World J. Gastroenterol.* **19**, 2445–2448 (2013).
 36. Mowat, A. M. & Agace, W. W. Regional specialization within the intestinal immune system. *Nat. Rev. Immunol.* **14**, 667–685 (2014).
 37. Kirsner, J. B. Historical aspects of inflammatory bowel disease. *J. Clin. Gastroenterol.* **10**, 286–297 (1988).
 38. Still, G. F. On a Form of Chronic Joint Disease in Children. *Med. Chir. Trans.* **80**, 47–60.9 (1897).

Chapter 2

Conserved human effector Treg cell transcriptomic and epigenetic signature in arthritic joint inflammation



Lisanne Lutter,^{1#} Gerdien Mijnheer,^{1#} Michal Mokry,^{1,2,3} Marlot van der Wal,¹ Rianne Scholman,¹ Veerle Fleskens,⁴ Aridaman Pandit,¹ Weiyang Tao,¹ Mark Wekking,³ Stephin Vervoort,^{1,5} Ceri Roberts,⁴ Alessandra Petrelli,¹ Janneke G.C. Peeters,¹ Marthe Knijff,¹ Sytze de Roock,¹ Sebastiaan Vastert,¹ Leonie S. Taams,⁴ Jorg van Loosdregt,^{1,5†} Femke van Wijk^{1†}

[#]These authors contributed equally

[†]These authors jointly supervised this work

¹Center for Translational Immunology, Pediatric Immunology & Rheumatology, Wilhelmina Children's Hospital, University Medical Center Utrecht, Utrecht University, Utrecht 3508 AB, the Netherlands.

²Regenerative Medicine Center Utrecht, Department of Pediatrics, University Medical Center Utrecht, Utrecht 3508 AB, The Netherlands.

³Epigenomics facility, University Medical Center Utrecht, Utrecht 3508 AB, The Netherlands.

⁴Centre for Inflammation Biology and Cancer Immunology, School of Immunology & Microbial Sciences, King's College London, London SE1 1UL, UK.

⁵Regenerative Medicine Center Utrecht, Center for Molecular Medicine, University Medical Center Utrecht, Utrecht 3508 AB, The Netherlands.

Nature Communications, 2021;12(1):2710

ABSTRACT

Treg cells are critical regulators of immune homeostasis, and environment-driven Treg cell differentiation into effector (e)Treg cells is crucial for optimal functioning. However, human Treg cell programming in inflammation is unclear. Here, we combine transcriptional and epigenetic profiling to identify a human eTreg cell signature. Inflammation-derived functional Treg cells have a transcriptional profile characterized by upregulation of both a core Treg cell (FOXP3, CTLA4, TIGIT) and effector program (GITR, BLIMP-1, BATF). We identify a specific human eTreg cell signature that includes the vitamin D receptor (VDR) as a predicted regulator in eTreg cell differentiation. H3K27ac/H3K4me1 occupancy indicates an altered (super-)enhancer landscape, including enrichment of the VDR and BATF binding motifs. The Treg cell profile has striking overlap with tumor-infiltrating Treg cells. Our data demonstrate that human inflammation-derived Treg cells acquire a conserved and specific eTreg cell profile guided by epigenetic changes, and fine-tuned by environment-specific adaptations.

INTRODUCTION

Forkhead box P3-expressing (FOXP3⁺) Treg cells are key players to control aberrant immune responses. Mutations in the *FOXP3* gene lead to severe autoimmunity and inflammation in both mice and humans^{1,2}. Because of their potential for clinical applications, Treg cells have been intensively studied over the last decades.

There is accumulating evidence from mouse models that specific environments such as inflammation or non-lymphoid tissues can induce further differentiation/adaptation into specialized activated Treg cell subsets, also referred to as effector (e)Treg cells^{3,4} (reviewed in ref. ⁵). Characteristic for eTreg cells appears to be the maintenance of FOXP3 expression, increased expression of several molecules related to their function such as ICOS, CTLA4 and TIGIT, and adaptation to the local environment. For example, recent studies in mice show that in visceral adipose tissue Treg cells play a dominant role in metabolic homeostasis⁶, whereas Treg cells in skin and gut can promote wound repair and are involved in local stem cell maintenance^{7,8}.

In mice, eTreg cells have been demonstrated to be crucial in specific inflammatory settings. Interestingly, inflammatory signals can induce the stable upregulation of typical Th cell transcription factors such as T-bet, allowing the Treg cells to migrate to the site of inflammation⁹. Moreover, co-expression of T-bet and Foxp3 is essential to prevent severe Th1 autoimmunity¹⁰. Studies using transgenic mice have contributed to the knowledge in this field, but how this can be translated to humans remains to be elucidated. Because of the interest in the use of Treg cells for therapeutic purposes in a variety of human diseases it is relevant to gain insight in human eTreg cell programming in inflammatory settings.

Also in humans there is evidence of environment-induced adaptation of human (e)Treg cells^{4,7,11} (reviewed in ref. ¹²) including tumor-infiltrating Treg cell signatures¹³⁻¹⁵. Pertinent issues that remain to be addressed are how diverse and stable human eTreg cell programming is in the inflammatory environment, and whether this is regulated at an epigenetic level.

In this work, we investigate the gene expression profile and active enhancer landscape of human Treg cells in a human autoimmune-associated inflammatory environment. We show that in an inflammatory setting Treg cells differentiate into eTreg and become adapted to the environment both on a transcriptomic and epigenetic level. Furthermore, we demonstrate that there is substantial overlap between the synovial fluid (SF) Treg cell signature and recently published human tumor-infiltrating Treg cell signatures. These findings indicate that human eTreg cell programming is epigenetically imprinted and may be commonly induced in inflammatory conditions ranging from autoimmune to tumor settings.

RESULTS

Enhanced core Treg cell signature in inflamed joints

To investigate whether the gene expression profile of human Treg cells in an inflammatory environment is different from circulating human Treg cells, CD3⁺CD4⁺CD25⁺CD127^{low} Treg cells

and CD3⁺CD4⁺CD25⁺CD127⁺ non-Treg cells were isolated from: synovial exudate obtained from inflamed joints of Juvenile Idiopathic Arthritis (JIA) patients, peripheral blood (PB) from JIA patients with active and inactive disease, and PB from healthy children and healthy adults (Supplementary Fig. 1a for gating strategy). More than 90% of the sorted Treg cell populations were FOXP3 positive (Supplementary Fig. 1b). The transcriptional landscape was determined with RNA-sequencing. An unsupervised principal component analysis (PCA) was performed to study the variability between Treg cells derived from different environments. Synovial fluid (SF)-derived Treg cells clearly clustered separately from PB-derived Treg cells (Fig. 1a), indicating that SF-derived Treg cells have a specific expression pattern compared to PB-derived Treg cells.

In accordance with previous publications we confirmed that SF-derived Treg cells were functional using an in vitro suppression assay (Fig. 1b and Supplementary Fig. 2a)^{16,17}. As expected, Treg cell signature genes were significantly enriched in SF Treg cells compared to SF CD4⁺ non-Treg cells (Fig. 1c, left panel). Treg cell signature genes were also enriched in SF compared to PB Treg cells derived from both healthy children and JIA patients (Fig. 1c right panel and Supplementary Fig. 2b). These included Treg cell hallmark genes important for Treg cell stability and function such as *FOXP3*, *CTLA4* and *TIGIT*, at both the transcriptional and protein level (Fig. 1d, e and Supplementary Figs. 1a and 2c)^{18,19}. In humans, CD3⁺CD4⁺non-Treg cells can upregulate FOXP3 and associated markers that as such can serve as markers for T cell activation³. We indeed observed a slight upregulation of FOXP3, CTLA4 and TIGIT at mRNA and protein level in SF non-Treg cells but not near the levels observed in SF Treg cells (Fig. 1d, e and Supplementary Figs. 1b and 2c), further confirming that SF Treg cells and non-Treg cells are distinct cell populations. Together these data demonstrate that the inflammatory environment reinforces the Treg cell-associated program.

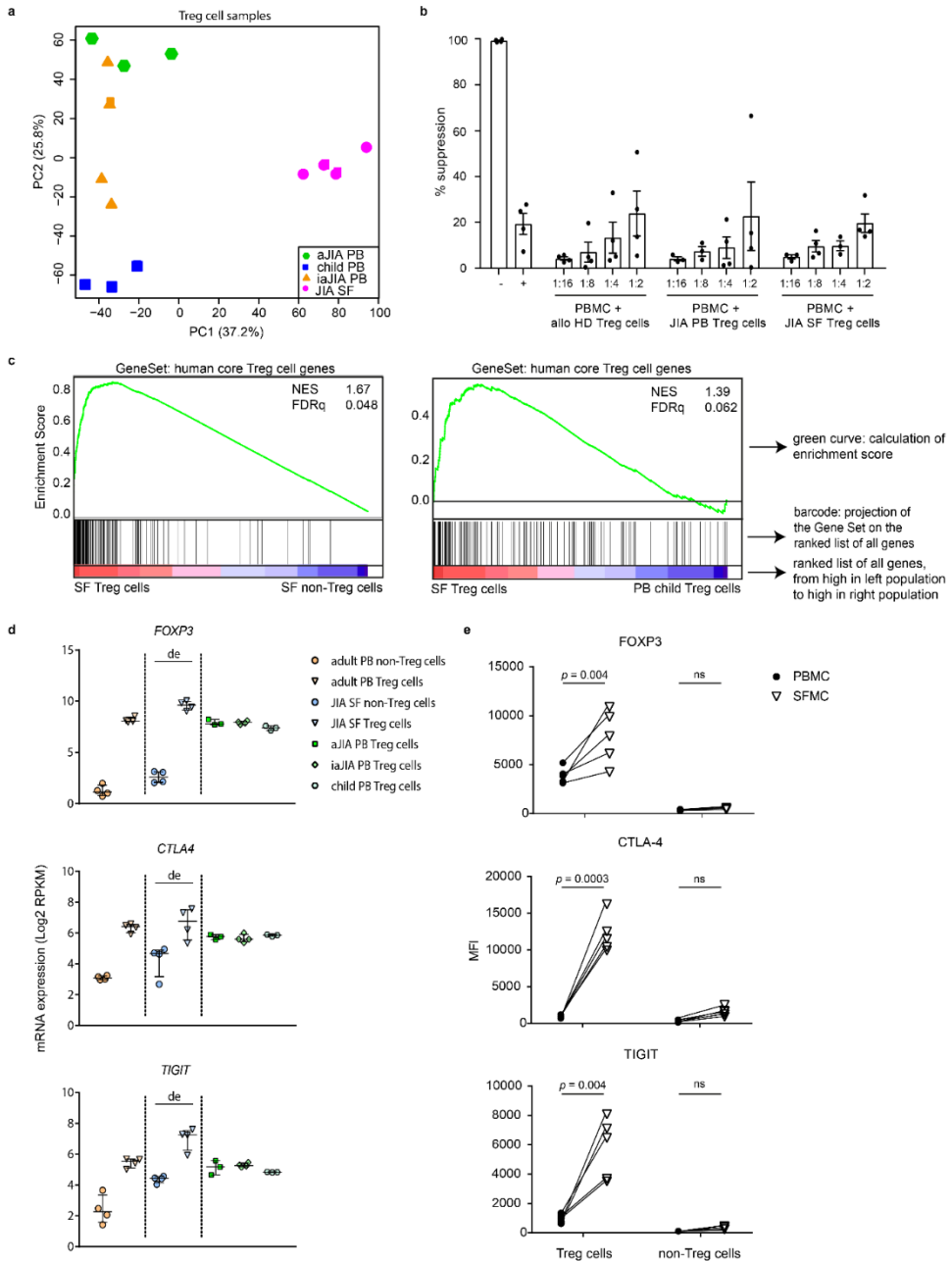


Figure 1. Distinct profile of human inflammation-derived and peripheral Treg cells. **a** Unsupervised Principal Component Analysis (PCA) of all Treg cell groups, synovial fluid (SF)- and peripheral blood (PB)-derived, from children. **b** Quantification of suppression (percentage) of CD4⁺ T cells by Treg cells from PB of healthy donors or juvenile idiopathic arthritis (JIA) patients and SF of JIA patients. 50,000 ctViolet labeled PBMC from an allogenic healthy donor were cultured with different ratios of Treg cells for 4 days in anti-CD3 coated plates ($n = 4$, mean \pm SEM). **c** Gene set enrichment analysis (GSEA) of human core Treg cell signature genes

(identified by Ferraro et al.³¹) in pairwise comparisons involving SF Treg cells and non-Treg cells, and SF Treg cells and healthy child PB Treg cells, represented by the normalized enrichment score (NES) and FDR statistical value (FDRq). **d** mRNA expression (log₂ RPKM) of *FOXP3*, *CTLA4* and *TIGIT* in Treg cells derived from PB of healthy adults (adult, *n* = 4), healthy children (child, *n* = 3), JIA patients with active (aJIA, *n* = 3) or inactive (iaJIA, *n* = 4) disease, SF of JIA patients (JIA SF, *n* = 4) and non-Treg cells (*n* = 3) from PB of healthy adults and SF of JIA patients (shown are median + IQR, de = differentially expressed according to log₂ fold change ≥ 0.6, adjusted (adj) *p*-value ≤ 0.05, mean of all normalized counts >10; adj *p*-values *FOXP3* = 1.1E⁻⁹⁵, *CTLA4* = 2.3E⁻⁰⁵, *TIGIT* = 1.9E⁻¹⁷) **e** Median Fluorescence Intensity (MFI) of FOXP3, CTLA4 and TIGIT in CD3⁺CD4⁺CD25⁺CD127^{low} Treg cells and CD3⁺CD4⁺CD25⁺CD127⁺ non-Treg cells from paired SFMC and PBMC from 5 JIA patients. Statistical comparisons were performed using two-way ANOVA with Sidak correction for multiple testing. **b**, **e** Data are representative of two independent experiments. Source data are provided as a Source Data file and deposited under GSE161426.

Inflammation-derived Treg cells have a specific effector profile

A pairwise comparison between SF- and PB-derived Treg cells from healthy children revealed many differentially expressed genes, including core Treg cell markers including *FOXP3* and *CTLA4*, but also markers that reflect more differentiated Treg cells, like *PRDM1* (encoding Blimp-1), *ICOS*, *BATF* and *BACH2* (Fig. 2a, Supplementary Data 1). Based on recent literature we analyzed the expression of markers related to eTreg cell differentiation in mice^{3,13,19–34}. Hierarchical clustering analysis confirmed that Treg cells clustered separately from non-Treg cells and revealed a cluster of core Treg cell genes with increased expression in all Treg cell groups including *CTLA4*, *FOXP3*, *IL2RA* (encoding CD25), *TIGIT* and *IKZF4* (encoding Helios) (Fig. 2b, box 1). Furthermore, clustering revealed genes that show molecular heterogeneity within the Treg cell groups. Some markers were expressed almost exclusively by SF Treg cells (including *GMZB*, *ICOS* and *IL10*) whereas others were highly expressed by SF Treg cells but with shared, albeit lower expression by SF non-Treg cells (including *PRDM1*, *BATF*, *TNFRSF18* encoding GITR, *TNFRSF1B* and *HAVCR2* encoding TIM-3) (Fig. 2b, box 2). A third cluster concerns genes most highly expressed in non-Treg cells (Fig. 2b, box 3). Some genes in this cluster shared expression with SF Treg cells, such as *LAG3*, *CXCR3* and *PDCD1* (encoding PD-1) whereas expression of *CD40LG*, *BACH2*, *SATB1*, *CCR7* and *TCF7* was clearly lower in SF Treg cells (Fig. 2b, box 2 and 3). Interestingly, the more heterogeneously expressed genes listed in box 2 and 3 were previously associated with an eTreg cell profile, including *ICOS*, *IL10*, *PRDM1*, *TNFRSF18* and *PDCD1*^{3,27,30,31,33}. The increased expression of ICOS, GITR and PD-1 was verified at protein level (Fig. 2c and Supplementary Fig. 3a). Besides the differential expression of these markers, we found a significant enrichment of genes within SF Treg cells recently described in mice to be up- or downregulated in eTreg cells³⁵ (Fig. 2d and Supplementary Fig. 3b), confirming the eTreg cell profile. Collectively, these data demonstrate that autoimmune-inflammation derived human Treg cells display an eTreg cell signature.

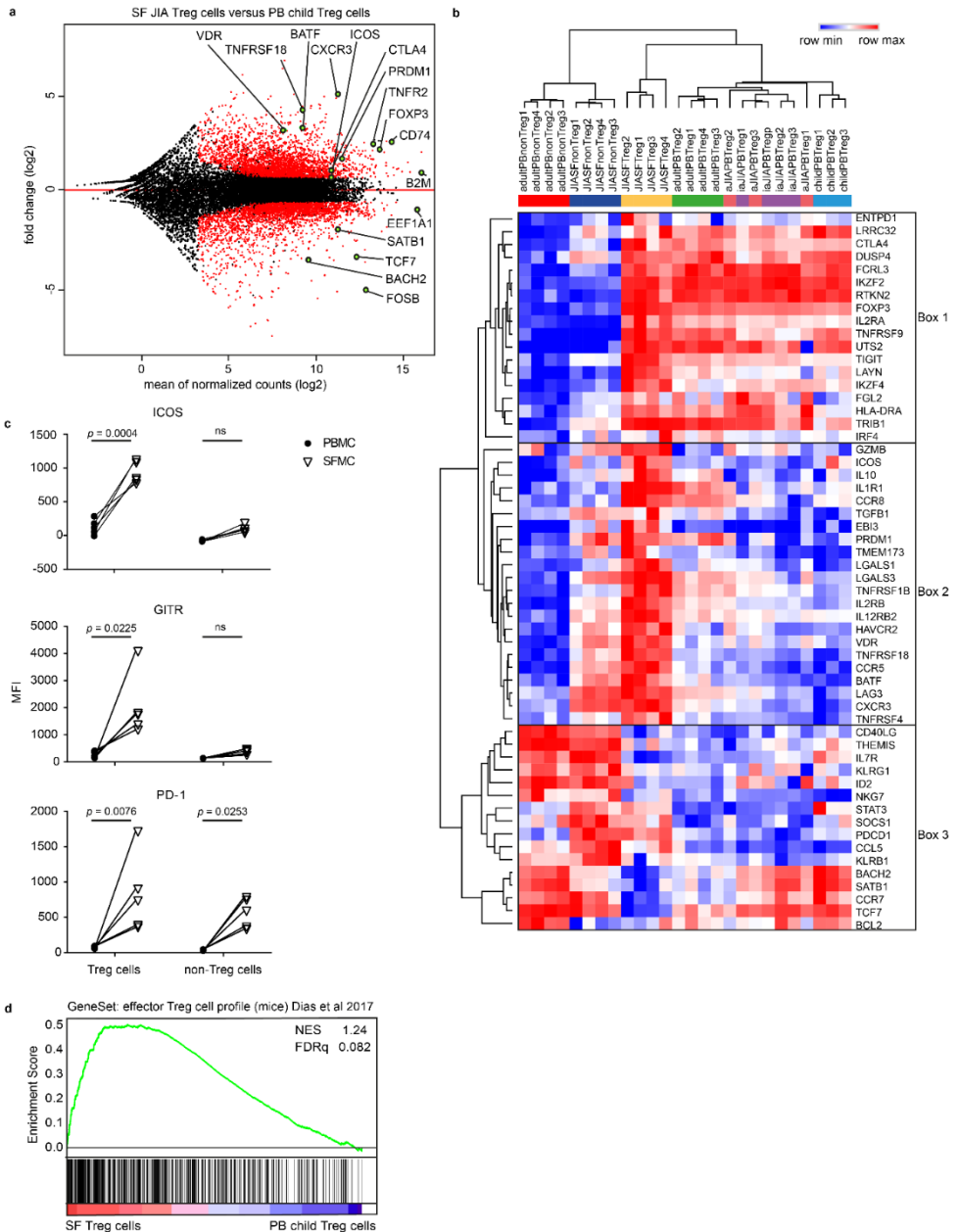


Figure 2. Inflammation-derived Treg cells have a specific effector profile. **a** MA plot of the differentially expressed genes between synovial fluid (SF, $n = 4$) and peripheral blood (PB, $n = 3$) Treg cells of healthy children with black dots reflecting no change, and red dots transcripts with an adjusted p -value < 0.05 (corrected for multiple testing using the Benjamini and Hochberg method), minimal mean of all normalized counts > 10 and \log_2 fold change > 0.6 . **b** Heatmap with hierarchical clustering analysis including all groups measured with RNA-sequencing selected genes based on recent literature (relative expression of \log_2 RPKM). **c** Median Fluorescence Intensity (MFI) of ICOS, GITR and PD-1 in gated CD3⁺CD4⁺CD25⁺CD127^{low} Treg cells and CD3⁺CD4⁺CD25⁺CD127⁺ non-Treg cells from paired SFMC and PBMC from 5 JIA patients. Statistical comparisons were performed using

two-way ANOVA with Sidak correction for multiple testing. Data are representative of two or more independent experiments. **d** Gene set enrichment analysis (GSEA) of effector Treg cell genes in mice (identified by Dias et al.⁵³) in pairwise comparisons involving SF Treg cells ($n = 4$) and PB Treg cells ($n = 3$) derived from healthy children, represented by the normalized enrichment score (NES) and FDR statistical value (FDRq, multiple hypothesis testing using sample permutation). Source data are provided as a Source Data file and deposited under GSE161426.

SF Treg cells adapt to the interferon-skewed inflammatory environment

To investigate the relationship between inflammatory environment-derived and PB-derived cells, we performed unsupervised PCA analysis on SF Treg cells and non-Treg cells, and PB Treg cells from healthy children. PB Treg cells were clearly separated from SF-derived cells, confirming that environment plays a dominant role in determining the transcriptional landscape (Fig. 3a). K-mean clustering analysis showed that SF Treg cells and non-Treg cells share increased expression of genes related to inflammation-associated pathways, including pathways linked to cytokine responses such as Interferon and IL-12 (Supplementary Fig. 4a). K-mean, and subsequent gene ontology analysis of SF Treg cells and all PB Treg cell groups derived from children demonstrated that pathways associated with Th1-skewing were specifically upregulated in SF Treg cells (Fig. 3b and Supplementary Fig. 4b, c). Indeed, expression of the Th1 key transcription factor *TBX21* (T-bet), the Th1 related chemokine receptor *CXCR3*, and IL-12 receptor β 2 (*IL12RB2*) in SF Treg cells was increased on both mRNA and protein level (Fig. 3c, d and Supplementary Fig. 4d). Expression of *TBX21* and *CXCR3* was equally high in both SF Treg cells and non-Treg cells, whilst *IL12RB2* showed a significantly higher expression in SF Treg cells (adjusted p -value = $6.8E^{-10}$). Accordingly, SF Treg cells in contrast to non-Treg cells showed co-expression of T-bet and FOXP3 protein excluding significant contamination of non-Treg cells potentially contributing to the high T-bet levels observed in SF Treg cells (Fig. 3e). These results indicate that SF Treg cells exhibit functional specialization to allow regulation of specific Th cell responses at particular tissue sites, as was previously established in mice³⁶⁻³⁸. In line herewith, we found an enrichment in SF Treg cells of the transcriptional signature of TIGIT⁺ Treg cells which have been identified as activated Treg cells selectively suppressing Th1 and Th17 cells in mice¹⁹ (Supplementary Fig. 4e). The higher frequency of memory Treg cells present in SF compared to PB did not explain the differences observed (Supplementary Figs. 2d and e, 3c and 4f).

The high expression of Th1-related proteins raised the question whether SF Treg cells may have acquired a Th1 phenotype. However, SF Treg cells failed to produce both IL-2 and IFN γ (Fig. 3f and Supplementary Fig. 4g) and responded dose-dependently to IL-2 with increasing pSTAT5 levels (Supplementary Fig. 4h), a signaling pathway pivotal for Treg cell survival and function³⁹. In fact, compared to PB Treg cells, SF Treg cells appeared to be even more responsive to IL-2. Altogether, our findings demonstrate adaptation of SF Treg cells to their inflammatory environment while maintaining Treg cell key features.

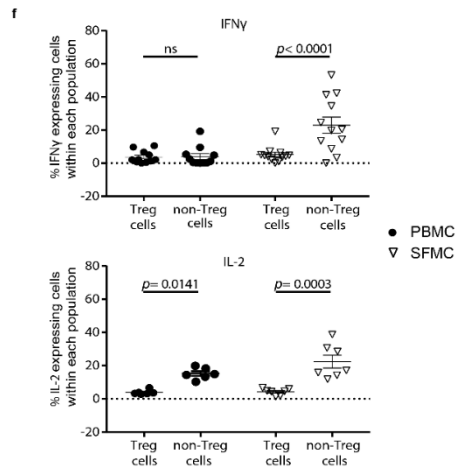
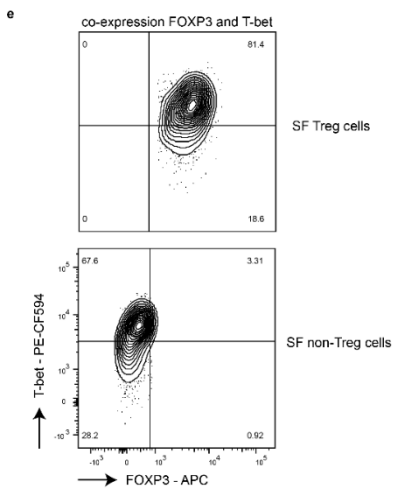
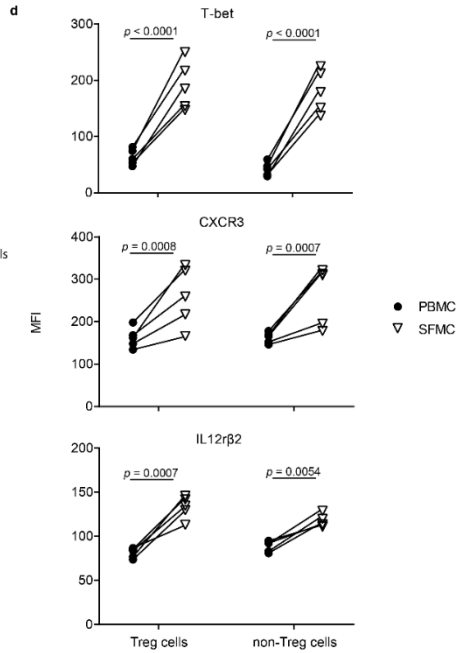
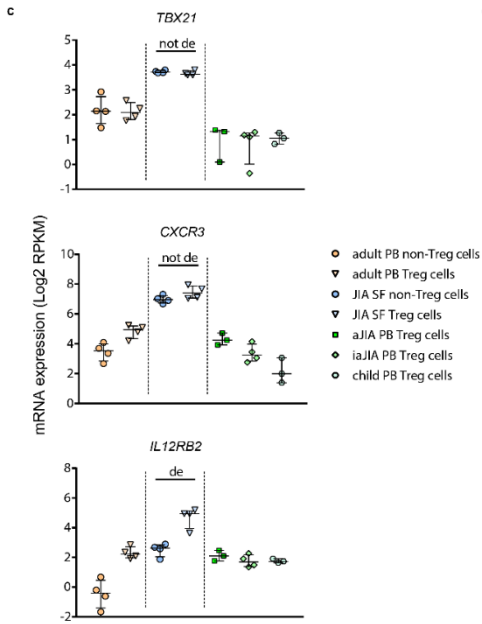
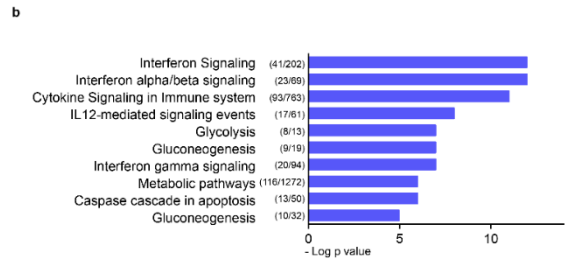
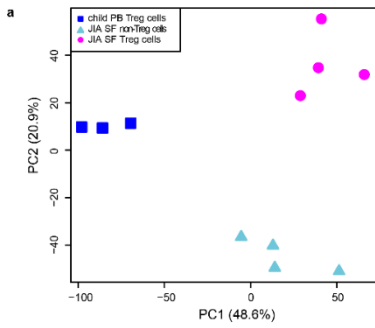


Figure 3. SF Treg cells adapt to the interferon-skewed inflammatory environment. **a** Unsupervised Principal Component Analysis (PCA) of synovial fluid (SF)-derived Treg cells and non-Treg cells (paired, $n = 4$) and peripheral blood (PB)-derived Treg cells ($n = 3$) from healthy children. **b** Gene ontology terms related to the 1791 genes specifically upregulated in SF ($n = 4$) compared to PB Treg cells derived from children (active juvenile idiopathic arthritis (JIA, ($n = 3$)), inactive JIA ($n = 4$) and healthy children ($n = 3$)), ranked by enrichment scores. The number of upregulated genes compared to the total number annotated in the gene ontology term are depicted before the terms. **c** mRNA expression (log₂ RPKM) of *TBX21*, *CXCR3* and *IL12RB2* in Treg cells derived from PB of healthy adults (adult, $n = 4$), healthy children (child, $n = 3$), JIA patients with active (aJIA, $n = 3$) or inactive (iaJIA, $n = 4$) disease, SF of JIA patients (JIA SF, $n = 4$) and non-Treg cells from PB of healthy adults ($n = 4$) and SF of JIA patients ($n = 4$) (shown as median + IQR, de = differentially expressed according to description in Fig. 1d). Adj p -value *TBX21* = 0.91, *CXCR3* = 0.44, *IL12RB2* = $6.83E^{-10}$. **d** Median Fluorescence Intensity (MFI) of T-bet, *CXCR3* and *IL12Rβ2* in $CD3^+CD4^+CD25^+CD127^{low}$ Treg cells and $CD3^+CD4^+CD25^+CD127^+$ non-Treg cells from paired SFMC and PBMC from 5 JIA patients. **e** Representative contourplot, for two independent experiments, of T-bet and FOXP3 in $CD3^+CD4^+CD25^+FOXP3^+$ Treg cells and $CD3^+CD4^+CD25^{int/-}FOXP3^-$ non-Treg cells from SFMC. **f** Percentage of IFN γ and IL-2 positive cells measured in $CD3^+CD4^+CD25^+FOXP3^+$ Treg cells and $CD3^+CD4^+CD25^{int/-}FOXP3^-$ non-Treg cells from SFMC and PMBC (IFN γ : $n = 11$ PB, $n = 12$ SF; IL-2: $n = 6$ PB, $n = 7$ SF, mean \pm SEM, p -values: IFN γ PB $p > 0.9999$, IFN γ SF $p < 0.0001$, IL-2 PB $p = 0.0051$, IL-2 SF $p < 0.0001$). **d**, **f** Data are representative of two independent experiments. Statistical comparisons were performed using two-way ANOVA with Sidak correction for multiple testing. Source data are provided as a Source Data file and deposited under GSE161426.

Regulation of effector Treg cells by the (super-)enhancer landscape

To explore the mechanistic regulation of the inflammation-adapted eTreg cell profile we analyzed the enhancer landscape of SF Treg cells. Enhancers are distal regulatory elements in the DNA that allow binding of transcription factors and as such coordinate gene expression. Epigenetic regulation of enhancers is critical for context-specific gene regulation⁴⁰. Enhancers can be defined by areas enriched for monomethylation of lysine 4 on histone H3 (H3K4me1 enrichment) and acetylation of lysine 27 on histone H3 (H3K27ac enrichment), where H3K27ac identifies active enhancers⁴¹. ChIP-seq performed for H3K27ac and H3K4me1 using SF Treg cells and healthy adult PB Treg cells revealed differences in enhancer profile and activity, with 3333 out of 37307 and 970 out of 10991 different peaks called between SF and PB Treg cells for H3K27ac and H3K4me1, respectively (Fig. 4a, Supplementary Fig. 5b, upper panel and Supplementary Data 2). We next assessed if the transcriptome of SF Treg cells is reflected at an epigenetic level. Genes that demonstrated increased H3K27ac and/or H3K4me1 were increased at the mRNA level and vice versa (Fig. 4a, Supplementary Fig. 5b, middle and lowest panel and Supplementary Data 2), confirming that gene expression and chromatin-acetylation and -monomethylation are interconnected in these cells.

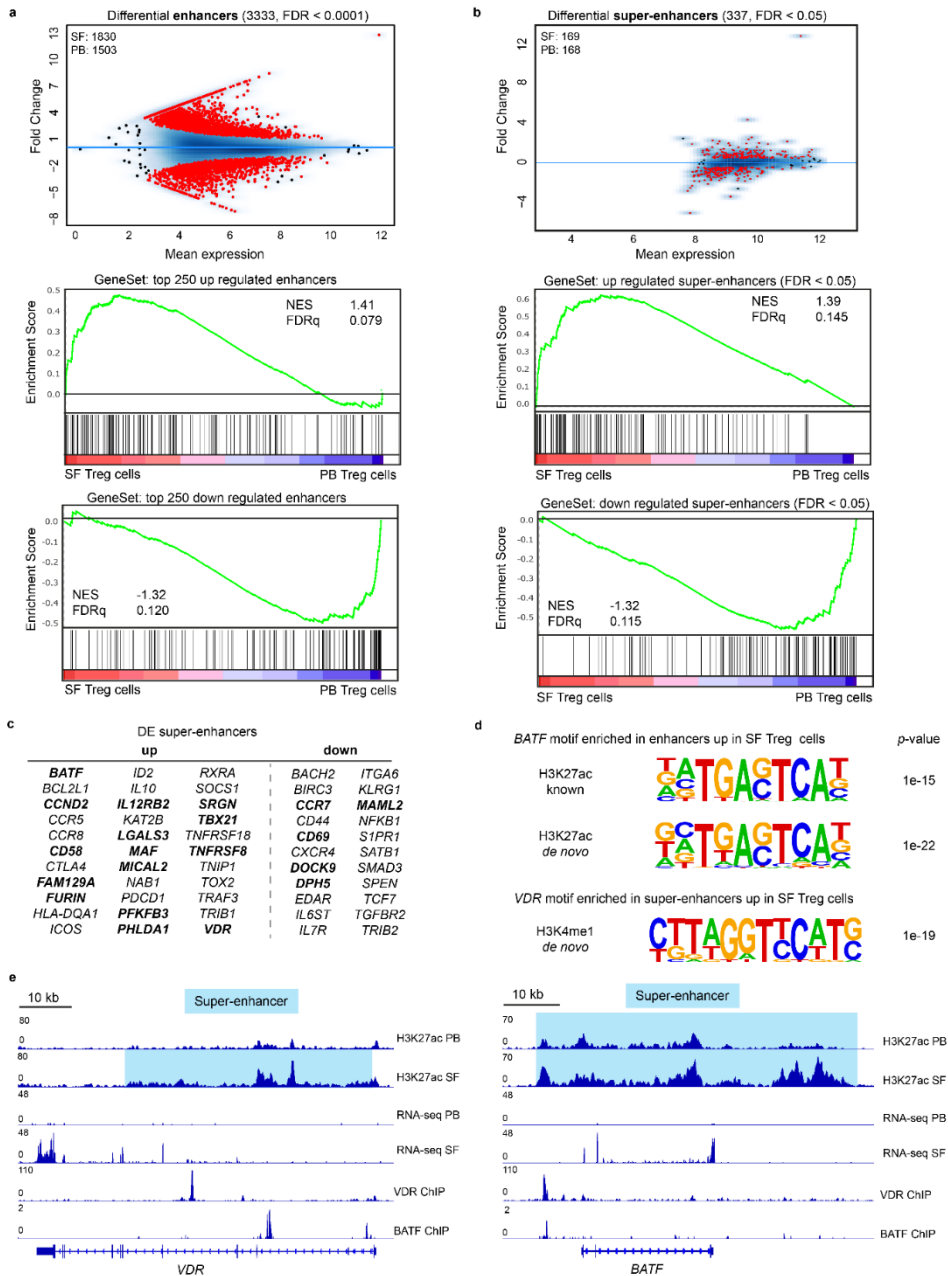


Figure 4. Environment-specific effector Treg cell profile is regulated by the (super-)enhancer landscape. a MA plots of differentially expressed enhancers (False Discovery Rate (FDR) < 0.0001) in synovial fluid (SF) versus peripheral blood (PB) Treg cells for H3K27ac ChIP-seq with the number of SF- and PB-specific enhancers indicated (top). Gene set enrichment analysis (GSEA) of the top 250 upregulated (middle) and downregulated (bottom) enhancers in pairwise comparisons involving transcriptome data of SF Treg cells and healthy adult PB Treg cells, represented by the normalized enrichment score (NES) and FDR statistical value (FDRq, multiple hypothesis testing using sample permutation). **b** Same as in **a** but for super-enhancers (FDR < 0.05). **c** Selection

of super-enhancers up- and downregulated in SF Treg cells versus healthy adult PB Treg cells for H3K27ac and H3K4me1 ChIP-seq (FDR < 0.05; bold = up/down for both and differentially expressed (DE) in SF versus PB Treg cells on transcriptome level, see also Supplementary Data 2). **d** Motifs, known and de novo, for transcription factor binding sites predicted using HOMER, enriched in the upregulated (super-)enhancers in SF Treg cells ($n = 3$) compared to healthy adult PB Treg cells ($n = 3$) for H3K27ac and H3K4me1 ChIP-seq. p -values: cumulative binomial distribution to calculate enrichment in target versus background sequences; *BATF* H3K27ac known $p = 1e^{-15}$, de novo $p = 1e^{-22}$ and *VDR* H3K4me1 $p = 1e^{-19}$. **e** Gene tracks for *VDR* and *BATF* (H3K27ac) displaying ChIP-seq signals, with the super-enhancer region highlighted in blue, in healthy adult PB Treg cells, SF Treg cells, *VDR*-specific (GSE89431) and a *BATF*-specific (GSE32465) ChIP-seq. RNA-seq signals for both *VDR* and *BATF* in child PB Treg cells and SF Treg cells are displayed as well. Representative samples for adult PB ($n = 3$), child PB ($n = 3$) and SF ($n = 3$ for ChIP-seq and $n = 4$ for RNA-seq) Treg cells are shown. For all panels FDR values were calculated using the Benjamini Hochberg method unless otherwise indicated. Source data are deposited under GSE161426 and GSE156426.

Super-enhancers are large clusters of enhancers that specifically regulate genes defining cell identity, both in health and disease^{42,43}. Super-enhancer-associated genes were identified as the nearest TSS to the center of the enhancer and super-enhancer locus using the ROSE algorithm. Also at super-enhancer level, we found significant enrichment in the transcribed genes, again indicating that the SF Treg cell profile is mediated by epigenetic changes (Fig. 4b and Supplementary Fig. 5c, middle and lowest panel). The analysis of differential super-enhancer-associated genes revealed 337 out of 791 and 317 out of 713 different gene loci for H3K27ac and H3K4me1, respectively (Fig. 4b and Supplementary Fig. 5c, upper panel). Specifically, we identified that super-enhancers associated with genes related to canonical Th1 differentiation, such as *TBX21* and *IL12RB2*, are increased in SF Treg cells (Fig. 4c) demonstrating epigenetic regulation of the environment-associated profile. Core Treg cell genes encoding the effector molecules *ICOS*, *IL10*, *CTLA4*, *TNFRSF18* and *PDCD1* were associated with increased super-enhancers as well as *FURIN* and *ID2* which are more putative functional Treg cell markers. eTreg cell differentiation was also reflected in the enhancer profile of SF Treg cells, with differential expression of super-enhancer-associated transcriptional regulators including *BATF*, *BACH2*, *SATB1*, *TRAF3* and *SOCS1*. Moreover, we found super-enhancers associated with markers not previously related to (e)Treg cell differentiation and mostly specific for human Treg cells, including *VDR* (encoding the vitamin D receptor), *RXRA* (encoding Retinoic acid receptor RXR-alpha), *KAT2B* (encoding p300/CBP-associated factor (PCAF)), *TOX2* (encoding TOX High Mobility Group Box Family Member 2) and *IL12RB2*^{3,4,6,44-53}. Inflammation related homing markers (*CCR2*, *CCR5*, *CCR7*) were associated with differential H3K27ac levels in SF Treg cells as well. Finally, regulation of cell cycling and apoptosis was also mirrored in the super-enhancer landscape of SF compared to PB Treg cells by increased activity of *DPH5*, *MICAL2*, *PHLDA1* and *CCND2*. Altogether, these super-enhancer-associated genes reflect adaptation and specialization of Treg cells within an inflammatory environment.

Motif analysis for *in silico* prediction of transcription factor binding sites in (super-)enhancers specifically upregulated in SF compared to PB Treg cells revealed motifs for Treg cell-specific transcription factors. These included STAT5 and Myb; the latter recently described

as a core transcription factor in eTreg cell differentiation⁵³. Recent papers further demonstrated BATF and RelA as crucial regulators for eTreg cells in mice^{47,49}. In support hereof, we found significant enrichment of BATF, TF65 (encoding RelA), and VDR motifs within the (super-)enhancer regions specifically upregulated in SF Treg cells (Fig. 4d and Supplementary Fig. 5d), thereby further strengthening the eTreg cell profile of SF Treg cells. The most prevalent motifs belong to the activator protein 1 (AP-1) transcription factor subfamily, part of the basic leucine zipper (bZIP) family (Supplementary Fig. 5d) indicating this subfamily is crucial in driving the eTreg cell signature, as similarly proposed by DiSpirito et al.⁵⁴ for pan-tissue Treg cells. Moreover, within the super-enhancers of both the transcriptional regulators VDR and BATF the binding sites for each of them were found, indicating that BATF (in complex with other proteins) and VDR regulate their own gene expression, and also control other eTreg cell genes (Fig. 4e). Together, these observations demonstrate that the inflammation-adapted effector phenotype of SF Treg cells observed on transcriptomic level is reflected at an epigenetic level, with a super-enhancer profile and enrichment of binding sites for eTreg cell genes, showing shared features with other Treg cells in chronically inflamed tissues.

Regulation of eTreg cell differentiation by the vitamin D3 receptor

To extract key gene regulators, based on human transcription factors and co-factors, in the differentiation from healthy PB to SF Treg cells a data-driven network and enrichment approach was performed (RegEnrich). A network of regulators and its targets was constructed (Fig. 5a) with the top predicted regulators driving the differentiation from PB to SF Treg cells were found to be *TCF7*, *LEF1*, *JUN*, *SPEN* (negative) and *ENO1*, *THRAP3* and *VDR* (positive) (Fig. 5a, b). *SPEN*, *THRAP3* and *VDR* have not been previously associated with eTreg cell differentiation. *VDR* associated downstream with core Treg cell genes including *FOXP3* and *STAT3*, but also *Tbx21* (Fig. 5a, c and Supplementary Data 3). In line herewith, there was a strong positive correlation for both FOXP3 ($r = 0.772$, $p < 0.0001$) and T-bet ($r = 0.937$, $p < 0.0001$) with VDR protein expression (Fig. 5d) reinforcing the predicted regulator network.

To investigate the direct effect of vitamin D₃ on driving Treg cells towards an effector profile we incubated sorted CD3/CD28-stimulated PB Treg cells with vitamin D₃ (calcitriol/1,25-dihydroxyvitaminD₃) and assessed the expression of (e)Treg cell function-related genes. Upon incubation with vitamin D₃ (10nM; the physiological vitamin D₃ level), increased expression of *IL2RA*, *CTLA4*, *TNFRSF8* (*CD30*) and *IL10*, as well as the eTreg cell transcription factors *TBX21* and *IRF4* was observed (Fig. 5e). On the protein level CD25, CTLA4 and TNFRSF8 were also significantly increased upon vitamin D₃ incubation (Fig. 5f). Additionally, in concordance with the epigenetic data, vitamin D₃ stimulation evoked a positive feedback loop on *VDR* expression (Fig. 5e). These findings support the hypothesis that vitamin D₃ signaling via VDR contributes to eTreg cell differentiation, while also being positively associated with core Treg cell marker expression.

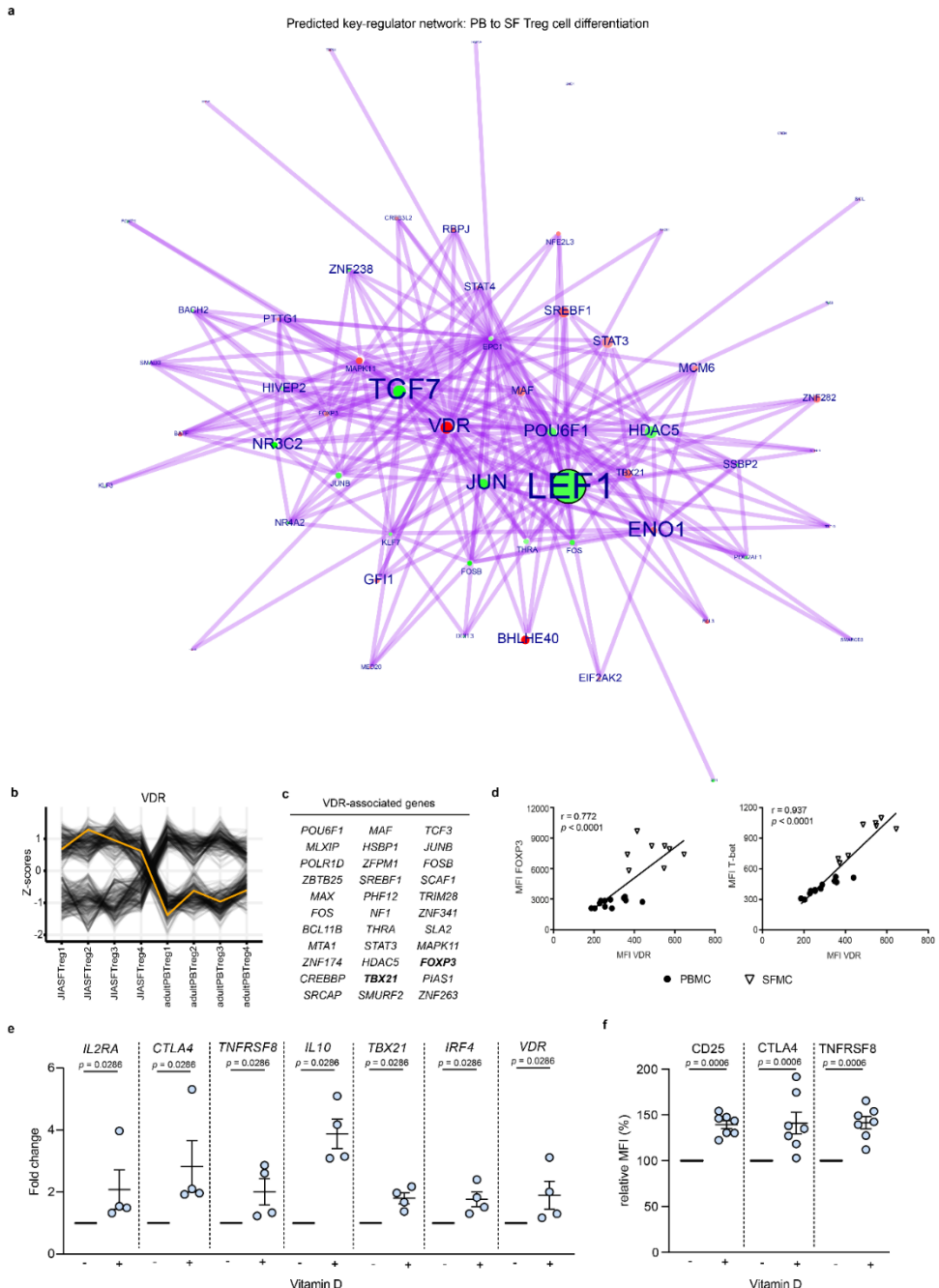


Figure 5. The vitamin D receptor is a predicted regulator of effector Treg cell differentiation. **a** Network inference of key-regulators driving peripheral blood (PB) to synovial fluid (SF) Treg cell differentiation on RNA level, based on unsupervised weighted correlation network analysis followed by Fisher's exact test of the transcription factors and co-factors (red=upregulation, green=downregulation). The purple lines depict connections between regulators and their targets. Circle size indicates $-\log_{10}(p)$ for each comparison, with the

p (-value) derived from differential expression analysis (log fold change > 1), and the text size represents the RegEnrich score; for both, larger indicates higher scores (see also Supplementary Data 3). **b** The RNA expression profile of *VDR* from JIA SF Treg cell samples 1-4 to adult PB Treg cell samples 1-4 indicated by the yellow line, with its associated genes in grey; values are normalized to the Z-score. **c** All genes associated with *VDR* defined by the key-regulator network inference. **d** Pearson's correlation plot of *VDR* and FOXP3 (left) and T-bet (right) Median Fluorescence Intensity (MFI's) in PB (circles) and SF (triangles) with the line fitted by linear regression ($n = 12$ PB HC and PB JIA (PBMC), $n = 8$ SF JIA (SFMC)). **e** Relative expression fold change ($2^{\Delta\Delta CT}$) of *IL2RA*, *CTLA4*, *TNFRSF8*, *IL10*, *TBX21*, *IRF4*, and *VDR* (lower left panel) on Treg cells upon incubation of 50,000 activated CD3⁺CD4⁺CD25⁺CD127^{low} sorted Treg cells from HC PB with 10 nM vitamin D compared to without vitamin D for 2 days ($n = 4$, mean \pm SEM). **f** Relative MFI changes of CD25 (*IL2RA*), *CTLA4* and *TNFRSF8* following experiment as per **e** with ($n = 7$, mean \pm SEM). **d-f** Data are representative of two independent experiments. Source data are provided as a Source Data file.

Similar eTreg cell profile in other inflammatory and tumor environments

To investigate whether the program identified in SF Treg cells is more general for human Treg cells exposed to inflammation, we compared our findings with Treg cells derived from PB and inflammatory joints of RA patients. Indeed, also in Treg cells from inflammatory exudate of Rheumatoid Arthritis (RA) patients similar eTreg cell genes were upregulated (Fig. 6a).

We then compared our data to recently published human tumor-infiltrating Treg cell specific signatures¹³⁻¹⁵. Strikingly, the tumor-infiltrating Treg cell signature from De Simone et al. was enriched in SF Treg cells (Normalized Enrichment Score (NES) 1.27, FDR statistical value (FDRq) 0.071; Fig. 6b). Vice versa, the differentially expressed genes in SF Treg cells versus PB Treg cells were enriched in tumor-infiltrating compared to normal tissue Treg cells (Plitas et al., 2016: NES 1.69, FDRq 0.017, Magnuson et al., 2018: NES 1.88, FDRq 0.002; Supplementary Fig. 6a, b). Hierarchical clustering analysis of the tumor-infiltrating gene signature from De Simone et al. further revealed separate clustering of SF Treg cells (Fig. 6c), indicating that the high expression of the signature genes is specific for human Treg cells at a site that is characterized with infiltration of immune cells. We also observed a small set of genes that were not upregulated in SF Treg cells, e.g. *CX3CR1*, *IL17REL*, *IL1RL1* and *IL1RL2*, implying environment-restricted adaptation (Fig. 6c). The three genes that were described as the most enriched and distinctive genes in tumor-infiltrating Treg cells, *LAYN*, *MAGEH1*, and *CCR8*, were selectively and highly upregulated in SF Treg cells (Fig. 6d). These data demonstrate that the Treg cell profile we observed is not restricted to the SF exudate from JIA and RA patients. In fact, it likely represents a more global profile of human Treg cells in inflammatory settings, likely fine-tuned by environment specific adaptations.

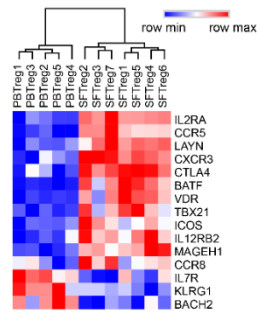
To investigate which cues might be specific for SF we explored the differences between upregulated genes in SF and tumor-infiltrating Treg cells. Relatively few pronounced SF-specific genes were found. On gene level, cytotoxic markers including *GZMM*, *GZMA* and *GNLY*, related to effector cell cytolysis and self-induced apoptosis of Treg cells⁵⁵ were SF-specific (Supplementary Fig. 6c). Gene ontology biological process analysis further revealed that in SF both active cell cycling and apoptotic pathways were upregulated, whereas in the tumor microenvironment cell activation and effector responses were prominent (Supplementary Fig. 6d). Additionally, tumor-infiltrating Treg cells showed distinct expression of chemokines and

chemokine receptors, e.g. IL-8 (CXCL8), CX3CR1, CXCR7 and CCR10 (Supplementary Fig. 6c), some of which have been proposed as prognostic marker and/or therapeutic target in cancer⁵⁶.

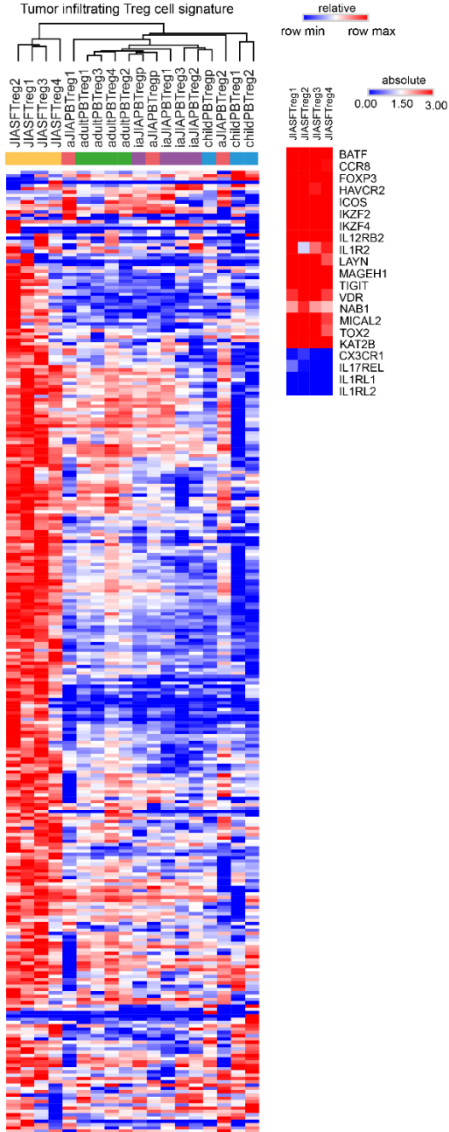
From the JIA, RA and tumor datasets we could deduce a set of genes that appear universally upregulated in eTreg cells, and also being reflected in the (super-)enhancer landscape of SF Treg cells (Fig. 6e). *ICOS*, *BATF*, *MAF*, *TNFRSF18* and *SRGN* were revealed as core markers previously also related to mouse eTreg cells. Additionally, *IL12RB2*, *VDR*, and *KAT2B*, were identified as core genes, as well as *PFKFB3* and *LDHA* involved in glycolysis and the apoptosis-related genes *MICAL2* and *TOX2*. The latter two have so far not been linked to Treg cells in human or mice, although both have independently been linked to human cancers^{57,58}. Indeed, gene set enrichment and leading edge analyses of activated, (shared) tissue, inflammatory and tumor-infiltrating Treg cell gene sets amongst others revealed sharing of the core eTreg cell genes, including *BATF*, *CCND2*, *CCR8*, *TNFRSF18*, and *VDR* (Supplementary Data 4). Even though SF Treg cells are highly activated, there was no enrichment for exhaustion nor exTreg cell-associated genes. Collectively, our results demonstrate that human Treg cells in different inflammatory settings share an effector profile and strongly indicates that inflammation drives eTreg cell differentiation in a comparable manner in different environments.

> Figure 6. The effector Treg cell and human tumor Treg cell signature overlap. **a** Heatmap with unsupervised hierarchical clustering analysis on peripheral blood (PB, $n = 5$) and (partially paired) synovial fluid (SF, $n = 7$) Treg cells from Rheumatoid Arthritis patients measured with a gene array, on selected signature genes identified from juvenile idiopathic arthritis (JIA) SF Treg cells and tumor-infiltrating Treg cells. **b** Gene set enrichment analysis (GSEA) of tumor-infiltrating Treg cell signature genes (identified by De Simone et al.¹³) in pairwise comparisons involving SF Treg cells ($n = 4$) and healthy child PB Treg cells ($n = 3$), represented by the normalized enrichment score (NES) and FDR statistical value (FDRq, multiple hypothesis testing using sample permutation). **c** Heatmap with hierarchical clustering analysis including all groups measured with RNA-sequencing on the identified tumor-infiltrating Treg cell signature genes (ref.¹³), with relative expression of log2 RPKM. Small heatmap on the right shows log2 RPKM values of a selection of genes in SF Treg cells. **d** mRNA expression (log2 RPKM) of *CCR8*, *MAGEH1* and *LAYN* in Treg cells from PB of healthy adults (adult, $n = 4$), healthy children (child, $n = 3$), JIA patients with active (aJIA, $n = 3$) or inactive (iaJIA, $n = 4$) disease, SF of JIA patients (JIA SF, $n = 4$) and non-Treg cells from PB of healthy adults ($n = 4$) and SF of JIA patients ($n = 4$) as determined by RNA-sequencing analysis (shown are median + IQR, de = differentially expressed according to description in Fig. 1d; adjusted p -values (Benjamini and Hochberg method) $CCR8 = 2.2E^{-13}$, $MAGEH1 = 1.2E^{-07}$, $LAYN = 1.2E^{-33}$). **e** Identification of a human effector Treg cell profile based on the overlapping genes upregulated in JIA SF Treg cells, RA SF Treg cells and tumor-infiltrating Treg cells (identified in several studies, see refs.^{13-15,89,90}), and reflected on the (super-)enhancer landscape of SF Treg cells. Source data are provided as a Source Data file and deposited under GSE161426.

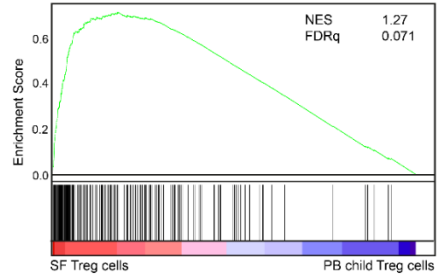
a Expression signature genes in Treg cells from Rheumatoid Arthritis patients



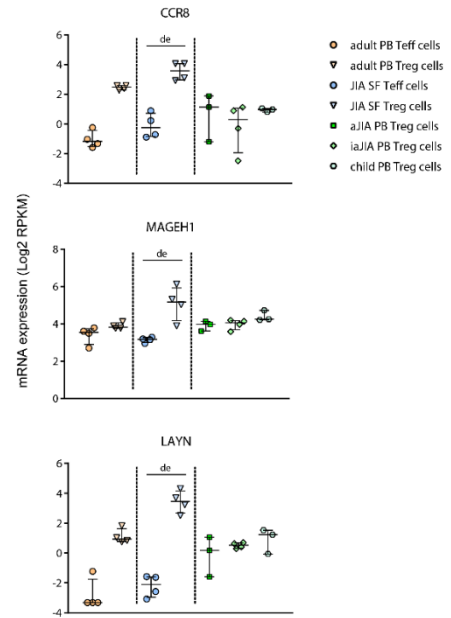
c Tumor infiltrating Treg cell signature



b GeneSet: tumor infiltrating Treg cell signature



d



e

shared eTreg cell signature

<i>ARPP19</i>	<i>HNRNP3L</i>	<i>PFKFB3</i>
<i>BATF</i>	<i>ICOS</i>	<i>PHLDA1</i>
<i>BCL2L1</i>	<i>IL12RB2</i>	<i>RBPJ</i>
<i>CCND2</i>	<i>IL1R1</i>	<i>SH2D2A</i>
<i>CCR8</i>	<i>IL1R2</i>	<i>SRGN</i>
<i>CD58</i>	<i>KAT2B</i>	<i>TMEM173</i>
<i>CTSC</i>	<i>LAIR2</i>	<i>TNFRSF18</i>
<i>ENTPD1</i>	<i>LGALS3</i>	<i>TNFRSF1B</i>
<i>FAM129A</i>	<i>MAF</i>	<i>TOX2</i>
<i>GAPDH</i>	<i>MICAL2</i>	<i>VDR</i>
<i>GCNT1</i>	<i>NAMPT</i>	

DISCUSSION

The discovery of eTreg cells in non-lymphoid tissues and inflammatory sites in mice have raised questions how human eTreg cells are transcriptionally and epigenetically programmed in different settings. The present study provides evidence that human Treg cells in a local inflammatory setting undergo further differentiation into specialized eTreg cells. This is reflected by high expression of TBX21 and CXCR3 and core Treg cell markers including FOXP3, CTLA4 and TIGIT. Essential Treg cell features are maintained, such as suppressive function, IL-2 responsiveness and absence of cytokine production. The transcriptional changes were mirrored at an epigenetic level, both in the enhancer and super-enhancer landscape, demonstrating that the profile is highly regulated. Additionally, we identify previously unappreciated and specific markers in human eTreg cells, like VDR, IL12R β 2, and BATF; with VDR as a predicted key-regulator in human eTreg cell differentiation. *In vitro*, vitamin D₃ incubation strengthened the core (e)Treg cell signature at both the protein and mRNA level. Finally, we demonstrate that the profile is not limited to autoimmune inflammation in JIA and RA, but shares almost complete overlap with tumor-infiltrating Treg cells. The similarity between a tumor and an autoimmune setting might seem counterintuitive, since the former reflects an immune-suppressive environment whereas the latter is associated with immune activation. Both environments however share features including immune cell infiltration and inflammation⁵⁹. This overlapping profile might therefore represent a more universal profile of human Treg cells in inflammatory environments. Because of the extensive genome-wide changes of Treg cells from an inflammatory environment insight in their functionality is important. In line with previous reports^{16,17}, we show that SF Treg cells are indeed suppressive and additionally highly responsive to IL-2 by phosphorylation of STAT5, excluding impaired IL-2 signaling^{60,61}. This advocates against an intrinsic defect of Treg cells in inflammation. Maintenance of inflammation may be explained by resistance of local effector cells, previously demonstrated in both JIA and RA^{17,62,63}.

In mice, functional specialization of Treg cells towards Th1 inflammation by upregulation of T-bet is described as essential to prevent Th1 autoimmunity^{9,10}. The remarkable co-expression of T-bet and FOXP3 in SF Treg cells in our study, with T-bet levels as high as in SF non-Treg cells, implies that functional specialization is translatable to a human setting. The increased expression of migration markers such as CXCR3 and CCR5 on protein, transcriptional and enhancer level further strengthens this, as high T-bet expression is crucial for migration and thus co-localization of Th1-specific Treg cells and Th1 effector T cells via upregulation of these chemokine receptors^{9,10}.

Contamination of Treg cells with non-Treg cells can be a concern when sorting *ex vivo* human cells. However, we exclude substantial contamination because 1) our data show robust transcriptomic differences between SF Treg cells and non-Treg cells, with increased expression of Treg cell hallmark genes in SF Treg cells, 2) sorted Treg cells are > 90% FOXP3⁺, 3) there is clear co-expression of FOXP3 and T-bet on the single cell level, 4) we show that SF Treg cells, while expressing high T-bet levels, lack cytokine production, potentially caused by high expression of FOXP3, SOCS1, EGR2 and EGR3 (Supplementary Data 1)^{64,65}. Nevertheless,

as recently shown by Miragaia et al.⁴ there may be heterogeneity within the eTreg cell population.

Our study investigated both the transcriptional and epigenetic regulation of eTreg cells in human inflammatory settings allowing us to discern human-specific eTreg cell regulation as well as commonalities between mice and humans. The findings on epigenetic level should still be demonstrated experimentally since although regions marked by H3K27ac/H3K4me1 are associated with active enhancers this is not prima facie evidence of enhancer function^{41,66}. Furthermore, we have identified (super-)enhancer associated genes as the nearest TSS to the center of the enhancer and super-enhancer locus. It is therefore possible that these (super-)enhancers can regulate other genes than predicted by our analyses⁴¹. This requires further studies into the spatial chromatin organization in Treg cells, especially under inflammatory conditions. The epigenetic landscape of human Treg cells is little explored, with only two papers studying H3K27acetylation and H3K4monomethylation of circulating human Treg cells^{67,68}. Arvey et al. conclude that the majority of Treg cell lineage-specific elements are not conserved between mice and human further emphasizing the lack of knowledge of the human Treg cell epigenetic landscape. Gao et al. focused on SNPs within enhancers of PB Treg cells from Type 1 diabetes patients, and in line with our data showed, that cell cycle and apoptosis regulation is highly reflected in the enhancer landscape of these patients. These data further underscore the need for additional studies, especially in non-lymphoid tissues during non-homeostatic conditions. We found similarities between mice and humans in eTreg cell differentiation regarding downregulation of *SATB1*, *BACH2*, *TCF7* and *LEF1*, all associated with a super-enhancer in PB but not SF Treg cells. Although all four genes are crucial for Treg cell development, recent reports show that downregulation of these regulators is necessary for further differentiation of Treg cells and preventing conversion into Th cells^{44,52,69-73}. *BACH2* can transcriptionally repress *PRDM1* (encoding Blimp-1) in T cells⁷², and in line herewith we observed increased acetylation and gene expression of *PRDM1* in SF Treg cells. This was further supported by the decrease in *TCF7* and *LEF1*, both negatively correlating with eTreg cell marker expression including *PRDM1*⁷³. Moreover, we found BATF as a prominent marker in SF Treg cells, with increased expression on both transcriptional and epigenetic level, and a binding site in upregulated super-enhancer associated genes. In addition, high BATF expression was also observed in RA SF Treg cells and tumor-infiltrating Treg cells, suggesting BATF is a key transcriptional regulator in both human and mice eTreg cells. We also found remarkable differences in eTreg cell signature markers compared to what is known from mice. Most pronounced is upregulation of *IL12RB2* at both the transcriptional and epigenetic level, and a binding site in upregulated super-enhancer associated genes, whereas in mice eTreg cells this marker is downregulated. Instead, impaired *IL-12Rβ2* expression has been reported as a key checkpoint preventing Treg cells from fully differentiating towards Th1 cells in mice³⁸. However, our data are in line with recent reports showing selective expression of *IL12RB2* in human PB Treg cells^{30,67}, suggesting this marker has different functions in human and mice.

Another unexpected finding is the upregulation of *VDR* in both JIA and RA SF Treg cells, on both transcriptional and epigenetic level, as well as in tumor-infiltrating Treg cells.

Although not highlighted, high VDR levels were present in breast tumor-infiltrating Treg cells¹⁴ and uterine eTreg cells⁷⁴. Besides the well-known tolerogenic effects of vitamin D₃⁷⁵, VDR is not well-studied in the Treg cell context, especially in humans. A recent study did show that memory CCR6⁺ Th cells gained a suppressive phenotype, including CTLA4 expression, and functional suppressive capacity similar to Treg cells upon incubation with vitamin D₃⁷⁶. Here we show VDR is a predicted key-regulator in SF eTreg cells, positively correlated with both FOXP3 and T-bet expression.

Another difference is absence of *KLRG1* upregulation in human eTreg cells. In mice, *KLRG1* is a key marker to identify eTreg cells, although not crucial for eTreg cell function⁷⁷. *KLRG1* is not upregulated on SF Treg cells and associated with a super-enhancer only in PB Treg cells. Additionally, in our data gene expression of *KLRG1* is restricted to non-Treg cells (both SF and PB). Confusing the findings are discrepancies possibly caused by the tissue measured or comparison made. Miragaia et al.⁴ showed upregulation of *PIM1* in non-lymphoid Treg cells compared to PB Treg cells in mice, but *PIM1* was not expressed in human tissue Treg cells. In our data however, *PIM1* is highly increased in SF compared to PB Treg cells of healthy adults and children (Supplementary Data 1). In summary, we show that human eTreg cells show similarities in eTreg cell differentiation markers identified in mice, but also found human-specific eTreg cell markers including IL-12Rβ2 and VDR, and absence of *KLRG1*.

Previous research has shown that ex vivo human Treg cells are highly glycolytic⁷⁸, in line with their high proliferative capacity⁷⁹. In mice increased glycolysis is required for eTreg cell differentiation and migration to inflammatory sites^{80,81}. In support hereof, glycolysis-associated genes including *PFKFB3*, *LDHA*, and *PKM2* were increased in SF Treg cells on both RNA and (super-)enhancer level. Finally, *ENO1*, encoding the glycolytic enzyme Enolase 1, is a predicted key-regulator of eTreg cell differentiation.

Lately, application of Treg cell-based therapies for autoimmune diseases and transplantation settings is gaining renewed interest. Promising data from animal models and clinical trials, both with cell therapy involving adoptive transfer and with low dose IL-2 administration, pave the way for Treg cell therapies to reach the clinic⁸². Our data show that circulating human Treg cells are markedly different from their counterparts derived from sites characterized by immune activation. This is reflected in the expression of effector markers and transcriptional regulators, but also in the expression of specific chemokine receptors. Regarding Treg cell-based therapies appreciating that specific environments may require adapted Treg cells, both for migration and function, is important. Moreover, in this study we profiled human eTreg cells abundantly present at sites of inflammation. This information can form a basis for follow-up studies that may eventually allow characterization of small amounts of circulating eTreg cells, for example to monitor patients undergoing treatment.

In conclusion, our study uncovered the transcriptional and epigenetic program that defines human inflammatory Treg cells. SF Treg cells display an environment-adapted as well as an eTreg cell phenotype established at the epigenetic level. Moreover, we describe striking similarities of the eTreg cell program with tumor-infiltrating Treg cells and SF Treg cells from RA patients. This revealed a set of genes shared with human eTreg cells from affected sites in

JIA, RA and cancer including BATF, VDR, MICAL2, TOX2, KAT2B, PFKFB3 and IL12R β 2. Finally, we show that THRAP3, ENO1 and VDR are predicted key-regulators driving human SF eTreg cell differentiation at the transcriptomic level.

METHODS

Collection of SF and PB Samples

Patients with JIA ($n = 41$) were enrolled by the Pediatric Rheumatology Department at University Medical Center of Utrecht (The Netherlands). Of the JIA patients $n = 8$ were diagnosed with extended oligo JIA and $n = 33$ with oligo JIA, according to the revised criteria for JIA⁴³, with an average age of 11.3 years (range 3.2-19 years) and a disease duration at the time of inclusion of 4.9 years (range 0.1-15 years). Active disease was defined by physician global assessment of ≥ 1 active joint (swelling, limitation of movement), and inactive disease was defined as the absence hereof. Additional parameters including the Juvenile Arthritis Disease Activity Score (JADAS), C-reactive protein (CRP) and erythrocyte sedimentation rate (ESR) were also taken into account. Patients with RA ($n = 7$) were enrolled by the rheumatology outpatient clinic at Guy's and St. Thomas' Hospital NHS Trust (United Kingdom). The average age of RA patients was 61 years (range 30-75 years). PB and synovial fluid (SF) was obtained when patients visit the outpatient clinic via vein puncture or intravenous drip, and by therapeutic joint aspiration of the affected joints, respectively. The study was conducted in accordance with the Institutional Review Board of the University Medical Center Utrecht (approval no. 11-499/C; JIA) and the Bromley Research Ethics Committee (approval no. 06/Q0705/20; RA). PB from healthy adult volunteers (HC, $n=20$, average age 41.7 years with range 27-62 years) was obtained from the Mini Donor Service at University Medical Center Utrecht. PB from $n=8$ healthy children (average age 11.4 years with range 7.3-15.6 years; approval no. 05-149/K) was obtained from a cohort of control subjects for a case-control clinical study. Informed consent was obtained from all the participants and/or from their parents/guardians/legally authorized representatives.

Isolation of SFMC and PBMC

SF of JIA patients was incubated with hyaluronidase (Sigma-Aldrich) for 30 min at 37°C to break down hyaluronic acid. Synovial fluid mononuclear cells (SFMCs) and peripheral blood mononuclear cells (PBMCs) were isolated using Ficoll Isopaque density gradient centrifugation (GE Healthcare Bio-Sciences, AB) and were used after freezing in Fetal Calf Serum (FCS) (Invitrogen) containing 10% DMSO (Sigma-Aldrich).

Suppression assay

CD3⁺CD4⁺CD25⁺CD127^{low} cells (Treg cells) were isolated from frozen PBMC (see Supplementary Fig. 1a for gating strategy), using the FACS Aria III (BD). Antibodies used for sorting are: anti-human CD3 BV510 (clone OKT3, 1:400), CD25 PE/Cy7 (clone M-A251, 1:25; BD), CD127 AF647 (clone HCD127, 1:50; Biolegend), CD4 FITC (clone RPA-T4, 1:200; eBioscience). To check for FOXP3 expression of the sorted populations cells were fixed and permeabilized by using

eBioscience Fixation and Permeabilization buffers (Invitrogen) and stained with anti-human FOXP3 eF450 (clone PCH101, 1:50; eBioscience) (see Supplementary Fig. 1b). Read out of proliferation is performed with the following antibodies: CD3 PerCP/Cy5.5 (clone UCHT1, 1:100; Biolegend), CD4 FITC (clone RPA-T4, 1:200; eBioscience), CD8 APC (clone SK1, 1:100; BD). Total PBMC were labeled with 2 μ M ctViolet (Thermo Fisher Scientific) and cultured alone or with different ratios of sorted Treg cells (1:16, 1:8, 1:4, 1:2). Cells were cultured in RPMI1640 media containing 10% human AB serum with addition of L-Glutamine and Penicillin/Streptomycin. PBMC were stimulated by 0,1 μ g/ml coated anti-CD3 (eBioscience) and incubated for four days in a 96 well round bottom plate (Nunc) at 37 °C. After 4 days cells were stained with CD3, CD4, and CD8 for read out of proliferation by flow cytometry performed on FACS Canto II (BD Biosciences) and data was analyzed using FlowJo Software v10 (Tree Star Inc.).

Cell phenotyping

PBMC and SFMC were thawed and stained by surface and intranuclear/cellular staining with the following antibodies: CD3 BV510 (clone OKT3, 1:400), CD3 AF700 (clone UCHT1, 1:50), CD127 PerCP-Cy5.5 (clone HCD127, 1:25), CD127 PE-Cy7 (clone HCD127, 1:50), CXCR3 FITC (clone G025H7, 1:40), IL2 PB (clone MQ1-17H12, 1:100; Biolegend), CD4 APC-eFluor780 (clone RPA-T4, 1:50), FOXP3 APC (clone PCH101, 1:25), TIGIT PerCP-eFluor710 (clone MBSA43, 1:50), FOXP3 eF450 (clone PCH101, 1:50), ICOS APC (clone ISA3, 1:20; eBioscience), CD127 BV421 (clone HIL-7R-M21, 1:40), CD25 PE/Cy7 (clone MA251, 1:25), CTLA4 PE (clone BNI3, 1:12.5), PD-1 BV711 (clone EH12.1, 1:100), IL12R β 2 PE (clone 2B6/12 β 2, 1:5), T-bet PE-CF594 (clone 04-46, 1:25), IFN γ PerCP-Cy5.5 (clone 4S.B3, 1:40), FOXP3 PE-CF594 (clone 259D/C7, 1:50; BD), GITR FITC (clone #110416, 1:8.3; R&D). For measurement of cytokines thawed cells were stimulated with 20ng/mL PMA (MP Biomedicals) and 1 μ g/mL ionomycin (Calbiochem) in RPMI supplemented with 10% AB. After 30 min incubation at 37 °C Golgi stop (BD Biosciences) was added followed by 3.5 hours of incubation at 37 °C. For intranuclear/cellular staining the Intracellular Fixation & Permeabilization Buffer Set (eBioscience) was used. See Supplementary Fig. 1a and c for gating strategy of FOXP3⁺ Treg cells and non-Treg cells, and Supplementary Figs. 2-4 for MFI plots of the markers of interest. Data acquisition was performed on a BD LSRFortessa (BD Biosciences) and analysis as above.

STAT5 Phosflow

PBMC and SFMC were thawed and resuspended in PBS (0,5 – 1,0 x 10⁶ living cells/tube). Surface staining of CD3 BV510 (clone OKT3, 1:400, Biolegend) and CD4 FITC (clone RPA-T4, 1:200, eBioscience) was performed for 25 min at 4°C. Cells were then stimulated with 0, 1, 10 or 100 IU/ml human (h)IL-2 (Proleukin; Novartis) for 30 min at 37°C, fixated and permeabilized by using buffers from the Transcription Factor Phospho Buffer Set (BD Biosciences). Intranuclear staining of FOXP3 eF450 (clone PCH101, 1:50), T-bet eF660 (clone eBio4B10, 1:50; eBioscience), CD25 PE/CY7 (clone M-A251, 1:25) and pSTAT5 PE (clone pY695, 1:25; BD) was performed for 50 min at 4°C. See Supplementary Fig. 1a and c for gating strategy of FOXP3⁺ Treg cells and non-

Treg cells, and Supplementary Fig. 4h for the gating of pSTAT5. Data acquisition and analysis as above.

RNA-sequencing

CD3⁺CD4⁺CD25⁺CD127^{low} and CD3⁺CD4⁺CD25⁺CD127⁺ cells were sorted by flow cytometry from HC PBMC and JIA patient SFMC and PBMC (see Supplementary Fig. 1a for gating strategy). Total RNA was extracted using the AllPrep DNA/RNA/miRNA Universal Kit (Qiagen) as specified by the manufacturer's instructions and stored at -80°C. Sequencing libraries were prepared using the Rapid Directional RNA-Seq Kit (NEXTflex). Libraries were sequenced using the Nextseq500 platform (Illumina), producing single end reads of 75bp (Utrecht Sequencing Facility). Sequencing reads were mapped against the reference human genome (hg19, NCBI37) using BWA (v0.7.5a, mem -t 7 -c 100 -M -R) (see Supplementary Data 5 for quality control information). Differential gene expression was performed using DESeq2 (v1.2). For K-means clustering and PCA analysis, genes with fold change between samples on 10th and 90th quantile at least 1 log₂ RPKM and expression at least 2 log₂ RPKM in the sample with the maximal expression were used. K-means clustering was done on gene expression medians per group, with an empirically chosen k of 14. The scripts used for analysis are available at⁸⁴. Gene Ontology pathway analyses were performed using ToppFun (<https://toppgene.cchmc.org/enrichment.jsp>) with as input genes belonging to the defined k-mean clusters, with an FDR-corrected *p*-value <0.05 defining significance. Gene set enrichment analysis (GSEA, v3.0 and v4.0.3)⁸⁵, with as input the log₂ RPKM data, was used to assess whether specific signatures were significantly enriched in one of the subsets. One thousand random permutations of the phenotypic subgroups were used to establish a null distribution of enrichment score against which a normalized enrichment score and FDR-corrected *q* values were calculated. Gene-sets were either obtained by analyzing raw data using GEO2R (NCBI tool) or downloaded from published papers, or self-made based on the H3K27ac/H3K4me1 data. In particular, the following published gene data sets were used: human core Treg cell signature: Ferraro et al.³¹; effector Treg cell signature in mice: Dias et al.⁵³; tumor-infiltrating Treg cell signature: De Simone et al.¹³, Plitas et al.¹⁴, Magnuson et al.¹⁵; effector Treg cell genes in mice: Levine et al.³⁵; TIGIT⁺ Treg cell signature in mice: Joller et al.¹⁹. Identification of key-regulators was performed using RegEnrich⁸⁶ v1.0.0 based on the differential gene expression data followed by unsupervised WGCNA for the network inference, mean RPKM counts > 0 were included, and Fisher's exact test was used for enrichment analysis. Heatmaps and subsequent hierarchical clustering analyses using One minus Pearson correlation were performed using Morpheus software (v0.1.1.1, <https://software.broadinstitute.org/morpheus/>).

H3K27ac and H3K4me1 ChIP-sequencing

PBMC from HC and SFMC from JIA patients were thawed and 0.5-1 million CD3⁺CD4⁺CD25⁺CD127^{low} cells were sorted by flow cytometry (see Supplementary Fig. 1a for gating strategy). For each sample, cells were crosslinked with 2% formaldehyde and crosslinking was stopped by adding 0.2 M glycine. Nuclei were isolated in 50 mM Tris (pH 7.5),

150 mM NaCl, 5 mM EDTA, 0.5% NP-40, and 1% Triton X-100 and lysed in 20 mM Tris (pH 7.5), 150mMNaCl, 2mMEDTA, 1% NP-40, 0.3% SDS. Lysates were sheared using Covaris microTUBE (duty cycle 20%, intensity 3, 200 cycles per burst, 60-s cycle time, eight cycles) and diluted in 20 mM Tris (pH 8.0), 150 mM NaCl, 2 mM EDTA, 1% X-100. Sheared DNA was incubated overnight with anti-histone H3 acetyl K27 antibody (ab4729; Abcam) or anti-histone H3 (mono methyl K4) antibody (ab8895; Abcam) pre-coupled to protein A/G magnetic beads. Cells were washed and crosslinking was reversed by adding 1% SDS, 100mM NaHCO₃, 200mM NaCl, and 300 µg/ml proteinase K. DNA was purified using ChIP DNA Clean & Concentrator kit (Zymo Research), end-repair, a-tailing, and ligation of sequence adaptors was done using Truseq nano DNA sample preparation kit (Illumina). Samples were PCR amplified, checked for the proper size range and for the absence of adaptor dimers on a 2% agarose gel and barcoded libraries were sequenced 75 bp single-end on Illumina NextSeq500 sequencer (Utrecht DNA sequencing facility). Sample demultiplexing and read quality assessment was performed using BaseSpace (Illumina) software. Reads with quality score of Q>30 were used for downstream analysis. Reads were mapped to the reference genome (hg19/hg38) with Bowtie 2.1.0 using default settings for H3K27ac ChIP-seq and BWA for H3K4me1 ChIP-seq (see Supplementary Data 5 for quality control information). SAM files were converted to BAM files using samtools version 0.1.19. Peaks were subsequently called using MACS-2.1.0. Enriched regions were identified compared to the input control using MACS2 callpeak--nomodel --exttsize 300 --gsize=hs -p 1e-9. The mapped reads were extended by 300bp and converted to TDF files with igvtools-2.3.36 and were visualized with IGV-2.7.2⁸⁷ for H3K27ac and H3K4me1 ChIP-seq. Differential binding analysis was performed using the R package DiffBind v1.8.5. In DiffBind read normalization was performed using the TMM technique using reads mapped to peaks which were background subtracted using the input control. Enhancer gene associations were determined as the nearest TSS to the center of the enhancer and super-enhancer locus. Super-enhancers were identified by employing the ROSE algorithm⁸⁸ using a stitching distance of the MACS2 called peaks of 12.5kb, peaks were excluded that were fully contained in the region spanning 1000bp upstream and downstream of an annotated TSS (-t 1000). The H3K27ac/H3K4me1 signal was corrected for background using the input control and subsequently ranked by increasing signal (Fig. S5A). Super-enhancer gene associations were determined as the nearest TSS to the center of the enhancer and super-enhancer locus using the ROSE algorithm. BEDtools v2.17.0 was used for general manipulation of peak bed-files. Motif enrichment analysis was performed using the HOMER software v4.11 (findMotifsGenome.pl; hg19/hg38; -size 200). ChIP-seq data for activated Treg cells, VDR and BATF were retrieved from GEO:GSE43119 (GSM1056948 and GSM1056952), GSE89431 (GSM2371449) and GSE32465 (GSM803538), respectively.

Vitamin D receptor and 1,25 vitamin D3 incubation assay

Thawed HC PBMC and JIA patient SFMC were stained by surface and intranuclear staining as described above with the following antibodies: anti-human fixable viability dye eF506 (1:1000), FOXP3 PerCP/Cy5.5 (clone PCH101, 1:50; eBioscience), CD3 AF700 (clone UCHT1, 1:50), CD4

BV785 (clone OKT4, 1:100; Biolegend), CD25 BV711 (clone 2A3, 1:50), CD127 BV605 (clone A019D5, 1:50; Sony Biotechnology), and VDR PE (clone D-6, 1:100; Santa Cruz Biotechnology). Additionally, CD4⁺ T cells were isolated from fresh PBMC using the CD4⁺ T cell isolation kit and LS column (Miltenyi Biotec). Sorted Treg cells (CD3⁺CD4⁺CD25⁺CD127^{low}, 50.000) were plated in a round bottom 96-wells plate in the presence of 10% human AB serum, anti-CD3/CD28 (Dynabeads Human T-activator CD3/CD28, Thermo Fisher Scientific) at a 1:5 ratio (1 bead to 5 cell ratio), 100 IU/ml (h)IL-2 (Proleukin; Novartis) for 2 days. In addition, 0 (control) or 10 nM 1 α ,25-Dihydroxyvitamin D3 (Sigma-Aldrich) was added. Expanded Treg cells were stained by surface and intranuclear staining as described above with the following antibodies: anti-human fixable viability dye eF506 (1:1000), FOXP3 eF450 (clone PCH101, 1:50; eBioscience), CD3 AF700 (clone UCHT1, 1:50), CD4 APC/Cy7 (clone RPA-T4, 1:100; Biolegend), CD25 BV711 (clone 2A3, 1:50), and CD30 FITC (clone Ber-H8, 1:12.5), and CTLA4 APC (clone BNI3, 1:12.5; BD). See Supplementary Figs. 1-2 for the gating strategy. Data acquisition and analysis as above. Furthermore, total RNA from expanded Treg cells was extracted using the PicoPure RNA Isolation Kit (Thermo Fisher Scientific) and RNA was reverse transcribed using the iScript cDNA Synthesis Kit (Bio-Rad). Quantitative RT-PCR was performed using SYBR Select Master Mix (Life Technologies) according to manufacturer's instructions and measured on a QuantStudio 12k Flex real-time PCR (Thermo Fisher Scientific). Fold change was calculated using the delta-delta Ct method ($2^{\Delta\Delta Ct}$) normalized to the housekeeping gene GUSB in Microsoft Excel 2016. The primers used are listed in Supplementary Table 1.

Microarray RA Treg cells

CD14⁺ monocytes (purity > 98%) were depleted through positive selection using CD14 MicroBeads (Miltenyi Biotec). CD4⁺ T cells were isolated from the CD14⁻ cell fraction by negative selection (Miltenyi Biotec) and stained with CD4 PerCP/Cy5.5 (clone SK3, 1:200), CD45RA APC/Cy7 (clone HI100, 1:50), CD45RO PB (clone UCHL1, 1:50), CD127 FITC (clone A019D5, 1:50; BioLegend), and CD25 PE (clone REA945, 1:50; Miltenyi Biotec). CD4⁺CD45RA⁻CD45RO⁺CD25⁺CD127^{low} cells (memory Treg cells, see Supplementary Fig. 1a for gating strategy), were sorted using a BD FACSAria II. Sorted Treg cell samples were lysed in 1000 μ l of TRIzol (Invitrogen). Chloroform (200 μ l) was added, and the samples were then whirl mixed and incubated for 2–3 minutes at room temperature. Following centrifugation (10,000g for 15 minutes at 4°C), the water phase was further purified using the ReliaPrepTM RNA Miniprep system (Promega) per manufacturer's instructions. RNA integrity was confirmed on an Agilent Technologies 2100 bioanalyzer. One hundred nanograms of total RNA was used to prepare the targets (Affymetrix) in accordance with the manufacturer's instructions. Hybridization cocktails were hybridized onto a Human Gene 2.0 ST Array. Chips were scanned and gene expression data were normalized using the RMA algorithm. Gene expression analysis was performed using Qlucore Omics Explorer software, version 3.0.

Statistics and reproducibility

For ChIP-seq and RNA-seq analysis, p -values were adjusted with the Benjamini-Hochberg procedure. Protein and cytokine expression was analyzed with Pearson's correlation, two-tailed Mann-Whitney U test, Two-way ANOVA with Sidak correction for multiple testing or a mixed-effects model with Dunnett post-hoc on paired data with missing values using GraphPad Prism. All experimental flow cytometry and sorting data concerns two or more independent experiments with similar results. RNA- and ChIP-sequencing runs were performed in one batch.

Data availability

RNA-seq and ChIP-seq data generated for this study have been deposited in the Gene Expression Omnibus (GEO) database under the accession codes: GSE161426 and GSE156418.

Code availability

The code used for RNA-seq analysis are available at https://github.com/mmokry/Mijnheer_Nat_Communications_2021⁸⁴.

Acknowledgements

We would like to thank J. van Velzen and P. Andriessen van der Burght for technical assistance, and Anoushka Samat for help with qPCR primer design. F. van Wijk is supported by a VIDI grant from ZonMw (91714332).

REFERENCES

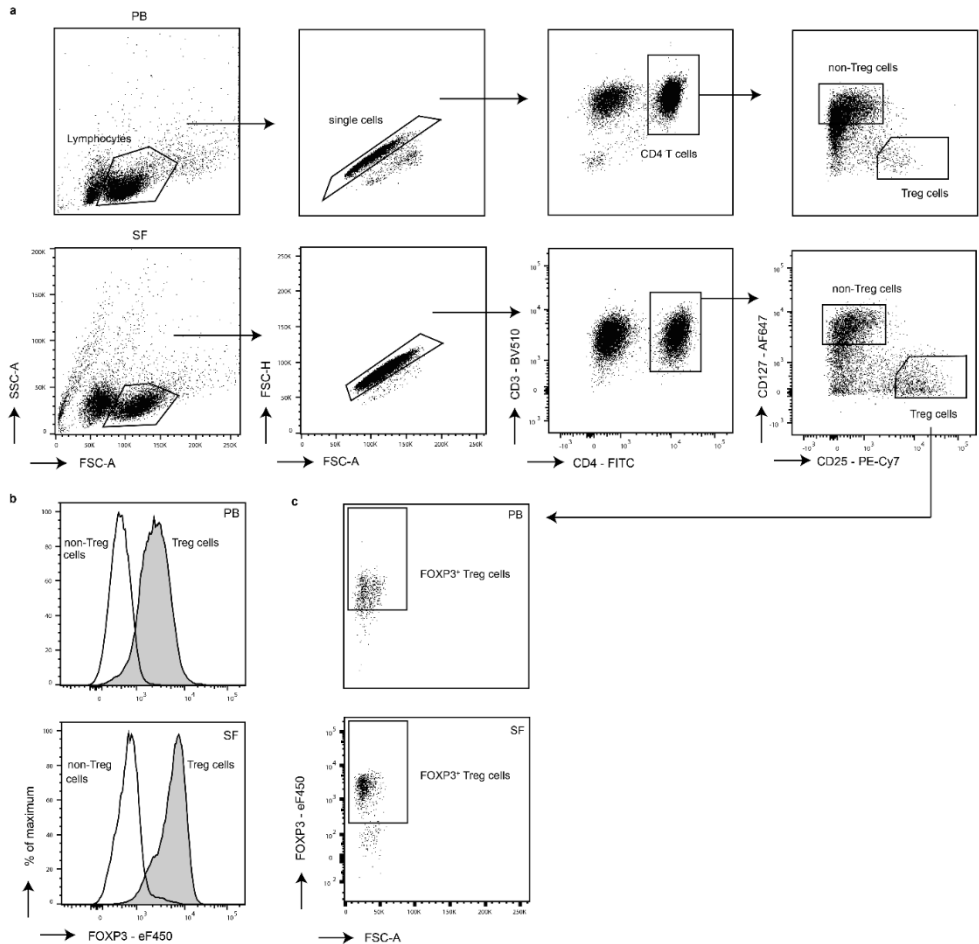
1. Brunkow, M. E. *et al.* Disruption of a new forkhead/winged-helix protein, scurfin, results in the fatal lymphoproliferative disorder of the scurfy mouse. *Nat. Genet.* **27**, 68–73 (2001).
2. Ochs, H. D. *et al.* The immune dysregulation, polyendocrinopathy, enteropathy, X-linked syndrome (IPEX) is caused by mutations of FOXP3. *Nat. Genet.* **27**, 20–21 (2001).
3. Cretney, E. *et al.* The transcription factors Blimp-1 and IRF4 jointly control the differentiation and function of effector regulatory T cells. *Nat Immunol* **12**, 304–311 (2011).
4. Miragaia, R. J. *et al.* Single-Cell Transcriptomics of Regulatory T Cells Reveals Trajectories of Tissue Adaptation. *Immunity* **50**, 493–504.e7 (2019).
5. Liston, A. & Gray, D. H. D. Homeostatic control of regulatory T cell diversity. *Nat. Rev. Immunol.* **14**, 154–165 (2014).
6. Vasanthakumar, A. *et al.* The transcriptional regulators IRF4, BATF and IL-33 orchestrate development and maintenance of adipose tissue-resident regulatory T cells. *Nat. Immunol.* **16**, 276–285 (2015).
7. Povoleri, G. A. M. *et al.* Human retinoic acid-regulated CD161 + regulatory T cells support wound repair in intestinal mucosa. *Nat. Immunol.* **19**, 1403–1414 (2018).
8. Kalekar, L. A. *et al.* Regulatory T cells in skin are uniquely poised to suppress profibrotic immune responses. *Sci. Immunol.* **4**, aaw2910 (2019).
9. Koch, M. A. *et al.* The transcription factor T-bet controls regulatory T cell homeostasis and function during type 1 inflammation. *Nat. Immunol.* **10**, 595–602 (2009).
10. Levine, A. G. *et al.* Stability and function of regulatory T cells expressing the transcription factor T-bet. *Nature* **546**, 421–425 (2017).
11. Miyara, M. *et al.* Functional Delineation and Differentiation Dynamics of Human CD4+ T Cells Expressing the FoxP3 Transcription Factor. *Immunity* **30**, 899–911 (2009).
12. Panduro, M., Benoist, C. & Mathis, D. Tissue Tregs. *Annu. Rev. Immunol.* **34**, 609–633 (2016).
13. De Simone, M. *et al.* Transcriptional Landscape of Human Tissue Lymphocytes Unveils Uniqueness of Tumor-Infiltrating T Regulatory Cells. *Immunity* **45**, 1135–1147 (2016).
14. Plitas, G. *et al.* Regulatory T Cells Exhibit Distinct Features in Human Breast Cancer. *Immunity* **45**, 1122–1134 (2016).
15. Magnuson, A. M. *et al.* Identification and validation of a tumor-infiltrating Treg transcriptional signature conserved across species and tumor types. *Proc. Natl. Acad. Sci. U. S. A.* **115**, E10672–E10681 (2018).
16. Van Amelsfort, J. M. R., Jacobs, K. M. G., Bijlsma, J. W. J., Lafeber, F. P. J. G. & Taams, L. S. CD4+CD25+ regulatory T cells in rheumatoid arthritis: Differences in the presence, phenotype, and function between peripheral blood and synovial fluid. *Arthritis Rheum.* **50**, 2775–2785 (2004).
17. Wehrens, E. J. *et al.* Functional human regulatory T cells fail to control autoimmune inflammation due to PKB/c-akt hyperactivation in effector cells. *Blood* **118**, 3538–3548 (2011).
18. Teh, P. P., Vasanthakumar, A. & Kallies, A. Development and Function of Effector Regulatory T Cells. in *Progress in Molecular Biology and Translational Science* (ed. Liston, A.) 155–174 (ScienceDirect, 2015). doi:10.1016/bs.pmbts.2015.08.005.
19. Joller, N. *et al.* Treg cells expressing the coinhibitory molecule TIGIT selectively inhibit proinflammatory Th1 and Th17 cell responses. *Immunity* **40**, 569–581 (2014).
20. Shalev, I. *et al.* Targeted deletion of fgl2 leads to impaired regulatory T cell activity and development of autoimmune glomerulonephritis. *J. Immunol.* **180**, 249–260 (2008).
21. Ye, L. *et al.* TCR usage, gene expression and function of two distinct FOXP3(+)Treg subsets within CD4(+)CD25(hi) T cells identified by expression of CD39 and CD45RO. *Immunol. Cell Biol.* **94**, 293–305 (2016).
22. Do, J.-S. *et al.* An IL-27/Lag3 axis enhances Foxp3+ regulatory T cell-suppressive function and therapeutic efficacy. *Mucosal Immunol.* **9**, 137–145 (2016).

23. Okubo, Y., Mera, T., Wang, L. & Faustman, D. L. Homogeneous expansion of human T-regulatory cells via tumor necrosis factor receptor 2. *Sci. Rep.* **3**, 3153 (2013).
24. Wang, R. *et al.* Expression of GARP selectively identifies activated human FOXP3+ regulatory T cells. *Proc. Natl. Acad. Sci. U. S. A.* **106**, 13439–44 (2009).
25. Bin Dhuban, K. *et al.* Coexpression of TIGIT and FCRL3 identifies Helios+ human memory regulatory T cells. *J. Immunol.* **194**, 3687–3696 (2015).
26. Fu, G. *et al.* Themis controls thymocyte selection through regulation of T cell antigen receptor-mediated signaling. *Nat. Immunol.* **10**, 848–856 (2009).
27. Ito, T. *et al.* Two Functional Subsets of FOXP3+ Regulatory T Cells in Human Thymus and Periphery. *Immunity* **28**, 870–880 (2008).
28. Müller, M., Herrath, J. & Malmström, V. IL-1R1 is expressed on both Helios(+) and Helios(-) FoxP3(+) CD4(+) T cells in the rheumatic joint. *Clin. Exp. Immunol.* **182**, 90–100 (2015).
29. Pan, F. *et al.* Eos mediates Foxp3-dependent gene silencing in CD4+ regulatory T cells. *Science* **325**, 1142–1146 (2009).
30. Bhairavabhotla, R. *et al.* Transcriptome profiling of human FoxP3(+) regulatory T cells. *Hum. Immunol.* **77**, 201–213 (2015).
31. Ferraro, A. *et al.* Interindividual variation in human T regulatory cells. *Proc. Natl. Acad. Sci. U. S. A.* **111**, E1111–1120 (2014).
32. Miyazaki, M. *et al.* Id2 and Id3 maintain the regulatory T cell pool to suppress inflammatory disease. *Nat. Immunol.* **15**, 767–776 (2014).
33. Mason, G. M. *et al.* Phenotypic Complexity of the Human Regulatory T Cell Compartment Revealed by Mass Cytometry. *J. Immunol.* **195**, 2030–2037 (2015).
34. Cheng, G. *et al.* IL-2 receptor signaling is essential for the development of Klrp1+ terminally differentiated T regulatory cells. *J. Immunol.* **189**, 1780–1791 (2012).
35. Levine, A. G., Arvey, A., Jin, W. & Rudensky, A. Y. Continuous requirement for the TCR in regulatory T cell function. *Nat. Immunol.* **15**, 1070–1078 (2014).
36. Chaudhry, A. *et al.* CD4+ regulatory T cells control TH17 responses in a Stat3-dependent manner. *Science* **326**, 986–991 (2009).
37. Zheng, Y. *et al.* Regulatory T-cell suppressor program co-opts transcription factor IRF4 to control T(H)2 responses. *Nature* **458**, 351–356 (2009).
38. Koch, M. A. *et al.* T-bet+ Treg Cells Undergo Abortive Th1 Cell Differentiation due to Impaired Expression of IL-12 Receptor β 2. *Immunity* **37**, 501–510 (2012).
39. Chinen, T. *et al.* An essential role for the IL-2 receptor in Treg cell function. *Nat. Immunol.* **17**, 1322–1333 (2016).
40. Heintzman, N. D. *et al.* Histone modifications at human enhancers reflect global cell-type-specific gene expression. *Nature* **459**, 108–112 (2009).
41. Creighton, M. P. *et al.* Histone H3K27ac separates active from poised enhancers and predicts developmental state. *Proc. Natl. Acad. Sci. U. S. A.* **107**, 21931–21936 (2010).
42. Hnisz, D. *et al.* XSuper-enhancers in the control of cell identity and disease. *Cell* **155**, 934–947 (2013).
43. Hu, Z. & Tee, W.-W. Enhancers and chromatin structures: regulatory hubs in gene expression and diseases. *Biosci. Rep.* **37**, BSR20160183 (2017).
44. Yang, B.-H. *et al.* TCF1 and LEF1 Control Treg Competitive Survival and Tfr Development to Prevent Autoimmune Diseases. *Cell Rep.* **27**, 3629–3645.e6 (2019).
45. DiSpirito, J. R. *et al.* Molecular diversification of regulatory T cells in nonlymphoid tissues. *Sci. Immunol.* **3**, (2018).
46. Koizumi, S. *et al.* JunB regulates homeostasis and suppressive functions of effector regulatory T cells. *Nat. Commun.* **9**, 5344 (2018).
47. Hayatsu, N. *et al.* Analyses of a Mutant Foxp3 Allele Reveal BATF as a Critical Transcription Factor in the Differentiation and Accumulation of Tissue Regulatory T Cells. *Immunity* **47**, 268–283.e9 (2017).

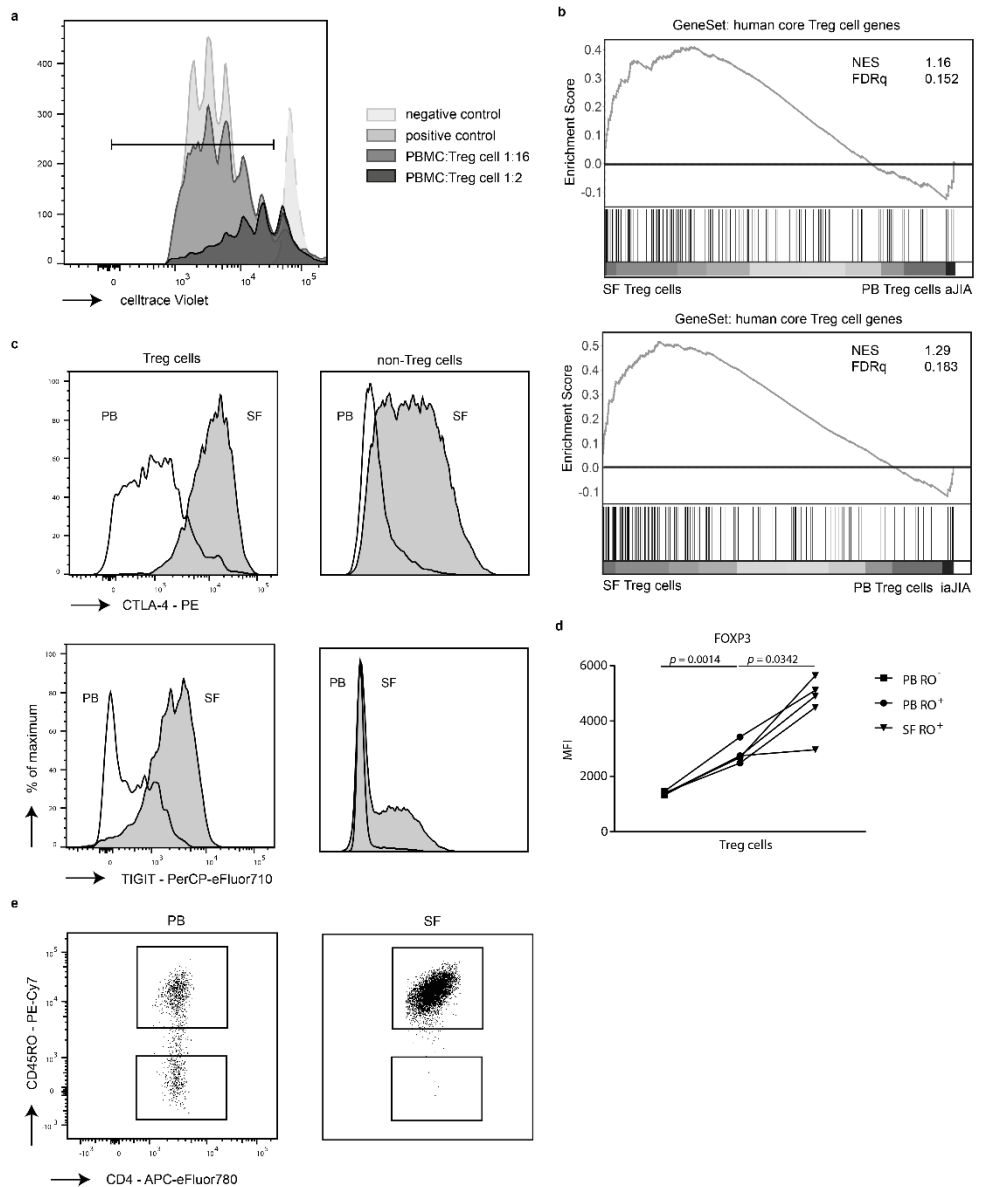
48. Vaeth, M. *et al.* Tissue resident and follicular Treg cell differentiation is regulated by CRAC channels. *Nat. Commun.* **10**, 1183 (2019).
49. Delacher, M. *et al.* Genome-wide DNA-methylation landscape defines specialization of regulatory T cells in tissues. *Nat. Immunol.* **18**, 1160–1172 (2017).
50. Sullivan, J. M., Höllbacher, B. & Campbell, D. J. Cutting Edge: Dynamic Expression of Id3 Defines the Stepwise Differentiation of Tissue-Resident Regulatory T Cells. *J. Immunol.* j11800917 (2018) doi:10.4049/jimmunol.1800917.
51. Alvisi, G. *et al.* IRF4 instructs effector Treg differentiation and immune suppression in human cancer. *J. Clin. Invest.* **130**, 3137–3150 (2020).
52. Roychoudhuri, R. *et al.* BACH2 represses effector programs to stabilize Treg-mediated immune homeostasis. *Nature* **498**, 506–510 (2013).
53. Dias, S. *et al.* Effector Regulatory T Cell Differentiation and Immune Homeostasis Depend on the Transcription Factor Myb. *Immunity* **46**, 78–91 (2017).
54. DiSpirito, J. R. *et al.* Molecular diversification of regulatory T cells in nonlymphoid tissues. *Sci. Immunol.* **3**, eaat5861 (2018).
55. Sula Karreci, E. *et al.* Human regulatory T cells undergo self-inflicted damage via granzyme pathways upon activation. *JCI insight* **2**, e91599 (2017).
56. Loyher, P.-L., Rodero, M. P., Combadière, C. & Boissonnas, A. Role of Chemokines and Chemokine Receptors in Cancer. in *Cancer Immunology: A Translational Medicine Context* (ed. Rezaei, N.) 235–262 (Springer International Publishing, 2020). doi:10.1007/978-3-030-30845-2_14.
57. Tessema, M. *et al.* Differential Epigenetic Regulation of TOX Subfamily High Mobility Group Box Genes in Lung and Breast Cancers. *PLoS One* **7**, e34850 (2012).
58. Mariotti, S. *et al.* MICAL2 is a novel human cancer gene controlling mesenchymal to epithelial transition involved in cancer growth and invasion. *Oncotarget* **7**, 1808–1825 (2016).
59. Elinav, E. *et al.* Inflammation-induced cancer: crosstalk between tumours, immune cells and microorganisms. *Nat. Rev. Cancer* **13**, 759–771 (2013).
60. Verbsky, J. W. & Chatila, T. A. Immune dysregulation, polyendocrinopathy, enteropathy, X-linked (IPEX) and IPEX-related disorders. *Curr. Opin. Pediatr.* **25**, 708–714 (2013).
61. Parackova, Z. *et al.* T regulatory lymphocytes in type 1 diabetes: Impaired CD25 expression and IL-2 induced STAT5 phosphorylation in pediatric patients. *Autoimmunity* **49**, 523–531 (2016).
62. Herrath, J. *et al.* The inflammatory milieu in the rheumatic joint reduces regulatory T-cell function. *Eur. J. Immunol.* **41**, 2279–2290 (2011).
63. Petrelli, A. *et al.* Self-Sustained Resistance to Suppression of CD8⁺ T_H1 Cells at the Site of Autoimmune Inflammation Can Be Reversed by Tumor Necrosis Factor and Interferon- γ Blockade. *Arthritis Rheumatol.* **68**, 229–236 (2016).
64. Singh, R. *et al.* Egr2 and 3 Inhibit T-bet-Mediated IFN- γ Production in T Cells. *J. Immunol.* **198**, 4394–4402 (2017).
65. Takahashi, R., Nakatsukasa, H., Shiozawa, S. & Yoshimura, A. SOCS1 Is a Key Molecule That Prevents Regulatory T Cell Plasticity under Inflammatory Conditions. *J. Immunol.* **199**, 149–158 (2017).
66. Wong, L., Jiang, K., Chen, Y. & Jarvis, J. N. Genetic insights into juvenile idiopathic arthritis derived from deep whole genome sequencing. *Sci. Rep.* **7**, 2657 (2017).
67. Arvey, A. *et al.* Genetic and epigenetic variation in the lineage specification of regulatory T cells. *Elife* **4**, e07571 (2015).
68. Gao, P. *et al.* Risk variants disrupting enhancers of TH1 and TREG cells in type 1 diabetes. *Proc. Natl. Acad. Sci.* **116**, 7581–7590 (2019).
69. Beyer, M. *et al.* Repression of the genome organizer SATB1 in regulatory T cells is required for suppressive function and inhibition of effector differentiation. *Nat. Immunol.* **12**, 898–907 (2011).
70. Vahedi, G. *et al.* Super-enhancers delineate disease-associated regulatory nodes in T cells. *Nature* **520**, 558–562 (2015).

71. Kitagawa, Y. *et al.* Guidance of regulatory T cell development by Satb1-dependent super-enhancer establishment. *Nat. Immunol.* **18**, 173–183 (2017).
72. Afzali, B. *et al.* BACH2 immunodeficiency illustrates an association between super-enhancers and haploinsufficiency. *Nat. Immunol.* **18**, 813–823 (2017).
73. Xing, S. *et al.* Tcf1 and Lef1 are required for the immunosuppressive function of regulatory T cells. *J. Exp. Med.* **216**, 847–866 (2019).
74. Wienke, J. *et al.* Human regulatory T cells at the maternal-fetal interface show functional site-specific adaptation with tumor-infiltrating-like features [preprint]. *bioRxiv* 820753 (2019) doi:10.1101/820753.
75. Bscheider, M. & Butcher, E. C. Vitamin D immunoregulation through dendritic cells. *Immunology* **148**, 227–236 (2016).
76. Dankers, W. *et al.* Human Memory Th17 Cell Populations Change Into Anti-inflammatory Cells With Regulatory Capacity Upon Exposure to Active Vitamin D. *Front. Immunol.* **10**, 1504 (2019).
77. Meinicke, H. *et al.* KLRG1 impairs regulatory T-cell competitive fitness in the gut. *Immunology* **152**, 65–73 (2017).
78. Procaccini, C. *et al.* The Proteomic Landscape of Human Ex Vivo Regulatory and Conventional T Cells Reveals Specific Metabolic Requirements. *Immunity* **44**, 406–421 (2016).
79. Vukmanovic-Stejic, M. *et al.* Human CD4⁺ CD25^{hi} Foxp3⁺ regulatory T cells are derived by rapid turnover of memory populations in vivo. *J. Clin. Invest.* **116**, 2423–2433 (2006).
80. Sun, I.-H. *et al.* mTOR Complex 1 Signaling Regulates the Generation and Function of Central and Effector Foxp3⁺ Regulatory T Cells. *J. Immunol.* **201**, 481–492 (2018).
81. Kishore, M. *et al.* Regulatory T Cell Migration Is Dependent on Glucokinase-Mediated Glycolysis. *Immunity* **47**, 875–889.e10 (2017).
82. Ferreira, L. M. R., Muller, Y. D., Bluestone, J. A. & Tang, Q. Next-generation regulatory T cell therapy. *Nat. Rev. Drug Discov.* **18**, 749–769 (2019).
83. Petty, R. E. *et al.* Revision of the proposed classification criteria for juvenile idiopathic arthritis: Durban, 1997. *J. Rheumatol.* **25**, 1991–1994 (1998).
84. Mokry, M. Conserved human effector Treg cell transcriptomic and epigenetic signature in inflammation. *Mijnheer_Nat_Communications_2021* (2021) doi:DOI: 10.5281/zenodo.4615296.
85. Subramanian, A. *et al.* Gene set enrichment analysis: a knowledge-based approach for interpreting genome-wide expression profiles. *Proc. Natl. Acad. Sci. U. S. A.* **102**, 15545–15550 (2005).
86. Tao, W., Radstake, T. R. D. J. & Pandit, A. RegEnrich: An R package for gene regulator enrichment analysis reveals key role of ETS transcription factor family in interferon signaling. *bioRxiv* 2021.01.24.428029 (2021) doi:10.1101/2021.01.24.428029.
87. Robinson, J. T. *et al.* Integrative genomics viewer. *Nature biotechnology* vol. 29 24–26 (2011).
88. Whyte, W. A. *et al.* Master transcription factors and mediator establish super-enhancers at key cell identity genes. *Cell* **153**, 307–319 (2013).
89. Zheng, C. *et al.* Landscape of Infiltrating T Cells in Liver Cancer Revealed by Single-Cell Sequencing. *Cell* **169**, 1342–1356.e16 (2017).
90. Vishwakarma, A. *et al.* Mapping the Immune Landscape of Clear Cell Renal Cell Carcinoma by Single-Cell RNA-seq [preprint]. *bioRxiv* 824482 (2019) doi:10.1101/824482.

SUPPLEMENTARY INFORMATION

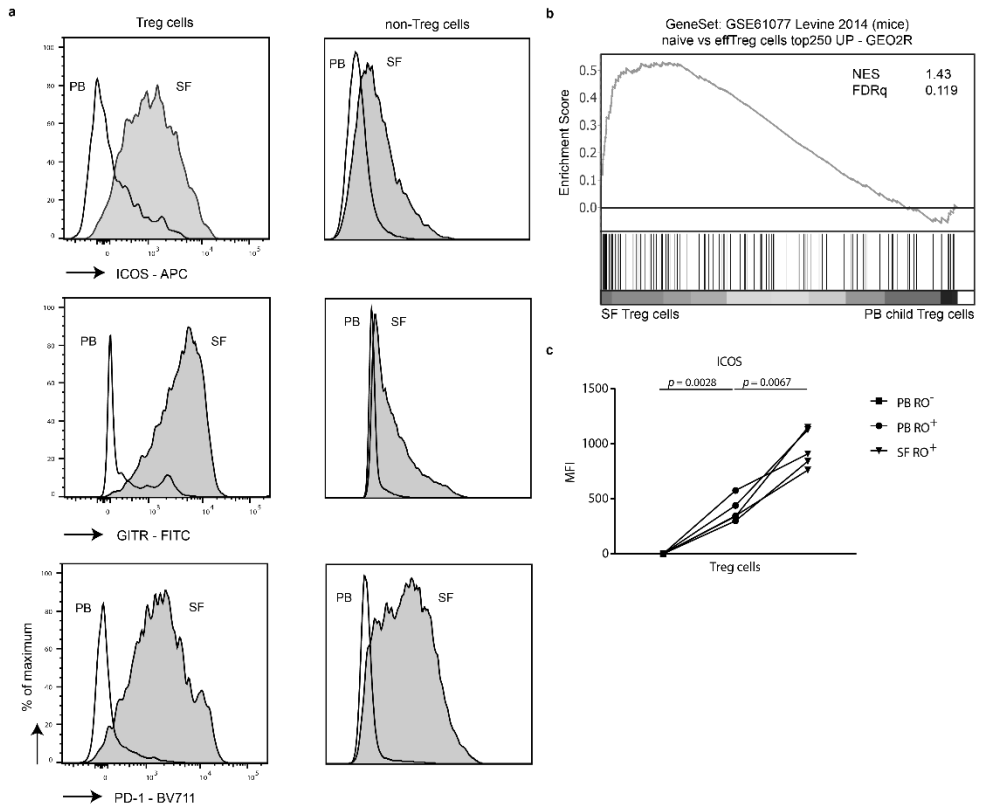


Supplementary Figure 1. Gating strategy and FOXP3 expression of sorted cells. **a** Representative gating strategy to sort and FACS both peripheral blood (PB)- and synovial fluid (SF)-derived Treg cells and non-Treg cells. **b** FOXP3 Median Fluorescence Intensity (MFI) plots of sorted SF- and PB-derived Treg cells and non-Treg cells. **c** Representative gating strategy of FOXP3 within Treg cells, gating as per **a**, in PB and SF. All panels are representative of two or more independent experiments.



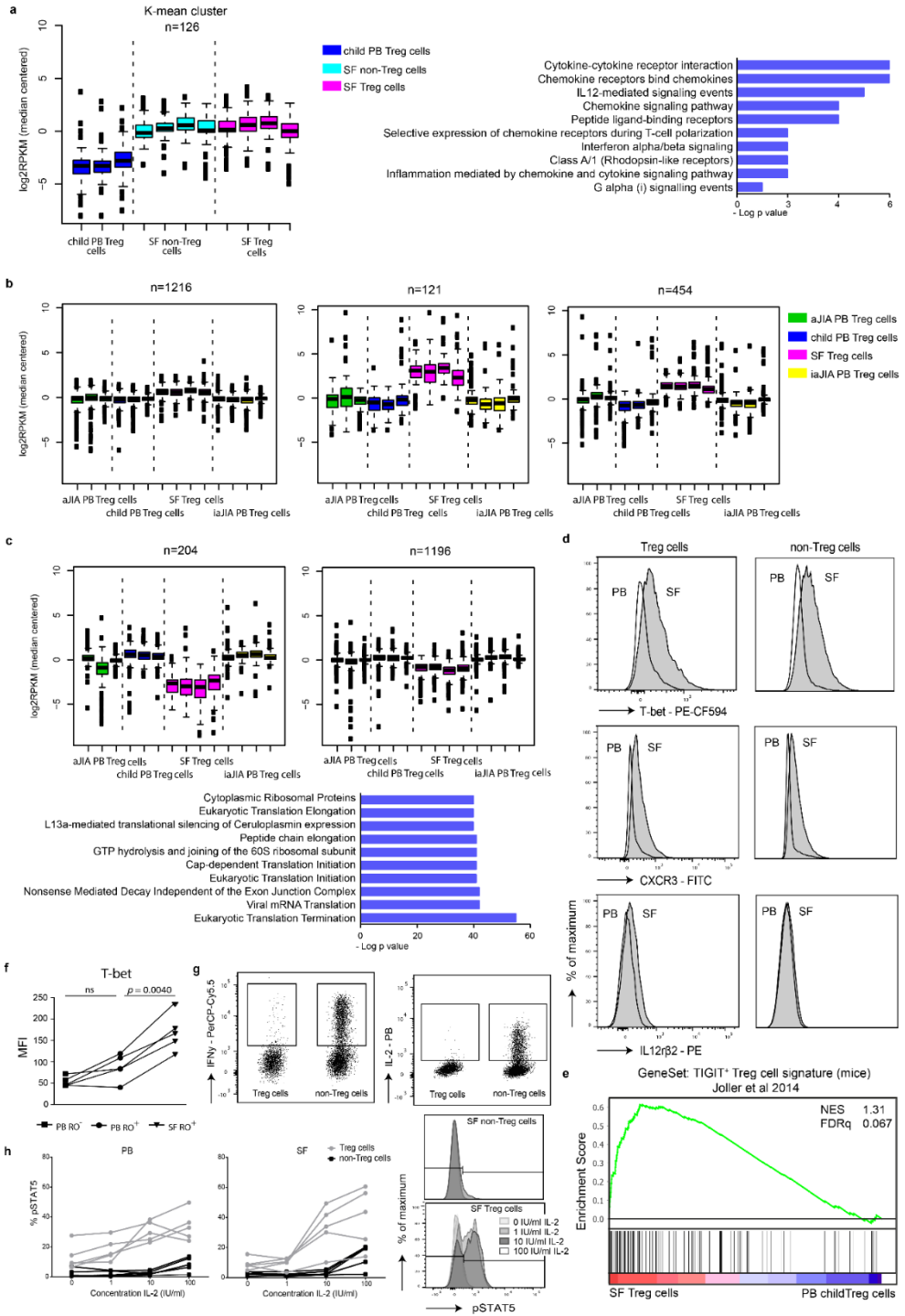
Supplementary Figure 2. GSEA and protein expression shows the Treg cell signature enriched in SF Treg cells. **a** Overview of the gating of proliferating peripheral blood mononuclear cells (PBMC), suppression assay as per Fig. 1b, without stimulation (negative control, dashed line), with stimulation (positive control, light gray fill), with 1:16 PBMC:Treg cells (dark gray fill) and with 1:2 PBMC:Treg cells (black fill). The bar shows the cells counted as proliferating. **b** GeneSet Enrichment Analysis (GSEA) of human core Treg cell signature genes (identified by Ferraro et al.⁷²) in pairwise comparison of synovial fluid (SF) and peripheral blood (PB) Treg cells derived from juvenile idiopathic arthritis (JIA) patients with active (left) or inactive (right) disease, represented by the normalized enrichment score (NES) and False Discovery Rate statistical value (FDRq, multiple hypothesis testing using sample permutation). **c** Representative MFI plots (for Fig. 1e) for both CTLA4 (top) and TIGIT (bottom) in Treg cells (left) and non-Treg cells (right) derived from paired SFMC (gray fill) and PBMC (no fill) of

JIA patients. **d** Comparison of the MFI of FOXP3 within PB CD45RO⁻ (PB RO⁻, square, healthy adults), PB CD45RO⁺ (PB RO⁺, circle, patients with active JIA), and SF CD45RO⁺ (SF RO⁺, triangle, patients with active JIA) ($n=5$ per subset). Statistical comparisons were performed using one-way ANOVA with Tukey correction for multiple testing. **e** Representative gating strategy of CD45RO⁺ and CD45RO⁻ Treg cells in PB and SF for **d**. **d**, **e** Data are representative of two independent experiments. **a**, **c** The graphs are representative for two independent experiments with $n = 4$ and $n = 5$ total, respectively. Source data are provided as a Source Data file.

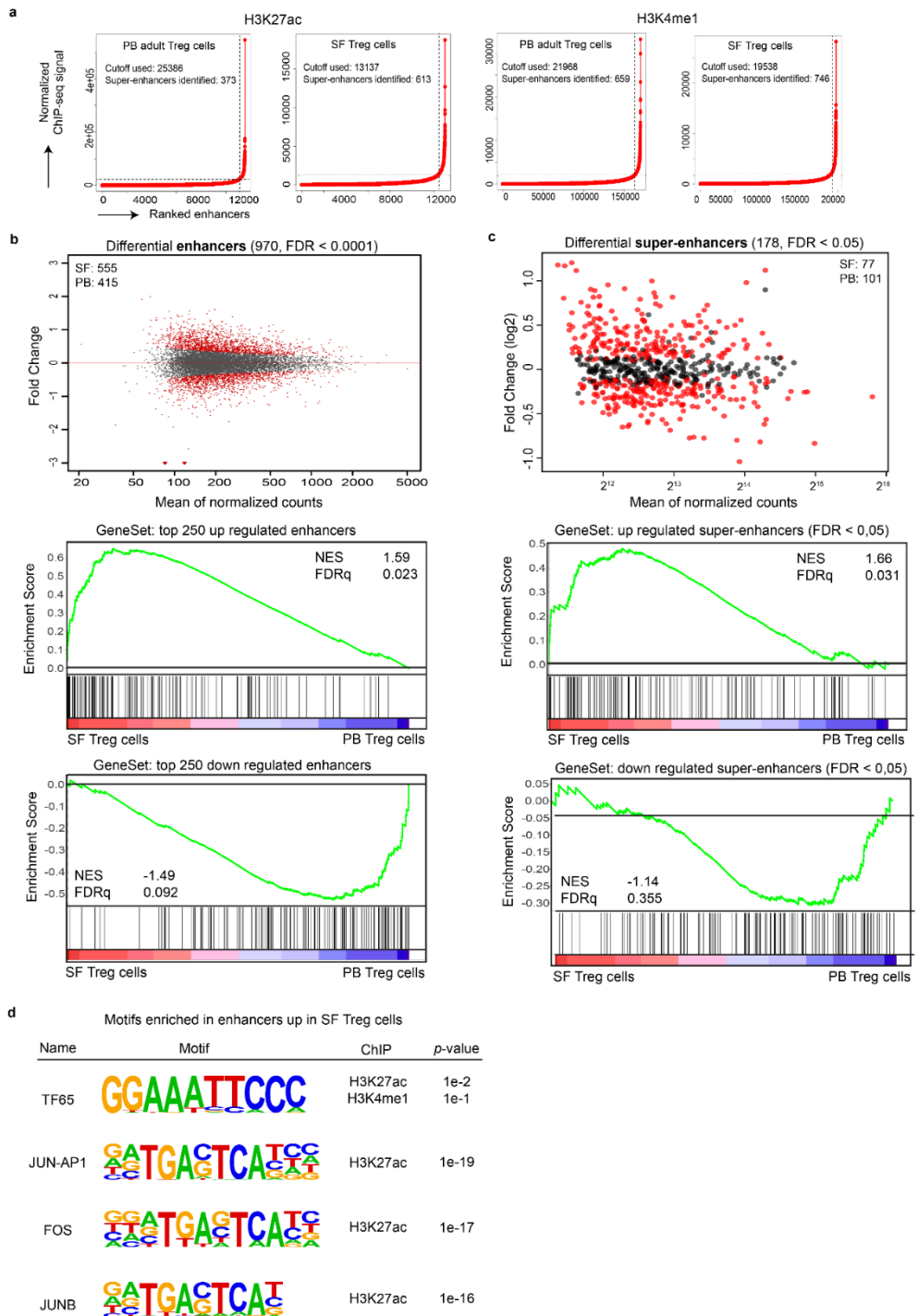


Supplementary Figure 3. GSEA and protein expression show an effector Treg cell signature in SF Treg cells.

a Representative Median Fluorescence Intensity (MFI) plots (for Fig. 2c) of ICOS (top), GITR (middle) and PD-1 (bottom) in paired synovial fluid (SF)- and peripheral blood (PB)-derived Treg cells (top) and non-Treg cells (bottom) from juvenile idiopathic arthritis (JIA) patients. SF: grey fill, PB: no fill. The graphs are representative for two independent experiments with $n = 5$ total. **b** Gene set enrichment analysis (GSEA) of effector eTreg cell genes (as identified with GEO2R as the top250 genes upregulated in naive versus eTreg cells, published in Levine et al.²¹) in pairwise comparison of SF ($n=4$) and healthy child PB ($n=3$) Treg cells, represented by the normalized enrichment score (NES) and FDR statistical value (FDRq, multiple hypothesis testing using sample permutation). **c** Comparison of the MFI of ICOS within PB CD45RO⁻ (PB RO⁻, square, healthy adults), PB CD45RO⁺ (PB RO⁺, circle, patients with active JIA), and SF CD45RO⁺ (SF RO⁺, triangle, patients with active JIA) ($n = 5$ per subset). See Supplementary Figure 2d for the gating strategy of CD45RO^{+/+} Treg cells. Statistical comparisons were performed using one-way ANOVA with Tukey correction for multiple testing. Source data are provided as a Source Data file.

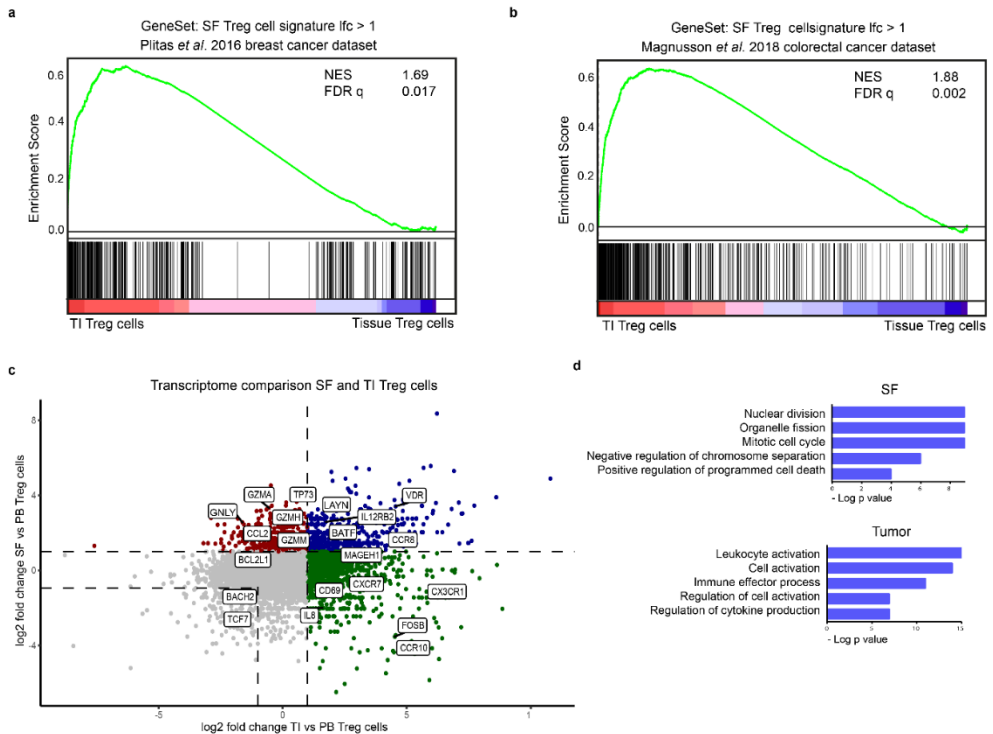


< Supplementary Figure 4. K-mean and GeneSet Enrichment analysis shows adaptation of SF Treg cells to Th1 environment. **a** K-mean analysis ($k = 14$) on peripheral blood (PB) Treg cells, synovial fluid (SF) Treg cells and SF non-Treg cells (paired, $n = 4$) with the cluster representing the genes upregulated in both SF Treg cells and non-Treg cells (n is the number of genes in the respective K-mean cluster; left) and the gene ontology pathway terms related to this cluster (right; top 10 ranked on p -value). Median + IQR with outliers are shown. **b** K-mean analysis ($k = 14$) on all Treg cell groups derived from children (PB Treg cells from healthy children ($n = 3$), juvenile idiopathic arthritis (JIA) patients with active ($n = 3$) or inactive ($n = 4$) disease and SF Treg cells from JIA patients ($n = 4$)) with the K-mean clusters shown representing upregulated genes in SF Treg cells compared to the rest (left). Median + IQR with outliers are shown. **c** Similar as in **b** but concerning downregulated genes in SF Treg cells (top) and gene ontology pathway terms (bottom; top 10 ranked on p -value). **d** Representative MFI plots (for Fig. 3d) of T-bet (top), CXCR3 (middle) and IL12r β 2 (bottom) in Treg cells (left) and non-Treg cells (right), derived from paired SFMC (grey fill) and PBMC of JIA patients. The graphs are representative for two independent experiments with $n = 5$ total. **e** Gene set enrichment analysis (GSEA) of TIGIT⁺ Treg cells signature genes (identified in mice by Joller et al.²⁰) in pairwise comparisons involving SF and healthy child PB Treg cells, represented by the normalized enrichment score (NES) and FDR statistical value (FDRq, multiple hypothesis testing using sample permutation). **f** Comparison of the MFI of T-bet within PB CD45RO⁻ (PB RO⁻, square, healthy adults), PB CD45RO⁺ (PB RO⁺, circle, patients with active JIA), and SF CD45RO⁺ (SF RO⁺, triangle, patients with active JIA) ($n = 5$ per subset). Statistical comparisons were performed using one-way ANOVA with Tukey correction for multiple testing. **g** Representative dotplots (for Fig. 3f) of IFN γ (left) and IL-2 (right) in SF Treg cells and non-Treg cells. The graphs are representative for two independent experiments. **h** Percentage and gating strategy (example of SF) of pSTAT5⁺ cells in PB- and SF-derived Treg cells and non-Treg cells in presence of increasing IL-2 concentrations ($n = 5$). Data are representative of two independent experiments. Source data are provided as a Source Data file and deposited under GSE161426.



Supplementary Figure 5. Environment-specific effector Treg cells profile is regulated by the (super)enhancer landscape. **a** Representative examples of the normalized distribution of H3K27ac (left two

panels) and H3K4me1 (right two panels) CHIP-seq. The plots show the enhancers ordered on the respective histone marker signal performed with the ROSE algorithm; a line with a slope of one tangent to the curve is used as a cutoff to distinguish super-enhancers above and typical enhancers below the point of tangency. **b** MA plots of differentially expressed enhancers derived from H3K4me1 CHIP-seq ($FDR < 0.0001$) in synovial fluid (SF) versus peripheral blood (PB) Treg cells with the number of SF- and PB-specific enhancers indicated (top). Gene set enrichment analysis (GSEA) of the top 250 upregulated (middle) and downregulated (bottom) enhancers in pairwise comparisons involving transcriptome data of SF Treg cells and PB Treg cells derived from healthy adults, represented by the normalized enrichment score (NES) and the FDR statistical value (FDRq, multiple hypothesis testing using sample permutation). **c** Same as in **a** but for super-enhancers ($FDR < 0.05$). **d** Motifs, known and de novo, for transcription factor binding sites predicted using HOMER, enriched in the upregulated (super-)enhancers in SF Treg cells compared to healthy adult PB Treg cells for H3K27ac and H3K4me1 CHIP-seq. *p*-values: cumulative binomial distribution to calculate enrichment in target versus background sequences. Source data are deposited under GSE156426.



Supplementary Figure 6. The effector Treg cells program is universal and overlaps with the human tumor Treg cells signature. **a** GeneSet Enrichment Analysis (GSEA) of the differentially expressed genes (\log_2 fold change (lfc) > 1, FDR < 0.05) in synovial fluid (SF) compared to peripheral blood (PB) Treg cells in pairwise comparisons involving tumor-infiltrating (TI) Treg cells and normal tissue Treg cells derived from breast cancer tissue (Plitas *et al.*¹⁶), represented by the normalized enrichment score (NES) and FDR statistical value (FDRq, multiple hypothesis testing using sample permutation). **b** Same as in **a** but concerning colorectal cancer (Magnusson *et al.*¹⁷). **c** Comparison of transcriptomes between SF and PB Treg cells to TI and normal tissue Treg cells. The \log_2 fold change of SF to PB Treg cells (y-axis) versus TI to PB Treg cells (x-axis; derived from Plitas *et al.*¹⁶) is shown. Each dot represents a gene present in both datasets; in grey unchanged/downregulated in both effector Treg cells subsets compared to PB Treg cells, in blue upregulated in both SF and TI Treg cells, in red upregulated in SF Treg cells and in green upregulated in TI Treg cells; selected genes are highlighted. **d** Gene ontology biological process terms related to genes specifically upregulated in SF (left) or TI (right) Treg cells from Plitas *et al.*¹⁶ compared to PB Treg cells in the respective datasets (healthy adults), ranked by enrichment scores. For all panels: SF Treg cells $n=4$, PB Treg cells $n=4$; Plitas TI Treg cells $n=3$, normal breast tissue Treg cells $n=7$; Magnusson TI Treg cells $n=11$ and normal colon tissue Treg cells $n=7$. Source data are deposited under GSE161426.

Supplementary Table 1. qPCR primer sequences.

Targets	
hGUSB_FW	CACCAGGGACCATCCAATACC
hGUSB_RV	GCAGTCCAGCGTAGTTGAAAAA
hCTLA4_FW	GGGGAATGAGTTGACCTTCCT
hCTLA4_RV	GGCACGGTTCTGGATCAATTA
hIL2RA_FW	CAATGCACAAGCTCTGCCACTC
hIL2RA_RV	ATCTGCCCCACCACGAAATGA
hTNFRSF8_FW	TTCTGGATGCAGGGCCAGT
hTNFRSF8_RV	CAGCTGCGTTGAGCTCCT
hFOXP3_FW	TCAAGCACTGCCAGGCG
hFOXP3_RV	CAGGAGCCCTTGTCGGAT
hIL10_FW	GAGGCTACGGCGCTGTCAT
hIL10_RV	CCACGGCCTTGCTCTTGTT
hIRF4_FW	AAGCCGGACCCTCCCACCTG
hIRF4_RV	TTGTGAACCTGCTGGGCTGGGA
hVDR_FW	TTCCGCTTCAGGATCATCTC
hVDR_RV	ACATCGGCATGATGAAGGA
hTBX21_FW	GGGAAACTAAAGCTCACAAC
hTBX21_RV	CCCCAAGGAATTGACAGTTG

Extended Supplementary Data can be found at: <https://github.com/lutterl/PhD-thesis-supplementary-data>.

Chapter 3

Human regulatory T cells locally differentiate and are functionally heterogeneous within the inflamed arthritic joint

Lisanne Lutter^{1,2}, M. Marlot van der Wal¹, Eelco C. Brand^{1,2}, Patrick Maschmeyer^{3,4}, Sebastiaan Vastert¹, Mir-Farzin Mashreghi^{3,5}, Jorg van Loosdregt¹, Femke van Wijk¹

¹Center for Translational Immunology, Wilhelmina Children's Hospital, University Medical Centre Utrecht, Utrecht University, Utrecht 3508 AB, the Netherlands.

²Department of Gastroenterology and Hepatology, University Medical Centre Utrecht, Utrecht University, Utrecht 3508 AB, the Netherlands.

³Therapeutic Gene Regulation, Deutsches Rheuma-Forschungszentrum (DRFZ), an Institute of the Leibniz Association, 10117 Berlin, Germany

⁴Present affiliation: Berlin Institute of Health at Charité – Universitätsmedizin Berlin, Charitéplatz 1, 10117 Berlin, Germany and Max-Delbrück-Center for Molecular Medicine in the Helmholtz Association (MDC), Berlin Institute for Medical Systems Biology (BIMSB), 10115 Berlin, Germany

⁵Berlin Institute of Health at Charité – Universitätsmedizin Berlin, BIH Center for Regenerative Therapies (BCRT), Charitéplatz 1, 10117 Berlin, Germany.

Clinical & Translational Immunology, 2022;11:e1420.

ABSTRACT

Objective: Tregs are crucial for immune regulation, and environment-driven adaptation of effector (e)Tregs is essential for local functioning. However, the extent of human Treg heterogeneity in inflammatory settings is unclear.

Methods: We combined single-cell RNA- and TCR-sequencing on Tregs derived from 3-6 patients with juvenile idiopathic arthritis (JIA) to investigate the functional heterogeneity of human synovial fluid (SF)-derived Tregs from inflamed joints. Confirmation and suppressive function of the identified Treg clusters was assessed by flow cytometry.

Results: Four Treg clusters were identified; incoming, activated eTregs with either a dominant suppressive or cytotoxic profile, and GPR56⁺CD161⁺CXCL13⁺ Tregs. Pseudotime analysis showed differentiation towards either classical eTreg profiles or GPR56⁺CD161⁺CXCL13⁺ Tregs supported by TCR data. Despite its most differentiated phenotype GPR56⁺CD161⁺CXCL13⁺ Tregs were shown to be suppressive. Furthermore, BATF was identified as an overarching eTreg regulator, with the novel Treg-associated regulon BHLHE40 driving differentiation towards GPR56⁺CD161⁺CXCL13⁺ Tregs, and JAZF1 towards classical eTregs.

Conclusion: Our study reveals a heterogeneous population of Tregs at the site of inflammation in JIA. SF Treg differentiate to a classical eTreg profile with a more dominant suppressive or cytotoxic profile that share a similar TCR repertoire, or towards GPR56⁺CD161⁺CXCL13⁺ Tregs with a more distinct TCR repertoire. Genes characterizing GPR56⁺CD161⁺CXCL13⁺ Tregs were also mirrored in other T cell subsets in both the tumor and autoimmune setting. Finally, the identified key regulators driving SF Treg adaptation may be interesting targets for autoimmunity or tumor interventions.

INTRODUCTION

Regulatory T cells (Tregs) comprise a subset of CD4⁺ T cells crucial in preserving immune homeostasis by antagonizing immune responses. The transcription factor (TF) FOXP3 characterizes Tregs, and mutations in the *FOXP3* gene lead to severe inflammation in both mice and humans^{1,2}. In recent years, potential therapeutic strategies targeting Tregs in both the autoimmune and tumor setting have been explored. In autoimmunity the number and/or functionality of Tregs should be enforced, whereas in the tumor milieu the suppressive capacity of Tregs should be dampened^{3,4}. This can, amongst others, be achieved by expanding Tregs, or by blocking Treg functioning via immune checkpoint blockade. PD-1 and CTLA-4 blockade are employed in the cancer setting and several other targets are currently tested in clinical trials⁴. Understanding the heterogeneity and plasticity of Tregs is essential in understanding immunodynamics at play in health and disease. This knowledge can then be exploited to develop and improve (potential) Treg-based therapeutic strategies.

Tregs are not identical in every tissue of residence, but are tailored to the environment in which they have to function, and can alter their phenotype according to micro-environmental changes over time^{5,6}. This plasticity enables continuous adaptation to changing immunodynamics. Upon activation, Tregs gain an effector profile (eTreg) and can initiate transcriptional programs associated with the dominant T helper (Th) response at the site of inflammation to enable Treg survival and suppression of the respective Th cells^{5,7,8}. These co-transcriptional programs include Th1 (T-bet), Th2 (GATA-3), Th17 (RORc), and T follicular regulatory cell (Tfr, Bcl6) programs⁹. We have recently demonstrated that in synovial fluid (SF) of patients with juvenile idiopathic arthritis (JIA), a predominantly Th1/Th17-associated disease¹⁰, Tregs retain a functional Treg core profile and obtain a Th1-skewed co-transcriptional profile on the proteomic, transcriptomic and epigenetic level⁷. Furthermore, it has been shown that some Tregs can acquire additional functions including stimulation of tissue repair in the intestine¹¹ and hair follicle growth in the skin¹². These additional functions further elucidate the local function and relevance of Tregs. An outstanding knowledge gap regarding human Tregs is the degree of heterogeneity of Tregs present within inflammation, if heterogeneity has consequences for Treg function, and how this relates to clonality and thus the T cell receptor (TCR)-repertoire of Tregs.

Tregs in tissues and peripheral blood (PB) have been shown to be heterogeneous^{5,7,8}, but data on local inflammatory environments in humans are lacking. Single cell (sc)RNA-sequencing enables us to map cellular states within an environment to facilitate our understanding of the phenotypic plasticity and functional diversity within the Treg population. SF-derived Tregs from JIA patients provide us with a relevant model of local autoimmune inflammation to determine the functional differentiation and clonality of inflammation-derived Tregs and its regulators. In this study we aimed to dissect the heterogeneity of SF-derived Tregs by employing scRNA-sequencing to further elucidate the immunodynamics at play in an inflammatory environment.

RESULTS

Heterogeneity within inflammatory synovial fluid Tregs

To assess the heterogeneity at the site of inflammation in JIA patients, SF Tregs (live CD3⁺CD4⁺CD127^{low}CD25^{high}) from three patients with oligoarticular JIA were sorted for single cell transcriptome analysis. Dimensionality reduction of 980 Tregs after quality control revealed presence of four clusters within the Treg population (Figure 1a), with each cluster present in all three patients (Figure 1b). All clusters were of Treg origin with the vast majority of cells (97%) expressing at least one FOXP3 mRNA molecule and in 99.96% of the Tregs the human core Treg signature as defined by Ferraro *et al.*¹³ was enriched (Supplementary figure 2b). There was no cluster-specific association with the cell cycle phase the Tregs resided in (Supplementary figure 2c; Pearson's Chi-squared test, *P*-value = 0.8512).

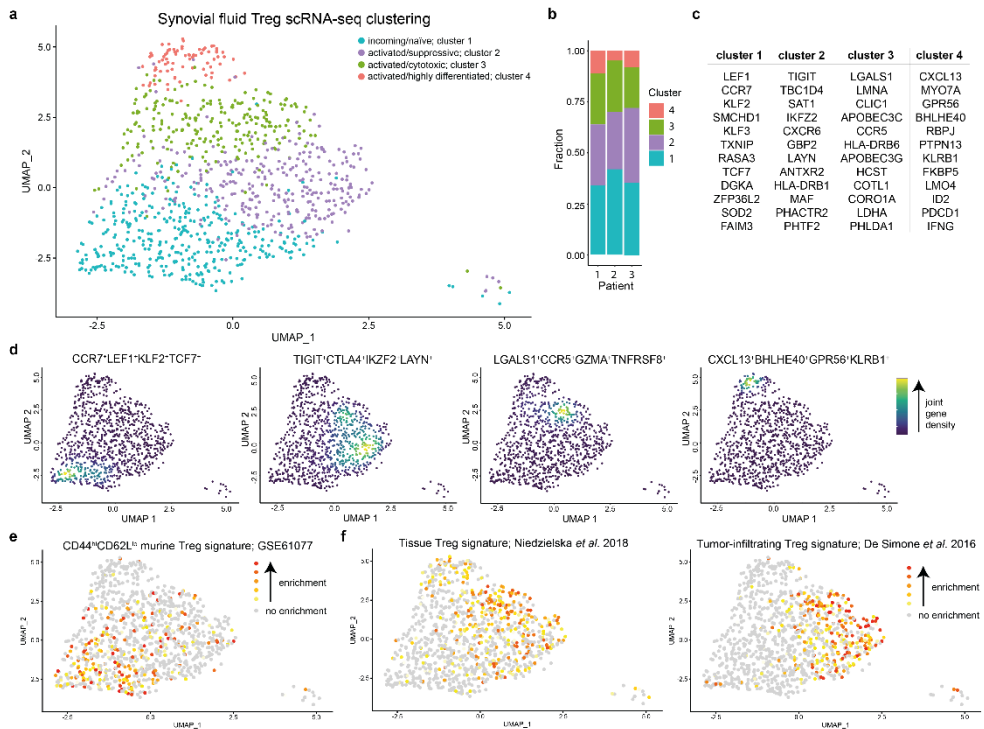


Figure 1. Heterogeneity and phenotypic profile of synovial fluid Tregs. **(a)** Dimensionality reduction (UMAP) of all synovial fluid (SF)-derived Tregs (sorted on live CD3⁺CD4⁺CD127^{low}CD25^{high}) of three Juvenile Idiopathic Arthritis (JIA) patients. Tregs are colored based on the assigned cluster. **(b)** Reproducible composition of the Tregs across the three included patients. Y-axis: fraction of cells colored based on the cluster as shown in **(a)** and separated per patient on the x-axis. **(c)** Top 12 upregulated genes, based on *P*-adjusted value, per cluster based on MAST differential gene expression analysis. **(d)** UMAPs of the combined expression of 2-4 selected differentially expressed genes per cluster shown in nebula density (kernel density estimation to handle sparsity of scRNA-sequencing data). The scale ranges from blue to yellow, with in yellow the highest kernel density, thus the highest (estimated) expression of all combined selected genes. **(e)** Gene set analysis of a gene module downregulated in naive versus memory CD4 T cells (GSE61077). Enrichment of a gene set is calculated

per cell; grey signifies no enrichment of the gene set and yellow to red represents increasing enrichment. **(f)** Similar to **(e)**, but for a human shared tissue Treg signature⁵⁶ and a human tumor-infiltrating Treg signature⁵⁷.

The largest cluster (37.24%), cluster 1, was characterized by genes that are downregulated upon activation and maturation of T cells. These genes included *CCR7*, *LEF1*, *KLF2*, *KLF3* and *TCF7*, suggesting a relatively quiescent/resting phenotype and probably representing Tregs that only recently migrated into the inflamed joint. The other three Treg clusters all displayed an activated gene signature including expression of many MHC class II genes (e.g. *HLA-DR*, *-DQ*, *-DP*, *-DM*), but also *DUSP4*, *CTSC*, *CTSB*, *ITM2A* and *LMNA* amongst others. Additional markers separated these clusters from each other. Both cluster 2 (31.22%; *TIGIT*, *CTLA4*, *IKZF2*, *LAYN*) and 3 (23.57%; *LGALS1*, *CXCR6*, *CCR5*, *TNFRSF8*, *GZMA*) showed high expression of genes associated with highly suppressive Tregs. The smallest activated Treg cluster, cluster 4 (7.96%), expressed a set of genes not commonly or previously associated with Tregs including *CXCL13*, *GPR56*, *MYO7A*, *BHLHE40*, *PTPN13*, and *KLRB1* (Figure 1c, d, Supplementary figure 2d, 3, Supplementary table 1). Overall, the three activated Treg clusters showed expression of a wide array of co-stimulatory and co-inhibitory markers to help suppress immune activation in a mostly contact-dependent manner but with a per cluster different potential dominant mode of suppression: e.g. *CTLA4* in cluster 2, *GZMA* in cluster 3, *LAG3* in cluster 4 (Supplementary table 1).

Area under the curve (AUC) analysis to determine whether a gene set is active in a cell¹⁴ supported the observation that cluster 1 comprises primarily resting Tregs with genes being upregulated in naive compared to memory Tregs (39.2% enriched Tregs in cluster 1 compared to 19.3%, 14.3% and 5.2% for cluster 2-4; Pearson's Chi-squared test P -value = 2.2×10^{-16}) or naive compared to effector memory CD4 T cells (37.6% of enriched Tregs in cluster 1 compared to 28.2%, 7% and 11.6% for cluster 2-4; Pearson's Chi-squared test P -value = 2.2×10^{-16}) (Figure 1e, Supplementary figure 2e). Gene signatures associated with eTregs as found in homeostatic tissues (37.3-41% enriched Tregs in cluster 2-4 compared to 18.1% for cluster 1; Pearson's Chi-squared test P -value = 2.502×10^{-10}) and the tumor tissue micro-environment (43.8/29.5% enriched Tregs in cluster 2/3 compared to 6.4/11.5% for cluster 1/4; Pearson's Chi-squared test P -value = 2.2×10^{-16}) were highly enriched in cluster 2 and 3 Tregs (Figure 1f). Subsequent gene ontology analysis also revealed that clusters 2-4 share upregulation of Th differentiation-associated genes, whereas cluster 1 showed downregulation of TCR-signaling pathways compared to clusters 2-4 indicative of resting Tregs. Additionally, cluster 3 and 4 shared pronounced upregulation of TCR- and Notch signaling, and of all SF-derived Tregs those from cluster 3 seemed to rely most on glycolysis (Supplementary table 2).

Microenvironmental cues can shape the transcriptomic signature of Tregs with a resulting co-transcriptional Th cell program^{5,7}. These can be distinguished based on the expression pattern of the chemokine receptors *CXCR3*, *CCR4*, *CCR6*, *CCR10* and *CXCR5*¹⁵. *CXCR5*, linked to Tfr, was not expressed in any of the SF Tregs. Cluster 1 harbored Tregs expressing mixed chemokine receptor profiles associated with Th2, Th22, Th1 and Th17 cells.

Overall expression of CCR4, CCR6 and CCR10 was low. In contrast, cluster 2-4 Tregs were for 51.7% positive for the Th1-associated CXCR3, (Supplementary figure 4). These data indicate that Tregs in the inflammatory SF environment are heterogeneous, and that local cues preferentially induce a Th1 co-transcriptional program in these Tregs.

Clonotype sharing amongst synovial fluid-derived Treg clusters

Next, we assessed whether the TCR of individual Tregs skews differentiation to a certain phenotype upon triggering. Therefore, we employed a 10X Genomics dataset, including both 5' gene expression and TCR sequences, published by Maschmeyer *et al.*¹⁶ containing SF-derived Tregs from JIA patients. Dimensionality reduction revealed similar Treg clusters as in our dataset indicating that the clustering is robust (Supplementary figure 5a).

On average, 55% of the detected clonotypes (full length combined TRA and TRB chain) were unique within a patient (range 34.8-72.7%), showing presence of clonal expansion. Exploratory analysis revealed that cluster 1 contained mostly single frequency clonotypes, whereas for cluster 2-4 this was less (average of 65.7% single clonotypes, range of 42.0-89.6% for cluster 1 and average of 49.2%, 44.3% and 61.4% for cluster 2-4, respectively) (Figure 2a). Clonal expansion was analyzed by dividing the detected clonotypes in 6 groups based on frequency. The proportional space filled by the most expanded clones revealed a gradient from cluster 1 to 4. In cluster 4, the most prevalent clonotypes comprised the greatest proportion of the total clones present (Figure 2b). A wide spread was observed for cluster 1 for the number of clonotypes comprising 10% of the total repertoire with an average of 16 clonotypes (Figure 2c). For cluster 2 and 3 only five clonotypes and for cluster 4 merely two different clonotypes were observed on average (Figure 2c). Several diversity indices indeed indicated that cluster 1 had the most diverse clonal repertoire compared to the three activated Treg clusters (Supplementary figure 5b).

We also determined presence of clonal sharing between the clusters, indicative of a shared origin. The overlap coefficient was calculated based on overlap of the complete TRA/TRB nucleotide sequences. This showed a clonotype overlap of 25% and 32.4% of cluster 1 with clusters 2 and 3, respectively. The latter two clusters shared 32.3% of their clonotypes. However, interestingly there was < 15% clonotype sharing on nucleotide level between cluster 4 and the other clusters, although on TRA/TRB chain level this was 21.1-28.5%. Overall, based on the Morisita similarity index, a measure that takes the total number of cells into account, it was indeed clear there was little similarity between clusters 1-3 and cluster 4 Tregs (Figure 2d). For the TRA chain alone the similarity between all four clusters was very high suggesting that the differences are primarily formed by the TRB (Figure 2e). We also assessed whether any of the SF Treg clusters showed a similar TCR repertoire to SF CD4 non-Treg cells. For none of the four SF Treg clusters a similar TCR repertoire to SF CD4 non-Treg cells was observed (Supplementary figure 5c). This suggests that there is minimal *in situ* differentiation of CD4 T cells to Tregs for any of the SF Treg clusters. Altogether, these data indicate that cluster 2 and 3 eTregs are relatively similar, as also suggested by their transcriptomic profile, whereas cluster 4 Tregs contain more distinct clonotypes primarily skewed by the TRB.

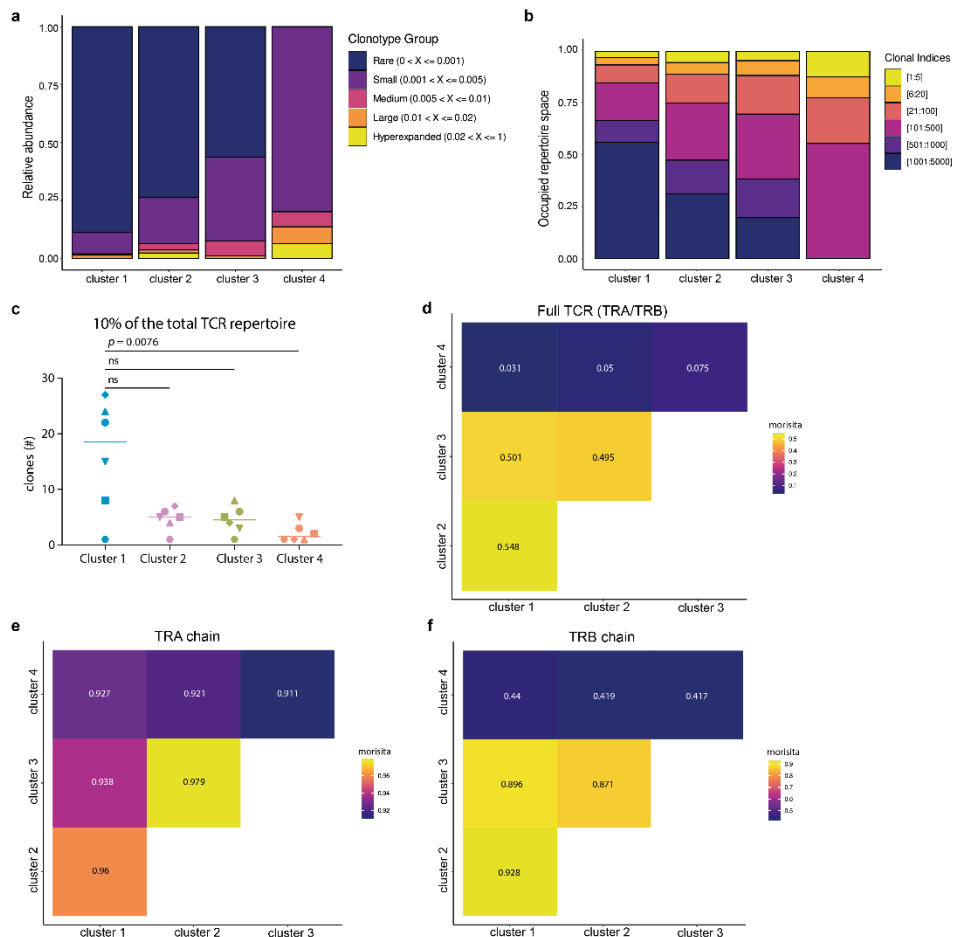


Figure 2. Clonal expansion and clonal overlap of synovial fluid-derived Tregs. **(a)** Histograms of the relative proportion filled up by clonotypes that form 1% (rare), 1-5% (small), 5-10% (medium), 10-20% (large) or > 20% (hyperexpanded) of the total repertoire, separated by cluster. 1% refers to clones that are present once (not expanded). **(b)** Histograms with the clones divided in 6 bins based on the frequency each clonotype is present. The bins are the top 1:5 clonotypes, 6:20, 21:100, 101:500, 501:1000, and 1001:5000. **(c)** Graph showing the least number of clonotypes (combined TRA and TRB chain) that comprise 10% of the TCR repertoire per patient ($n = 6$, different symbols) per cluster (colors as per Supplementary figure 5a). Comparison was performed with a Friedman's test followed by Dunn's post hoc analysis. **(d)** Morisita diversity index for the similarity of the TCR repertoire between all four SF Treg clusters based on the nucleotide sequence of both the TRA and TRB chain. The scale ranges from 0 to 1, with 0 indicating no overlap and 1 indicating identical repertoires. **(e)** Similar to **(d)** but for the nucleotide sequence of the TRA chain. **(f)** Similar to **(d)** but for the nucleotide sequence of the TRB chain.

Non-linear differentiation of Tregs within synovial fluid

To further explore how the SF Treg clusters are related, we employed pseudotime analyses to estimate Treg differentiation within SF based on transcriptional similarities. We applied

Monocle v3^{17,18} to perform trajectory inference and pseudotime plotting (Figure 3a, b). Mathematical assessment of the potential starting node for the differentiation trajectory pointed towards cluster 1 Tregs. Those Tregs were indeed highest in (combined) expression of the genes *CCR7*, *LEF1*, *TCF7* and *KLF2* associated with a naive state (Figure 3c). The identified trajectory suggests that upon arrival within the SF environment, Tregs are skewed towards a classical eTreg phenotype (clusters 2 and 3) or towards cluster 4 Tregs. Cluster 4 Tregs may, however, also pass a cluster 3 phenotype along the differentiation trajectory (Figure 3a, b).

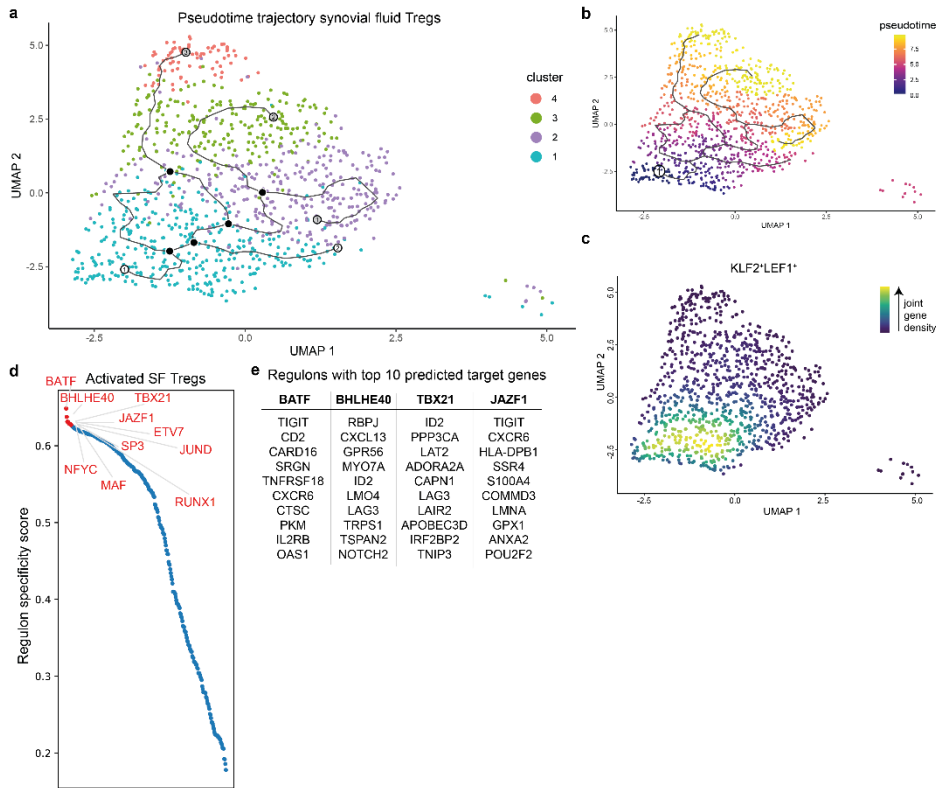


Figure 3. Predicted differentiation trajectory and regulation of synovial fluid Tregs. **(a)** Predicted differentiation trajectory of Tregs within the synovial fluid (SF) environment plotted on the UMAP as per Figure 1a. White circles represent predicted starting points, black circles designate decision points setting a cell upon a trajectory, and grey circles (ending in all three activated Treg clusters) depict end points. **(b)** Similar to **(a)** but colored based on pseudotime with early cells in blue and end stage cells in yellow. The circle with number 1 is the mathematically determined starting node. **(c)** UMAP of the combined expression of *CCR7*, *LEF1*, *KLF2* and *TCF7* in nebulosa density. The scale ranges from blue to yellow, with the highest kernel density displayed in yellow, thus representing the highest (estimated) expression of all combined selected genes. **(d)** Top 10 predicted regulons (transcription factor and its target genes) to drive differentiation of cluster 1 to activated cluster 2-4 (e) Tregs. The regulons are ranked by the regulon specificity score for cluster 2-4 Tregs shown on the y-axis ranging from 0 to 1, with 1 indicating complete specificity of the regulon for the cell type. **(e)** Selected regulons with their top 10 calculated target genes.

TFs interact with cis-regulatory elements and regulate cell differentiation, and together with their target genes it forms a regulon. SCENIC can be employed for gene regulatory network analysis to deduce active regulons per cell. Here, we compared cluster 1 recently migrated Tregs with cluster 2-4 activated (e)Tregs. There was no clear binarization of the regulons per cluster indicating that there is a gradual differentiation of SF Tregs. The top regulons were all upregulated in cluster 2-4 Tregs and associated with differentiation or maintenance of the Treg phenotype indicating that upon migration to the SF-environment cluster 1 Tregs differentiate towards cluster 2-4 Tregs and not in the opposite way (Figure 3d). BATF is a known key driver in eTreg differentiation^{7,19,20}, and indeed, our analysis revealed BATF as the primary local regulon for differentiation of Tregs that recently migrated to SF. RUNX1 and NFYC have also been previously associated with Treg development, maintenance and differentiation, and TBX21 is a possible driver of the Th1-associated co-transcriptional program^{7,21,22}, whereas for example SP3 is associated with generic processes including proliferation, apoptosis and metabolism²³. BHLHE40 was identified as a novel regulon for eTreg differentiation, and target genes mostly comprised cluster 4-associated genes including *CXCL13*, *GPR56* and *KLRB1*. However, also amongst its target genes are genes required for Treg differentiation and survival such as *ID2*²⁴. Other BHLHE40 associated genes, such as, *RBPJ* and *RFX1* have been linked to inhibiting Th2 and Th17 differentiation respectively^{25,26}. Another novel identified regulator, i.e. JAZF1, primarily drives SF Treg differentiation towards cluster 2-3 Tregs. Its target genes include the (e)Treg genes *TIGIT* and *CXCR6*^{6,7}, but also *POU2F2* which regulates a shift towards aerobic glycolysis²⁷ (Figure 3e). Overall, these data indicate that Tregs arriving in the inflamed SF-environment can differentiate into activated (e)Tregs via different routes in a non-linear fashion, facilitated by key regulators including BATF, TBX21, RUNX1, and the newly (e)Treg-associated regulons BHLHE40 and JAZF1.

GPR56⁺/CD161⁺/CXCL13⁺ synovial fluid Tregs are highly differentiated and suppressive

Cluster 4 Tregs were defined by genes not commonly associated with Tregs which warranted further investigation. On protein level, we could confirm presence of Tregs expressing GPR56 and/or CD161 (average of 18.1%, range 10.3-32.3%). This subset was specifically enriched for CXCL13 expression. In PB Tregs, expression of GPR56 and/or CD161 averaged 4.6%, with no CXCL13⁺ Tregs present (Figure 4a). In line with the transcriptomic data, GPR56⁺CD161⁺CXCL13⁺ SF Tregs expressed high levels of PD-1 and LAG3 (Figure 4b). We also confirmed FOXP3 protein expression within these Tregs. Although the intensity of FOXP3 expression in GPR56 and/or CD161 positive CXCL13⁺ SF Tregs was lower compared to other SF Tregs it was higher than in PB Tregs and PB and SF non-Tregs (Figure 4c). In addition, a gradual decline of Helios-expressing Tregs was observed from PB Tregs to CXCL13⁺ SF Tregs. However, compared to non-Tregs about 5.5x more cells expressed Helios: 53.9% for CXCL13⁺ SF Treg versus 9.9% for CXCL13⁺ SF non-Treg (Figure 4d). Even though Helios cannot distinguish thymic- and peripherally-derived Tregs, its expression in FOXP3⁺ Tregs indicates a stable and activated phenotype^{28,29}, suggesting that CXCL13⁺ Tregs maintain fundamental Treg characteristics.

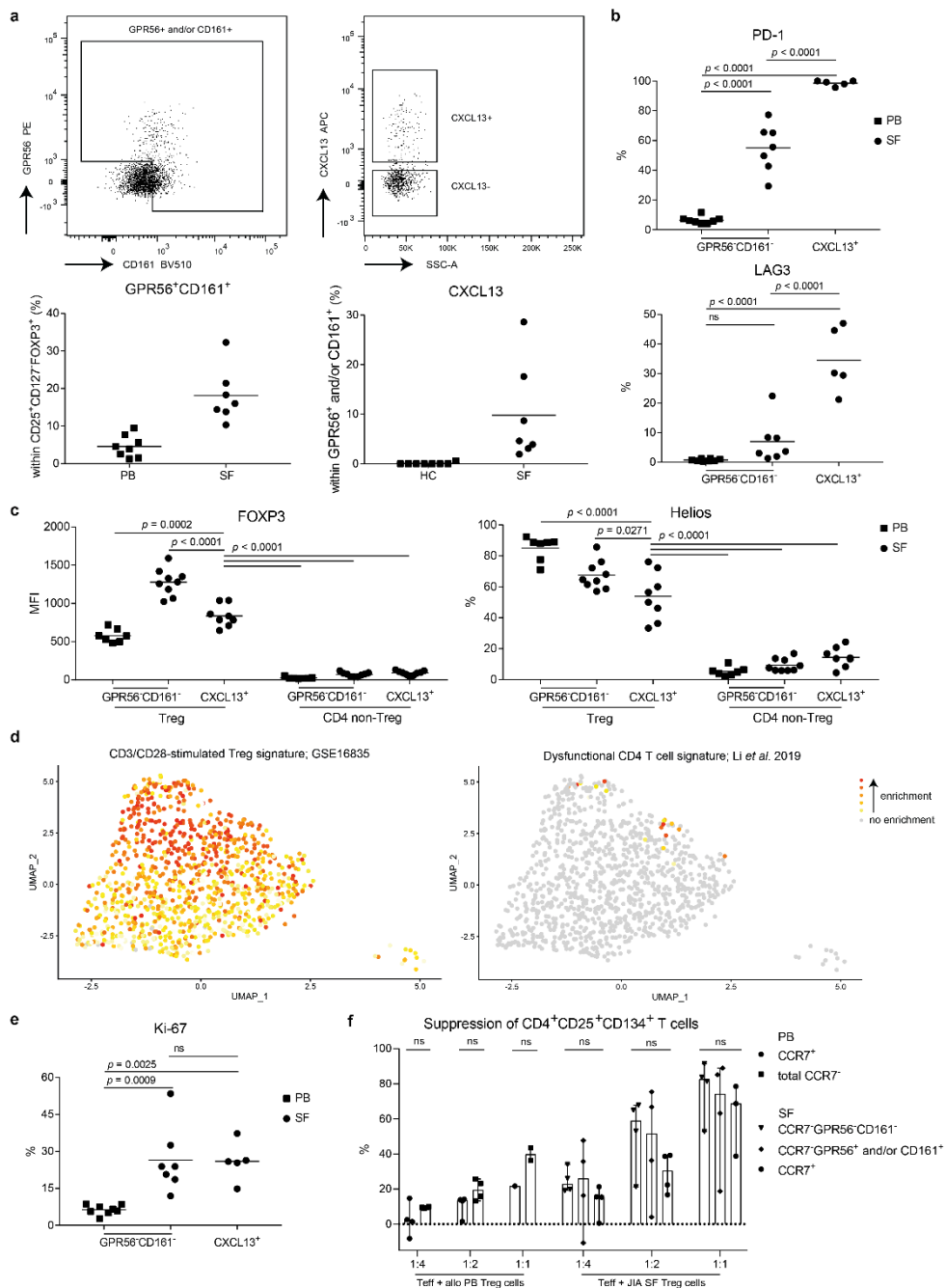


Figure 4. CD161⁺GPR56⁺CXCL13⁺ synovial fluid Tregs are highly differentiated and suppressive. **(a)** Representative gating (upper row) and quantification (lower row) of GPR56⁺ and/or CD161⁺ expression within CD127^{low}CD25^{high}FOXP3⁺ Tregs (left) and CXCL13 expression within this subset (left). Quantification is shown in control peripheral blood (PB) Tregs ($n = 8$) and synovial fluid (SF)-derived Treg from Juvenile Idiopathic Arthritis (JIA) patients ($n = 7$). **(b)** Quantification of PD-1 (upper) and LAG3 (lower) within control PB GPR56⁺CD161⁺ ($n = 8$),

synovial fluid (SF) GPR56⁺CD161⁻ ($n = 7$) and SF CXCL13⁺ (GPR56⁺ and/or CD161⁻, and CXCL13⁺; $n = 5$) Tregs. **c** Quantification of Helios (left) and FOXP3 (right) within control PB GPR56⁺CD161⁻ ($n = 7$), SF GPR56⁺CD161⁻ ($n = 9$) and SF CXCL13⁺ (GPR56⁺ and/or CD161⁻, and CXCL13⁺; $n = 8$) Tregs and CD4 non-Tregs (CD127⁺CD25^{low}FOXP3⁺). **(d)** Gene set analysis of a CD3/CD28 stimulated Treg (GSE16835) (left) and a dysfunctional CD4 T cell signature⁴¹ (right). Enrichment is calculated per cell; grey signifies no enrichment and yellow to red shows increasing enrichment. **(e)** As per **(b)** for Ki-67. **(f)** Suppression of CD4 effector T cells, assay as per Long et al.³¹. Sorted CD3⁺CD25⁻ T cells (10.000) were cultured with Tregs (CCR7⁺ (cluster 1), CCR7⁻, CCR7⁻GPR56⁺CD161⁻ (cluster 2-3), CCR7⁻GPR56⁺ and/or CD161⁺ (cluster 4)) derived from control PB or SF of JIA patients in varying ratio's (1:4, 1:2, 1:1) to quantify the suppression induced by Tregs. Control PB $n = 4$, SF $n = 3-4$. Statistical comparisons were performed using Friedman's test. **(c, e, f)** Data are representative of two independent experiments. **(c and e)** Statistical comparisons were performed using one-way ANOVA with Tukey's correction for multiple testing.

Genes associated with TCR stimulation showed the highest enrichment in clusters 3 and 4 (Figure 4d). Upregulation of TCR signaling was also reflected in the gene ontology analysis and their previously shown clonality (Supplementary table 2 and Figure 2a-c). Ongoing TCR stimulation has been associated with exhaustion, but exhaustion-associated genes were enriched in only 1.84% (18/980 Tregs) of the Tregs, and not particularly in cluster 4 (Figure 4d). Supporting the absence of exhaustion-associated gene signatures in cluster 4 is the high expression of Ki-67, a marker for recent proliferation, similar to other SF-derived Tregs (Figure 4e).

CD4⁺ non-Treg cells can transiently express FOXP3 upon activation, while maintaining effector functions³⁰. To verify that our Tregs are *bona fide* suppressor cells, we assessed Treg-specific characteristics. On transcriptome level we observed higher expression of *BHLHE40*, *IFNG* and *ID2* in cluster 4 compared to the other SF Tregs, which are TFs associated with cytokine expression. However, on protein level we could not detect significant levels of IFN γ (1.63%), IL-2 (3.88%) or IL-17 (2.2%) produced by GPR56/CD161⁺ CXCL13⁺ SF Tregs (Supplementary figure 6a) indicating that these cells are true Tregs. In addition, we performed a suppression assay as developed by Long et al.³¹ to assess the suppressive capacity of cluster 4 Tregs. We sorted cluster 4 Tregs based on CCR7-GPR56 and/or CD161 expression (for gating strategy see Supplementary figure 6b), which includes CXCL13 expressing Tregs. In contrast, within the CD161⁻GPR56⁻ Treg population CXCL13⁺ Tregs comprised only 0.8% of the cells. In addition, we included CCR7⁺ Tregs for resting/quiescent Tregs and CCR7⁻ Tregs negative for both GPR56 and CD161 from both SF and control PB. As expected, we observed that a higher ratio of Tregs to CD4 effector T cells resulted in a higher percentage of CD4 effector T cell suppression. Furthermore, similar levels of CD4 effector T cell suppression were observed by all sorted SF Treg subsets (Figure 4f). These data show that Tregs from cluster 4 are proficient suppressor cells without any clear differences among Treg clusters present in SF.

DISCUSSION

We show that even though Tregs in SF of JIA patients obtain a dominant Th1 co-transcriptional program, substantial heterogeneity can be observed. The largest proportion of SF Tregs actually comprise of recently arrived cells (*CCR7*, *KLF2*, *TCF7*, *LEF1*) which seem to differentiate

to three activated (e)Treg phenotypes that are not completely discrete but form a gradient of transcriptional states. Two of these phenotypes are more classical eTregs characterized by *CTLA4*, *TIGIT*, *GZMA*, *TNFRSF8*, *CCR5*, and *TBX21*, whereas the third activated Treg cluster contains Tregs expressing *CXCL13*, *GPR56*, and *KLRB1*. Tregs from the latter cluster bear a more distinct TCR profile, while the eTregs of clusters 2 and 3 are more closely related. Lastly, next to BATF as shared regulator in eTreg differentiation, the here identified Treg regulators BHLHE40 and JAZF1 regulate primarily genes associated with cluster 4 and clusters 2/3 Tregs, respectively. The TF BHLHE40 (also known as DEC1 or BHLHB2) is upregulated upon TCR activation. BHLHE40 in Th-cells is associated with a pro-inflammatory phenotype^{32,33}; however, in Tregs this TF seems crucial for long-term maintenance of the Treg pool, and adoptive transfer of BHLHE40 expressing Tregs in a colitis model in mice prevents wasting disease³⁴. JAZF1 (TIP27) has been mostly studied for its role in gluconeogenesis and lipid metabolism in relation to the development of type 2 diabetes mellitus, and its signaling also results in decreased expression of proinflammatory cytokines^{35,36}. Our data suggest that JAZF1, and its downstream target genes, skew Treg metabolism in the chronic inflammatory setting, but this remains to be fully elucidated. These data support the notion that Tregs within SF follow different and unique routes of adaptation.

In both mice and humans, studies have explored PB to tissue Treg differentiation. However, data on functional adaptation pathways of Tregs in inflamed tissues is lacking. Here we show that infiltrating Tregs are heterogeneous in chemokine receptor expression upon migration to SF indicating partial unspecific homing in response to inflammatory signals, with local cues and antigen(s) inducing preferential differentiation to, and expansion of, Th1-skewed Tregs. The acquisition of a Th-associated co-transcriptional program is crucial for Treg survival and function in those inflammatory environments³⁷. The demonstrated heterogeneity also suggests that upon local cues Tregs can induce subtle shifts in phenotype, possibly to suppress immune responses under changing inflammatory conditions. Especially for cluster 2 and 3 Tregs this seems likely since they share many clonotypes but show phenotypic differences in functional Treg markers. For GPR56⁺CD161⁺CXCL13⁺ Tregs (cluster 4), however, clonotypes are less overlapping suggesting a more predetermined route of these Tregs, perhaps based on TCR-specificity or affinity, when migrating to the site of inflammation. Thereby the question rises where the imprinting of Treg differentiation occurs. Chemokine receptor expression is determined in secondary lymphoid structures and functional marker heterogeneity seems to be partially predetermined in the periphery³⁸⁻⁴⁰. Our data suggests that there is further extensive local plasticity and differentiation, which is supported by the observation that different T cell subsets show a similar phenotypical adaptation in local inflammatory environments.

Several scRNA-sequencing studies in autoimmune and tumor settings have shown presence of CD4 and CD8 T cell subsets characterized by CXCL13 and inhibitory immune checkpoints^{16,41-44} indicating a partial mirrored phenotype amongst inflammation-derived T cells. However, for FOXP3⁺ Tregs this phenotype has not been described before. These CXCL13⁺ subsets express high levels of PD-1 and other inhibitory immune checkpoints, proliferate, are

clonally expanded and have lost classical CD4 and CD8 T cell effector functions including cytokine production^{16,41-44}. These cells have a T peripheral helper-like phenotype with respect to CXCL13 and PD-1 expression as well as absence of CXCR5 and Bcl6⁴³, but do not produce IL-21. Genes such as *PDCD1*, *CCL5*, *GNLY*, *HAVCR2* and *CCL4* expressed by these cells suggest a terminal stage of differentiation. However, Li *et al.*⁴¹ showed that these dysfunctional cells are tumor-reactive, and gaining CXCL13 expression might indicate acquisition of novel functions⁴⁴. TCR stimulation, presence of inflammatory cytokines including type I interferons and especially TGF β are known to induce CXCL13 expression⁴⁵, which are all abundant in inflammatory environments. That these cells are not found in the periphery indicates that CXCL13 expression is acquired locally. CXCL13 expression suggests a role in ectopic lymphoid structure (ELS) formation as CXCL13 is a known B-cell attractant. Although, Tregs can regulate B-cell maturation within lymphoid structures it is unknown if they can also help forming ELS via CXCL13 expression. Supportive hereof could be expression of extracellular matrix organization-related genes, such as *ADAM19*, *COL6A3*, *COL9A2*, *CTSH*, *CCL4*, and *CCL5* by a fraction of these CXCL13⁺ Tregs. Expression of these genes could also indicate an involvement in tissue repair via extracellular matrix organization after inflammation-related damage in JIA patients⁴⁶. Furthermore, in a murine model tissue repair recently has been shown as a function of Tregs at the site of myocardial infarctions⁴⁷. Additional markers expressed by CXCL13⁺ cells, such as GPR56 for SF Tregs, seem more cell-specific since they are not co-expressed in CXCL13⁺ (SF) non-Tregs. Furthermore, for SF GPR56⁺CD161⁺ Tregs (containing CXCL13⁺ Tregs) there is no loss of classical functioning as these Tregs remain proficient suppressors. This indicates that CXCL13 expression and expression of inhibitory immune checkpoints is likely dependent on the T cell subset concerned. Whether these CXCL13⁺ T cell subsets, and specifically CXCL13⁺ Tregs, in the autoimmune setting are beneficial or pathogenic needs to be elucidated.

Limitations of this study include the risk of contamination of the sorted Tregs with non-Tregs. However, CD127^{high}CD25^{low} Tregs were sorted with a purity > 98% with a FOXP3 intracellular staining confirming > 90% FOXP3 expression and 96.7% of the Tregs contained at least one FOXP3 transcript. Another concern could be the sample size of 3 JIA patients for the scRNA-sequencing. Therefore, we confirmed our findings in a public 10x Genomics sequenced SF T cell dataset including Tregs. We could also confirm presence of CXCL13⁺ Tregs at protein level further supporting our transcriptomic findings. Furthermore, there is still a limited understanding of gene signatures representing functions or states in human Tregs. For example, a definition of exhausted Tregs is lacking with many of the genes defined for CD8 and CD4 T cells actually signifying enhanced Treg activity such as *PDCD1*, *ENTPD1* (CD39), and *LAG3*. It is of importance to further explore (human) Tregs in inflammatory settings to improve our understanding of their (dys)function.

In recent years, several Treg-targeted therapeutic strategies have been implemented in the clinic or are in clinical trial including inhibitory immune checkpoints such as CTLA-4 and LAG3⁴. Our data suggest that not all Tregs will be targeted equally since expression of inhibitory immune checkpoints differs amongst Tregs in one environment. It would be valuable to study patient inter- and intra-variability (if heterogeneity is dynamic) regarding

Treg heterogeneity since this could aid in improving personalized Treg-based therapeutic strategies; is for example PD-1, LAG3 or a combination better suited for a patient?⁴⁸ Additionally, when aiming to prevent adverse side-effects it might be more specific to target chemokine receptors such as CCR4 in clinical trial⁴ because expression of this chemokine receptor depends on the environment.

In conclusion, our study reveals a heterogeneous population of Tregs at the site of inflammation in JIA. SF Treg differentiate to a classical eTreg profile with a more dominant suppressive or cytotoxic profile that share a similar TCR repertoire, or towards GPR56⁺CD161⁺CXCL13⁺ Tregs with a more distinct TCR repertoire. The latter cluster of Tregs is also mirrored in other T cell subsets at the site of inflammation. Finally, the novel Treg regulon BHLHE40 seems to drive differentiation towards primarily GPR56⁺CD161⁺CXCL13⁺ Tregs and JAZF1 towards the classical eTreg phenotype.

METHODS

Patient samples

For scRNA-sequencing, patients with oligo JIA ($n = 3$, 3/3 female) were enrolled in the pediatric rheumatology department at the University Medical Center of Utrecht (the Netherlands). The average age was 9.3 years (range 7-12 years) with a disease duration at the time of inclusion of 7 years (range 4-10 years). Two patients were without medication, and one received methotrexate maintenance therapy. HLA-B27 status has not been assessed. For flow cytometry, patients with oligo JIA ($n = 17$; 40% female, average age 14.2 [2-19 years]) of which 30% had extended and 55% persistent oligo-articular disease were included. Ten patients were without medication, 5 on methotrexate, 2 on NSAIDs and 3 on anti-TNF maintenance therapy. In addition, PB of controls ($n = 21$; 58% female, average age 39.3 [25-62 years]) were included.

Active disease was defined by physician global assessment of ≥ 1 active joint (swelling, limitation of movement), and inactive disease was defined as the absence hereof. During an outpatient clinic visit, SF was obtained by therapeutic joint aspiration of the affected joints, and blood was withdrawn via vein puncture or an intravenous drip catheter. The study was conducted in accordance with the Institutional Review Board of the University Medical Center Utrecht (approval no. 11-499/C). PB from healthy adult volunteers was obtained from the Mini Donor Service at University Medical Center Utrecht. The research was carried out in compliance with the Declaration of Helsinki. Informed consent was obtained from all the participants and/or from their parents/guardians/legally authorized representatives.

SF of JIA patients was incubated with hyaluronidase (Sigma-Aldrich, Saint Louis) for 30 min at 37°C to break down hyaluronic acid. Synovial fluid mononuclear cells (SFMCs) and peripheral blood mononuclear cells (PBMCs) were isolated using Ficoll Isopaque density gradient centrifugation (GE Healthcare Bio-Sciences, Chicago).

Single-cell mRNA-sequencing

Live CD3⁺CD4⁺CD25⁺CD127^{low} cells were sorted from fresh SF (Supplementary figure 1a) into 384-well hard shell plates (Biorad, Hercules) with 5 µl of vapor-lock (QIAGEN, Hilden, Germany) containing 100-200 nl of RT primers, dNTPs and synthetic mRNA Spike-Ins and immediately spun down and frozen to -80°C. Cells were prepared for SORT-seq as previously described⁴⁹. Illumina sequencing libraries were then prepared with the TruSeq small RNA primers (Illumina, San Diego) and sequenced single-end at 75 basepair read length with 60.000 reads per cell on a NextSeq500 platform (Illumina). Sequencing reads were mapped against the reference human genome (GRCh38) with BWA.

Single-cell mRNA-sequencing analysis

Quality control was performed in R with the scater package v1.12.2⁵⁰ and cells were dropped when the number of genes, number of UMI's and/or the percentage of mitochondrial genes was over 3 median absolute deviations under/above the median. Afterwards principal component analysis (PCA)-outliers were removed with the package mvoutlier v1. The raw data expression matrices were subsequently analyzed using Seurat v2-4⁵¹⁻⁵³ following the outline provided by the distributor (<https://satijalab.org/seurat/>). Each dataset was normalized and the cell-cycle was regressed out using SCTransform⁵⁴. Thereupon, the SF datasets were integrated with PrepSCTIntegration followed by FindIntegrationAnchors and IntegrateData for SCTransform-processed data.

For dimensionality reduction first the principal components (PCs) were calculated (RunPCA) and clustering was performed with UMAP (RunUMAP: 30 dimensions; FindNeighbors: clustering resolution of 1). One cluster was removed from further analyses (Supplementary figure 2a) since it was of ambiguous origin (e.g. hybrid, transferred extracellular vesicles or doublets). Subsequent differential gene expression was performed using the MAST test (standard settings) with a *P*-adjusted value < 0.05 considered statistically significant. For visualization the functions DoHeatmap, Dimplot, Featureplot and plot_density were employed. UMAPs were plotted with raw mRNA counts or using the new nebuloza algorithm⁵⁵ based on kernel density estimation to handle sparsity of scRNA-sequencing data.

Gene set enrichment analysis was performed with gene sets derived from the literature (Ferraro *et al.*¹³ for a human Treg signature, Niedzielska *et al.*⁵⁶ for a shared tissue Treg signature, De Simone *et al.*⁵⁷ for a tumor-infiltrating Treg signature, and Li *et al.*⁴¹ for a dysfunctional signature of CD4⁺ T cells) or the MSigDB C7 database (GSE61077 for CD44^{hi}CD62L^{lo} versus CD44^{lo}CD62L^{hi} murine Tregs, GSE11057 for naive T cells versus effector memory human CD4 T cells, GSE16835 for CD3/CD28 stimulated versus *ex vivo* Treg) with AUCell¹⁴. The cut-off for enrichment of a gene set in a cell was defined using the AUC. Per cluster the proportion of cells enriched for the gene set was calculated and compared with the Chi-square test. Gene Ontology pathway analyses implementing the probability density function were performed using ToppFun (<https://toppgene.cchmc.org/enrichment.jsp>) with as input the differentially expressed genes belonging to each Treg cluster, with a false discovery rate (FDR)-corrected *P*-value < 0.05 defining significance.

For pseudotime trajectory analysis Monocle v3¹⁷ was used with a trajectory predicted using standard settings based on the clustering previously performed with Seurat. The principal root node was estimated mathematically with the function `get_earliest_principal_node`. Network inference analysis employing SCENIC¹⁴ was performed in python v3.6 with Jupyter Notebook v6.1.5 using the UMAP clustering as starting point to define regulons. In short, co-expression based on the raw count data and DNA motif analysis is used to obtain transcription factors and their target genes using standard settings. Activity of these potential TFs and targets (regulons) are analyzed per cell and finally the scores per cell were combined to compare clusters with each other to define regulators that might drive differentiation within the SF environment. The scRNA-sequencing count data generated for this study have been submitted to a public repository on GitHub (<https://github.com/lutterl/JIA-synovial-fluid-Tregs-scRNAseq>). Raw data files will be made publicly available before publication.

Single cell TCR-sequencing analysis

RNA- and TCR-sequencing profiling data of single cell SF Tregs employing 10X genomics were downloaded from GSE160097 [<https://www.ncbi.nlm.nih.gov/geo/query/acc.cgi?acc=GSE160097>]. TCR-sequencing data was analyzed using scRepertoire following the outlined guidelines⁵⁸. In short, T cell receptor alpha locus (TRA) and TCR beta locus (TRB) data was combined based on the cell barcode. If there was more than one TRA and/or TRB chain detected the most prevalent chain was selected for integration. RNA-sequencing and TCR-sequencing data was combined and subsequent T cell clustering was performed with Seurat as described above. TCR-sequencing analysis was performed on the nucleotide level.

Flow cytometry

Immunophenotyping

PBMCs and SFMCs were thawed and resuspended in RPMI1640 (Gibco, Waltham) supplemented with 10% Fetal Bovine Serum (FBS). For measurements of CXCL13 the cells were cultured for 5 hours at 37°C in RPMI supplemented with 10% human AB serum and GolgiStop (1/1500; BD Biosciences, New Jersey). For cytokine measurements the cells were plated in the presence of anti-CD3/CD28 (Dynabeads® Human T-activator CD3/CD28, ThermoFisher Scientific, Waltham) at a 1:5 ratio (bead:cell) at 37°C. After 19 hours cells were incubated for 5 hours with GolgiStop. After stimulation, cells were stained with surface antibodies for 20 min at 4°C. The following antibodies were used: fixable viability dye eF780 or eF506 (eBioscience, San Diego), anti-human CD3 AF700 (clone UCHT1), GPR56 PE-Cy7 (clone CG4), PD-1 PerCP-Cy5.5 (clone EH12.2H7; Biolegend, San Diego), CD4 BV785 (clone OKT4; eBioscience), CD25 BV711 (clone 2A3), CD161 BV510 (clone DX12), CD161 PE-Cy5 (clone DX12), Helios PE (clone 22F6; BD), CD127 BV605 (clone A019D5; Sony Biotechnology, San Jose), and LAG-3 PE (polyclonal; R&D, Minneapolis). For intranuclear/cellular staining the Intracellular Fixation & Permeabilization Buffer Set (eBioscience) was used, and staining was performed for 30 minutes at 4°C. The following antibodies were used: Ki-67 FITC (clone mip1; Dako, Jena, Germany), CXCL13 APC (clone 53610; R&D), IFN γ PerCP-Cy5.5 (clone 4S.B3), FOXP3 eF450

(clone PCH101), IL-17 FITC (clone eBio64DEC17; eBioscience), FOXP3 PE-CF594 (clone 259D/C7), IL-2 PE (clone MQ1-17H12; BD). Data acquisition was performed on a BD LSRFortessa (BD Biosciences) and data were analyzed using FlowJo Software v10 (Tree Star Inc., Ashland).

Suppression assay

Suppression assays were performed according to the outline provided by Long *et al.*³¹. In short, effector cells (live CD3⁺CD25⁻, lowest 50% of CD25 stained CD3⁺ T cells) and Tregs (CD3⁺CD4⁺CD127^{low}CD25^{high} subdivided into CCR7⁺, CCR7⁻GPR56⁺CD161⁻ (DN) and CCR7⁻GPR56⁺ and/or CD161⁺) were isolated from frozen PBMC and SFMC using the FACS Aria III (BD). Both PBMC and SFMC were 'rested' for 24 hours in RPMI1640 supplemented with 10% FBS at 37°C prior to sorting. Antibodies used for sorting were: CD3 AF700 (clone UCHT1), CD127 AF647 (clone HCD127), GPR56 PE-Cy7 (clone CG4; Biolegend), CD25 BV711 (clone 2A3), CD161 BV510 (clone DX12; BD), CD4 FITC (clone RPA-T4), and CCR7 PE (clone 3D12; eBioscience). Effector cells were labeled with 2µM ctViolet (Thermo Fisher) and cultured alone or with different ratios of sorted Tregs (1:1, 1:2, 1:4). Cells were cultured in RPMI1640 media containing 10% human AB serum with addition of L-Glutamine and Penicillin/Streptomycin. Effector cells were stimulated by anti-CD3/CD28 dynabeads at a 1:28 ratio (ThermoFisher), and incubated for 48 hours at 37°C. Read out on a BD LSRFortessa (BD Biosciences) was performed using Fixable viability dye eF506 (eBioscience), ctViolet (ThermoFisher), CD8 PE-Cy7 (clone SK1; BD), CD4 BV785 (clone OKT4), CD25 BV711 (clone 2A3; eBioscience), CD3 AF700 (clone UCHT1) and CD134 PerCP-Cy5.5. (OX40, clone Ber-ACT35; Biolegend), with CD25 and CD134 as surrogate markers for proliferation³¹. Data were analyzed using FlowJo Software v10 (Tree Star Inc.).

Statistical analysis

Statistical analyses were performed with Pearson's Chi-squared test, a Friedman's test with Dunn's post hoc, or a one-way ANOVA with Tukey's post-hoc test if applicable. Paired data comparisons with missing values were analyzed with a mixed-effect model (Restricted Maximum Likelihood). Analyses were performed in Graphpad Prism v7.04 and v8.3 (San Diego), Excel Office v2017 (Washington) and R v3.5.2-4.1.0 (Cincinnati).

ACKNOWLEDGEMENTS

We thank Sytze de Roock for help with selecting donor samples, Single Cell Discoveries for running our single cell RNA-sequencing (SORT-seq), and Pawel Durek for providing us with the single cell TCR-sequencing data. E.C. Brand was supported by the Alexandre Suerman program for MD and PhD candidates of the University Medical Centre Utrecht, Netherlands. F. van Wijk is supported by a VID1 grant from the Netherlands Organization for Scientific Research (ZonMw, 91714332). E.C. Brand and F. van Wijk are co-applicants on an Investigator Initiated research grant of Pfizer unrelated to this manuscript.

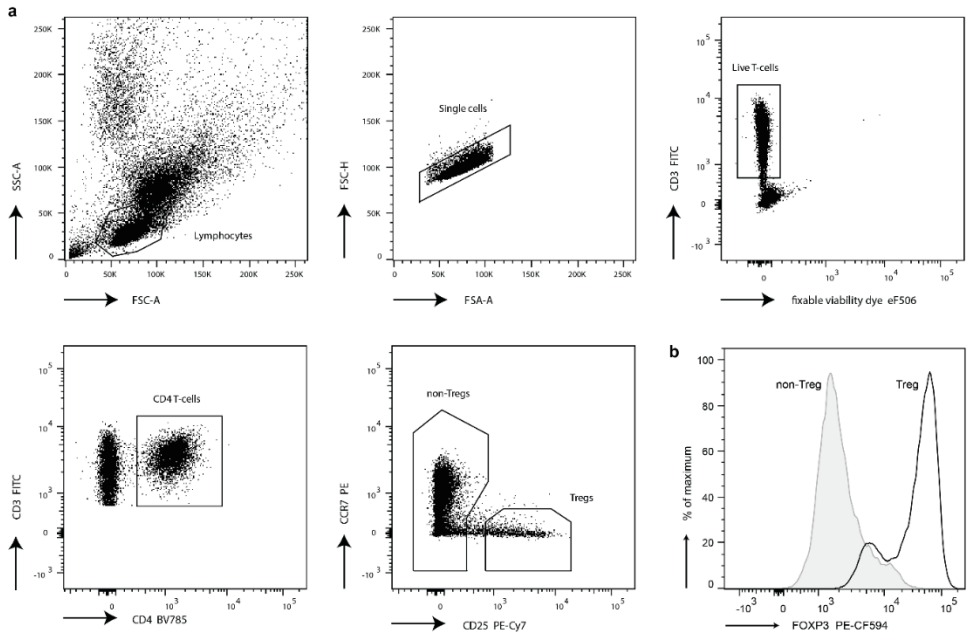
REFERENCES

- 1 Brunkow ME, Jeffery EW, Hjerrild KA *et al.* Disruption of a new forkhead/winged-helix protein, scurfin, results in the fatal lymphoproliferative disorder of the scurfy mouse. *Nat Genet* 2001; **27**: 68–73.
- 2 Ochs HD, Bennett CL, Christie J *et al.* The immune dysregulation, polyendocrinopathy, enteropathy, X-linked syndrome (IPEX) is caused by mutations of FOXP3. *Nat Genet* 2001; **27**: 20–21.
- 3 Raffin C, Vo LT, Bluestone JA. T(reg) cell-based therapies: challenges and perspectives. *Nat Rev Immunol* 2020; **20**: 158–172.
- 4 Li C, Jiang P, Wei S, Xu X, Wang J. Regulatory T cells in tumor microenvironment: new mechanisms, potential therapeutic strategies and future prospects. *Mol Cancer* 2020; **19**: 116.
- 5 Liston A, Gray DHD. Homeostatic control of regulatory T cell diversity. *Nat Rev Immunol* 2014; **14**: 154–65.
- 6 Miragaia RJ, Gomes T, Chomka A *et al.* Single-Cell Transcriptomics of regulatory T cells reveals trajectories of tissue adaptation. *Immunity* 2019; **50**: 493-504.e7.
- 7 Mijnheer G, Lutter L, Mokry M *et al.* Conserved human effector Treg cell transcriptomic and epigenetic signature in arthritic joint inflammation. *Nat Commun* 2021; **12**: 2710.
- 8 Wienke J, Brouwers L, van der Burg LM *et al.* Human Tregs at the materno-fetal interface show site-specific adaptation reminiscent of tumor Tregs. *JCI insight* 2020; **5**: e137926.
- 9 Zhu J, Yamane H, Paul WE. Differentiation of effector CD4 T cell populations. *Annu Rev Immunol* 2010; **28**: 445–489.
- 10 Maggi L, Mazzoni A, Cimaz R, Liotta F, Annunziato F, Cosmi L. Th17 and Th1 lymphocytes in oligoarticular juvenile idiopathic arthritis. *Front Immunol* 2019; **10**: 450.
- 11 Povoleri GAM, Nova-Lamperti E, Scottà C *et al.* Human retinoic acid–regulated CD161⁺ regulatory T cells support wound repair in intestinal mucosa. *Nat Immunol* 2018; **19**: 1403–1414.
- 12 Ali N, Zirak B, Rodriguez RS *et al.* Regulatory T Cells in skin facilitate epithelial stem cell differentiation. *Cell* 2017; **169**: 1119-1129.e11.
- 13 Ferraro A, D’Alise AM, Raj T, Asinovski N, Phillips R, Ergun A *et al.* Interindividual variation in human T regulatory cells. *Proc Natl Acad Sci U S A* 2014; **111**: 34–37.
- 14 Aibar S, González-Blas CB, Moerman T *et al.* SCENIC: single-cell regulatory network inference and clustering. *Nat Methods* 2017; **14**: 1083–1086.
- 15 Duhon T, Duhon R, Lanzavecchia A, Sallusto F, Campbell DJ. Functionally distinct subsets of human FOXP3⁺ Treg cells that phenotypically mirror effector Th cells. *Blood* 2012; **119**: 4430–4440.
- 16 Maschmeyer P, Heinz GA, Skopnik CM *et al.* Antigen-driven PD-1⁺TOX⁺BHLHE40⁺ and PD-1⁺TOX⁺EOMES⁺ T lymphocytes regulate juvenile idiopathic arthritis in situ. *Eur J Immunol* 2021; **51**: 915-929.
- 17 Trapnell C, Cacchiarelli D, Grimsby J *et al.* The dynamics and regulators of cell fate decisions are revealed by pseudotemporal ordering of single cells. *Nat Biotechnol* 2014; **32**: 381–386.
- 18 Cao J, Spielmann M, Qiu X *et al.* The single-cell transcriptional landscape of mammalian organogenesis. *Nature* 2019; **566**: 496–502.
- 19 Delacher M, Imbusch CD, Weichenhan D *et al.* Genome-wide DNA-methylation landscape defines specialization of regulatory T cells in tissues. *Nat Immunol* 2017; **18**: 1160-1172.
- 20 Hayatsu N, Miyao T, Tachibana M *et al.* Analyses of a mutant Foxp3 allele reveal BATF as a critical transcription factor in the differentiation and accumulation of tissue regulatory T cells. *Immunity* 2017; **47**: 268-283.e9.
- 21 Ono M. Control of regulatory T cell differentiation and function by T cell receptor signalling and Foxp3 transcription factor complexes. *Immunology* 2020; **160**: 24–37.
- 22 Oh SA, Li MO. TETs link hydrogen sulfide to immune tolerance. *Immunity* 2015; **43**: 211–213.
- 23 Meinders M, Kulu DI, van de Werken HJG *et al.* Sp1/Sp3 transcription factors regulate hallmarks of megakaryocyte maturation and platelet formation and function. *Blood* 2015; **125**: 1957–1967.
- 24 Miyazaki M, Miyazaki K, Chen S *et al.* Id2 and Id3 maintain the regulatory T cell pool to suppress

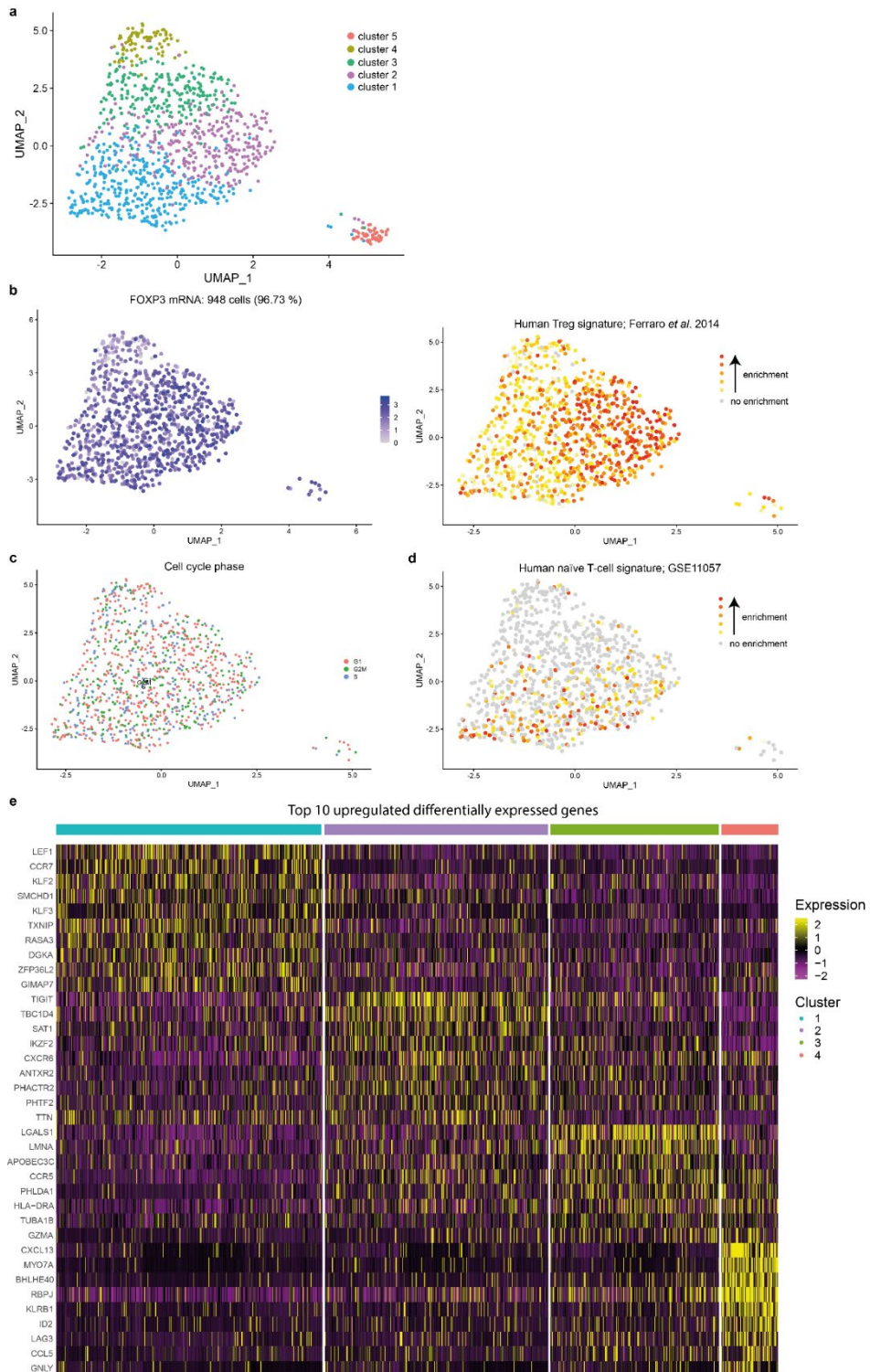
- inflammatory disease. *Nat Immunol* 2014; **15**: 767–776.
- 25 Delacher M, Schmidl C, Herzog Y *et al.* Rbpj expression in regulatory T cells is critical for restraining TH2 responses. *Nat Commun* 2019; **10**: 1621.
- 26 Zhao M, Tan Y, Peng Q *et al.* IL-6/STAT3 pathway induced deficiency of RFX1 contributes to Th17-dependent autoimmune diseases via epigenetic regulation. *Nat Commun* 2018; **9**: 583.
- 27 Yang R, Wang M, Zhang G, Li Y, Wang L, Cui H. POU2F2 regulates glycolytic reprogramming and glioblastoma progression via PDPK1-dependent activation of PI3K/AKT/mTOR pathway. *Cell Death Dis* 2021; **12**: 433.
- 28 Himmel ME, MacDonald KG, Garcia RV, Steiner TS, Levings MK. Helios⁺ and Helios⁻ Cells coexist within the natural FOXP3⁺ T regulatory cell subset in humans. *J Immunol* 2013; **190**: 2001-2008.
- 29 Elkord E. Helios should not be cited as a marker of human thymus-derived Tregs. commentary: Helios⁺ and Helios⁻ Cells coexist within the natural FOXP3⁺ T regulatory cell subset in humans. *Front. Immunol.* 2016; **7**: 276.
- 30 Miyara M, Yoshioka Y, Kitoh A *et al.* Functional delineation and differentiation dynamics of human CD4⁺ T Cells expressing the FoxP3 transcription factor. *Immunity* 2009; **30**: 899–911.
- 31 Long AE, Tatum M, Mikacenic C, Buckner JH. A novel and rapid method to quantify Treg mediated suppression of CD4 T cells. *J Immunol Methods* 2017; **449**: 15–22.
- 32 Emming S, Bianchi N, Polletti S *et al.* A molecular network regulating the proinflammatory phenotype of human memory T lymphocytes. *Nat Immunol* 2020; **21**: 388–399.
- 33 Lin C-C, Bradstreet TR, Schwarzkopf EA *et al.* Bhlhe40 controls cytokine production by T cells and is essential for pathogenicity in autoimmune neuroinflammation. *Nat Commun* 2014; **5**: 3551.
- 34 Miyazaki K, Miyazaki M, Guo Y *et al.* The role of the basic helix-loop-helix transcription factor Dec1 in the regulatory T cells. *J Immunol* 2010; **185**: 7330–7339.
- 35 Meng F, Hao P, Du H, Zhou Z. Effects of Adenovirus-mediated overexpression of JAZF1 on chronic inflammation: an *in vitro* and *in vivo* study. *Med Sci Monit Basic Res* 2020; **26**: e924124.
- 36 Yang M, Dai J, Jia Y *et al.* Overexpression of juxtaposed with another zinc finger gene 1 reduces proinflammatory cytokine release via inhibition of stress-activated protein kinases and nuclear factor- κ B. *FEBS J* 2014; **281**: 3193–3205.
- 37 Koch MA, Tucker-Heard G, Perdue NR, Killebrew JR, Urdahl KB, Campbell DJ. The transcription factor T-bet controls regulatory T cell homeostasis and function during type 1 inflammation. *Nat Immunol* 2009; **10**: 595–602.
- 38 Ito T, Hanabuchi S, Wang Y-H *et al.* Two functional subsets of FOXP3⁺ regulatory T cells in human thymus and periphery. *Immunity* 2008; **28**: 870–880.
- 39 Mohr A, Malhotra R, Mayer G, Gorochov G, Miyara M. Human FOXP3⁺ T regulatory cell heterogeneity. *Clin & Transl Immunol* 2018; **7**: e1005.
- 40 Baecher-Allan C, Wolf E, Hafler DA. MHC class II expression identifies functionally distinct human regulatory T cells. *J Immunol* 2006; **176**: 4622–4631.
- 41 Li H, van der Leun AM, Yofe I *et al.* Dysfunctional CD8 T Cells form a proliferative, dynamically regulated compartment within human melanoma. *Cell* 2019; **176**: 775-789.e18.
- 42 Zhang L, Yu X, Zheng L *et al.* Lineage tracking reveals dynamic relationships of T cells in colorectal cancer. *Nature* 2018; **564**: 268–272.
- 43 Rao DA. T cells that help B cells in chronically inflamed tissues. *Front Immunol* 2018; **9**: 1924.
- 44 van der Leun AM, Thommen DS, Schumacher TN. CD8⁺ T cell states in human cancer: insights from single-cell analysis. *Nat Rev Cancer* 2020; **20**: 218–232.
- 45 Kobayashi S, Watanabe T, Suzuki R *et al.* TGF- β induces the differentiation of human CXCL13-producing CD4⁺ T cells. *Eur J Immunol* 2016; **46**: 360–371.
- 46 Wojdas M, Dąbkowska K, Winsz-Szczołka K. Alterations of extracellular matrix components in the course of juvenile idiopathic arthritis. *Metabolites* 2021; **11**: 132.
- 47 Xia N, Lu Y, Gu M *et al.* A unique population of regulatory T cells in heart potentiates cardiac protection

- from myocardial infarction. *Circulation* 2020; **142**: 1956–1973.
- 48 Kumagai S, Togashi Y, Kamada T *et al.* The PD-1 expression balance between effector and regulatory T cells predicts the clinical efficacy of PD-1 blockade therapies. *Nat Immunol* 2020; **21**: 1346–1358.
- 49 Muraro MJ, Dharmadhikari G, Grün D *et al.* A single-cell transcriptome atlas of the human pancreas. *Cell Syst* 2016; **3**: 385–394.e3.
- 50 McCarthy DJ, Campbell KR, Lun ATL, Wills QF. Scater: pre-processing, quality control, normalization and visualization of single-cell RNA-seq data in R. *Bioinformatics* 2017; **33**: 1179–1186.
- 51 Butler A, Hoffman P, Smibert P, Papalexi E, Satija R. Integrating single-cell transcriptomic data across different conditions, technologies, and species. *Nat Biotechnol* 2018; **36**: 411–420.
- 52 Stuart T, Butler A, Hoffman P *et al.* Comprehensive integration of single-cell data. *Cell* 2019; **177**: 1888–1902.e21.
- 53 Hao Y, Hao S, Andersen-Nissen E *et al.* Integrated analysis of multimodal single-cell data. *Cell* 2021; **184**: 3573–3587.e29.
- 54 Hafemeister C, Satija R. Normalization and variance stabilization of single-cell RNA-seq data using regularized negative binomial regression. *Genome Biol* 2019; **20**: 296.
- 55 Alquicira-Hernandez J, Powell JE. Nebulosa recovers single-cell gene expression signals by kernel density estimation. *Bioinformatics* 2021; **37**: 2485–2487.
- 56 Niedzielska M, Israelsson E, Angermann B *et al.* Differential gene expression in human tissue resident regulatory T cells from lung, colon, and blood. *Oncotarget* 2018; **9**: 36166–36184.
- 57 De Simone M, Arrigoni A, Rossetti G *et al.* Transcriptional Landscape of Human Tissue Lymphocytes Unveils Uniqueness of Tumor-Infiltrating T Regulatory Cells. *Immunity* 2016; **45**: 1135–1147.
- 58 Borchering N, Bormann NL, Kraus G. scRepertoire: An R-based toolkit for single-cell immune receptor analysis. *F1000Research* 2020; **9**: 47.

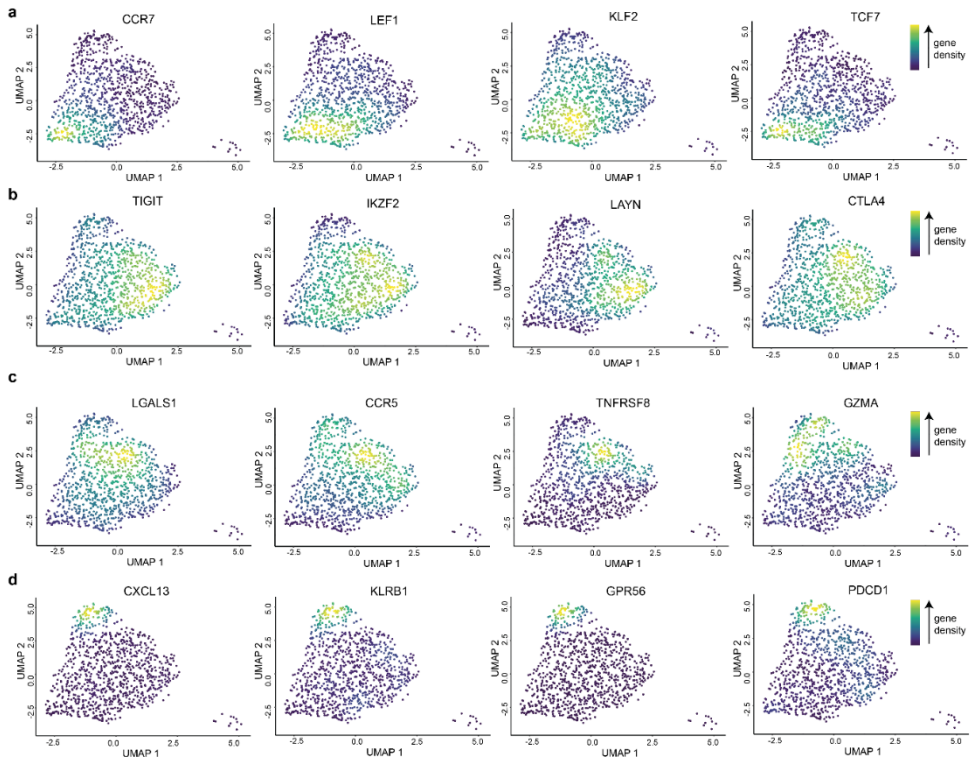
SUPPLEMENTARY INFORMATION



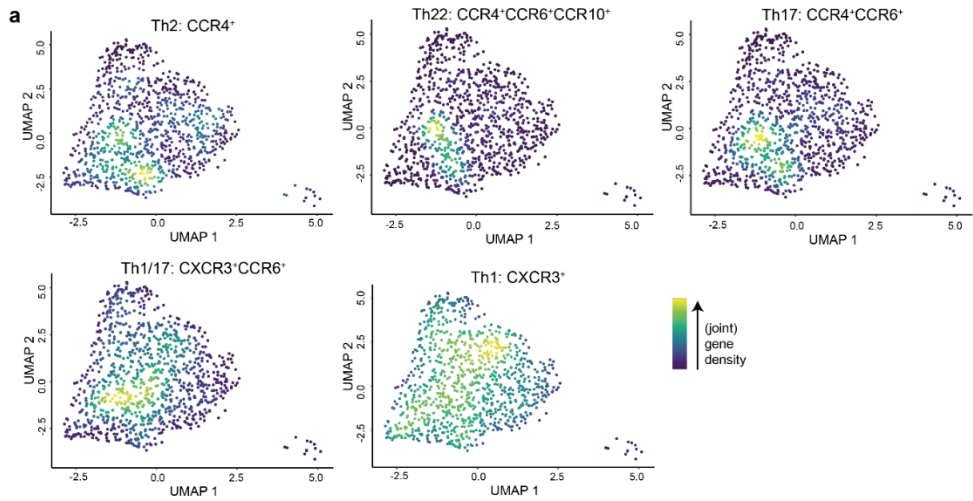
Supplementary figure 1. Gating strategy of synovial fluid derived Tregs. **(a)** Representative gating strategy to sort Tregs derived from synovial fluid (SF). **(b)** Representative FOXP3 median fluorescence.



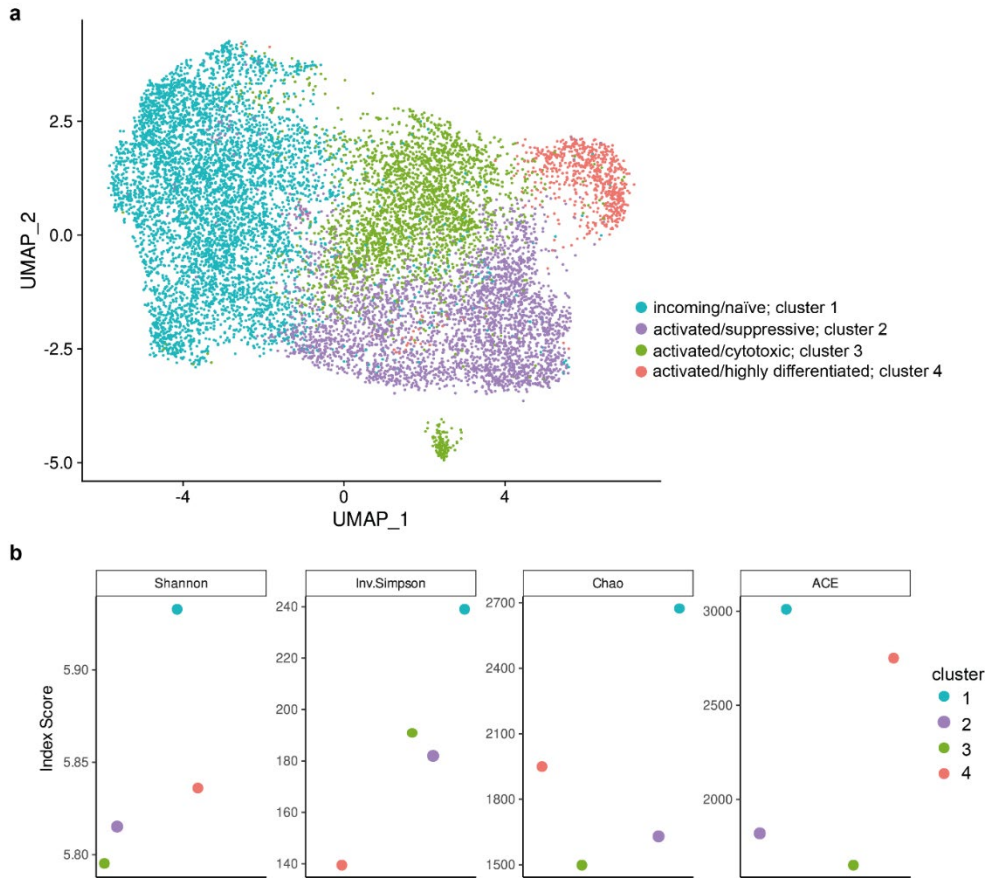
< Supplementary figure 2. Heterogeneity and phenotypical profile of synovial fluid Tregs. **(a)** Dimensionality reduction (UMAP) of all sequenced Tregs that passed the quality control. Cluster 5 is of ambiguous composition (e.g. hybrid, transferred extracellular vesicles or doublets) and not included in further analysis. **(b)** mRNA FOXP3 expression (left) and gene set enrichment of a human core Treg signature¹⁹ (right). Grey means no FOXP3 mRNA expression or Treg signature enrichment, with in blue cells with FOXP3 mRNA (left), and yellow to red increasing shows enrichment of the Treg signature (right). **(c)** UMAP with the cells colored by phase of the cell cycle; pink = G1, green = G2M, blue = S. Pearson's Chi-squared test revealed no association between the cell cycle phase and the clustering ($P = 0.8512$). **(d)** Heatmap of the top 10 upregulated differentially expressed genes, based on \log_2 fold change, per cluster. Expression ranges from purple (no raw count mRNA expression) to yellow (presence of mRNA expression of the concerned gene). **(e)** Similar to **(b)** but for a gene set upregulated in naïve compared to effector memory human CD4 T-cells (GSE11057).



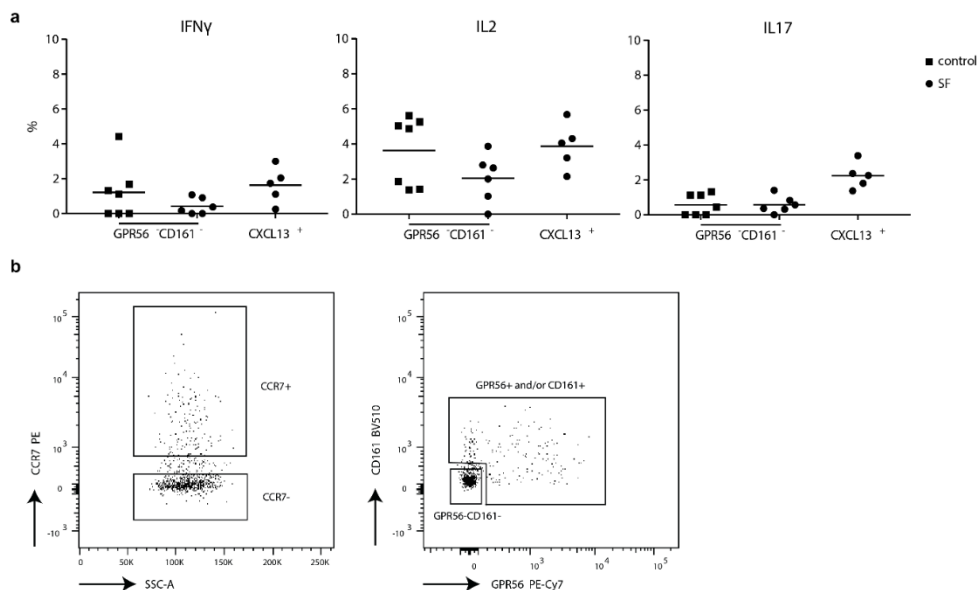
Supplementary figure 3. Synovial fluid Treg cluster-identifying genes. **(a)** UMAPs showing the nebuloza density of the selected differentially expressed genes *CCR7*, *LEF1*, *KLF2*, and *TCF7* for cluster 1 Tregs. The nebuloza density (based on kernel density) ranges from blue to yellow, with in yellow the highest kernel density, thus the highest (estimated) expression of the shown gene. **(b)** Similar to **(a)** but for *TIGIT*, *IKZF2* (encoding Helios), *LAYN*, and *CTLA4* which are differentially expressed by cluster 2 Tregs. **(c)** Similar to **(a)** but for *LGALS1*, *CCR5*, *TNFRSF8*, and *GZMA* which are differentially expressed by cluster 3 Tregs. **(d)** Similar to **(a)** but for *CXCL13*, *KLRB1*, *GPR56*, and *PDCD1* which are differentially expressed by cluster 4 Tregs.



Supplementary figure 4. Preferential expansion of Th1-skewed Tregs in synovial fluid. **(a)** UMAPs showing the nebulosa density of chemokine receptor gene expression combinations (positive expression) that are associated with Tregs that have obtained a T helper (Th)-type co-transcriptional program. Upper row from right to left: *CCR4* for Th2-skewed Tregs, *CCR6*, *CCR4* and *CCR10* expression for Th22-skewed Tregs, and *CCR6* and *CCR4* expression for Th17-skewed Tregs. Lower row from right to left: *CXCR3* and *CCR6* for Th1/Th17-skewed Tregs and *CXCR3* for Th1-skewed Tregs. The nebulosa density (based on kernel density) ranges from blue to yellow, with in yellow the highest kernel density, thus the highest (estimated) expression of the combination of genes.



Supplementary figure 5. Clonal expansion and clonal overlap of synovial fluid-derived Tregs. **(a)** Dimensionality reduction (UMAP) similar to Figure 1a but of a 10X genomics sequenced synovial fluid (SF)-derived Treg dataset (GSE160097) with the cells colored by cluster. Colors are identical to the clustering of Figure 1a. **(b)** Morisita, inverse Simpson, Chao and ACE diversity indexes calculated per SF Treg cluster. Each index is a measure for the diversity of the T-cell receptor repertoire per cluster with higher values indicating less diversity of the repertoire. **(c)** Morisita diversity index for the similarity of the TCR repertoire the four SF Treg clusters and SF CD4 non-Treg cells based on the nucleotide sequence of both the TRA and TRB chain. The scale ranges from 0 to 1, with 0 indicating no overlap and 1 indicating identical repertoires.



Supplementary figure 6. CD161⁺GPR56⁺CXCL13⁺ synovial fluid Tregs are highly differentiated and suppressive cells. **(a)** Percentages of IFN γ (left), IL-2 (middle) and IL-17 (right) expression within control peripheral blood (PB) GPR56⁻CD161⁻, synovial fluid (SF) GPR56⁻CD161⁻ and SF CXCL13⁺ (GPR56⁺ and/or CD161⁺, and CXCL13⁺) Tregs (CD127^{low}CD25^{high}FOXP3⁺). control PB $n = 7$, SF $n = 6$. Data are representative of two independent experiments. **(b)** Representative gating strategy to sort CCR7⁺, CCR7⁻ (in PB), CCR7⁻GPR56⁻CD161⁻ (in SF) and CCR7⁻GPR56⁺ and/or CD161⁺ (in SF) Tregs for the suppression assay (gating of Tregs as per Supplementary figure 1a).

Extended Supplementary Data can be found at: <https://github.com/lutterl/PhD-thesis-supplementary-data>.

Chapter 4

Regulation of human regulatory T cell differentiation and functional adaptation in tissue and disease

Lisanne Lutter^{1,2}, Femke van Wijk¹

¹Center for Translational Immunology, Wilhelmina Children's Hospital, University Medical Centre Utrecht, Utrecht University, Utrecht 3508 AB, the Netherlands.

²Department of Gastroenterology and Hepatology, University Medical Centre Utrecht, Utrecht University, Utrecht 3508 AB, the Netherlands.

Manuscript in preparation

ABSTRACT

Regulatory T (Treg) cells are essential in immune homeostasis. Adaptation to tissue microenvironments is crucial for the survival and optimal functioning of Tregs. There seems to be more overlap in adaptation to, and differentiation of, inflamed and tumor tissue-derived Tregs than previously thought. However, there is still an incomplete picture of the similarities and discrepancies in the transcriptional program of Tregs derived from inflammatory and tumor tissue microenvironments. Here, we integrated publicly available bulk RNA-sequencing datasets. We explored shared and distinct genes, pathways and key regulators characterizing the transcriptional program of Tregs comparing PB to homeostatic tissue, and homeostatic tissue to inflammatory/tumor tissue. Tregs first adapt to the tissue microenvironment regulated by HOX genes followed by activation, interaction with and influence on the local tissue architecture and eTreg differentiation. Differentiation of Tregs in inflammatory/tumor conditions seems to coincide with increased oxidative phosphorylation. *BATF* is an important transcription factor in tissue adaptation and differentiation independent of the state of the tissue. *FOXP3*, *HDGF* and *NR3C2* are shared regulators of the transcriptional program in both inflamed and tumor tissue-derived Tregs. These data enable exploration of tissue- and setting-specific Treg markers that could be employed in therapeutic strategies in the inflammatory and tumor microenvironment.

INTRODUCTION

Regulatory T cells (Tregs) are key players in preserving immune homeostasis by maintaining unresponsiveness to self-antigens and suppressing proinflammatory immune responses. The importance of Tregs is shown by mutations in the Treg transcription factor (TF) FOXP3 resulting in severe autoimmune responses in both mice and humans.^{1,2} Like other T cell subsets, Tregs can reside and exert their function in tissues. In tissue sites, Tregs differentiate into specialized activated effector (e)Tregs. eTregs maintain a strong core Treg signature with high expression of FOXP3, IKZF2 (encoding Helios) and IL2RA (encoding CD25) compared to peripheral blood (PB) Tregs. eTregs also acquire effector molecules including PDCD1 (encoding PD1), TNFRSF8 and ICOS.³⁻¹⁰ Moreover, Tregs can adapt to the local microenvironment by obtaining key TFs and chemokine receptor expression associated with the specific microenvironment.⁴ For example, in T helper (Th)-1 polarized inflammatory microenvironments such as the synovial fluid of patients with juvenile idiopathic arthritis Tregs co-express a Th1-program including T-bet and CXCR3.^{8,11} Adaptation to the local microenvironment can also lead to new roles for Tregs. In visceral adipose tissue, Tregs play a dominant role in metabolic homeostasis,¹² whereas Tregs in skin and gut can promote wound repair and are involved in local stem cell maintenance.^{13,14} Tregs in the tumor microenvironment prevent antitumor responses via suppression of the effector tumor-infiltrating lymphocytes, and thus can promote tumor progression.¹⁵ Overall, adaptation of Tregs to the local microenvironment ensures survival of Tregs and enables their local functioning.

An open question that remains to be addressed is to what extent the transcriptional program of Tregs adapting to effector tissue sites is conserved irrespective of the tissue type. Furthermore, the TF network that is crucial in adaptation to, and differentiation of, homeostatic, inflamed and tumor tissue environments are not fully clear. This knowledge will help our understanding of Treg adaptation and functioning at tissue sites. This might also identify tissue- or state-specific markers to be employed in therapeutic strategies, both in cancer and autoimmunity. In cancer, the holy grail is to identify tumor specific Treg targets/regulators that when targeted have limited side effects. Recent studies, however, indicate that Tregs from an (auto)inflammatory versus tumor microenvironment are more similar than previously thought.⁸ There is still an incomplete picture of the overlap and discrepancies between Tregs derived from inflammatory and tumor tissue environments. Here, we have integrated publicly available bulk RNA-sequencing datasets consisting of PB Tregs in homeostatic conditions, homeostatic tissue Tregs, chronic inflammation-derived tissue Tregs and tumor-derived tissue Tregs. We assessed which genes characterize PB to homeostatic tissue adaptation, and homeostatic to inflammatory/tumor tissue adaptation. Lastly, we performed regulatory gene network and enrichment analyses to identify which TFs regulate these adaptational transitions. The integrated PB and tissue-derived Treg data reveal that Tregs upon migration from the periphery first adapt to the tissue environment regulated by HOX genes. This is followed by activation, interaction with and influence on the local tissue architecture and eTreg differentiation with the eTreg profile becoming stronger in inflamed

and tumor tissue. Differentiation of Tregs in inflammatory/tumor conditions seems to coincide with increased oxidative phosphorylation. *BATF* is an important TF in this adaptation and differentiation independent of the state of the tissue. *FOXP3*, *HDGF* and *NR3C2* are shared important regulators of the transcriptional program in both inflamed and tumor tissue-derived Tregs. Further defining inflamed and tumor tissue-derived Tregs were chemokines and chemokine receptors, with *CCL4* being specifically upregulated in inflamed and tumor but not homeostatic tissue-derived Tregs.

RESULTS AND DISCUSSION

HOX genes are involved in tissue adaptation of Tregs

We set out to define the transcriptional program of a Treg that migrates from the PB to homeostatic tissue, and subsequently to inflamed or tumor tissue. This concerned the shared programming irrespective of the type of tissue, the type of inflammation and the type of tumor. Clustering analyses indicated that Tregs derived from homeostatic tissue sites are diverging from PB-derived Tregs, but some overlap is still observed. In contrast, inflammation- and tumor-derived Tregs overlap but cluster separately from PB-derived Tregs (Supplementary Figure 1A). Several HOX genes were highly upregulated in homeostatic tissue-derived compared to PB-derived Tregs (i.e. *HOXC10*, *HOXB6*, *HOXC6*, *HOXA3*, *HOXA7* and *HOXA9*) (Figure 1A). HOX genes are crucial TFs in the embryonic development via regulation of proliferation, differentiation, migration and apoptosis. Expression of HOX genes has also been shown in organ tissue of adults which indicates that HOX genes are also of importance in tissue maintenance.¹⁶ Upregulation of HOX genes in tissue sites suggests that the cellular identity of tissue Tregs is modified or fine-tuned. In addition, migration towards homeostatic tissue sites coincides with upregulation of pathways associated with cell activation (Figure 1B).

Most HOX genes were downregulated again in inflamed and tumor tissue Tregs compared to homeostatic tissue Tregs (Figure 1A). Previous research has shown that PB-derived T cells downregulate HOX genes upon activation.¹⁷ Indeed, besides HOX gene downregulation both inflammation- and tumor-derived Tregs showed extensive upregulation of the activation-associated HLA class II genes, *TNFRSF9* (CD137), *TNFRSF4* (OX40), *IL1R1* (CD121a) and *IL1R2* (CD121b) (Figure 1A).¹⁸⁻²² These were upregulated in all tissue Tregs, except for *ENTPD1* (CD39) which was only upregulated in tumor-derived tissue Tregs (Figure 1A). Gene ontology analysis also indicated that inflammation- and tumor-derived Tregs showed further activation with upregulation of TCR, NFκB and cytokine-mediated signaling (Figure 1C). Together these data indicate that HOX genes enable Tregs to establish themselves at tissue sites, with activation further fine-tuning the Treg transcriptional program.

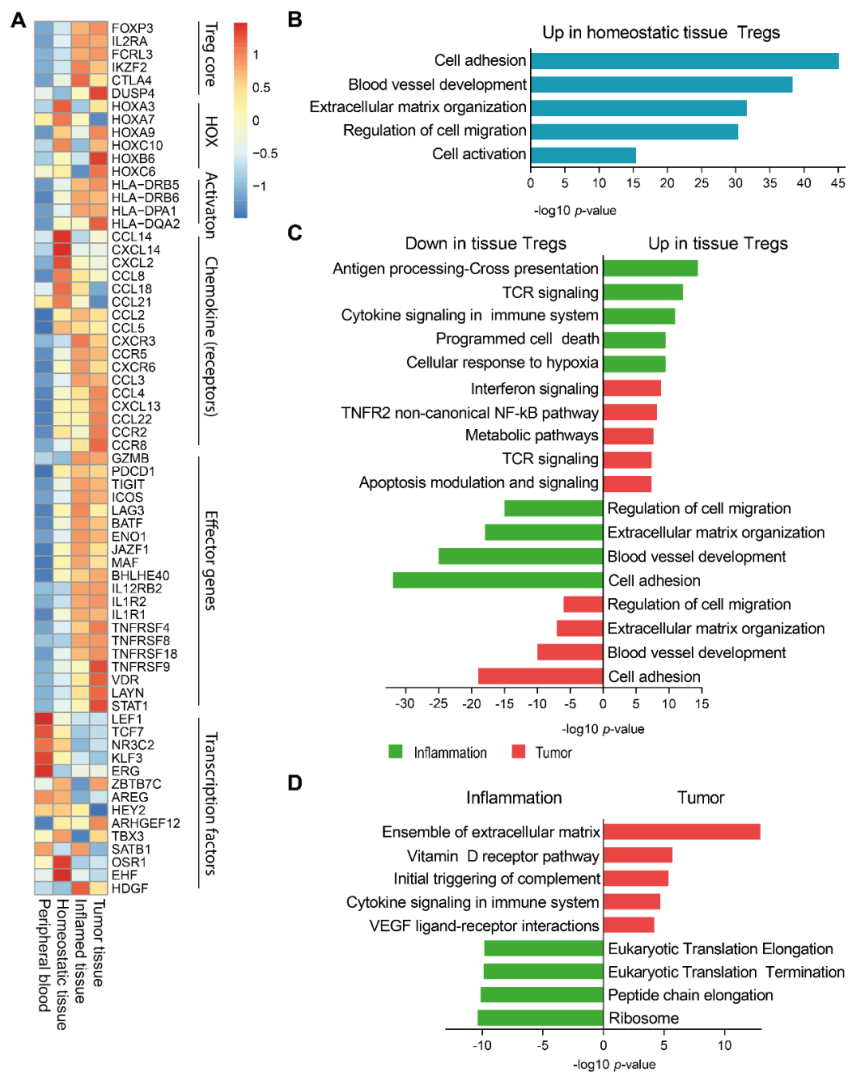


Figure 1. Treg tissue adaptation and effector Treg differentiation. (A) Heatmap of selected genes in the RNA-sequencing dataset, based on differential gene expression analysis (p -adjusted value < 0.1) and literature. The transformed median gene expression count data per group; homeostatic peripheral blood (PB) Tregs, homeostatic tissue Tregs, inflamed tissue Tregs and tumor tissue Tregs, are plotted. The genes are centered and scaled per row. (B) Selected upregulated biological process and pathway terms related to PB versus homeostatic tissue Tregs. No pathways or processes were downregulated. (C) Similar to B but comparing homeostatic tissue and inflammatory/tumor tissue Tregs (green = inflammation, red = tumor). (D) Similar to B but comparing inflamed and tumor tissue-derived Tregs.

Treg migration to tissue is associated with upregulation of chemokine (receptor) expression

Tregs have to migrate from the periphery to the tissue. Gene ontology analysis indeed revealed upregulation of processes related to adhesion, organization of cell migration and extracellular

matrix organization in homeostatic tissue Tregs compared to PB Tregs. Genes involved include the integrin-coding genes (e.g. *ITGA1*, *ITGA2*, *ITGB4*), matrix metalloproteinases (e.g. *MMP2*, *MMP7*, *MMP19*) and collagen chains (e.g. *COL4A6*, *COL5A1*, *COL5A2*). These pathways were downregulated again in inflamed and tumor tissue (Figure 1B,C), except for expression of most chemokines and chemokine receptors (Figure 1A). Comparing PB to homeostatic tissue-derived Tregs there was increased expression of many chemokines and chemokine receptors (e.g. *CCL21*, *CXCL13*, *CXCR3*, *CCR5*, *CXCR6* and *CCL8*) (Figure 1A). Chemokines and chemokine receptors allow for migration of cells themselves, the attraction of, and communication with other cells, but also the differentiation of a cell.²³ This wide range of chemokine and chemokine receptor expression suggests that Tregs are capable of contributing to the local tissue architecture by attracting both immune and stromal cells, and perform cell-cell communication with a variety of cells. Interestingly, in murine models of experimental autoimmune encephalitis and islets allograft rejection both CCL4 and CCL3 were expressed by Tregs. This allowed for attraction of pathogenic CD4 and CD8 T cells to enable immunosuppression by Tregs for which they need to be in close proximity of the target cell.²⁴ In our analysis, CCL3 was only upregulated in Tregs from inflamed compared to homeostatic tissue and CCL4 in Tregs from both inflamed and tumor compared to homeostatic tissue, but not in homeostatic tissue Tregs compared to PB Tregs. Blockade of CCL4 in the tumor microenvironment could therefore be explored to block immunosuppression of CD4 and CD8 T cells, and allow for tumor cell killing by effector T cells.

Comparing Tregs derived from inflamed and tumor tissue revealed that tumor-derived Tregs showed enrichment of extracellular matrix organization, VEGF(R) signaling and adhesion indicating a role for tissue organization in tumors, which is less apparent in inflammation (Figure 1D). In the tumor setting the formation of lymph and blood vessels and remodeling of the tissue is observed.²⁵ It seems that tumor-derived Tregs may contribute to the remodeling process. In inflammation there is less tissue remodeling but mainly loss of tissue architecture, such as loss of crypts and epithelial cells in the intestinal mucosa of patients with Crohn's disease.²⁶

Strengthened core Treg signature in tissue Tregs

Activation of Tregs after antigen-recognition and migration to effector sites is followed by local eTreg differentiation. We and others have recently shown the acquisition of an eTreg phenotype in homeostatic, tumor and inflamed tissue sites in humans. The eTreg phenotype is defined by upregulation of several effector molecules to enhance the suppressive function of Tregs. Effector molecules include ICOS, PDCD1, VDR and TNF receptor super family (TNFRSF) members.³⁻¹⁰ We indeed observed expression of eTreg-associated genes in homeostatic tissue- compared to PB-derived Tregs, which increased even more in both inflamed and tumor tissue-derived Tregs (Figure 1A). Upon activation and eTreg differentiation, Tregs maintain their core Treg signature. This core signature consists of *FOXP3*, *CTLA4*, *DUSP4*, *IKZF2* (encoding Helios), *IL2RA* (encoding CD25) and *FCRL3* among others.^{27,28} Homeostatic tissue Tregs did not show a strengthened core Treg signature compared to PB-

derived Tregs, but both inflammation- and tumor-derived Tregs did show higher expression of core Treg genes (Figure 1A). Strengthening of the core Treg signature seems to coincide with acquisition of a Th co-transcriptional program in inflammatory/tumor conditions.⁸ This upregulated core Treg signature could therefore be required to maintain the Treg functional profile and prevent acquisition of Th-specific functions or loss of regulatory functions. Indeed, loss of FOXP3 in Tregs and conversion to ‘exTregs’ that are autoreactive and produce cytokines turning them pathogenic has been shown to occur in non-physiological conditions (reviewed in ²⁹). Tregs derived from inflamed tissue showed high expression of *SATB1*. FOXP3 represses *SATB1* expression which is crucial to maintain the Treg phenotype and suppressive function, while preventing effector T cell differentiation.³⁰ In seasonal allergic rhinitis, *SATB1*-expressing Tregs were not able to suppress the ongoing Th2-responses.³¹ If *SATB1* is not sufficiently repressed by FOXP3 in inflammatory conditions this could impair their suppressive function, and allow adaptation of Th-related cytokine production. *TGFB1* was more highly expressed in inflamed versus homeostatic tissue-derived Tregs as well as in inflamed compared to tumor tissue-derived Tregs. TGF- β suppresses the expression of *SATB1*,^{32,33} and could be an additional autoregulatory mechanism to maintain the Treg profile and function while also allowing adaptation to a Th-polarized environment via *SATB1*.

Gene set enrichment analysis of hallmark gene sets representing well-defined biological states or processes supported that Tregs in a non-homeostatic tissue (i.e. tumor and inflamed tissue) are further differentiated compared to homeostatic tissue Tregs. Hallmark pathways associated with cytokine responses were all enriched in inflamed and tumor compared to homeostatic tissue-derived Tregs, and not in homeostatic tissue compared to PB-derived Tregs. Especially type I and type II interferon signaling as well as IL-6 signaling were enriched in inflamed and tumor tissue-derived compared to homeostatic tissue-derived Tregs (Figure 2A). Interestingly, although *VDR* is upregulated in both homeostatic and inflamed tissue-derived Tregs, the highest expression of *VDR* was observed in the tumor setting (Figure 1A). The vitamin D receptor pathway was also enriched in tumor versus inflamed tissue Tregs (Figure 1D). *VDR* has tolerogenic effects and seems to increase Treg effector molecule expression. There might be a tissue or inflammation specific effect at play since we did previously show that *VDR* is a key regulator of synovial fluid-derived Tregs.⁸ These data reveal both extensive overlap in adaptive processes as well as some differences between Tregs derived from inflamed and tumor tissue. Overall, genes and pathways more highly associated tumor tissue-derived Tregs seem to be connected with enforcing a tolerogenic profile.

Activation of T cells is commonly associated with glycolysis but there was no enrichment for glycolysis observed in any of the tissue-derived Tregs, even though mTORC1 and PI3K-AKT signaling were enriched (Figure 2A). PI3K/Akt/mTOR activation are known to induce a shift towards aerobic glycolysis via *Glut1*.^{34,35} Moreover, oxidative phosphorylation was enriched in inflamed and tumor tissue-derived Tregs (Figure 2A). FOXP3 itself can drive the gene set involved in fatty acid metabolism and oxidative phosphorylation.³⁶ Both in inflamed and tumor compared to homeostatic tissue the expression of FOXP3 was upregulated which may drive this metabolic pathway. Oxidative phosphorylation can protect

cells from fatty acid-induced cell death which is observed in both the inflamed and tumor tissue microenvironments.³⁶ In summary, these data indicate that there is a gradual differentiation of Tregs with maintenance of the core Treg signature and a possible protective increase of oxidative phosphorylation in Tregs in non-homeostatic tissues.

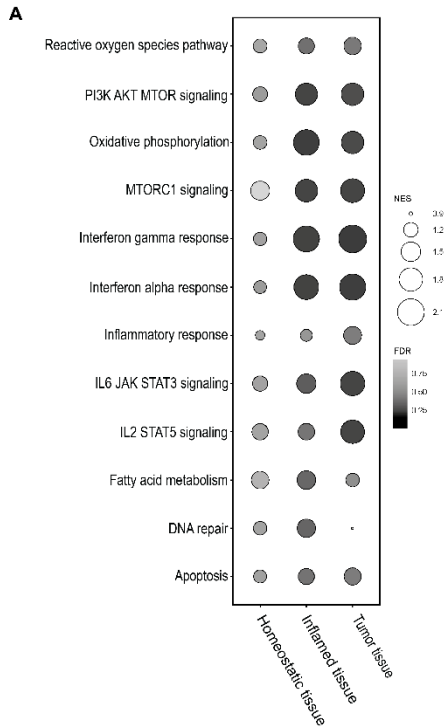


Figure 2. Hallmark gene set enrichment in non-homeostatic tissue-derived Tregs. (A) Gene set enrichment analysis of selected Hallmark gene sets (MSigDB) in pairwise comparisons involving peripheral blood (PB) Tregs and homeostatic tissue Tregs (right), homeostatic tissue Tregs and inflamed tissue Tregs (middle) and homeostatic tissue Tregs and tumor tissue Tregs (left). Circle size represent the normalized enrichment score (NES, bigger means more enrichment) and color represents the FDR statistical value (FDRq, multiple hypothesis testing using sample permutation; darker means more significantly enriched). Only hallmark gene sets that were significantly enriched in at least one of the comparisons are shown.

BATF, FOXP3, HDGF and NR3C2 are key regulators of the Treg transcriptional program in non-homeostatic tissue

Lastly, we performed a data-driven network and enrichment analysis (RegEnrich³⁷). We assessed which key regulators, based on TFs and co-factors, are important in differentiation of Tregs from PB to homeostatic tissue, and from homeostatic tissue to inflamed and tumor tissue. Predicted key regulators of PB to homeostatic tissue Treg differentiation included HOX genes, *ZBTB7*, *TBX3*, *HEY2* and *ETV7* which were all first described for their role in embryonic development.³⁸ This set of regulators were not linked to Treg function or differentiation but seem to establish tissue adaptation. On the other hand, *BATF*, *BHLHE40*, *AHRGEF12*, *VDR* and

MAF were predicted key regulators with downstream linked genes involved in activation and eTreg differentiation. *BATF*, *VDR* and *MAF* have also previously been described as important TFs in both tissue Tregs and eTreg differentiation.^{5,7-9} Regulators that are downregulated in tissue Tregs included *TCF7* and *BACH2* (Figure 3A), with loss of *TCF7* associated with maturation of eTreg cells.³⁹

BATF, *FOXP3*, *HDGF* (positive) and *NR3C2* (negative) were predicted top key regulators in both inflammation and tumor-derived Tregs (Figure 3B,C). *HDGF*, hepatoma-derived growth factor, has been shown to induce Tregs,⁴⁰ but its role in eTregs in non-homeostatic tissue conditions remains to be elucidated. *NR3C2* encodes the mineralocorticoid receptor which has been linked to an inflammatory phenotype in immune cells.⁴¹ Its downregulation in non-homeostatic conditions could thus be a protective mechanism to prevent proinflammatory differentiation of Tregs. Downstream genes of *NR3C2* were involved in the TNFR2 signaling pathway. TNFR2 signaling is involved in immunomodulation and tissue regeneration. Upon activation of Tregs TNFR2 signaling is upregulated. Although not required for maintenance of immune homeostasis in non-inflammatory conditions, its absence in Tregs derived from inflammatory conditions is associated with autoimmunity.⁴² *TNFRSF1B* (encoding TNFR2) was only increased in tumor compared to homeostatic tissue-derived Tregs, but other TNFRSF members in the TNFR2 signaling pathway (e.g. *TNFRSF8* and *TNFRSF18*) were increased in both inflamed and tumor tissue-derived Tregs.

In addition to the shared key regulators there were also regulators that were more specific for inflamed or tumor tissue-derived Tregs. *EHF* was the top predicted negative regulator for inflamed compared to homeostatic tissue-derived Tregs (Figure 3B,C). Its suppression can induce Tregs and their proliferation.⁴³ *ENO1*, encoding the glycolytic enzyme enolase 1, is known to be upregulated upon activation and eTreg differentiation.⁸ This was a positive key regulator of Tregs from inflamed tissue. Genes downstream of *ENO1* related to activation, cytokine-cytokine receptor signaling and TNF receptor superfamily signaling involved in the effector function of Tregs. We have also previously identified *VDR* as key regulator of eTreg differentiation and showed that vitamin D increases eTreg gene expression.⁸ The predicted key regulator network of tumor-derived tissue Tregs reveals that *VDR* is especially important in the tumor microenvironment, also supported by upregulation of the *VDR* pathway on gene ontology level (Figure 1B). *STAT1* was also identified as a tumor-derived Treg specific regulator. *STAT1* is typically associated with Tregs present in a Th1-polarized environment. The tumor types included in the integrated RNA-sequencing dataset comprised colorectal cancer, melanoma and breast cancer. These are not typically characterized by a predominant Th1-polarized environment. The genes downstream of *STAT1* did include *CCR1* and *CCR5* but not *TBX21* or *CXCR3*. *STAT1* was associated with many effector genes such as *CTLA4*, *ICOS*, *LTA*, *LTB* and *ICOS*. Whether *STAT1* itself is active in eTreg differentiation in the tumor environment will also depend on its phosphorylation status, which has to be further addressed. In summary, these data show that the TF network important in tissue Tregs consistently show *BATF* as crucial in tissue adaptation. *FOXP3*, *HDGF* and *NR3C2* are predicted to be important in Treg adaptation in non-homeostatic conditions. Divergence of the TF

network in inflamed and tumor tissue-derived Tregs is also observed. This indicates that although much of the transcriptional program in tissue microenvironments is conserved, inflammation and tumor-specific differences are present. In conclusion, the differences between Tregs derived from homeostatic, inflamed and tumor tissue could be explored for setting-specific targeting of Tregs in therapeutic strategies.

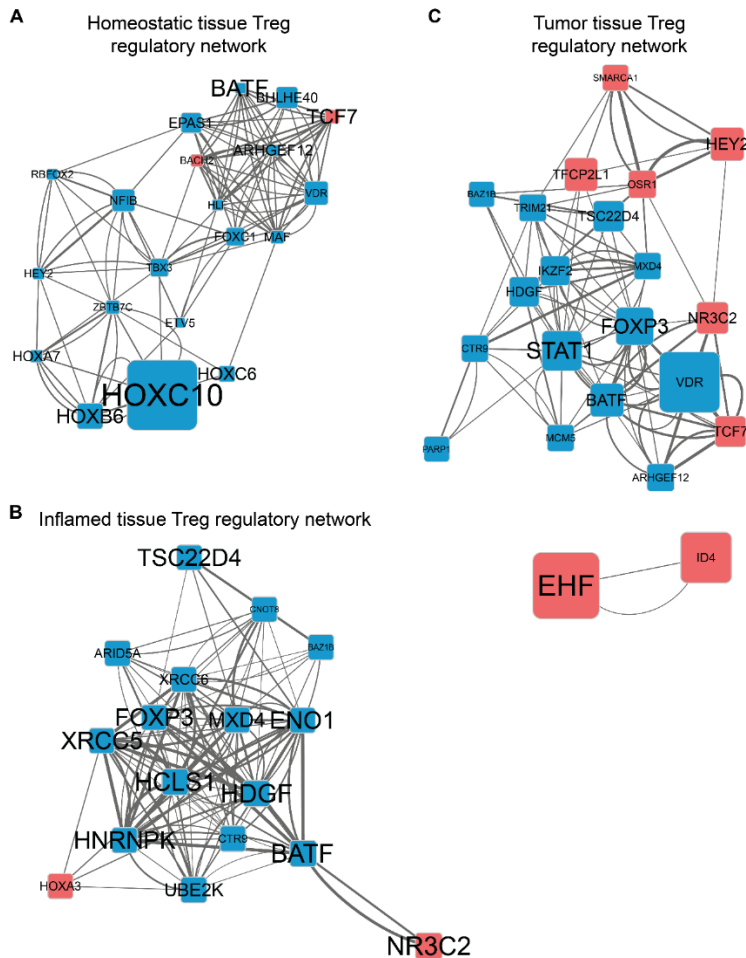


Figure 3. Predicted key regulators Treg tissue adaptation. (A) Network inference of the top 20 key regulators correlating with peripheral blood to homeostatic tissue Treg adaptation, based on unsupervised gene regulatory network analysis followed by gene set enrichment analysis of the transcription factors (TFs) and co-factors (pink = downregulation, blue = upregulation). The grey lines indicate connections between regulators (TFs) and their downstream targets (only TFs are shown), the line thickness represents the correlation weight (thicker = higher correlation). Square size indicates $-\log_{10}(p)$ for each comparison, with the p -value derived from differential expression analysis (\log_2 fold change >1 and p -adjusted value <0.1), text size represents the RegEnrich score; for both, larger indicates higher scores. (B) Similar to A but for homeostatic to inflamed tissue-derived Tregs. (C) Similar to A but for homeostatic to tumor tissue-derived Tregs. Square and text size, and line thickness of the network graphs are not comparable amongst the networks.

METHODS

Transcriptome data

Datasets were derived in-house or searched on the NCBI-GEO database and Pubmed according to the following criteria: regulatory T cells (Tregs), *Homo Sapiens* and high throughput sequencing (i.e. bulk RNA-seq, single cell RNA-seq and microarray datasets were not included). Subsequently, the datasets containing FACS-sorted Tregs derived from tissue sites, with or without concordant PB-derived Tregs, were included. Table 1 contains an overview of the included datasets. All the selected external datasets were downloaded as FASTQ files using the fastq-dump tool from sratoolkit. Quality of the FASTQ files was assessed with FASTQC, and Trimmomatic v0.39⁴⁴ was used to remove low quality reads and adapter contamination. For GSE89225, samples were run on multiple lanes and the FASTQ files of the different lanes were concatenated before further processing. FASTQ files were then aligned to the reference genome (GRCh38.103) using the HISAT2 aligner,⁴⁵ and converted to BAM files with samtools.⁴⁶ The resulting BAM files were used to calculate the count of the aligned reads using the Rsubread⁴⁷ package featureCounts in R v4.0. In-house datasets were processed as previously described.^{8,9,48} Shortly, the reads were demultiplexed and aligned to the human cDNA reference genome (hg38) using BWA (version 0.7.13). Multiple reads mapping to the same gene with the same unique molecular identifier were counted as a single read, and raw counts of splice variants were summed. In-house dataset (GSE161426) was aligned to a reference transcriptome. Subsequently, quality control of the samples was performed within each dataset. The number of samples in Table 1 refer to the samples that passed the quality control. The publicly available and in-house datasets were mapped with different mappers (BWA and HISAT2); however, a recent publication showed that the influence of which mapper was used has no significant impact on the final results. The program employed for differential gene expression program is of higher impact on correctly identifying differentially expressed genes, with DESeq2 being most true compared to qPCR output regarding differentially expressed genes.⁴⁹

Table 1. Description of the regulatory T cell RNA-sequencing datasets.

Series	Platform	Reads	Sort (within CD4 ⁺)	Control/disease	Sample type	Number (excluded)
In-house ⁸ / GSE161426	Illumina NextSeq 500	75 bp SE	CD127 ⁺ CD25 ^{hi}	Control	PB	n = 4
				adult	PB	n = 4
				Control child JIA child	SF	n = 4
In-house ⁹	Illumina NextSeq 500	75 bp PE	CD127 ⁺ CD25 ^{hi}	Pregnan cy (paired)	PB	n = 5
					Uterus incision	n = 4
					Uterus placentabed	n = 5
In-house ⁴⁸	Illumina NextSeq 500	75 bp PE	CD127 ⁺ CD25 ^{hi}	Control	Ileum	
					- Epithelium	n = 1
					- Lamina propria Ileum NI	n = 3

				Crohn's disease	- Epithelium - Lamina propria Ileum I	n = 4 n = 4
				Crohn's disease (paired)	- Epithelium - Lamina propria	n = 3 n = 3
In-house	Illumina NextSeq 500	75 bp PE	CD25 ^{hi}	Crohn's disease CRC	Colon NI - Epithelium - Lamina propria Colon homeostatic - Epithelium	n = 5 n = 4 n = 1
GSE139341 ⁵⁰	Illumina HiSeq 2500	50 bp PE	CD25 ⁺ CD27 ⁺	Control Psoriasis	Skin Skin	n = 4 n = 5
GSE139372 ⁵⁰	Illumina HiSeq 2500	50 bp PE	CD25 ⁺ CD27 ⁺	Melanoma	Skin	n = 2
GSE74102 ⁵¹	ABI solid4 system	50 bp SE	CD127 ⁻ CD25 ⁺	CRC (paired)	Colon - steady state - tumor	n = 6
GSE116347 ⁵²	Illumina NextSeq 500	25 bp PE	CD127 ⁻ CD25 ⁺	Control FL RLN	LN LN LN	n = 10 n = 11 n = 4
GSE89225 ⁵³	Illumina HiSeq 2500	50 bp PE	CD25 ^{hi}	Breast cancer (1 paired sample)	Controlateral breast (control) Breast tumor	n = 5 n = 3
GSE89225 ⁵³	Ion Torrent	200 bp SE	CD25 ^{hi} CD45R A ^{+/-}	Control (paired) Breast cancer	PB - memory - naïve Breast	n = 4 n = 4 n = 3
GSE115898 ⁵⁴	Illumina HiSeq 2500	100 bp PE	CD25 ⁺ CD27 ⁺	Control	Skin	n = 4
E-MTAB-9112 ⁵⁵	Illumina HiSeq 2500	100 bp PE	CD25 ⁺ CD45RA ⁻	Breast cancer	Non-invaded LN Invaded LN Breast	n = 2 n = 2 n = 2

bp, base pairs; CRC, colorectal cancer; FL, follicular lymphoma; I, inflamed; JIA, Juvenile Idiopathic Arthritis; LN, lymph node; NI, non-inflamed; PB, peripheral blood, PE, paired-end; RLN, reactive lymph node; SE, single-end; SF, synovial fluid.

Data integration

The ensemble gene annotations were converted to HGNC gene symbols with BioMart,⁵⁶ with the highest expressed ensemble gene selected if multiple ensemble annotations mapped to the same HGNC gene symbol. All gene count data files were concatenated with zero's filled out for

genes that were not detected in a respective dataset. The data were then filtered based on a median gene expression > 1 among all samples before integration. The filtered data were GC content percentage normalized (withinLaneNormalization; upper-quartile normalization, 10 bins), and between-sample normalization was performed (betweenLaneNormalization; full normalization).^{57,58} Thereafter, the RUVg method was employed to identify residual factors contributing to the batch effect ($k = 11$).⁵⁹ The k was chosen based on when the RLE plots were evenly distributed and zero-centered, correlation between the PCs and the parameters of interest (especially the type of sample; e.g. homeostatic, inflamed, tumor Tregs derived from PB or tissue) was optimal and with study minimal, and clustering on the PCA plot was void of an observable study batch effect. Negative control genes used to determine the residual factors were comprised of the genes that were not differentially expressed ($p > 0.1$) nor outliers in pairwise comparisons of the Tregs within each dataset separately. The genes curated from these comparisons that were present in every dataset were selected resulting in a gene set of 88 control genes that do not change across conditions (Supplementary Table 1).

Transcriptome analysis

The resulting data matrix consisted of 25,174 genes with a total of 130 samples. Differential analysis was performed using DESeq2⁶⁰ (Wald's test) with a p -adjusted value < 0.1 considered statistically significant. Comparisons were made from PB to tissue Tregs during homeostasis, and from tissue Tregs in homeostatic conditions to both inflammation-derived and tumor tissue Tregs. This was performed irrespective of the type of tissue and the type of inflammation or tumor. For visualization purposes the R package pheatmap and ggplot2 were employed. The counts were transformed employing $\log_2(\text{offset counts} + 1)$ transformation. We then used the median gene expression for each tissue-type (homeostatic PB, homeostatic tissue, inflamed tissue and tumor tissue) for the heatmaps. Pathway analysis was performed on the differentially expressed genes as input in Topfun with standard settings. Gene set enrichment analysis (GSEA v4.2.3⁶¹), with as input the normalized data (output DESeq2) was used to assess enrichment of the hallmark gene sets (H collection MSigDB). One thousand random permutations of the gene sets were used to establish a null distribution of enrichment score against which a normalized enrichment score and FDR-corrected q values were calculated. Identification of key regulators was performed using RegEnrich v1.0.1³⁷ based on the differential gene expression data followed by unsupervised gene regulatory network inference (GENIE3) to construct a network based on the raw gene count data, and GSEA was used for enrichment analysis (standard settings). Network visualization was performed with Cytoscape v3.2.1.⁶²

Acknowledgements

We thank Aridaman Pandit and Judith Wienke for discussions on data analysis, and Michal Mokry for providing us with the raw count matrices of the in-house RNA-sequencing datasets.

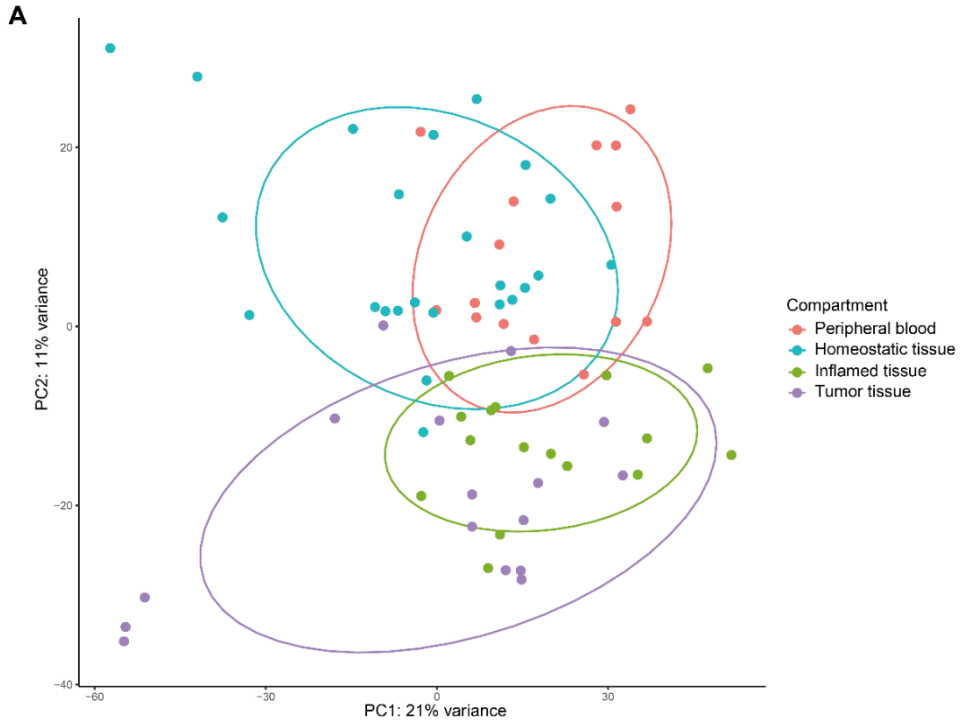
REFERENCES

1. Brunkow, M. E. *et al.* Disruption of a new forkhead/winged-helix protein, scurfin, results in the fatal lymphoproliferative disorder of the scurfy mouse. *Nat. Genet.* **27**, 68–73 (2001).
2. Ochs, H. D. *et al.* The immune dysregulation, polyendocrinopathy, enteropathy, X-linked syndrome (IPEX) is caused by mutations of FOXP3. *Nat. Genet.* **27**, 20–21 (2001).
3. Teh, P. P., Vasanthakumar, A. & Kallies, A. Development and Function of Effector Regulatory T Cells. in *Progress in Molecular Biology and Translational Science* 155–174 (2015).
4. Liston, A. & Gray, D. H. D. Homeostatic control of regulatory T cell diversity. *Nat. Rev. Immunol.* **14**, 154–65 (2014).
5. Miragaia, R. J. *et al.* Single-Cell Transcriptomics of Regulatory T Cells Reveals Trajectories of Tissue Adaptation. *Immunity* **50**, 493–504.e7 (2019).
6. Delacher, M. *et al.* Genome-wide DNA-methylation landscape defines specialization of regulatory T cells in tissues. *Nat. Immunol.* **18**, 1160–1172 (2017).
7. Hayatsu, N. *et al.* Analyses of a Mutant Foxp3 Allele Reveal BATF as a Critical Transcription Factor in the Differentiation and Accumulation of Tissue Regulatory T Cells. *Immunity* **47**, 268–283 (2017)
8. Mijnheer, G. *et al.* Conserved human effector Treg cell transcriptomic and epigenetic signature in arthritic joint inflammation. *Nat. Commun.* **12**, 2710 (2021).
9. Wienke, J. *et al.* Human Tregs at the materno-fetal interface show site-specific adaptation reminiscent of tumor Tregs. *JCI insight* **5**, e137926 (2020).
10. Vasanthakumar, A. *et al.* The TNF Receptor Superfamily-NF- κ B Axis Is Critical to Maintain Effector Regulatory T Cells in Lymphoid and Non-lymphoid Tissues. *Cell Rep.* **20**, 2906–2920 (2017).
11. Lutter, L. *et al.* Human regulatory T-cells locally differentiate and are functionally heterogeneous within the inflamed arthritic joint. *bioRxiv* 2022.02.18.480998 (2022).
12. Vasanthakumar, A. *et al.* The transcriptional regulators IRF4, BATF and IL-33 orchestrate development and maintenance of adipose tissue-resident regulatory T cells. *Nat. Immunol.* **16**, 276–285 (2015).
13. Povoleri, G. A. M. *et al.* Human retinoic acid-regulated CD161 + regulatory T cells support wound repair in intestinal mucosa. *Nat. Immunol.* **19**, 1403–1414 (2018).
14. Kalekar, L. A. *et al.* Regulatory T cells in skin are uniquely poised to suppress profibrotic immune responses. *Sci. Immunol.* **4**, aaw2910 (2019).
15. Plitas, G. *et al.* Regulatory T Cells Exhibit Distinct Features in Human Breast Cancer. *Immunity* **45**, 1122–1134 (2016).
16. Takahashi, Y. *et al.* Expression profiles of 39 HOX genes in normal human adult organs and anaplastic thyroid cancer cell lines by quantitative real-time RT-PCR system. *Exp. Cell Res.* **293**, 144–153 (2004).
17. Morgan, R. & Whiting, K. Differential expression of HOX genes upon activation of leukocyte subpopulations. *Int. J. Hematol.* **87**, 246–249 (2008).
18. Holling, T. M., van der Stoep, N., Quinten, E. & van den Elsen, P. J. Activated human T cells accomplish MHC class II expression through T cell-specific occupation of class II transactivator promoter III. *J. Immunol.* **168**, 763–770 (2002).
19. Tran, D. Q. *et al.* Selective expression of latency-associated peptide (LAP) and IL-1 receptor type I/II (CD121a/CD121b) on activated human FOXP3+ regulatory T cells allows for their purification from expansion cultures. *Blood* **113**, 5125–33 (2009).
20. Schoenbrunn, A. *et al.* A converse 4-1BB and CD40 ligand expression pattern delineates activated regulatory T cells (Treg) and conventional T cells enabling direct isolation of alloantigen-reactive natural Foxp3+ Treg. *J. Immunol.* **189**, 5985–5994 (2012).
21. Seddiki, N. *et al.* Human antigen-specific CD4+CD25+CD134+CD39+ T cells are enriched for regulatory T cells and comprise a substantial proportion of recall responses. *Eur. J. Immunol.* **44**, 1644–1661 (2014).
22. Bacher, P. *et al.* Regulatory T Cell Specificity Directs Tolerance versus Allergy against Aeroantigens in

- Humans. *Cell* **167**, 1067-1078.e16 (2016).
23. Hughes, C. E. & Nibbs, R. J. B. A guide to chemokines and their receptors. *FEBS J.* **285**, 2944–2971 (2018).
 24. Patterson, S. J. *et al.* T regulatory cell chemokine production mediates pathogenic T cell attraction and suppression. *J. Clin. Invest.* **126**, 1039–1051 (2016).
 25. Markert, E. K., Levine, A. J. & Vazquez, A. Proliferation and tissue remodeling in cancer: the hallmarks revisited. *Cell Death Dis.* **3**, e397–e397 (2012).
 26. Geboes, K. Histopathology of Crohn's disease and ulcerative colitis. *Inflamm. Bowel Dis.* (2003).
 27. Ferraro, A. *et al.* Interindividual variation in human T regulatory cells. *Proc. Natl. Acad. Sci. U. S. A.* **111**, 34–37 (2014).
 28. Pfoertner, S. *et al.* Signatures of human regulatory T cells: an encounter with old friends and new players. *Genome Biol.* **7**, R54 (2006).
 29. Saxena, V., Lakhani, R., Iyyathurai, J. & Bromberg, J. S. Mechanisms of exTreg induction. *Eur. J. Immunol.* **51**, 1956–1967 (2021).
 30. Beyer, M. *et al.* Repression of the genome organizer SATB1 in regulatory T cells is required for suppressive function and inhibition of effector differentiation. *Nat. Immunol.* **12**, 898–907 (2011).
 31. Froese van Dijck, A. *et al.* SATB1 is repressed in FoxP3+Tregs following Grass Pollen Subcutaneous and Sublingual Immunotherapy and Correlates with Clinical efficacy. *J. Allergy Clin. Immunol.* **139**, AB192 (2017).
 32. He, J. *et al.* Suppressive effect of SATB1 on hepatic stellate cell activation and liver fibrosis in rats. *FEBS Lett.* **589**, 1359–1368 (2015).
 33. Stephen, T. L. *et al.* SATB1 Expression Governs Epigenetic Repression of PD-1 in Tumor-Reactive T Cells. *Immunity* **46**, 51–64 (2017).
 34. MacIver, N. J., Michalek, R. D. & Rathmell, J. C. Metabolic Regulation of T Lymphocytes. *Annu. Rev. Immunol.* **31**, 259–283 (2013).
 35. Pearce, E. L., Poffenberger, M. C., Chang, C.-H. & Jones, R. G. Fueling immunity: insights into metabolism and lymphocyte function. *Science* **342**, 1242454 (2013).
 36. Howie, D. *et al.* Foxp3 drives oxidative phosphorylation and protection from lipotoxicity. *JCI Insight* **2**, e89160 (2017).
 37. Tao, W., Radstake, T. R. D. J. & Pandit, A. RegEnrich: An R package for gene regulator enrichment analysis reveals key role of ETS transcription factor family in interferon signaling. *bioRxiv* 2021.01.24.428029 (2021).
 38. Weizman Institute of Science. GeneCards The Human Gene Database. www.genecards.org. Accessed: May 20th 2022.
 39. Koizumi, S. & Ishikawa, H. Transcriptional Regulation of Differentiation and Functions of Effector T Regulatory Cells. *Cells* **8**, 939 (2019).
 40. Sun, A.-M. *et al.* Hepatocarcinoma cell-derived hepatoma-derived growth factor (HDGF) induces regulatory T cells. *Cytokine* **72**, 31–35 (2015).
 41. Muñoz-Durango, N. *et al.* Modulation of Immunity and Inflammation by the Mineralocorticoid Receptor and Aldosterone. *Biomed Res. Int.* **2015**, 652738 (2015).
 42. Yang, S., Wang, J., Brand, D. D. & Zheng, S. G. Role of TNF–TNF Receptor 2 Signal in Regulatory T Cells and Its Therapeutic Implications. *Frontiers in Immunology* **19**, 784 (2018).
 43. Liu, J. *et al.* Tumoral EHF predicts the efficacy of anti-PD1 therapy in pancreatic ductal adenocarcinoma. *J. Exp. Med.* **216**, 656–673 (2019).
 44. Bolger, A. M., Lohse, M. & Usadel, B. Trimmomatic: a flexible trimmer for Illumina sequence data. *Bioinformatics* **30**, 2114–2120 (2014).
 45. Kim, D., Paggi, J. M., Park, C., Bennett, C. & Salzberg, S. L. Graph-based genome alignment and genotyping with HISAT2 and HISAT-genotype. *Nat. Biotechnol.* **37**, 907–915 (2019).
 46. Li, H. *et al.* The Sequence Alignment/Map format and SAMtools. *Bioinformatics* **25**, 2078–2079 (2009).
 47. Liao, Y., Smyth, G. K. & Shi, W. The R package Rsubread is easier, faster, cheaper and better for

- alignment and quantification of RNA sequencing reads. *Nucleic Acids Res.* **47**, e47–e47 (2019).
48. Lutter, L. *et al.* Compartment-driven imprinting of intestinal CD4 (regulatory) T cells in inflammatory bowel disease and homeostasis. *bioRxiv* 2022.05.06.490870 (2022).
 49. Costa-Silva, J., Domingues, D. & Lopes, F. M. RNA-Seq differential expression analysis: An extended review and a software tool. *PLoS One* **12**, e0190152–e0190152 (2017).
 50. Lowe, M. M. *et al.* Regulatory T cells use arginase 2 to enhance their metabolic fitness in tissues. *JCI insight* **4**, e129756 (2019).
 51. Nedelkovska, H. *et al.* Follicular Lymphoma Tregs Have a Distinct Transcription Profile Impacting Their Migration and Retention in the Malignant Lymph Node. *PLoS One* **11**, e0155347 (2016).
 52. Magnuson, A. M. *et al.* Identification and validation of a tumor-infiltrating Treg transcriptional signature conserved across species and tumor types. *Proc. Natl. Acad. Sci. U. S. A.* **115**, E10672–E10681 (2018).
 53. Plitas, G. *et al.* Regulatory T Cells Exhibit Distinct Features in Human Breast Cancer. *Immunity* **45**, 1122–1134 (2016).
 54. Ahn, R. S. *et al.* Transcriptional landscape of epithelial and immune cell populations revealed through FACS-seq of healthy human skin. *Sci. Rep.* **7**, 1343 (2017).
 55. Núñez, N. G. *et al.* Tumor invasion in draining lymph nodes is associated with Treg accumulation in breast cancer patients. *Nat. Commun.* **11**, 3272 (2020).
 56. Durinck, S., Spellman, P. T., Birney, E. & Huber, W. Mapping identifiers for the integration of genomic datasets with the R/Bioconductor package biomaRt. *Nat. Protoc.* **4**, 1184–1191 (2009).
 57. Risso, D., Schwartz, K., Sherlock, G. & Dudoit, S. GC-content normalization for RNA-Seq data. *BMC Bioinformatics* **12**, 480 (2011).
 58. Bullard, J. H., Purdom, E., Hansen, K. D. & Dudoit, S. Evaluation of statistical methods for normalization and differential expression in mRNA-Seq experiments. *BMC Bioinformatics* **11**, 94 (2010).
 59. Risso, D., Ngai, J., Speed, T. P. & Dudoit, S. Normalization of RNA-seq data using factor analysis of control genes or samples. *Nat. Biotechnol.* **32**, 896–902 (2014).
 60. Love, M. I., Huber, W. & Anders, S. Moderated estimation of fold change and dispersion for RNA-seq data with DESeq2. *Genome Biol.* **15**, 550 (2014).
 61. Subramanian, A. *et al.* Gene set enrichment analysis: a knowledge-based approach for interpreting genome-wide expression profiles. *Proc. Natl. Acad. Sci. U. S. A.* **102**, 15545–50 (2005).
 62. Shannon, P. *et al.* Cytoscape: a software environment for integrated models of biomolecular interaction networks. *Genome Res.* **13**, 2498–2504 (2003).

SUPPLEMENTARY INFORMATION

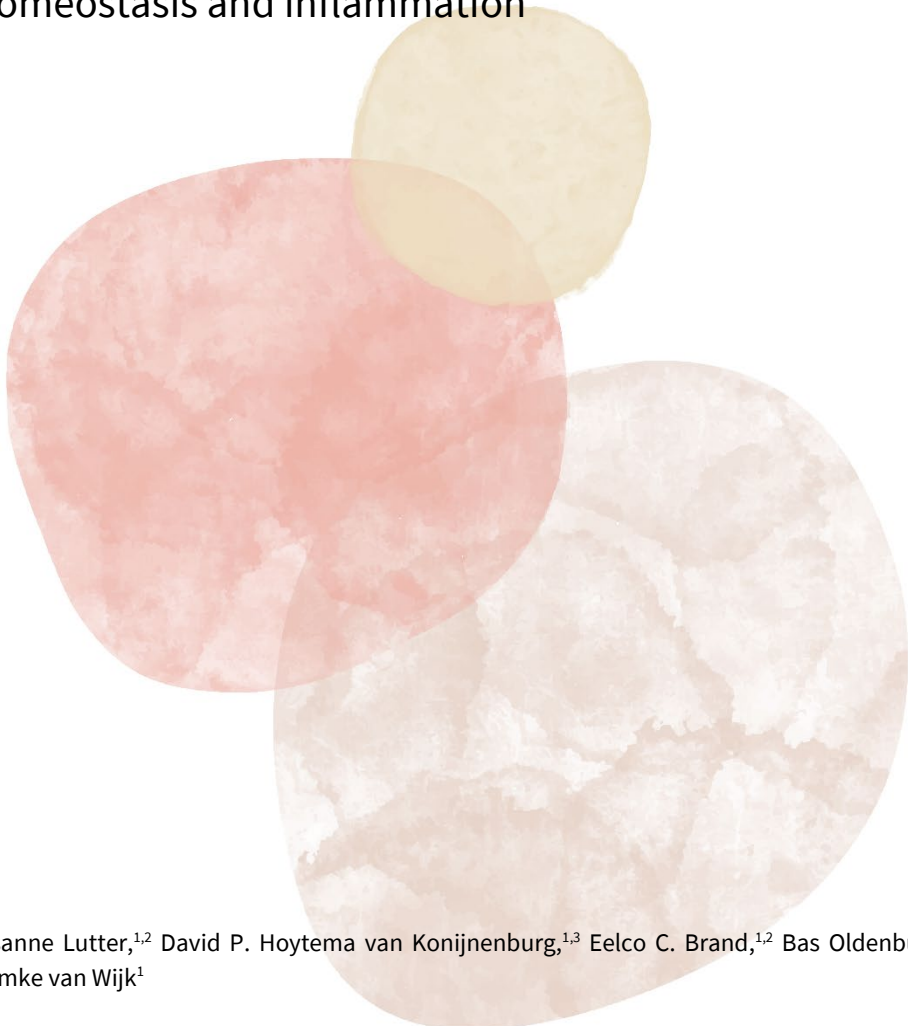


Supplementary Figure 1. Clustering of peripheral blood and tissue-derived Tregs. (A) Principal component analysis plot of Tregs derived from homeostatic peripheral blood (pink), homeostatic tissue (blue), inflamed tissue (green) and tumor tissue (purple). Ellipses are drawn with a 80% confidence level.

Extended Supplementary Data can be found at: <https://github.com/lutterl/PhD-thesis-supplementary-data>.

Chapter 5

The elusive case of human intraepithelial T cells in gut homeostasis and inflammation



Lisanne Lutter,^{1,2} David P. Hoytema van Konijnenburg,^{1,3} Eelco C. Brand,^{1,2} Bas Oldenburg,² Femke van Wijk¹

¹ Laboratory of Translational Immunology, University Medical Center Utrecht, Utrecht, the Netherlands

² Department of Gastroenterology and Hepatology, University Medical Center Utrecht, Utrecht, the Netherlands

³ Laboratory of Mucosal Immunology, The Rockefeller University, New York, USA

ABSTRACT

The epithelial barrier of the gastrointestinal tract is home to numerous intraepithelial T cells (IETs). IETs are functionally adapted to the mucosal environment and are among the first adaptive immune cells to encounter microbial and dietary antigens. They possess hallmark features of tissue-resident T cells: they are long-lived nonmigratory cells capable of rapidly responding to antigen challenges independent of T cell recruitment from the periphery. Gut-resident T cells have been implicated in the relapsing and remitting course and persisting low-grade inflammation of chronic gastrointestinal diseases, including IBD and coeliac disease. So far, most data regarding IETs have been derived from experimental animal models; however, IETs and the environmental makeup differ between mice and humans. With advances in techniques, the number of human studies has grown exponentially in the past 5 years. Here, we review the literature on the involvement of human IETs in gut homeostasis and inflammation, and how these cells are influenced by the microbiota and dietary antigens. Finally, targeting of IETs in therapeutic interventions is discussed. Broad insight into the function and role of human IETs in gut homeostasis and inflammation is essential to identify future diagnostic, prognostic and therapeutic strategies.

KEY POINTS

- Intraepithelial T cells (IETs), residing at the epithelial barrier in the gastrointestinal tract, are an epitome of tissue-resident T cells.
- Tissue-resident T cells are long-lived, nonrecirculating T cells that provide rapid immune responses independent of peripheral T cell recruitment.
- IETs have an important role in immunosurveillance whilst simultaneously inducing tolerance for nonpathogenic antigens, consequently preserving the integrity of the single-layer epithelial membrane.
- IBD and coeliac disease are characterized by a predominance of (recurrent) gastrointestinal inflammation
- The longevity and abundant presence of IETs at the intestinal epithelial barrier suggests a role for IETs in the relapsing and remitting course and persisting low-grade inflammation of these diseases.
- As tissue-specific and potentially pathogenic cells, IETs are an ideal target for therapeutic (non-systemic) intervention in chronic tissue-specific inflammatory diseases such as IBD.

INTRODUCTION

The human gut immune system comprises a diverse set of immune and nonimmune cells distributed over the intestinal layers. These cells maintain a balance between immune tolerance and tissue homeostasis on the one hand, and rapid protective immunity on the other hand. Responses against external stimuli need to be tightly controlled to prevent destruction of the single-cell membrane separating the human body from the external environment. Active immunity is provided by a complex innate and adaptive immune system intertwined within the mucosa¹ (Fig. 1). The gut-associated lymphoid tissue consists of organized lymphoid aggregates (for example, Peyer's patches or colonic patches), mesenteric lymph nodes, and isolated lymphoid follicles. In addition, both the lamina propria and epithelium are seeded with immune cells. A broad representation of leukocytes (including dendritic cells, B cells, T cells, and macrophages) is found in the lamina propria, whereas T cells make up the vast majority of the immune cells permanently populating the epithelium¹. Historically, the immune cells in the epithelium have been referred to as intraepithelial lymphocytes (IELs), but we refer to the epithelial T cell population as IETs¹⁻³.

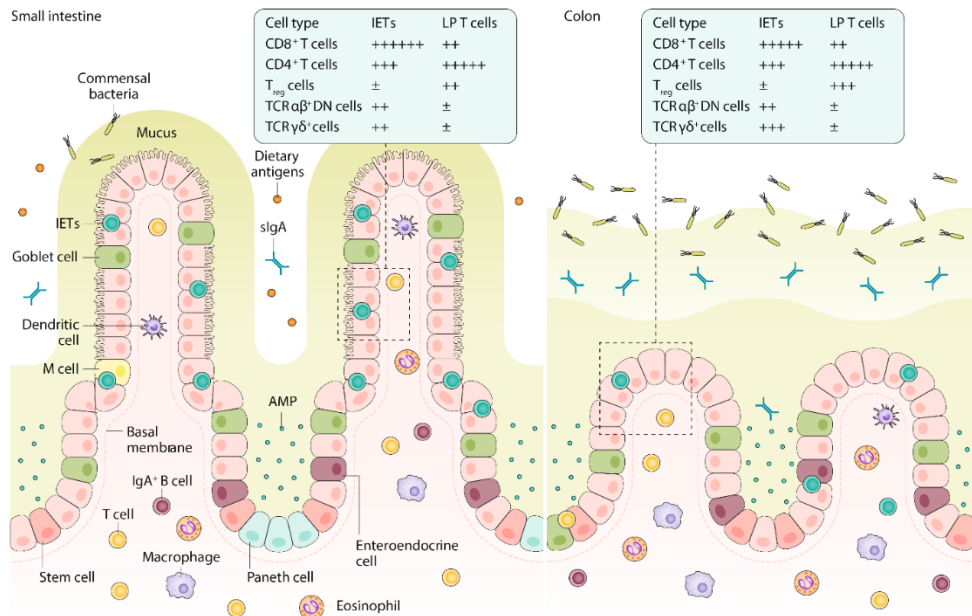


Figure 1. Overview of the intestinal mucosa and distribution of immune cells. The small intestine consists of villi and crypts covered in mucus, creating a large surface area for its digestive function, whereas the colon has no villi and a thicker mucus layer as less digestion takes place there. Many adaptive and innate immune cells are found in the lamina propria (LP), including macrophages, mast cells, eosinophils, dendritic cells, B cells and T cells. Stem cells at the base of the crypts give rise to all intestinal epithelial cells (IECs). IECs consist of enterocytes with absorptive function, goblet cells that produce mucus and Paneth cells (only in the small intestine) that secrete factors to aid in digestion and immune function. Intraepithelial T cells (IETs) are located between these IECs and the basal membrane, and they decrease in number along the intestinal tract. The two panels show the relative T cell receptor (TCR)αβ⁺ and TCRγδ⁺ T cell distribution in the epithelium and lamina propria. Many CD8αβ⁺ T cells reside in the epithelium, in contrast to a dominance of CD4⁺ T cells in the lamina propria; in particular regulatory T (Treg) cells are relatively far more abundant in the lamina propria.

Furthermore, TCR $\gamma\delta^+$ and TCR $\alpha\beta^+$ DN T cells make up a higher percentage of the T cell compartment in the epithelium than in the lamina propria. AMP, antimicrobial protein; DN, double negative; IgA, immunoglobulin A; sIgA, secretory immunoglobulin A.

The intestinal tract is in fact home to one of the largest T cell populations in the body⁴ (Box 1). Mucosal T cells are essential for homeostasis and protective immunity, but also have a role in uncontrolled (chronic) mucosal inflammation, as seen in coeliac disease or IBD, and possibly even in tumour development⁵. In inflammatory or infectious settings, primed T cells are temporarily recruited to the gut from the circulation, but a large population of T cells permanently resides in the gut and is maintained independently of lymphoid and circulating memory populations⁵. These T cells mostly consist of T cell receptor (TCR) $\alpha\beta^+$ CD8 $\alpha\beta^+$ and TCR $\alpha\beta^+$ CD4⁺ tissue-resident memory T cells, but regulatory T (T_{reg}) cells (TCR $\alpha\beta^+$ CD4⁺FOXP3⁺), TCR $\gamma\delta^+$ T cells, natural killer (NK) T cells, and mucosal-associated invariant T cells also establish long-term residence in the gut⁶⁻⁸. Here we review the latest insights on human gut T cells with a focus on IETs, and discuss their tissue residency and role in homeostasis and disease.

Box 1. T cell subsets

T cell progenitors derive from hematopoietic stem cells in the bone marrow. They migrate to the thymus, where they mature to become T cells. Subsequently, T cells migrate through secondary lymphoid organs scanning presented antigens for their cognate antigen. This process is performed by the T cell receptor (TCR), which is antigen-specific and initiates T cell activation upon antigen recognition. The TCR of most T cells consists of a linked TCR α and TCR β chain (TCR $\alpha\beta$), whereas a minority of T cells express a linked TCR γ and TCR δ chain (TCR $\gamma\delta$)³.

TCR $\alpha\beta^+$ T cells recognize antigens presented by a peptide bound to a major histocompatibility complex (MHC) molecule on an antigen-presenting cell. Two major TCR $\alpha\beta^+$ subsets exist, depending on the expressed co-receptor that aids in antigen-recognition: CD4⁺ T cells (T helper (T_H) cells) and CD8 $\alpha\beta^+$ T cells (cytotoxic T cells). Antigens presented by MHCII molecules are recognized by CD4⁺ T cells, whereas antigens presented by MHCI complexes are recognized by CD8⁺ T cells³.

Naive CD4⁺ T cells that are activated differentiate into several subsets depending on their function, including T_H1, T_H2, T_H9, T_H17 and regulatory T (T_{reg}) cells. T_H1 and T_H9 cells have a proinflammatory profile: T_H1 cells show pronounced interferon- γ and TNF expression, and T_H9 cells mainly express IL-9. T_H2 cells secrete anti-inflammatory molecules, such as IL-4, IL-5 and IL-13. T_H17 cells preferentially produce IL-17 and IL-22 and are known for mediating recruitment of neutrophils and macrophages to sites of inflammation. T_{reg} cells secrete anti-inflammatory cytokines, including IL-10 and transforming growth factor- β (TGF β), and suppress inflammation³.

TCR $\gamma\delta^+$ T cells do not express a co-receptor (double negative (DN); CD4⁻CD8⁻) and thus do not recognize antigens presented by classical MHC complexes. CD8 $\alpha\alpha$ (co-)expressing T cells (Box 2) and DN TCR $\alpha\beta^+$ T cells can be found in some tissues. These T cells seem able to recognize whole peptides and nonpeptide antigens presented by nonclassical MHCI molecules, such as CD1d displaying lipid antigens and MHC class I polypeptide-related sequence A (MICA) and MICB, among others^{3,63,64,182}.

Intestinal IETs

The gut epithelium has long been known to harbour a large and unique collection of T cells that is retained within this single-cell layer⁹, the so-called IETs. Like tissue-resident memory T cells, the majority of IETs express CD69 and CD103 (also known as integrin $\alpha\epsilon$), and

permanently reside in the epithelium¹⁰. IETs are not static however; in vivo imaging in mice has revealed extensive vertical circulation patterns throughout the villi and ‘flossing’ movements (snake-like movements into the lateral intercellular space between the intestinal epithelial cells (IECs))^{9,11}. In addition to the IETs, other innate immune cell populations residing in the human epithelium have been described. These cells include innate lymphoid 1 (ILC1)-like cells^{12,13} and CD3⁺CD7⁺ cells,^{14,15} which both have NK activity and a pro-inflammatory cytokine profile. The relative numbers of these cells have been shown to be altered in coeliac disease and Crohn’s disease^{12,14}; however, their role in gut homeostasis or disease remains largely unknown. For the rest of this Review, we focus solely on the T cells. Human IETs have long remained elusive to study, mostly due to practical reasons, but novel techniques are helping to reveal their unique features.

The ratio of IETs to IECs decreases along the intestinal tract from 13 to 22 per 100 in the distal part of the duodenum to ~ 5 per 100 in the colon, but with an increase in the rectum up to 20 per 100^{16–20}. This pattern of distribution has so far not been explained, but heterogeneity in antigen exposure probably has an important role. In the small intestine, dietary antigens are most abundant, whereas the colon hosts the bulk of the gut microbiota^{21,22}. In addition, both the small intestine and the colon have a loose outer mucous layer colonized by the gut microbiota; however, the colon also has an inner mucous layer that is impenetrable to bacteria during homeostasis, thus pathogen penetration through the mucous layer differs between the small intestine and colon²².

A special feature of the IET compartment is the unique composition of T cell lineages. Besides conventional TCR $\alpha\beta$ ⁺CD4⁺ and TCR $\alpha\beta$ ⁺CD8 $\alpha\beta$ ⁺ T cells, the epithelium harbours large populations of natural IETs including TCR $\gamma\delta$ ⁺ and CD4⁺CD8⁻ double-negative cells (Table 1). Evidence indicates that the fate of natural IETs is determined during thymic development and not via antigen-induced differentiation in the periphery, hence the term natural. After leaving the thymus, these cells migrate directly to the gut epithelium¹⁰. Substantial heterogeneity exists within natural IETs and their precursors^{23,24}, and there is also variability in major histocompatibility complex (MHC) restriction (classical versus nonclassical MHC; Box 1; Table 1). In contrast to conventional IETs, several natural IET populations show enrichment for self-reactive cells as well as oligoclonality^{10,23,25}. The natural IETs seed to the gut long before birth; for example, TCR $\gamma\delta$ ⁺ T cells are found in the primitive gut of humans as early as 6–9 weeks of gestation²⁶. In mice, the number of natural IETs declines and the number of TCR $\alpha\beta$ ⁺ IETs increases owing to increased antigen exposure after birth¹⁰. In humans, the percentage of TCR $\gamma\delta$ ⁺ T cells decreases from 20% to 10% of all IETs immediately after birth²⁷. Furthermore, upon introduction of foreign antigens, the TCR $\alpha\beta$ ⁺ IET composition shifts from mainly double-negative (35–70%) to conventional TCR $\alpha\beta$ ⁺ IETs expressing CD4 or CD8 $\alpha\beta$ (only 6% double negative)^{25,27}, with an expanded TCR repertoire²⁸. More than 80% of the TCR $\alpha\beta$ ⁺ IETs express CD8 $\alpha\beta$ ¹⁷, independent of age²⁹, in contrast to most locations in the body where CD4⁺ T cells are predominant (including the lamina propria). In addition, about 10% of the T cells in the lamina propria are naive³⁰, whereas all IETs have an antigen-experienced phenotype^{31,32}.

Table 1. Main subsets and characteristics of human and mouse IETs

IET	Subset	Prevalence (%) ^a		Development	TCR repertoire	Kinetics of accumulation
		Small intestine	Colon			
Human						
Natural	TCR $\alpha\beta$ ⁻ DN	0	>0	Evade negative selection; evidence suggests partial extrathymic maturation	Nonclassical MHC (for example, HLA-E); oligoclonal expansion	Present at birth; stable in absolute numbers but decrease in the IET:IEC ratio with age
	TCR $\gamma\delta$ ⁺ ^b	1–4	15–20			
Conventional ^c	TCR $\alpha\beta$ ⁺ CD4 ⁺ ^d	15–40	8–11	Conventional thymus-derived T cells migrate from SLOs to intestinal epithelium; CD8 $\alpha\alpha$ ⁺ phenotype is probably acquired there	MHC class I and II; oligoclonal expansion	Present at birth; increase in absolute numbers but the IET:IEC ratio remains stable
	TCR $\alpha\beta$ ⁺ CD8 $\alpha\beta$ ⁺ ^d	60–99	64–72			
Mouse						
Natural	TCR $\alpha\beta$ ⁺ ^b	11.0–17.5	6–17	Evade negative selection; leave as DN and acquire CD8 $\alpha\alpha$ ⁺ phenotype in the intestinal epithelium	Nonclassical MHC (for example, Qa1); oligoclonal expansion	Present at birth; decrease with age
	TCR $\gamma\delta$ ⁺ ^b	25–65	2–18			
Conventional ^c	TCR $\alpha\beta$ ⁺ CD4 ⁺ ^d	2–7	15.0–72.5	Conventional thymus-derived T cells migrate from SLOs to intestinal epithelium where CD8 $\alpha\alpha$ ⁺ phenotype is acquired	MHC class I and II; oligoclonal expansion	Absent at birth; increase with age
	TCR $\alpha\beta$ ⁺ CD8 $\alpha\beta$ ⁺ ^d	26–41	3.5–50.0			

DN, double negative; IEC, intestinal epithelial cell; IET, intraepithelial T cell; MHC, major histocompatibility complex; SLOs, secondary lymphoid organs; TCR, T cell receptor. ^aThe range is for all IETs (including CD3⁺; for some studies, different subsets were not well defined). ^bCells can be DN or express CD8 $\alpha\alpha$ ⁺ (Box 2). ^cConventional TCR $\alpha\beta$ ⁺CD4⁺ and TCR $\alpha\beta$ ⁺CD8 $\alpha\beta$ ⁺ IETs are also called induced IETs. ^dCD8 $\alpha\alpha$ ⁺ can be upregulated, but percentages are usually not subspecified. IETs in the small intestine are more than three times as abundant in absolute numbers when compared with the colon.

When comparing mice with humans, there are clear similarities in IET composition, but major differences are also notable (Table 1). For example, in mice, up to 50% of all IETs are TCR $\gamma\delta$ ⁺¹⁰, whereas in humans this figure is 10–20% of all IETs²⁷. To date the majority of data on IETs are derived from mouse studies, which might not be directly translatable to the human setting. Nevertheless, general concepts about IET migration, differentiation and tissue adaptations and interactions seem to be conserved between the species. Notably, human studies regarding IETs usually do not define subsets within the TCR $\alpha\beta$ ⁺CD4⁺, TCR $\alpha\beta$ ⁺CD8 $\alpha\beta$ ⁺ or TCR $\gamma\delta$ ⁺ subsets, or they focus on only one population. It is now becoming clear that environmental cues can drive differential functional programmes and cell dynamics that might have a role in health and disease, and where possible, the subsets are discussed separately in this Review.

Migration, differentiation and tissue adaptation of IETs

Gut-homing of T cells depends predominantly on induction of homing marker expression by retinoic acid metabolized from vitamin A by dendritic cells³³. The main gut-homing marker on T cells is integrin $\alpha 4\beta 7$, which adheres to mucosal addressin cell adhesion molecule 1 (MadCAM-1) on vascular endothelium (Fig. 2). Co-expression with CC-chemokine receptor 9 (CCR9) homes T cells to the small intestine by attraction to the chemokine C-C motif ligand 25 (CCL25) produced by IECs; G-protein-coupled-receptor 15 (GPR15) expressed on T cells, which has an unknown ligand, seems to attract effector T cells to the colon^{34–38}. After homing to lymphoid aggregates, T cells migrate to the lamina propria^{37,39}. Subsequently, T cells downregulate integrin $\alpha 4$ expression and upregulate integrin αE expression that, together with $\beta 7$ integrin, can adhere to E-cadherin on the basolateral side of human small intestinal and colonic epithelium^{39,40}. These consecutive changes in homing markers, among others, help

establish IETs for long-term residency in the epithelium. The mentioned integrins are not all-encompassing, however; for example, T cells missing integrin $\alpha 4\beta 7$ can still home to the gut⁴¹, and in a humanized mouse model of Crohn's disease integrin $\alpha 4\beta 1$ is crucial for effector T cell homing to the ileum⁴². Whereas *in vivo* experiments in mice have demonstrated that many T cells migrate from the lamina propria to the epithelium, only a very limited number re-migrate to the lamina propria⁹. Migration patterns within the lamina propria and epithelium, and regional differences in expression of chemoattractants and adhesion molecules, remain to be fully elucidated.

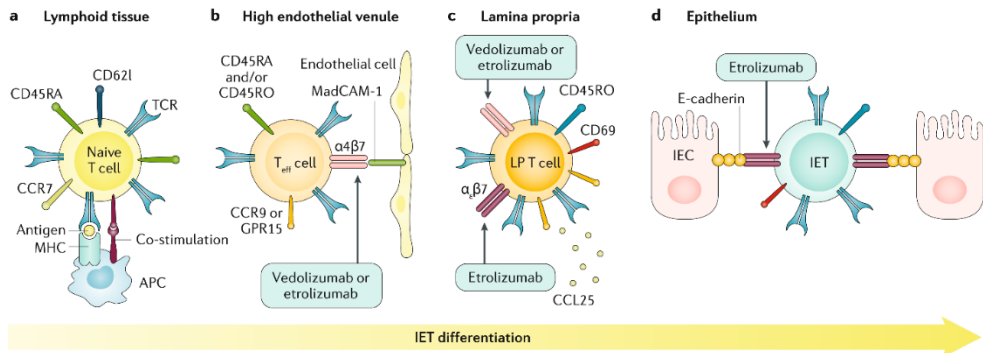


Figure 2. Differentiation from naive T cell to IET in the gut. **a** | Naive T cells are characterized by the expression of CD62L, CD45RA and CC-chemokine receptor 7 (CCR7). These surface markers ensure that naive T cells circulate in the peripheral blood and pass secondary lymphoid organs, including gut-associated lymphoid tissue. Here, naive T cells interact with antigen-presenting cells (APCs) via the major histocompatibility complex (MHC)-antigen-T cell receptor (TCR) complex and co-stimulation. **b** | TCR stimulation results in T effector (Teff) cell differentiation accompanied by a loss of naive T cell surface marker expression and upregulation of the memory marker CD45RO, including induction of gut-homing receptors. Among other processes, this entails upregulation of integrin $\alpha 4\beta 7$ that can bind to the mucosal vascular addressin cell adhesion molecule 1 (MadCAM1) and upregulation of CC-chemokine receptor 9 (CCR9) attracted to C-C motif ligand 25 (CCL25) expressed by epithelial cells in the small intestine or G-protein-coupled receptor 15 (GPR15) binding with an unknown ligand in the colon. Natural intraepithelial T cell (IET) antigen recognition occurs predominantly in the thymus, followed by upregulation of gut-homing factors as described above. Subsequently, activated T cells exit the lymphoid tissue and re-enter circulation. When passing through post-capillary venules, rolling, tethering, arrest and transmigration ensures translocation to the gut. Vedolizumab (currently used as therapy in IBD) and etrolizumab (in phase III clinical trials) target gut-homing receptors and perhaps long term maintenance of tissue-resident T cells by inhibiting integrin $\alpha 4\beta 7$ and integrin $\beta 7$, respectively. **c** | The Teff cells in the lamina propria (LP) downregulate $\alpha 4$ and upregulate CD69 and CD103 (integrin αE). The local changes in markers ensure tissue residency. Naive T cells can also be found in tissues, with ~20% of the naive T cells upregulating CD69, probably characterizing tissue retention⁴³. **d** | IETs ultimately adapted to the intestinal environment reside in the epithelial layer. Maintenance depends, among other factors, on continuous persistence of antigen, interaction with epithelial cells. IEC, intestinal epithelial cell.

Local microenvironmental cues are essential to establish and maintain the IET phenotype. For example, human colonic TCR $\gamma\delta^+$ T cells that express the γ -chain V4 mature and proliferate upon recognition of butyrophilins, which are immunomodulatory molecules expressed on IECs⁴⁴. Furthermore, transforming growth factor β (TGF β) is responsible for the upregulation of integrin αE and CD69 on IETs^{45–48}. Pathways that preserve tissue residency are not identical between the epithelium and lamina propria; for example, in mice, integrin $\alpha_v\beta 6$ expression by

IECs is crucial for continued tissue residency in the epithelium but not in the lamina propria⁴⁹. IECs also express cytokines that can induce IET proliferation, including IL-7 and IL-15. In particular, IL-15 is important for IET proliferation and survival⁵⁰, and production of these cytokines is highly increased in inflammation, such as in coeliac disease⁵¹⁻⁵³. Microbial pattern recognition via Toll-like receptor 2 (TLR2) expressed on the apical side of IECs and via the intracellular receptor nucleotide-binding oligomerization domain-containing protein 2 (NOD2) in antigen-presenting cells (APCs) can induce IL-15 expression^{50,54}.

T cells with a cytotoxic profile are rare (~5% of all T cells) in the blood^{55,56}, whereas T cells with a cytotoxic profile dominate in the intestinal epithelium¹⁷. This abundance of cytotoxic T cells is a unique adaptation to the local environment. Cytotoxic activity includes production of perforin and granzyme B, and is accompanied by expression of NK receptors. Interestingly, in addition to the TCR $\alpha\beta^+$ CD8 $\alpha\beta^+$ IETs, TCR $\alpha\beta^+$ CD4 $^+$ IETs can also obtain a cytotoxic profile^{57,58}. Studies in mice have shown that upon migration to the gut epithelium, TCR $\alpha\beta^+$ CD4 $^+$ T cells can lose expression of the classical CD4 transcription factor ThPOK^{9,57,58}, followed by upregulation of transcription factors associated with TCR $\alpha\beta^+$ CD8 $\alpha\beta^+$ cytotoxic cells, such as T-box transcription factor TBX21 (TBET) and runt-related transcription factor 3 (RUNX3). Locally abundant factors, including TGF β , retinoic acid and TBET-inducing cytokines, are crucial for differentiation^{57,58}. Altogether this process leads to a complete change in functional profile, mostly characterized by adoption of a cytotoxic and/or regulatory signature. Another feature of these differentiated TCR $\alpha\beta^+$ CD4 $^+$ IETs is expression of CD8 $\alpha\alpha$ homodimer, a negative regulator of T cell activation⁵⁹ (Box 2). TCR $\alpha\beta^+$ CD4 $^+$ IETs co-expressing CD8 $\alpha\alpha$ can also be found in humans, and the limited data available suggest that these cells acquire regulatory features such as expression of IL-10 and cytotoxic T lymphocyte-associated molecule 4 (CTLA4)⁵⁹. Altogether, these findings indicate that the intestinal epithelial barrier promotes and supports unprecedented functional and phenotypical changes in T cells to meet its unique needs.

Box 2. CD8 α

CD8 α is a cell surface glycoprotein that can be expressed either as a disulfide-linked heterodimer together with CD8 β or as a homodimer. The T cell co-receptor CD8 $\alpha\beta$ enhances T cell sensitivity to antigen; however, studies indicate that CD8 α has the opposite effect and acts as a co-repressor. CD8 α can be upregulated after T cell receptor (TCR) stimulation on both TCR $\gamma\delta^+$ and TCR $\alpha\beta^+$ T cells. CD8 α has low affinity for major histocompatibility complex I (MHC I) molecules and does not mediate cell–cell adhesion¹⁸³; thus, it evades negative selection and does not act as a co-receptor for T cell activation. Co-expression of CD8 α on TCR $\alpha\beta^+$ CD8 $^+$ or TCR $\alpha\beta^+$ CD4 $^+$ T cells even diminishes the functional avidity between the TCR and MHC-peptide complex¹⁸⁴. It seems that co-expression of CD8 α can be upregulated and downregulated⁹³; this plasticity might be important in maintaining immunological tolerance. In animal models, cells expressing TCRs with high antigen affinity also expressed CD8 α , thus enforcing quiescence⁹³. Furthermore, CD8 α expression in human natural killer (NK) cells protects NK cells of self-induced apoptosis, enabling them to target multiple cells successively¹⁸⁵. Delaying apoptosis might also be a mechanism of survival for other T cells expressing CD8 α ⁸⁸.

CD8 α induction is often observed in the intestinal mucosa in particular. In mice, the mechanism behind this phenomenon has been well described in TCR $\alpha\beta^+$ CD4 $^+$ T cells, and these so-called TCR $\alpha\beta^+$ CD4 $^+$ cytotoxic T lymphocytes have been shown to have regulatory functions^{9,57}. In the human intestine, co-expression of CD8 α has been described on several T cell subsets, including TCR $\gamma\delta^+$, TCR $\alpha\beta^+$ CD8 $^+$ and TCR $\alpha\beta^+$ CD4 $^+$ T cells. Human TCR $\alpha\beta^+$ CD4 $^+$ CD8 α^+ T cells lack forkhead box protein P3 (FOXP3) but do express regulatory markers and functions of FOXP3 $^+$ regulatory T cells⁵⁹.

Functional profile of IETs

Interactions between IETs and surrounding cells ensure the integrity of the epithelial barrier and protection from pathogenic organisms (Fig. 3). *Salmonella* or *Toxoplasma* infection in TCR $\gamma\delta^+$ IET-depleted or knockout mice leads to increased and earlier pathogen invasion^{11,60–62}, illustrating the importance of IETs in preventing pathogen dissemination. All IETs perform local immunosurveillance by sampling antigens presented by APCs and IECs^{63,64}, but also by interacting with stress ligands and cytokines^{65,66}. Despite their differences, IET subsets share a dominant functional profile and an ‘activated yet resting’ phenotype, illustrated by low basal cytokine production and little proliferation^{29,67}. Quantitatively, TCR $\alpha\beta^+$ IETs produce more cytokines than TCR $\gamma\delta^+$ IETs, with the TCR $\alpha\beta^+$ CD8 $\alpha\beta^+$ subset producing higher cytokine levels than the TCR $\alpha\beta^+$ CD4 $^+$ subset at steady state. IETs can be rapidly activated, responding with a pronounced T helper 1 (T_H1)-type cytokine profile of IL-2, TNF and interferon- γ (IFN γ)^{29,36,68–73} (Table 2). IFN γ has a protective function in infection, but also causes epithelial membrane disruption by inducing IEC apoptosis and by severing cell–cell connections via reduced transcription of tight junction proteins and degradation of E-cadherin^{74–76}.

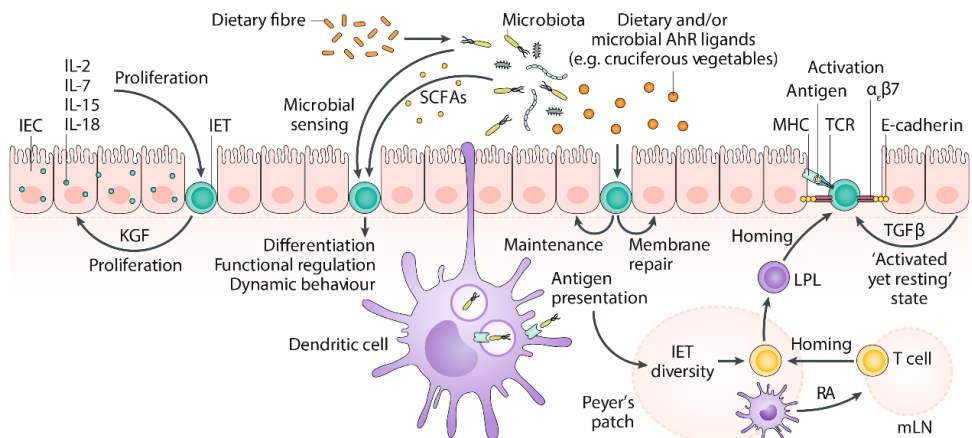


Figure 3. Interactions of human IETs with the mucosal environment. To highlight the interactions, an overrepresentation of intraepithelial T cells (IETs) proportionate to intestinal epithelial cells (IECs) is depicted, and IETs are not enclosed by IECs. Gut-homing factors are induced by dendritic cells (DCs) through retinoic acid (RA) signalling. Once in the epithelium, IECs maintain IETs long term through interaction of E-cadherin on IECs and integrin $\alpha_E\beta_7$ on IETs. IECs present antigens to IETs without co-stimulation, maintain the 'activated yet resting' state of IETs through transforming growth factor- β (TGF β) expression and can induce IET proliferation via IL-7 and IL-15 cytokine expression, among other actions. Keratinocyte growth factor (KGF) secreted by IETs inhibits apoptosis and induces proliferation of IECs, contributing to maintenance of the epithelial layer. Furthermore, the gut microbiota is partially responsible for IET expansion, probably via presentation of microbial antigens by DCs in lymphoid aggregates to IETs. The microbiota and its metabolites can also induce T cell differentiation, regulate T cell functions and, via microbial sensing by IECs, regulate IET motility patterns in mice. Dietary and microbial aryl hydrocarbon receptor (AhR) ligands are assumed to induce epithelial membrane repair, immune defense and IET maintenance. LPL, lamina propria lymphocyte; MHC, major histocompatibility complex; mLN, mesenteric lymph node; SCFAs, short chain fatty acids; TCR, T cell receptor.

Upon activation, IETs can also display cytotoxicity and induce apoptosis of target cells through granzyme B, perforin, and Fas–Fas ligand interaction^{71,77,79,80,88–90}. Furthermore, both inhibitory and activating NK receptors involved in target cell lysis (such as NK group member 2 (NKG2) receptors), are expressed on IETs^{10,91}. Stress signals upregulate the NK receptor ligands⁹¹, and NK receptor-mediated cytotoxicity is a way to maintain the intestinal barrier by eliminating stressed cells. Many NK receptor ligands are shared between mice and humans, but for NKG2 receptors, the ligands differ⁹². For humans, the ligands expressed on IECs include HLA-E, and MHC class I polypeptide-related sequence A (MICA) and MICB. These properties illustrate that IETs can be very efficient killers and suggest that IETs can sense epithelial stress via innate receptors and kill infected or stressed cells.

Inappropriate strong responses of IETs to any type of luminal or self-antigen would have disastrous consequences for the epithelial barrier. Therefore, IETs are thought to be kept in check by inhibitory receptors such as CD8 α ⁹³ (Box 2) and by interaction with the environment. Thus, although IETs are thought to recognize microbial and dietary antigens^{94,95}, this process does not elicit a destructive immune response. IETs themselves might also have a role in homeostasis or tolerance induction by producing anti-inflammatory cytokines such as

IL-10^{59,72} and keratinocyte growth factor (KGF; also known as FGF7)^{84,85}, which can stimulate IEC proliferation^{86,96} and epithelial reconstitution⁸⁷.

Table 2. Phenotypic characteristics of human intestinal intraepithelial T cells

Effector function	TCR αβ ⁺ CD4 ⁺ (CD8 αα ⁺)	TCR αβ ⁺ CD8 αβ ⁺	TCR γδ ⁺ (DN or CD8 αα ⁺)
Cytokines			
IL-1α	+		
IL-1β	++	+	+
IL-2	++	++	++
IL-3	–	–	–
IL-4	–	–	–
IL-5	–	–	–
IL-6	±	±	±
IL-7	–	–	–
IL-8	++	+	+
IL-10	+	+	+ ^b
IL-13	–	–	–
IL-17A	+	+	ND
IL-17B	ND	ND	ND
TGFβ1	+	+	+ ^c
IFNγ	++	++	++
TNF	++	++	++
Cytotoxic factors			
NKG2A	ND	+	++ ^d
NKG2C	ND	+	+
NKG2D	– ^e	++	+
Cytotoxic granules			
Fas and FasL	++/+		
ADCC	–		
SCMC	+		
Growth factors^c			
KGF	±		
GM-CSF	+		
M-CSF	+		

The presence or absence of mRNA mediators is shown, along with functional expression of (cytotoxic) effector molecules. The + and – signs are used to denote approximate values, interpreted and weighed from the available literature. ± denotes low expression. Comparisons can be made across rows but not between columns. If not subspecified per intraepithelial T cell (IET) subset, + or – is depicted at the start of the row; some subsets might not express the respective mediator. ADCC, antibody-dependent cell-mediated cytotoxicity; DN, double negative; FasL: Fas ligand; GM-CSF, granulocyte-macrophage colony-stimulating factor; IFNγ, interferon-γ; KGF, keratinocyte growth factor; M-CSF, macrophage colony-stimulating factor; ND, not determined; NKG2A, NKG2-A/NKG2-B type II integral membrane protein; NKG2C, NKG2-C type II integral membrane protein (also known as KLRC2); SCMC, spontaneous cell-mediated cytotoxicity; TCR, T cell receptor; TGFβ1, transforming growth factor-β1. ^aThe presence of T helper 2 (T_H2)-type cytokines such as IL-4, IL-5 and IL-13, has so far not been found on IETs. For further information on the human IET functional profile, see elsewhere^{19,29,36,59,68,70–73,77–83}. ^bProduction only upon activation. ^cFor further information on human IET growth factor expression, see elsewhere^{84–87}. ^dTCRγδ⁺CD8⁺ IETs express more NKG2A compared to TCRγδ⁺DN IETs⁸¹. ^eNKG2D⁺ CD4⁺ IETs are unusual, but some are seen in Crohn's disease⁸².

Interplay between IETs and environment

Microbial diversity and richness are essential for the TCR $\alpha\beta^+$ CD4 $^+$ and TCR $\alpha\beta^+$ CD8 $\alpha\beta^+$ IET compartment in both humans and mice as antigen-experienced IETs expand in the presence of higher bacterial diversity⁹⁷. Human gut microbiota transferred to germ-free mice can induce moderate changes in T cell subset proportions and function⁹⁸. In germ-free, but also dietary-protein-free mice, the TCR $\alpha\beta^+$ IETs are greatly reduced in number^{94,95}, with restoration of normal TCR $\alpha\beta^+$ numbers after introduction of intestinal microbiota⁹⁹. The gut microbiota is also important in the unique programming of IETs; in mice, Treg conversion to TCR $\alpha\beta^+$ CD4 $^+$ CD8 $\alpha\alpha^+$ T cells in the intestinal epithelium is microbiota-dependent⁹. The gut microbiota induces regulatory functions in TCR $\alpha\beta^+$ CD4 $^+$ T cells while reducing effector functions¹⁰⁰. The dynamic movement patterns of TCR $\gamma\delta^+$ IETs in the steady state have been shown to be strongly influenced by the microbiota¹¹. Short-chain fatty acids (microbial metabolites processed from dietary fibre) can induce TCR $\alpha\beta^+$ CD4 $^+$ T_H1 and T_H17 differentiation, and they can induce IL-10 secretion by CD4 (non-Treg) T cells in mice¹⁰¹. Furthermore, expression of the activating NK receptor 2B4 on all cytotoxic TCR $\alpha\beta^+$ IETs (TCR $\gamma\delta^+$ IETs not assessed) in both mice and humans is driven by the gut microbiota. Stimulation of this receptor in mouse TCR $\alpha\beta^+$ CD8 $\alpha\beta^+$ IETs results in reduced proliferation and enhanced regulatory function of these cells^{102,103}.

Unlike other immune-cells, mouse IETs depend on aryl hydrocarbon receptor (AhR) signalling for their development, diversity and residency in the gut¹⁰⁴. Transcriptomic profiling of all IETs combined in ileal biopsy samples from healthy humans also found high expression of AhR³⁶. AhR has both endogenous and exogenous ligands, including dietary products (for example, compounds found in cruciferous vegetables), toxins (such as dioxins)¹⁰⁴, and microbial molecules (for example, tryptophan metabolites such as indoles)¹⁰⁵. The AhR pathway has mostly been implicated in epithelial membrane repair and defense against bacteria but can also be destructive, depending on the ligand and ligand exposure time¹⁰⁶. Loss of gut microbiota that produce AhR ligands or reduced ingestion of dietary AhR ligands in mice results in increased bacterial load and risk of autoimmune disease via reduction of IET cytotoxicity and increased epithelial permeability¹⁰⁴. Finally, in mice, AhR stimulation reduces mucosal inflammation¹⁰⁷, and AhR expression on total mucosal T cells is reduced in active inflammatory lesions in patients with Crohn's disease^{108,109}, although this phenomenon was not studied for IETs and lamina propria T cells separately. These data emphasize the importance of external stimuli in the maintenance and function of all IETs (Fig. 3), although the mechanisms and function of direct interaction between the environment and human IETs remain to be determined.

Relevance of IETs in disease

Several studies suggest a role for tissue-resident T cells, including IETs (Fig. 4), in intestinal chronic inflammatory diseases. In particular, tissue-resident T cells responding to allergens, self-antigens, or those that are cross-reactive towards luminal antigens, might elicit unwanted immune responses. These cells are, for example, the main suspects in the relapsing and remitting course and persisting low-grade inflammation of IBD, because tissue-resident T cells

do not recirculate, are found in local inflamed tissue with sharp margins and respond within 24–48 hours upon antigen presentation by dendritic cells^{5,7}. The ‘activated yet resting’ phenotype of IETs enables them to respond within even a few hours^{10,68}. Furthermore, chronic inflammatory diseases tend to worsen over time, which could be due to progressive accumulation of tissue-resident cells, and relapses are often seen at the same location¹¹⁰. For the latter, recurrence of Crohn’s disease at the anastomosis after ileocollectomy is a good example^{111,112}.

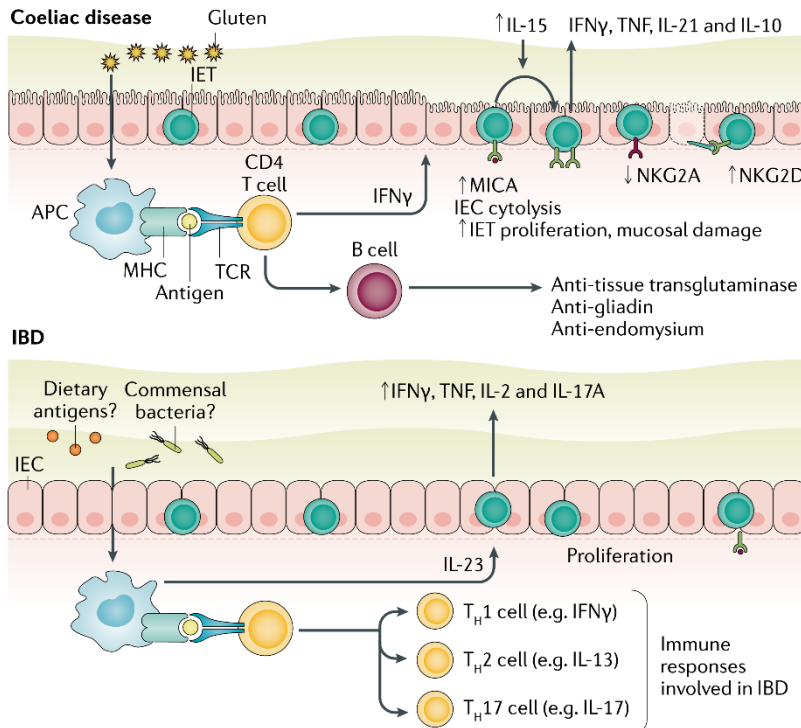


Figure 4. Intestinal immune responses in coeliac disease and IBD. The immune changes for IBD in general are shown, although many differences in the immune response exist between Crohn’s disease and ulcerative colitis. In coeliac disease, gluten-specific T cells residing in the lamina propria induce an inflammatory response that results in IL-15 production by intestinal epithelial cells (IECs). IL-15 stimulates T cell receptor (TCR) $\alpha\beta^+$ CD8 $\alpha\beta^+$ intraepithelial T cell (IET) proliferation and effector function, which is correlated with mucosal damage, including villus atrophy. During homeostasis, NKG2-A/NKG2-B type II integral membrane protein (NKG2A) on TCR $\alpha\beta^+$ CD8 $\alpha\beta^+$ IETs can suppress TCR $\alpha\beta^+$ CD8 $\alpha\beta^+$ IETs, but NKG2A is downregulated in coeliac disease. Furthermore, IETs upregulate NKG2D, which can induce cytolysis. The TCR $\alpha\beta^+$ CD4 $^+$ cells in the lamina propria provide help for B cell differentiation and production of the autoantibodies present in coeliac disease. In IBD, TCR $\alpha\beta^+$ CD8 $\alpha\beta^+$ IET proliferation and effector function are also increased. This increase is primarily due to IL-23 produced by macrophages situated in the lamina propria, although other immune changes in the lamina propria also induce epithelial disruption. In Crohn’s disease, this response is more pronounced than in ulcerative colitis. In both coeliac disease and IBD, the IET compartment is skewed towards TCR $\alpha\beta^+$ CD8 $\alpha\beta^+$ IETs, which are destructive (whereas TCR $\gamma\delta^+$ IETs seem protective). APC, antigen-presenting cell; MHC, major histocompatibility complex; MICA, MHC class I polypeptide-related gene A; T_H, T helper.

In chronic gastrointestinal diseases, IET numbers can increase, leading to intraepithelial lymphocytosis, which is defined as >25 IETs per 100 IECs. Intraepithelial lymphocytosis with intact villous structure can also be observed in small intestinal bacterial overgrowth, in IBD, in patients with coeliac disease on a gluten-free diet and in patients using NSAIDs^{113,114}. Intraepithelial lymphocytosis with villous atrophy is more often seen in active coeliac disease, non-gluten protein hypersensitivity and gastrointestinal infections^{113,114}. Even though intraepithelial lymphocytosis is a nonspecific determinant, it is a reason for further diagnostic evaluation^{115,116}.

Coeliac disease

Patients with coeliac disease show an autoimmune reaction to gliadin, a derivative from gluten. The glutamines in gliadin are converted to glutamic acid by tissue transglutaminase. Hereupon, APCs can present these gliadin peptides on MHC-II HLA-DQ2 and MHC-II HLA-DQ8 to gluten-specific CD4⁺ T cells in the lamina propria¹¹⁷. This induces an inflammatory response resulting in small intestinal enteropathy¹¹⁸. Interestingly, although no IETs are gluten-specific¹¹⁹, coeliac disease is associated with profound changes in IET function, resulting in increased cytotoxic effector function¹²⁰ (Fig. 4). In addition, histological studies have suggested a change in IET distribution in patients with coeliac disease. In steady state, IETs showed a decrease in number along the villi from the junction of the crypts to the villous tips (decrescendo pattern)¹¹⁴; however, in coeliac disease a crescendo pattern (that is, increasing in number towards the villous tips) was observed^{114,115,121}. The intraepithelial lymphocytosis comprises an increase in absolute numbers of TCRγδ⁺ and TCRαβ⁺CD8αβ⁺ IETs and a relative decrease in TCRαβ⁺CD4⁺ IETs¹²². Persons at risk of developing coeliac disease, that is people with anti-transglutaminase antibodies but no histological lesions, have IET proportions similar to those of patients with coeliac disease¹²². This finding suggests that IET composition changes even before disease symptoms appear. Cytotoxic TCRαβ⁺CD8αβ⁺ IETs are crucial effectors in villous atrophy, although disease starts with the gluten-specific lamina propria T cells^{117,123}. Lamina propria T cell activation results in IL-15 production by IECs and lamina propria mononuclear cells, which mediates expression of MICA and MICB on IECs^{53,119,123,124}, stimulates TCRαβ⁺CD8αβ⁺ proliferation and cytotoxic effector function, and suppresses the effect of TGFβ^{125,126}. In coeliac disease the inhibitory receptor NKG2-A/NKG2-B type II integral membrane protein (NKG2A; also known as KLRC1) is downregulated whereas the activating receptor NKG2-D type II integral membrane protein (NKG2D; also known as KLRK1) is upregulated on IETs^{117,126,127}. The high levels of IL-15 in coeliac disease^{53,123} can result in TCR-independent NKG2D-mediated cytotoxicity. In TCR-independent functioning, the level of specificity for T cell activation decreases substantially, thereby carrying the risk of losing self-tolerance and ultimately evoking an autoimmune response. NKG2D-mediated cytotoxicity depends on type IV cytosolic phospholipase A2 (cPLA2), which is highly upregulated in IETs in coeliac disease¹²⁸. Furthermore, both NKG2D and IL-15 signaling can induce arachidonic acid release from membrane phospholipids^{128,129}. Arachidonic acid is processed into prostaglandins and leukotrienes, such as cysteinyl leukotrienes (CystLTs). In active coeliac disease, the CystLTs pathway is upregulated, stimulating NKG2D-mediated cytotoxicity by IETs via autocrine CystLTs signalling¹²⁹. Finally, stimulated by IL-15, TCRαβ⁺CD4⁺ IETs produce TNF, IL-10 and IL-

21 in active coeliac disease¹³⁰, with IL-21 shown to upregulate perforin-mediated cytotoxicity^{131,132}. Altogether these changes result in epithelial damage and villous atrophy.

When patients are placed on a gluten-free diet, expression of NKG2A on TCR $\gamma\delta^+$ IETs and MICA and MICB expression on IECs normalizes¹³³. However, even after recovery of normal villous structure, duodenal lymphocytosis persists for > 10 years¹³⁴. Whereas the TCR $\alpha\beta^+$ CD8 $\alpha\beta^+$ IET levels normalize¹³⁵, the absolute number of TCR $\gamma\delta^+$ IETs remains elevated^{135,136}, which might contribute to re-establishing epithelial homeostasis^{137,138}. Thus, although a clear pathogenic role exists for TCR $\alpha\beta^+$ CD8 $\alpha\beta^+$ IETs in particular in coeliac disease, TCR $\gamma\delta^+$ IETs in general might have an important role in epithelial repair.

IBD

The pathogenesis of Crohn's disease and ulcerative colitis, together comprising IBD, is complex and not fully elucidated⁵². Mucosal lymphocytes are altered in number and function in patients with IBD compared with those in healthy control individuals¹³⁹, and are thought to play a pivotal part in the pathogenic process. Intraepithelial lymphocytosis is observed in IBD^{20,113,140-142}, with a higher total IET count in Crohn's disease than in ulcerative colitis¹⁴², but lower count than in coeliac disease¹⁴³. Although the absolute number of TCR $\alpha\beta^+$ CD8 $\alpha\beta^+$ IETs is considerably increased, TCR $\gamma\delta^+$ IET numbers remain largely unchanged¹⁴⁴⁻¹⁴⁷. Even non-involved and once-involved colonic regions in patients with ulcerative colitis show some degree of increased total IET numbers²⁰ (Fig. 4).

In IBD, especially in Crohn's disease, APCs produce increased levels of IL-23¹⁴⁸. In addition, the IL-23 receptor is upregulated on TCR $\alpha\beta^+$ CD8 $\alpha\beta^+$ IETs, and stimulation by IL-23 leads to production of proinflammatory cytokines, including IFN γ , TNF, IL-2 and IL-17A. Furthermore, IET cytotoxicity is increased in patients with IBD, even compared with cytotoxicity in patients with colitis due to *Salmonella* infection¹⁴⁸. The elevated cytotoxicity executed by TCR $\alpha\beta^+$ CD8 $\alpha\beta^+$ IETs¹⁴⁷ is believed to be a main contributor to the mucosal damage that characterizes both IBD and coeliac disease^{60,147}. TCR $\alpha\beta^+$ CD4 $^+$ IETs might also contribute to epithelial damage by upregulating NKG2D⁸². Although IETs can be damaging in IBD, the local inflammatory response is probably more dependent on (infiltrating) lamina propria cells such as TCR $\alpha\beta^+$ CD4 $^+$ T_H subsets that produce inflammatory cytokines, but the exact mechanisms are presently unknown^{52,149}. The impaired intestinal barrier of patients with IBD might, however, change the dynamics of lamina propria T cells and IETs. IBD is characterized by massive lymphocyte infiltrations spanning the intestinal mucosa, and in Crohn's disease, even transmural inflammation is seen¹⁵⁰. This destructive inflammation might result in exchange of immune cells between the intestinal compartments, enabling cells without specific gut-homing markers to infiltrate. In addition, aberrant expression of proinflammatory cytokines that alter the local microenvironment might impede the differentiation from peripheral T cell to tissue-resident IET. Whether resident IETs, infiltrating cells or a combination of both are the contributing T cells of the epithelial compartment in the pathogenesis of IBD is unclear.

Colorectal cancer

Extensive, long-standing colitis is an established risk factor for colorectal cancer (CRC), with the severity of histological inflammation in these patients being a key risk factor¹⁵¹⁻¹⁵³. Tumour-infiltrating lymphocytes (TILs) in several gastrointestinal tract neoplasms share many

phenotypic and functional characteristics with IETs, including CD103 and immune checkpoint expression (for example CTLA4 and programmed death 1 (PD1)) and a memory phenotype¹⁵⁴⁻¹⁵⁶. Moreover, until a tumour has developed its own blood supply (or infiltrated lymphatic vessels), lymphocytes are hypothesized to reach the tumour via a direct mucosal and/or epithelial route, and therefore in early stage tumours, TILs might originate from IETs. In support of this suggestion, both TCR $\gamma\delta^+$ IETs and CRC TCR $\gamma\delta^+$ TILs preferably express the TCR V δ 1 region⁶⁹, which is in contrast to peripheral TCR $\gamma\delta^+$ T cells which express the V δ 2 region. Because of low-grade inflammation within and surrounding the developing tumour, TILs might additionally be recruited from the periphery. Conversely, the absence of TCR β gene overlap from CRC and adjacent mucosal tissue, independent of the distance¹⁵⁷, suggests that TCR $\alpha\beta^+$ TILs do not originate from TCR $\alpha\beta^+$ IETs.

Even if IETs are not (all) the progenitors of TILs, they might contribute to antitumour activity. In vitro, TCR $\gamma\delta^+$ IETs are able to eliminate epithelial cancer cells with similar histology to CRC cells¹⁵⁸. One elimination pathway might be NKG2D signalling via ligand interaction on CRC cells resulting in IET Fas ligand production and Fas-ligand-mediated cytotoxicity¹⁵⁹. TNF and IFN γ production by IETs, together with IET α_E adhesion to E-cadherin on target cells, were found to be crucial for optimal cytolysis. Thus, on the one hand, TCR $\alpha\beta^+$ CD8 $\alpha\beta^+$ IETs might contribute to the increased risk of tumorigenesis in IBD by promoting inflammation, whereas on the other hand, peritumoral TCR $\gamma\delta^+$ IETs could play a protective role by targeting tumour cells.

Targeting IETs in therapy

Coeliac disease

Currently, the treatment for coeliac disease is a lifelong gluten-free diet. Nonresponders, who strictly adhere to a gluten-free diet but continue to have symptoms not due to comorbidity, make up ~1% of all patients with coeliac disease¹⁶⁰. Given that coeliac disease is characterized by chronic overexpression of IL-15, assessing the clinical efficacy of an IL-15 blocking antibody in these patients seems worthwhile. IL-15 inhibition could also be of value to aid mucosal healing in patients starting a gluten-free diet. In transgenic mice that overexpressed human IL-15 – resulting in villous atrophy and duodeno-jejunal inflammation – blocking IL-15 restored the intestinal mucosa¹⁶¹. The first phase II clinical trial is currently testing the efficacy of an IL-15 blocking antibody in patients with nonresponsive coeliac disease¹⁶². Blocking IL-15 might affect IETs in several ways¹⁶³. In the short term, it might diminish or normalize IET cytotoxic function and prevent TCR-independent NKG2D-mediated cytolysis, consequently reducing epithelial destruction; however, long-term blocking of IL-15 might affect IET proliferation and survival, given that low levels of IL-15 are needed for these processes.

IBD

IBD treatment largely relies on targeting the (mucosal) immune system. Even if IETs are less involved than lamina propria T cells in the pathogenesis of IBD, targeting gut-homing and/or resident T cells in general might be essential in limiting epithelial damage^{139,142,147}. Current first-line therapies in IBD, including 5-aminosalicylates (5-ASA), corticosteroids and anti-TNF

compounds, have systemic anti-inflammatory effects^{164–166}. Even after the introduction of anti-TNF drugs, ~20% of patients with IBD still require surgery within 2–5 years to control disease¹⁶⁷. Novel therapies specifically targeting the intestinal immune system and T cell migration include the integrin inhibitors vedolizumab (anti- $\alpha4\beta7$, GEMINI trials^{168,169}) and etrolizumab (anti- $\beta7$, ETRO trials in phase III¹⁷⁰).

Vedolizumab is effective in inducing and maintaining remission in patients with IBD, especially for ulcerative colitis. It binds integrin $\alpha4\beta7$, which, in vitro results in internalization of the vedolizumab- $\alpha4\beta7$ complex and blocking $\alpha4\beta7$ binding to MadCAM1¹⁷¹. Functional $\alpha4\beta7$ membrane expression is rapidly restored after discontinuation of vedolizumab¹⁷¹. T cell function and proliferation are not affected by short-term blocking of $\alpha4\beta7$ ^{171,172}. Blocking $\alpha4\beta7$ in mice that are healthy or have acute dextran sodium sulfate-induced colitis results in loss of intestinal B cells and Foxp3⁺ Treg cells, but the TCR $\alpha\beta^+$ CD4⁺ and TCR $\alpha\beta^+$ CD8 $\alpha\beta^+$ T cell populations remain unchanged¹⁷³. However, in mice with chronic T-cell-mediated colitis, all mucosal T cells are reduced in number and function by blocking $\alpha4\beta7$ ¹⁷³. The local immune changes induced by vedolizumab in humans are less clear, but in ulcerative colitis, the FOXP3⁺ Treg cells in particular seem to be reduced in number¹⁷². This effect is a marked specificity of anti- $\alpha4\beta7$ therapy, and it is unknown whether this uneven reduction in T cell subsets has negative effects in the long term. Blocking $\alpha4\beta7$ can result in expression of alternative, less gut-specific homing markers to ensure lymphocyte-trafficking to the gut⁴². Furthermore, altered migrational behaviour due to the upregulation of other homing markers on peripheral lymphocytes in the blood could be responsible for the extraintestinal autoimmune symptoms observed as adverse effects of vedolizumab¹⁷⁴.

Etrolizumab targets all gut-specific T cells, including IETs, that express integrin $\alpha\epsilon\beta7$ ³⁷ and therefore affects a broader set of lymphocytes. Short term blocking of $\beta7$ seems to interfere with the trafficking of $\beta7^+$ T cells to the intestines but does not decrease the total numbers of intestinal $\beta7^+$ T cells. However, a trend towards decreased numbers of $\alpha\epsilon^+$ T cells in the epithelium was observed¹⁷⁰. Whether vedolizumab and etrolizumab penetrate the mucosa is unknown, but these therapies mainly seem to affect lymphocyte gut-homing and do not directly target the resident intestinal lymphocytes. This observation could explain the relatively slow response time for these drugs (remission is achieved after ~10 weeks with vedolizumab¹⁶⁸). Importantly, even though prolonged maintenance therapy (5 years) with vedolizumab does not result in increased numbers of adverse events including infections¹⁷⁵, no data are available on how the local immune compartment is affected in the long term. In particular, etrolizumab could affect the maintenance of the intestinal tissue-resident T cell pool and its function if used for a long period of time. For example, $\beta7$ -deficient mice have severely impaired gut-associated lymphoid tissue, whereas lymphocyte development in other organs is unaffected¹⁷⁶. Targeting markers specifically implicated in gut-homing during inflammation could therefore be an attractive option for long term maintenance therapy. In this context, the novel therapeutic target GPR15 seems promising, especially in ulcerative colitis. GPR15 is expressed on pathogenic T cells in patients with ulcerative colitis¹⁷⁷, and in a

humanized mouse model, anti-GPR15 therapy effectively blocked T effector cell gut-homing¹⁷².

Gut-homing markers are differentially expressed between T cell subsets, between the small intestine and colon, between diseases and between species^{172,177,178}. Therefore, non-humanized mouse-models will not suffice to test novel therapies, and this differential expression also complicates elucidation of the exact mechanisms involved in gut-homing. Prediction of therapeutic responses could be derived from an improved understanding of these mechanisms and could thus be of great importance from the patient and clinical perspective, given that only a subset of patients responds to gut-homing targeted therapies¹⁶⁸⁻¹⁷⁰.

CONCLUSIONS

IETs are non-recirculating, resident T cells located at the one-cell-layer-thick epithelial barrier. IETs have an 'activated yet resting' phenotype, with a unique cytotoxic profile capable of rapid responsiveness. Furthermore, IETs have a function in epithelial maintenance via the expression of growth factors. Their predominant T_H1-type cytokine profile and cytotoxic capabilities warrant tight regulation to maintain the balance between inflammation and tolerance. In chronic intestinal inflammation, as seen in coeliac disease and IBD, TCR $\alpha\beta$ ⁺CD8 $\alpha\beta$ ⁺ IETs in particular seem able to disrupt the epithelial membrane with dire consequences.

Studies aiming to define and understand the local immune response in the human gastrointestinal tract often overlook the IETs, or these cells are studied pooled with the lamina propria T cells. Studying IETs separately from lamina propria T cells is essential to expand our understanding of the intestinal mucosal immune system, as this different effector population experiences other environmental cues and performs different functions. Although animal models are invaluable to broaden our understanding of immunological mechanisms, the immune system is under substantial selective pressure, and with 65 million years of evolution between mouse and humans, differences are inevitable¹⁷⁹. In addition, it is important to consider the influence of the diverse microbial composition seen with geographical variation and age¹⁸⁰, the diversity of diet and living environments and, to a lesser extent, of genetics¹⁸¹ on the local immune balance.

In the near future, mechanistic studies in humans will be challenging because IETs do not survive well *ex vivo*, and *in vivo* studies are limited by technical and ethical concerns. However, techniques to study human resident T cells have advanced tremendously, especially the omic techniques to decipher characteristics and explore interactions. Greater emphasis on human IETs, as a separate entity from lamina propria T cells, will enable us to establish their role in health and disease and could lead to a fuller understanding of human physiology in general and eventually might lead to targeted disease diagnosis, treatment and prognostication.

Acknowledgements

The authors apologize to those colleagues whose relevant work was not included in this Review owing to space constraints. The authors thank J. ten Hove for critically reading the

manuscript and for helpful comments. F.v.W. is supported by a VIDI career development grant (016.146.332) from The Netherlands Organization for Health Research and Development (ZonMw). D.P.H.v.K. and E.C.B. are supported by the Alexandre Suerman program for MD and PhD students of the University Medical Center Utrecht, Netherlands.

REFERENCES

1. Mowat, A. M. & Agace, W. W. Regional specialization within the intestinal immune system. *Nat. Rev. Immunol.* **14**, 667–685 (2014).
2. Peterson, L. W. & Artis, D. Intestinal epithelial cells: regulators of barrier function and immune homeostasis. *Nat. Rev. Immunol.* **14**, 141–153 (2014).
3. Murphy, K. & Weaver, C. *Janeway's Immunobiology*. (Garland Science, 2016).
4. Ganusov, V. V & De Boer, R. J. Do most lymphocytes in humans really reside in the gut? *Trends Immunol.* **28**, 514–518 (2007).
5. Park, C. O. & Kupper, T. S. The emerging role of resident memory T cells in protective immunity and inflammatory disease. *Nat. Med.* **21**, 688–697 (2015).
6. Masopust, D. Preferential Localization of Effector Memory Cells in Nonlymphoid Tissue. *Science* **291**, 2413–2417 (2001).
7. Fan, X. & Rudensky, A. Y. Hallmarks of Tissue-Resident Lymphocytes. *Cell* **164**, 1198–1211 (2016).
8. Burzyn, D., Benoist, C. & Mathis, D. Regulatory T cells in nonlymphoid tissues. *Nat. Immunol.* **14**, 1007–1013 (2013).
9. Sujino, T. *et al.* Tissue adaptation of regulatory and intraepithelial CD4(+) T cells controls gut inflammation. *Science* **352**, 1581–1586 (2016).
10. Cheroutre, H., Lambolez, F. & Mucida, D. The light and dark sides of intestinal intraepithelial lymphocytes. *Nat. Rev. Immunol.* **11**, 445–456 (2011).
11. Hoytema van Konijnenburg, D. P. *et al.* Intestinal epithelial and intraepithelial T cell crosstalk mediates a dynamic response to infection. *Cell* **171**, 783–794.e13 (2017).
12. Fuchs, A. *et al.* Intraepithelial type 1 innate lymphoid cells are a unique subset of IL-12- and IL-15-responsive IFN-gamma-producing cells. *Immunity* **38**, 769–781 (2013).
13. Simoni, Y. *et al.* Human Innate Lymphoid Cell Subsets Possess Tissue-Type Based Heterogeneity in Phenotype and Frequency. *Immunity* **46**, 148–161 (2017).
14. Spencer, J. *et al.* Changes in intraepithelial lymphocyte subpopulations in coeliac disease and enteropathy associated T cell lymphoma (malignant histiocytosis of the intestine). *Gut* **30**, 339–346 (1989).
15. Leon, F. *et al.* Human small-intestinal epithelium contains functional natural killer lymphocytes. *Gastroenterology* **125**, 345–356 (2003).
16. Rostami, K. *et al.* ROC-king onwards: intraepithelial lymphocyte counts, distribution & role in coeliac disease mucosal interpretation. *Gut* **66**, 2080–2086 (2017).
17. Hirata, I., Berrebi, G., Austin, L. L., Keren, D. F. & Dobbins, W. O. Immunohistological characterization of intraepithelial and lamina propria lymphocytes in control ileum and colon and in inflammatory bowel disease. *Dig. Dis. Sci.* **31**, 593–603 (1986).
18. Bednarska, O., Ignatova, S., Dahle, C. & Ström, M. Intraepithelial lymphocyte distribution differs between the bulb and the second part of duodenum. *BMC Gastroenterol.* **13**, 111 (2013).
19. Austin, L. L. & Dobbins, W. O. Intraepithelial leukocytes of the intestinal mucosa in normal man and in Whipple's disease: a light- and electron-microscopic study. *Dig. Dis. Sci.* **27**, 311–320 (1982).
20. Ahn, J. Y. *et al.* Colonic mucosal immune activity in irritable bowel syndrome: Comparison with healthy controls and patients with ulcerative colitis. *Dig. Dis. Sci.* **59**, 1001–1011 (2014).
21. Faderl, M., Noti, M., Corazza, N. & Mueller, C. Keeping bugs in check: The mucus layer as a critical component in maintaining intestinal homeostasis. *IUBMB Life* **67**, 275–285 (2015).
22. Hansson, G. C. Role of mucus layers in gut infection and inflammation. *Curr. Opin. Microbiol.* **15**, 57–62 (2012).
23. Ruscher, R., Kummer, R. L., Lee, Y. J., Jameson, S. C. & Hogquist, K. A. CD8 α phaalalpha intraepithelial lymphocytes arise from two main thymic precursors. *Nat. Immunol.* **18**, 771–779 (2017).
24. Klose, C. S. N. *et al.* A committed postselection precursor to natural TCR $\alpha\beta$ intraepithelial lymphocytes. *Nat. Publ. Gr.* 1–12 (2017).
25. van Wijk, F. & Cheroutre, H. Intestinal T cells: Facing the mucosal immune dilemma with synergy and diversity. *Seminars in Immunology* **21**, 130–138 (2009).
26. McVay, L. D., Jaswal, S. S., Kennedy, C., Hayday, A. & Carding, S. R. The generation of human gammadelta T cell repertoires during fetal development. *J. Immunol.* **160**, 5851–5860 (1998).
27. Spencer, J., Isaacson, P. G., Walker-Smith, J. A. & MacDonald, T. T. Heterogeneity in intraepithelial lymphocyte subpopulations in fetal and postnatal human small intestine. *Journal of pediatric*

- gastroenterology and nutrition* **9**, 173–177 (1989).
28. Mold, J. E. *et al.* Fetal and adult hematopoietic stem cells give rise to distinct T cell lineages in humans. *Science* **330**, 1695–1699 (2010).
 29. Sathaliyawala, T. *et al.* Distribution and Compartmentalization of Human Circulating and Tissue-Resident Memory T Cell Subsets. *Immunity* **38**, 187–197 (2013).
 30. Thome, J. J. C. *et al.* Early-life compartmentalization of human T cell differentiation and regulatory function in mucosal and lymphoid tissues. *Nat. Med.* **22**, 72–77 (2016).
 31. Jarry, A., Cerf-bensussan, N., Brousse, N., Selz, F. & Guy-grand, D. Subsets of CD3+ (T cell receptor α/β or γ/δ) and CD3- lymphocytes isolated from normal human gut epithelium display phenotypical features different from their counterparts in peripheral blood. *Eur. J. Immunol.* **20**, 1097–1103 (1990).
 32. Steinert, E. M. *et al.* Quantifying Memory CD8 T Cells Reveals Regionalization of Immunosurveillance. *Cell* **161**, 737–749 (2015).
 33. Bakdash, G., Vogelpoel, L. T., van Capel, T. M., Kapsenberg, M. L. & de Jong, E. C. Retinoic acid primes human dendritic cells to induce gut-homing, IL-10-producing regulatory T cells. *Mucosal Immunol.* **8**, 265–278 (2015).
 34. Zabel, B. A. *et al.* Human G protein-coupled receptor GPR-9-6/CC chemokine receptor 9 is selectively expressed on intestinal homing T lymphocytes, mucosal lymphocytes, and thymocytes and is required for thymus-expressed chemokine-mediated chemotaxis. *J. Exp. Med.* **190**, 1241–1256 (1999).
 35. Cerf-Bensussan, N., Bègue, B., Gagnon, J. & Meo, T. The human intraepithelial lymphocyte marker HML-1 is an integrin consisting of a $\beta 7$ subunit associated with a distinctive α chain. *Eur. J. Immunol.* **22**, 273–277 (1992).
 36. Raine, T., Liu, J. Z., Anderson, C. A., Parkes, M. & Kaser, A. Generation of primary human intestinal T cell transcriptomes reveals differential expression at genetic risk loci for immune-mediated disease. *Gut* **64**, 250–259 (2015).
 37. Briskin, M. *et al.* Human mucosal addressin cell adhesion molecule-1 is preferentially expressed in intestinal tract and associated lymphoid tissue. *Am. J. Pathol.* **151**, 97–110 (1997).
 38. Habtezion, A., Nguyen, L. P., Hadeiba, H. & Butcher, E. C. Leukocyte Trafficking to the Small Intestine and Colon. *Gastroenterology* **150**, 340–354 (2016).
 39. Salmi, M. & Jalkanen, S. Lymphocyte homing to the gut: Attraction, adhesion, and commitment. *Immunological Reviews* **206**, 100–113 (2005).
 40. Dogan, A., Wang, Z. D. & Spencer, J. E-cadherin expression in intestinal epithelium. *J Clin Pathol* **48**, 143–146 (1995).
 41. Kuklin, N. A. *et al.* Alpha4beta7 independent pathway for CD8+ T cell-mediated intestinal immunity to rotavirus. *J. Clin. Invest.* **106**, 1541–1552 (2000).
 42. Zundler, S. *et al.* The alpha4beta1 Homing Pathway Is Essential for Ileal Homing of Crohn's Disease Effector T Cells In Vivo. *Inflamm. Bowel Dis.* **23**, 379–391 (2017).
 43. Thome, J. J. C. *et al.* Longterm maintenance of human naive T cells through in situ homeostasis in lymphoid tissue sites. *Sci. Immunol.* **1**, eaah6506, (2016).
 44. Di Marco Barros, R. *et al.* Epithelia Use Butyrophilin-like Molecules to Shape Organ-Specific gammadelta T Cell Compartments. *Cell* **167**, 203–218.e17 (2016).
 45. Laidlaw, B. J. *et al.* CD4+ T Cell Help Guides Formation of CD103+ Lung-Resident Memory CD8+ T Cells during Influenza Viral Infection. *Immunity* **41**, 633–645 (2014).
 46. Mackay, L. K. *et al.* The developmental pathway for CD103+CD8+ tissue-resident memory T cells of skin. *Nat. Immunol.* **14**, 1294–1301 (2013).
 47. Zhang, N. & Bevan, M. J. Transforming growth factor-beta signaling controls the formation and maintenance of gut-resident memory T cells by regulating migration and retention. *Immunity* **39**, 687–696 (2013).
 48. Mackay, L. K. *et al.* T-box Transcription Factors Combine with the Cytokines TGF- β and IL-15 to Control Tissue-Resident Memory T Cell Fate. *Immunity* **43**, 1101–1111 (2015).
 49. Mohammed, J. *et al.* Stromal cells control the epithelial residence of DCs and memory T cells by regulated activation of TGF- β . *Nat. Immunol.* **17**, 414–421 (2016).
 50. Jiang, W. *et al.* Recognition of gut microbiota by NOD2 is essential for the homeostasis of intestinal intraepithelial lymphocytes. *J. Exp. Med.* **210**, 2465–2476 (2013).
 51. Muzes, G., Molnar, B., Tulassay, Z. & Sipos, F. Changes of the cytokine profile in inflammatory bowel diseases. *World J. Gastroenterol.* **18**, 5848–5861 (2012).
 52. Park, J. H., Peyrin-Biroulet, L., Eisenhut, M. & Shin, J. II. IBD immunopathogenesis: A comprehensive

- review of inflammatory molecules. *Autoimmun. Rev.* **16**, 416–426 (2017).
53. Meresse, B. *et al.* Coordinated induction by IL15 of a TCR-independent NKG2D signaling pathway converts CTL into lymphokine-activated killer cells in celiac disease. *Immunity* **21**, 357–366 (2004).
 54. Qiu, Y. *et al.* TLR2-Dependent Signaling for IL-15 Production Is Essential for the Homeostasis of Intestinal Intraepithelial Lymphocytes. *Mediators Inflamm.* **2016**, 4281865 (2016).
 55. Lanier, L. L., Le, A. M., Civin, C. I., Loken, M. R. & Phillips, J. H. The relationship of CD16 (Leu-11) and Leu-19 (NKH-1) antigen expression on human peripheral blood NK cells and cytotoxic T lymphocytes. *J. Immunol.* **136**, 4480–4486 (1986).
 56. Ohkawa, T. *et al.* Systematic characterization of human CD8+ T cells with natural killer cell markers in comparison with natural killer cells and normal CD8+ T cells. *Immunology* **103**, 281–290 (2001).
 57. Mucida, D. *et al.* Transcriptional reprogramming of mature CD4(+) helper T cells generates distinct MHC class II-restricted cytotoxic T lymphocytes. *Nat. Immunol.* **14**, 281–289 (2013).
 58. Reis, B. S., Hoytema van Konijnenburg, D. P., Grivennikov, S. I. & Mucida, D. Transcription factor T-bet regulates intraepithelial lymphocyte functional maturation. *Immunity* **41**, 244–256 (2014).
 59. Sarrabayrouse, G. *et al.* CD4CD8 $\alpha\alpha$ lymphocytes, a novel human regulatory T cell subset induced by colonic bacteria and deficient in patients with inflammatory bowel disease. *PLoS Biol.* **12**, e1001833 (2014).
 60. Dalton, J. E. *et al.* Intraepithelial gammadelta+ lymphocytes maintain the integrity of intestinal epithelial tight junctions in response to infection. *Gastroenterology* **131**, 818–829 (2006).
 61. Ismail, A. S., Behrendt, C. L. & Hooper, L. V. Reciprocal interactions between commensal bacteria and gamma delta intraepithelial lymphocytes during mucosal injury. *J. Immunol.* **182**, 3047–3054 (2009).
 62. Edelblum, K. L. *et al.* gammadelta Intraepithelial Lymphocyte Migration Limits Transepithelial Pathogen Invasion and Systemic Disease in Mice. *Gastroenterology* **148**, 1417–1426 (2015).
 63. Perera, L. *et al.* Expression of nonclassical class I molecules by intestinal epithelial cells. *Inflamm. Bowel Dis.* **13**, 298–307 (2007).
 64. Lin, X. P., Almqvist, N. & Telemeo, E. Human small intestinal epithelial cells constitutively express the key elements for antigen processing and the production of exosomes. *Blood Cells, Mol. Dis.* **35**, 122–128 (2005).
 65. Strid, J., Sobolev, O., Zafirova, B., Polic, B. & Hayday, A. The intraepithelial T cell response to NKG2D-ligands links lymphoid stress surveillance to atopy. *Science* **334**, 1293–1297 (2011).
 66. Vantourout, P. *et al.* Immunological visibility: posttranscriptional regulation of human NKG2D ligands by the EGF receptor pathway. *Sci. Transl. Med.* **6**, 231ra49 (2014).
 67. Hayday, A., Theodoridis, E., Ramsburg, E. & Shires, J. Intraepithelial lymphocytes: exploring the Third Way in immunology. *Nat Immunol* **2**, 997–1003 (2001).
 68. Shires, J., Theodoridis, E. & Hayday, A. C. Biological Insights into TCR $\gamma\delta$ + and TCR $\alpha\beta$ + Intraepithelial Lymphocytes Provided by Serial Analysis of Gene Expression (SAGE). *Immunity* **15**, 419–434 (2001).
 69. Deusch, K. *et al.* A major fraction of human intraepithelial lymphocytes simultaneously expresses the gamma/delta T cell receptor, the CD8 accessory molecule and preferentially uses the V delta 1 gene segment. *Eur. J. Immunol.* **21**, 1053–1059 (1991).
 70. Lundqvist, C. *et al.* Phenotype and cytokine profile of intraepithelial lymphocytes in human small and large intestine. *Ann. N. Y. Acad. Sci.* **756**, 395–399 (1995).
 71. Lundqvist, C., Melgar, S., Yeung, M. M., Hammarström, S. & Hammarström, M. L. Intraepithelial lymphocytes in human gut have lytic potential and a cytokine profile that suggest T helper 1 and cytotoxic functions. *J. Immunol.* **157**, 1926–1934 (1996).
 72. Hoang, P., Crotty, B., Dalton, H. R. & Jewell, D. P. Epithelial cells bearing class II molecules stimulate allogeneic human colonic intraepithelial lymphocytes. *Gut* **33**, 1089–1093 (1992).
 73. Booth, J. S. *et al.* Characterization and functional properties of gastric tissue-resident memory T cells from children, adults, and the elderly. *Front. Immunol.* **5**, 1–15 (2014).
 74. Youakim, A. & Ahdieh, M. Interferon-gamma decreases barrier function in T84 cells by reducing ZO-1 levels and disrupting apical actin. *Am. J. Physiol.* **276**, G1279–88 (1999).
 75. Smyth, D., Leung, G., Fernando, M. & McKay, D. M. Reduced surface expression of epithelial E-cadherin evoked by interferon-gamma is Fyn kinase-dependent. *PLoS One* **7**, e38441 (2012).
 76. Qiu, Y. & Yang, H. Effects of Intraepithelial Lymphocyte-Derived Cytokines on Intestinal Mucosal Barrier Function. *J. Interf. Cytokine Res.* **33**, 551–562 (2013).
 77. Chott, A. *et al.* Intraepithelial lymphocytes in normal human intestine do not express proteins associated with cytolytic function. *Am. J. Pathol.* **151**, 435–442 (1997).

78. Cerf-Bensussan, N. *et al.* A monoclonal antibody (HML-1) defining a novel membrane molecule present on human intestinal lymphocytes. *Eur. J. Immunol.* **17**, 1279–1285 (1987).
79. Russell, G. J., Nagler-Anderson, C., Anderson, P. & Bhan, A. K. Cytotoxic potential of intraepithelial lymphocytes (IELs). Presence of TIA-1, the cytolytic granule-associated protein, in human IELs in normal and diseased intestine. *Am. J. Pathol.* **143**, 350–354 (1993).
80. Hongo, T. *et al.* Functional expression of Fas and Fas ligand on human colonic intraepithelial T lymphocytes. *J. Int. Med. Res.* **28**, 132–142 (1999).
81. Bhagat, G. *et al.* Small intestinal CD8+TCR $\gamma\delta$ +NKG2A+ intraepithelial lymphocytes have attributes of regulatory cells in patients with celiac disease. *J. Clin. Investig.* **118**, 281–293 (2008).
82. Allez, M. *et al.* CD4+NKG2D+ T Cells in Crohn's Disease Mediate Inflammatory and Cytotoxic Responses Through MICA Interactions. *Gastroenterology* **132**, 2346–2358 (2007).
83. Deusch, K. *et al.* Lymphokine repertoire and proliferative capacity of human intestinal intraepithelial lymphocytes. *Gastroenterology* **100**, A574 (1991).
84. Finch, P. W., Pricolo, V., Wu, A. & Finkelstein, S. D. Increased expression of keratinocyte growth factor messenger RNA associated with inflammatory bowel disease. *Gastroenterology* **110**, 441–451 (1996).
85. Finch, P. W. & Cheng, A. L. Analysis of the cellular basis of keratinocyte growth factor overexpression in inflammatory bowel disease. *Gut* **45**, 848–855 (1999).
86. Rubin, J. S. *et al.* Purification and characterization of a newly identified growth factor specific for epithelial cells. *Proc. Natl. Acad. Sci. U. S. A.* **86**, 802–806 (1989).
87. Sturm, A. & Dignass, A. U. Epithelial restitution and wound healing in inflammatory bowel disease. *World J. Gastroenterol.* **14**, 348–353 (2008).
88. Cerf-Bensussan, N., Guy-Grand, D. & Griscelli, C. Intraepithelial lymphocytes of human gut: isolation, characterisation and study of natural killer activity. *Gut* **26**, 81–88 (1985).
89. Dobbins, W. O. 3rd. Human intestinal intraepithelial lymphocytes. *Gut* **27**, 972–985 (1986).
90. Di Sabatino, A. *et al.* Intraepithelial and lamina propria lymphocytes show distinct patterns of apoptosis whereas both populations are active in Fas based cytotoxicity in coeliac disease. *Gut* **49**, 380–386 (2001).
91. Rautel, D. H. Roles of the NKG2D immunoreceptor and its ligands. *Nat. Rev. Immunol.* **3**, 781–790 (2003).
92. Colucci, F., Di Santo, J. P. & Leibson, P. J. Natural killer cell activation in mice and men: different triggers for similar weapons? *Nat. Immunol.* **3**, 807–813 (2002).
93. Cheroutre, H. & Lambolez, F. Doubting the TCR Coreceptor Function of CD8 $\alpha\alpha$. *Immunity* **28**, 149–159 (2008).
94. Menezes, J. da S. *et al.* Stimulation by food proteins plays a critical role in the maturation of the immune system. *Int. Immunol.* **15**, 447–455 (2003).
95. Bandeira, A. *et al.* Localization of gamma/delta T cells to the intestinal epithelium is independent of normal microbial colonization. *J. Exp. Med.* **172**, 239–244 (1990).
96. Yang, H., Antony, P. A., Wildhaber, B. E. & Teitelbaum, D. H. Intestinal Intraepithelial Lymphocyte -T Cell-Derived Keratinocyte Growth Factor Modulates Epithelial Growth in the Mouse. *J. Immunol.* **172**, 4151–4158 (2004).
97. Sundin, J. *et al.* Altered faecal and mucosal microbial composition in post-infectious irritable bowel syndrome patients correlates with mucosal lymphocyte phenotypes and psychological distress. *Aliment. Pharmacol. Ther.* **41**, 342–351 (2015).
98. Geva-Zatorsky, N. *et al.* Mining the Human Gut Microbiota for Immunomodulatory Organisms. *Cell* **168**, 928–943.e11 (2017).
99. Umesaki, Y., Setoyama, H., Matsumoto, S. & Okada, Y. Expansion of axF T-cell receptor-bearing intestinal intraepithelial lymphocytes after microbial colonization in germ-free mice and its independence from thymus. *Immunology* **79**, 32–37 (1993).
100. Semenkovich, N. P. *et al.* Impact of the gut microbiota on enhancer accessibility in gut intraepithelial lymphocytes. *Proc. Natl. Acad. Sci. U. S. A.* **113**, 201617793 (2016).
101. Park, J. *et al.* Short chain fatty acids induce both effector and regulatory T cells by suppression of histone deacetylases and regulation of the mTOR-S6K pathway. *Mucosal Immunol.* **8**, 80–93 (2015).
102. Cabinian, A. *et al.* Gut symbiotic microbes imprint intestinal immune cells with the innate receptor SLAMF4 which contributes to gut immune protection against enteric pathogens. *Gut* **67**, 847–859 (2017).
103. O'Keefe, M. S. *et al.* SLAMF4 Is a Negative Regulator of Expansion of Cytotoxic Intraepithelial CD8+ T Cells That Maintains Homeostasis in the Small Intestine. *Gastroenterology* **148**, 991–1001.e4 (2015).

104. Li, Y. *et al.* Exogenous stimuli maintain intraepithelial lymphocytes via aryl hydrocarbon receptor activation. *Cell* **147**, 629–640 (2011).
105. Hubbard, T. D. *et al.* Adaptation of the human aryl hydrocarbon receptor to sense microbiota-derived indoles. *Sci. Rep.* **5**, 12689 (2015).
106. Julliard, W., Fechner, J. H. & Mezrich, J. D. The aryl hydrocarbon receptor meets immunology: Friend or foe? A little of both. *Front. Immunol.* **5**, 458 (2014).
107. Ji, T. *et al.* Aryl Hydrocarbon Receptor Activation Down-Regulates IL-7 and Reduces Inflammation in a Mouse Model of DSS-Induced Colitis. *Dig. Dis. Sci.* **60**, 1958–1966 (2015).
108. Monteleone, I., Pallone, F. & Monteleone, G. Aryl hydrocarbon receptor and colitis. *Semin. Immunopathol.* **35**, 671–675 (2013).
109. Monteleone, I. *et al.* Aryl hydrocarbon receptor-induced signals up-regulate IL-22 production and inhibit inflammation in the gastrointestinal tract. *Gastroenterology* **141**, 237–248 (2011).
110. Clark, R. A. Resident memory T cells in human health and disease. *Sci. Transl. Med.* **7**, 269rv1–269rv1 (2015).
111. Rutgeerts, P. *et al.* Natural history of recurrent Crohn's disease at the ileocolonic anastomosis after curative surgery. *Gut* **25**, 665–672 (1984).
112. Pascua, M., Su, C., Lewis, J. D., Brensinger, C. & Lichtenstein, G. R. Meta-analysis: factors predicting post-operative recurrence with placebo therapy in patients with Crohn's disease. *Aliment. Pharmacol. Ther.* **28**, 545–556 (2008).
113. Brown, I., Mino-Kenudson, M., Deshpande, V. & Lauwers, G. Y. Intraepithelial lymphocytosis in architecturally preserved proximal small intestinal mucosa: An increasing diagnostic problem with a wide differential diagnosis. *Archives of Pathology and Laboratory Medicine* **130**, 1020–1025 (2006).
114. Chang, F., Mahadeva, U. & Deere, H. Pathological and clinical significance of increased intraepithelial lymphocytes (IELs) in small bowel mucosa. *APMIS* **113**, 385–399 (2005).
115. Schmidt, E., Smyrk, T. C., Faubion, W. A. & Oxentenko, A. S. Duodenal intraepithelial lymphocytosis with normal villous architecture in pediatric patients: Mayo Clinic experience, 2000–2009. *J. Pediatr. Gastroenterol. Nutr.* **56**, 51–55 (2013).
116. Parihar, V. *et al.* Clinical Outcome of Patients with Raised Intraepithelial Lymphocytes with Normal Villous Architecture on Duodenal Biopsy. *Digestion* **95**, 288–292 (2017).
117. Jabri, B. & Sollid, L. M. T Cells in Celiac Disease. *J. Immunol.* **198**, 3005–3014 (2017).
118. Green, P. H. R. & Cellier, C. Celiac Disease. *N. Engl. J. Med.* **357**, 1731–1743 (2007).
119. Meresse, B., Malamut, G. & Cerf-Bensussan, N. Celiac disease: an immunological jigsaw. *Immunity* **36**, 907–919 (2012).
120. Abadie, V., Discepolo, V. & Jabri, B. Intraepithelial lymphocytes in celiac disease immunopathology. *Semin. Immunopathol.* **34**, 551–556 (2012).
121. Goldstein, N. S. & Underhill, J. Morphologic features suggestive of gluten sensitivity in architecturally normal duodenal biopsy specimens. *Am. J. Clin. Pathol.* **116**, 63–71 (2001).
122. Steenholt, J. V. *et al.* The composition of T cell subtypes in duodenal biopsies are altered in coeliac disease patients. *PLoS One* **12**, 1–17 (2017).
123. Hue, S. *et al.* A direct role for NKG2D/MICA interaction in villous atrophy during celiac disease. *Immunity* **21**, 367–377 (2004).
124. Allegretti, Y. L. *et al.* Broad MICA/B Expression in the Small Bowel Mucosa: A Link between Cellular Stress and Celiac Disease. *PLoS One* **8**, e73658 (2013).
125. Fehniger, T. A. & Caligiuri, M. A. Interleukin 15: biology and relevance to human disease. *Blood* **97**, 14–32 (2001).
126. Jabri, B. *et al.* Selective expansion of intraepithelial lymphocytes expressing the HLA-E-specific natural killer receptor CD94 in celiac disease. *Gastroenterology* **118**, 867–879 (2000).
127. Setty, M. *et al.* Distinct and Synergistic Contributions of Epithelial Stress and Adaptive Immunity to Functions of Intraepithelial Killer Cells and Active Celiac Disease. *Gastroenterology* **149**, 681–691.e10 (2015).
128. Tang, F. *et al.* Cytosolic PLA2 is required for CTL-mediated immunopathology of celiac disease via NKG2D and IL-15. *J. Exp. Med.* **206**, 707–719 (2009).
129. Tang, F. *et al.* Cysteinyl leukotrienes mediate lymphokine killer activity induced by NKG2D and IL-15 in cytotoxic T cells during celiac disease. *J. Exp. Med.* **212**, 1487–1495 (2015).
130. Sarra, M. *et al.* IL-15 positively regulates IL-21 production in celiac disease mucosa. *Mucosal Immunol.* **6**, 244–255 (2013).

131. Ebert, E. C. Interleukin 21 up-regulates perforin-mediated cytotoxic activity of human intra-epithelial lymphocytes. *Immunology* **127**, 206–215 (2009).
132. Ciccocioppo, R. *et al.* Cytolytic mechanisms of intraepithelial lymphocytes in coeliac disease (CoD). *Clin. Exp. Immunol.* **120**, 235–240 (2000).
133. Long, E. O. *et al.* Killer cell inhibitory receptors: Diversity, specificity, and function. *Immunological Reviews* vol. 155 135–144 (1997).
134. Tuire, I. *et al.* Persistent duodenal intraepithelial lymphocytosis despite a long-term strict gluten-free diet in celiac disease. *Am. J. Gastroenterol.* **107**, 1563–1569 (2012).
135. Kutlu, T. *et al.* Numbers of T cell receptor (TCR) alpha beta+ but not of TCR gamma delta+ intraepithelial lymphocytes correlate with the grade of villous atrophy in coeliac patients on a long term normal diet. *Gut* **34**, 208–214 (1993).
136. Järvinen, T. T. *et al.* Intraepithelial lymphocytes in celiac disease. *Am. J. Gastroenterol.* **98**, 1332–1337 (2003).
137. Chen, Y., Chou, K., Fuchs, E., Havran, W. L. & Boismenu, R. Protection of the intestinal mucosa by intraepithelial gamma delta T cells. *Proc. Natl. Acad. Sci. U. S. A.* **99**, 14338–14343 (2002).
138. Ismail, A. S., Behrendt, C. L. & Hooper, L. V. Reciprocal Interactions between Commensal Bacteria and $\gamma\delta$ Intraepithelial Lymphocytes during Mucosal Injury. *J. Immunol.* **182**, 3047 LP – 3054 (2009).
139. Fiocchi, C., Battisto, J. R. & Farmer, R. G. Gut mucosal lymphocytes in inflammatory bowel disease: isolation and preliminary functional characterization. *Dig. Dis. Sci.* **24**, 705–717 (1979).
140. Walker, M. M. *et al.* Duodenal mastocytosis, eosinophilia and intraepithelial lymphocytosis as possible disease markers in the irritable bowel syndrome and functional dyspepsia. *Aliment. Pharmacol. Ther.* **29**, 765–773 (2009).
141. Posnett, D. N. *et al.* T cell antigen receptor V gene usage. Increases in V beta 8+ T cells in Crohn's disease. *J. Clin. Invest.* **85**, 1770–1776 (1990).
142. Mitomi, H. *et al.* Contribution of TIA-1+ and granzyme B+ cytotoxic T lymphocytes to cryptal apoptosis and ulceration in active inflammatory bowel disease. *Pathol. Res. Pract.* **203**, 717–723 (2007).
143. Hardee, S., Alper, A., Pashankar, D. S. & Morotti, R. A. Histopathology of Duodenal Mucosal Lesions in Pediatric Patients with Inflammatory Bowel Disease: Statistical Analysis to Identify Distinctive Features. *Pediatr. Dev. Pathol.* **17**, 450–454 (2014).
144. Trejdosiewicz, L. K. *et al.* Gamma delta T cell receptor-positive cells of the human gastrointestinal mucosa: occurrence and V region gene expression in *Helicobacter pylori*-associated gastritis, coeliac disease and inflammatory bowel disease. *Clin. Exp. Immunol.* **84**, 440–444 (1991).
145. Cuvelier, C. A., Wever, N. D. E., Mielants, H., Vos, M. D. E. & Veyst, E. M. Expression of T cell receptors patients with Crohn's disease and with spondylarthropathy. *Clin. Exp. Immunol.* **90**, 275–279 (1992).
146. Vidali, F. *et al.* Increased CD8+ intraepithelial lymphocyte infiltration and reduced surface area to volume ratio in the duodenum of patients with ulcerative colitis. *Scand. J. Gastroenterol.* **45**, 684–689 (2010).
147. Nüssler, N. C. *et al.* Enhanced cytolytic activity of intestinal intraepithelial lymphocytes in patients with Crohn's disease. *Langenbecks. Arch. Surg.* **385**, 218–224 (2000).
148. Liu, Z. *et al.* The increased expression of IL-23 in inflammatory bowel disease promotes intraepithelial and lamina propria lymphocyte inflammatory responses and cytotoxicity. *J. Leukoc. Biol.* **89**, 597–606 (2011).
149. Silva, F. A. R., Rodrigues, B. L., Ayrizono, M. de L. S. & Leal, R. F. The Immunological Basis of Inflammatory Bowel Disease. *Gastroenterol. Res. Pract.* **2016**, 2097274 (2016).
150. Hendrickson, B. A., Gokhale, R. & Cho, J. H. Clinical Aspects and Pathophysiology of Inflammatory Bowel Disease. *Clin. Microbiol. Rev.* **15**, 79–94 (2002).
151. Rutter, M. *et al.* Severity of inflammation is a risk factor for colorectal neoplasia in ulcerative colitis. *Gastroenterology* **126**, 451–459 (2004).
152. Gupta, R. B. *et al.* Histologic inflammation is a risk factor for progression to colorectal neoplasia in ulcerative colitis: a cohort study. *Gastroenterology* **133**, 1091–1099 (2007).
153. Ullman, T. A. & Itzkowitz, S. H. Intestinal inflammation and cancer. *Gastroenterology* **140**, 1807–1816 (2011).
154. Galon, J. *et al.* Type, density, and location of immune cells within human colorectal tumors predict clinical outcome. *Science* **313**, 1960–1964 (2006).
155. Chirica, M. *et al.* Phenotypic analysis of T cells infiltrating colon cancers: Correlations with oncogenetic status. *Oncoimmunology* **4**, e1016698 (2015).

156. Gentles, A. J. *et al.* The prognostic landscape of genes and infiltrating immune cells across human cancers. *Nat. Med.* **21**, 938–945 (2015).
157. Sherwood, A. M. *et al.* Tumor-infiltrating lymphocytes in colorectal tumors display a diversity of T cell receptor sequences that differ from the T cells in adjacent mucosal tissue. *Cancer Immunol. Immunother.* **62**, 1453–1461 (2013).
158. Maeurer, M. J. *et al.* Human intestinal Vdelta1+ lymphocytes recognize tumor cells of epithelial origin. *J. Exp. Med.* **183**, 1681–1696 (1996).
159. Ebert, E. C. & Groh, V. Dissection of spontaneous cytotoxicity by human intestinal intraepithelial lymphocytes: MIC on colon cancer triggers NKG2D-mediated lysis through Fas ligand. *Immunology* **124**, 33–41 (2008).
160. Dewar, D. H. *et al.* Celiac disease: management of persistent symptoms in patients on a gluten-free diet. *World J. Gastroenterol.* **18**, 1348–1356 (2012).
161. Yokoyama, S. *et al.* Antibody-mediated blockade of IL-15 reverses the autoimmune intestinal damage in transgenic mice that overexpress IL-15 in enterocytes. *Proc. Natl. Acad. Sci. U. S. A.* **106**, 15849–15854 (2009).
162. Clinicaltrials.gov. A Study to Evaluate the Efficacy and Safety of AMG 714 in Adult Patients With Celiac Disease.
163. Jabri, B. & Abadie, V. IL-15 functions as a danger signal to regulate tissue-resident T cells and tissue destruction. *Nat. Rev. Immunol.* **15**, 771–783 (2015).
164. Gomollon, F. *et al.* 3rd European Evidence-based Consensus on the Diagnosis and Management of Crohn's Disease 2016: Part 1: Diagnosis and Medical Management. *J. Crohns. Colitis* **11**, 3–25 (2017).
165. Terdiman, J. P., Gruss, C. B., Heidelbaugh, J. J., Sultan, S. & Falck-Ytter, Y. T. American Gastroenterological Association Institute guideline on the use of thiopurines, methotrexate, and anti-TNF-alpha biologic drugs for the induction and maintenance of remission in inflammatory Crohn's disease. *Gastroenterology* **145**, 1459–1463 (2013).
166. American Gastroenterological Association. Crohns disease clinical care pathway. Available at: <http://campaigns.gastro.org/algorithms/IBDCarePathway/pdf/IBDCarePathway.pdf>. (Accessed: 7th November 2017).
167. Peyrin-Biroulet, L. & Lemann, M. Review article: remission rates achievable by current therapies for inflammatory bowel disease. *Aliment. Pharmacol. Ther.* **33**, 870–879 (2011).
168. Sandborn, W. J. *et al.* Vedolizumab as Induction and Maintenance Therapy for Crohn's Disease. *N. Engl. J. Med.* **369**, 711–721 (2013).
169. Feagan, B. G. *et al.* Vedolizumab as Induction and Maintenance Therapy for Ulcerative Colitis. *N. Engl. J. Med.* **369**, 699–710 (2013).
170. Vermeire, S. *et al.* Etorlizumab as induction therapy for ulcerative colitis: A randomised, controlled, phase 2 trial. *Lancet* **384**, 309–318 (2014).
171. Wyant, T., Yang, L. & Fedyk, E. In vitro assessment of the effects of vedolizumab binding on peripheral blood lymphocytes. *MAbs* **5**, 842–850 (2013).
172. Fischer, A. *et al.* Differential effects of alpha4beta7 and GPR15 on homing of effector and regulatory T cells from patients with UC to the inflamed gut in vivo. *Gut* **65**, 1642–1664 (2016).
173. Wang, C. *et al.* Effect of $\alpha\beta 7$ Blockade on Intestinal Lymphocyte Subsets and Lymphoid Tissue Development. *Inflamm. Bowel Dis.* **16**, 1751–1762 (2010).
174. Lissner, D. *et al.* P617 Extraintestinal autoimmune phenomena during treatment with vedolizumab. *J. Crohn's Colitis* **11**, S394–S395 (2017).
175. Loftus, E. V *et al.* Long-term effectiveness and safety of vedolizumab in patients with ulcerative colitis: 5-year cumulative exposure of GEMINI 1 completers rolling into the GEMINI open-label extension study. *J. Crohns Colitis* **11**, S182–S183 (2017).
176. Wagner, N. *et al.* Critical role for beta7 integrins in formation of the gut-associated lymphoid tissue. *Nature* **382**, 366–370 (1996).
177. Nguyen, L. P. *et al.* Role and species-specific expression of colon T cell homing receptor GPR15 in colitis. *Nat. Immunol.* **16**, 207–213 (2015).
178. Ho, J. *et al.* A CD8+/CD103high T cell subset regulates TNF-mediated chronic murine ileitis. *J. Immunol.* **180**, 2573–2580 (2008).
179. Mestas, J. & Hughes, C. C. W. Of mice and not men: differences between mouse and human immunology. *J. Immunol.* **172**, 2731–2738 (2004).
180. Yatsunenkov, T. *et al.* Human gut microbiome viewed across age and geography. *Nature* **486**, 222–227

- (2012).
181. Brodin, P. *et al.* Variation in the Human Immune System Is Largely Driven by Non-Heritable Influences. *Cell* **160**, 37–47 (2015).
 182. Dutronc, Y. & Porcelli, S. a. The CD1 family and T cell recognition of lipid antigens. *Tissue Antigens* **60**, 337–353 (2002).
 183. Wyer, J. R. *et al.* T cell receptor and coreceptor CD8 alphaalpha bind peptide-MHC independently and with distinct kinetics. *Immunity* **10**, 219–225 (1999).
 184. Cawthon, A. G., Lu, H. & Alexander-Miller, M. A. Peptide requirement for CTL activation reflects the sensitivity to CD3 engagement: correlation with CD8alphabeta versus CD8alphaalpha expression. *J. Immunol.* **167**, 2577–2584 (2001).
 185. Srour, E. F., Leemhuis, T., Jenks, L., Redmond, R. & Jansen, J. Cytolytic activity of human natural killer cell subpopulations isolated by four-color immunofluorescence flow cytometric cell sorting. *Cytometry* **11**, 442–446 (1990).

Chapter 6

Compartment-driven imprinting of intestinal CD4 (regulatory) T cells in inflammatory bowel disease and homeostasis

Lisanne Lutter^{1,2}, José J.M. ter Linde^{1,2}, Eelco C. Brand^{1,2}, David P. Hoytema van Konijnenburg^{1,3}, Britt Roosenboom⁴, Carmen Horjus Talabur-Horje⁴, Bas Oldenburg², Femke van Wijk¹

¹Centre for Translational Immunology, University Medical Centre Utrecht, Utrecht, The Netherlands

²Department of Gastroenterology and Hepatology, University Medical Centre Utrecht, Utrecht, The Netherlands

³Division of Immunology, Boston Children's Hospital and Department of Pediatrics, Harvard Medical School, Boston, MA, USA

⁴Department of Gastroenterology and Hepatology, Rijnstate Hospital, Arnhem, The Netherlands

Manuscript submitted

ABSTRACT

Objective: The mucosal immune system is implicated in the etiology and progression of inflammatory bowel diseases. The lamina propria and epithelium of the gut mucosa constitute two separate compartments, containing distinct T cell populations. Human CD4 T cell programming and regulation of lamina propria and epithelium CD4 T cells, especially during inflammation, remains incompletely understood.

Methods: We performed imaging mass cytometry, flow cytometry, bulk and single-cell RNA-sequencing to profile ileal lamina propria and intraepithelial CD4 T cells (CD4CD8 α , regulatory T cells (Tregs), CD69⁻ and CD69^{high} Trm T cells) in controls and Crohn's disease (CD) patients (paired non-inflamed and inflamed).

Results: Inflammation results in alterations of the CD4 T cell population with a pronounced increase in Tregs and migrating/infiltrating cells. On a transcriptional level, inflammation within the epithelium induced T cell activation, increased IFN γ responses and an effector Treg profile. Conversely, few transcriptional changes within the lamina propria were observed. Key regulators including the chromatin remodelers *ARID4B* and *SATB1* were found to drive compartment-specific transcriptional programming of CD4 T(reg) cells.

Conclusion: Inflammation in CD patients primarily induces changes within the epithelium and not the lamina propria. Additionally, there is epithelium and lamina propria compartment-specific CD4 T cell imprinting driven by regulators shared among CD4 T cells. The main consequence of epithelial adaptation, irrespective of inflammation, seems to be an overall dampening of broad (pro-inflammatory) responses and tight regulation of lifespan. These data suggest differential regulation of the lamina propria and epithelium, with a specific regulatory role in the inflamed epithelium.

INTRODUCTION

Inflammatory bowel disease (IBD), comprising Crohn's disease (CD) and ulcerative colitis, is a chronic relapsing-remitting inflammatory disease with a multifactorial and not fully elucidated pathogenesis.¹ Both the innate and adaptive immune system have been implicated in the etiology and progression of disease.¹ The lamina propria and epithelium of the gut mucosa constitute two separate compartments, containing distinct populations of T cells.² Intraepithelial T cells, interspersed between the single layer of epithelial cells, are in direct contact with food and microbiota-derived antigens, whereas T cells in the lamina propria are surrounded by a variety of other immune and stromal cells. In the lamina propria, most T cells are of the CD4 lineage, while CD8 T cells predominate in the epithelium.³ CD4 T cells are commonly divided in T helper (Th, effector) cells, regulatory T cells (Tregs) and CD4CD8 α T cells. Many of these are considered residents of the mucosal environment; tissue-resident memory T (Trm) cells, expressing CD69.^{3,4} In CD patients, CD4 T cells are increased in both the lamina propria and epithelium⁵⁻⁸ and changes of the phenotypic profile of several CD4 T cell subsets have been observed, including an increased percentage of double/multiple cytokine producing CD4 regulatory and pro-inflammatory T cells, and a more cytotoxic profile of these CD4 T cells.⁹⁻¹⁴ Additionally, it is now clear that microenvironmental cues can steer functional programs and cell dynamics that might have a role in health and disease. However, since studies reporting on CD4 T cells primarily focused on lamina propria or on the bulk of mucosal cells, our understanding of CD4 T cell programming in different mucosal compartments remains incompletely understood. This includes programming of Tregs and CD4CD8 α T cells, both associated with regulation,^{15,16} and the differential regulation of CD4 T cells derived from the lamina propria and epithelium, especially in inflammation. Studying tissue- and compartment-specific resident CD4 T cell regulation in IBD may improve our understanding of chronic and locally recurrent inflammation as well as open up new avenues for targeted treatment.

To assess these questions, we profiled surface marker-based CD4 T cell subsets with bulk RNA-sequencing as well as an unbiased CD4 T cell single-cell RNA-sequencing exploration, to map the CD4 T cell compartment in the epithelium and lamina propria of the human ileum, complemented with imaging mass cytometry (IMC), in control subjects and paired inflamed and non-inflamed ileal biopsies from patients with CD. Our results uncover compartment-specific CD4 T cell imprinting in the epithelium compared to the lamina propria driven by key regulators regulating effector function and lifespan in the epithelium.

RESULTS

Increased epithelial and lamina propria regulatory and effector CD4 T cells in (active) ileal Crohn's disease

We first analyzed the composition of major T cell populations in the epithelium and lamina propria of the human ileum. Therefore, we obtained ileal biopsies from control subjects as well as paired non-inflamed and inflamed ileal biopsies from patients with CD (gating strategy: supplemental figure 1A). We assessed the presence of the following T cell subsets: T cell

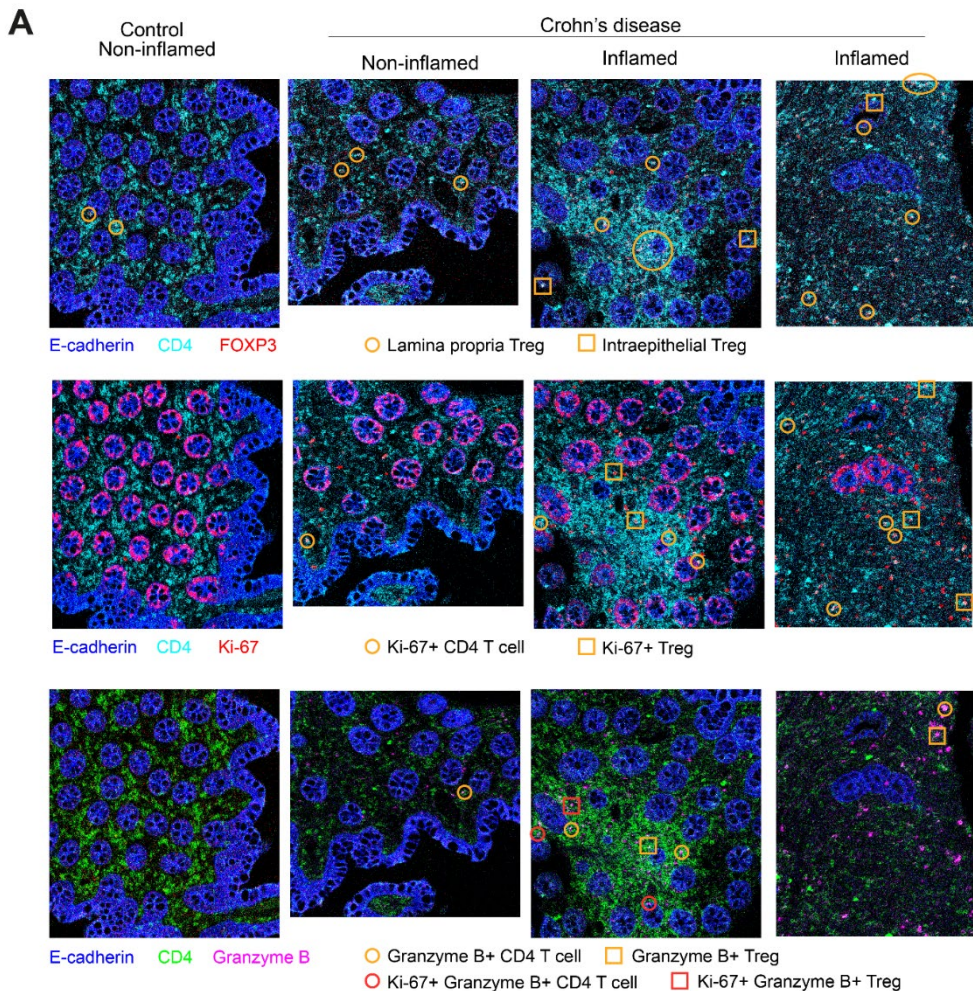
receptor (TCR) $\gamma\delta$, TCR $\gamma\delta$ -CD8-CD4, CD8, CD4CD8 α of which the vast majority is expected to be CD4CD8 α , effector (CD4⁺CD127⁺CD25⁻), and Treg (CD4⁺CD127^{low}CD25^{high}) cells (supplemental figure 2A). The non-inflamed of control subjects and patients with CD was found to display a comparable T cell subset composition, except for an increase in Tregs in the lamina propria of patients with CD ($p = 0.0295$). Inflammation resulted in a further increase in Tregs ($p = 0.0078$) and a decrease in CD4CD8 α T cells ($p = 0.0391$) in the lamina propria compared to the paired non-inflamed ileum of patients with CD. The epithelium of the inflamed ileum displayed increased percentages of Tregs and CD4 effector T cells as well ($p = 0.0156$ and 0.0078 , respectively), with a concomitant decrease in CD8 T cells ($p = 0.0156$). Furthermore, within the CD4 effector T cell subset, an increase in CD69⁻ cells was observed in CD patients ($p = 0.0451$ for lamina propria CD45RA⁻CD69⁻ in CD versus control subjects), which was most pronounced in the inflamed epithelium ($p = 0.0078$ for CD45RA⁻CD69⁻ and CD45RA⁺CD69⁻ in inflamed versus non-inflamed epithelium and lamina propria, supplemental figure 2B), indicating infiltration/expansion of CD69^{low} effector memory and naive CD4 T cells. Thus, most inflammation-associated changes in the overall T cell composition impact the regulatory and migrating/infiltrating CD69^{low} CD4 effector subset content, and occur within the epithelium.

To additionally assess potential changes in CD4 T cell distribution throughout the mucosal compartment, we performed IMC on paired inflamed and non-inflamed ileal tissue derived from two control subjects and three patients with CD (figure 1A). In the inflamed lamina propria of CD patients diffuse CD4 T cell infiltrates were present (figure 1A, upper row), and loss of normal mucosal architecture can be observed (figure 1A, upper row outer right). FOXP3⁺ Tregs were predominantly located within CD4-rich regions in the lamina propria, especially in the inflamed ileum (figure 1A, upper row). Within the ileal mucosa of control subjects no Ki-67⁺ or Granzyme B⁺ CD4 T cells were observed (figure 1A, outer left panels). In patients with CD, the non-inflamed lamina propria contained a few Ki-67⁺ CD4 T cells and Ki-67⁺ Tregs (FOXP3⁺), as well as Granzyme B⁺ CD4 T cells (figure 1A, inner left panels). However, in inflamed tissue a higher ratio of CD4 and FOXP3⁺ CD4 T cells expressing Ki-67⁺ or Granzyme B⁺ was found (figure 1A, right panels), and within the inflamed lamina propria some Ki-67 and Granzyme B double-positive CD4 T cells were observed (figure 1A, right panels). Altogether, these IMC data indicate that CD4 (FOXP3⁺) T cells both proliferate locally and gain cytotoxic effector function in CD patients, especially in the inflamed mucosa.

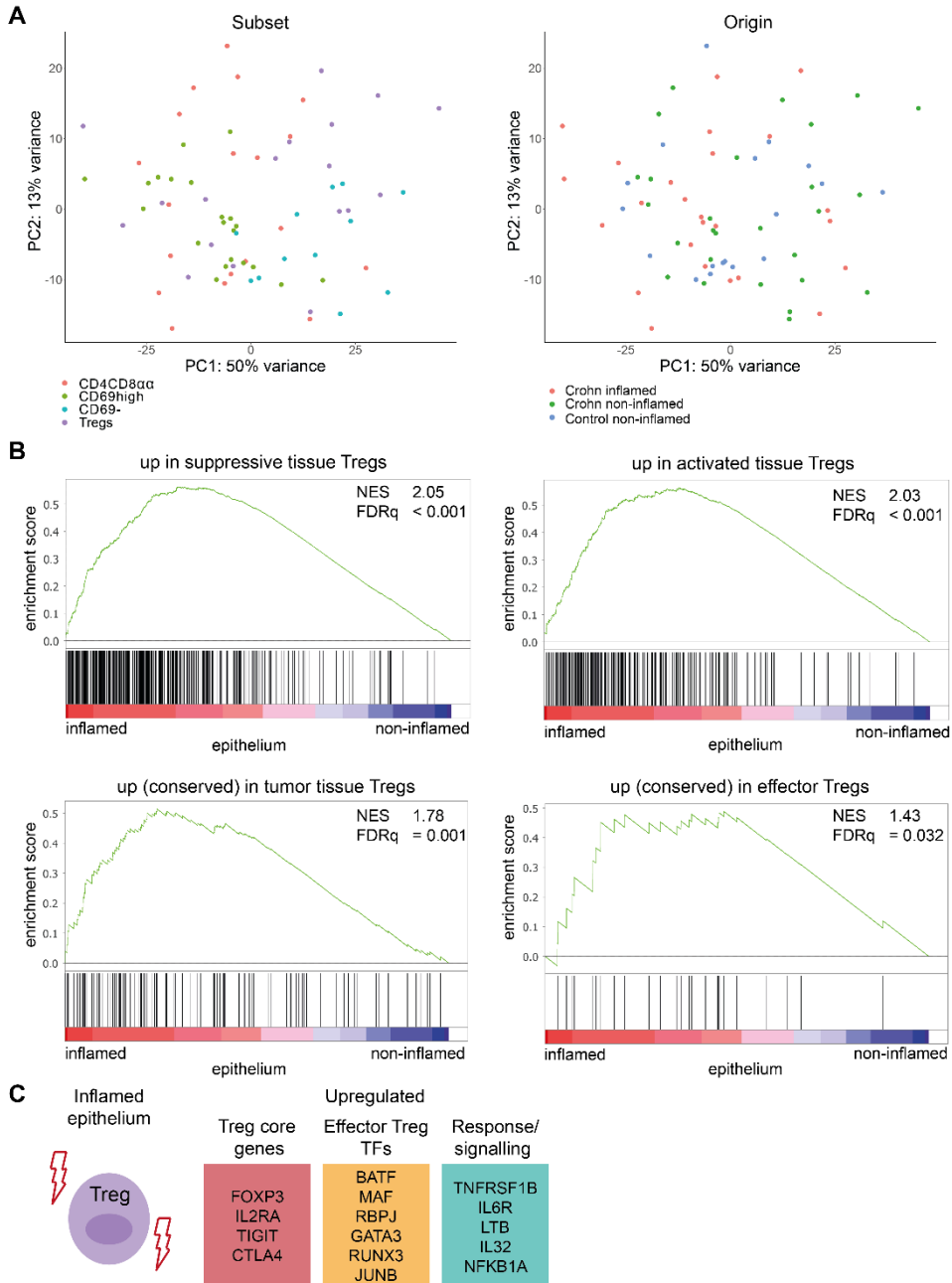
Inflammation is associated with an effector Treg profile in the epithelium.

We then performed bulk RNA-sequencing of sorted CD4CD8 α T cells, Tregs (CD4⁺CD127^{low}CD25⁺), and effector T cells (CD4⁺CD127⁺CD25⁻) subdivided in CD69⁻ and CD69^{high} (Trm cells) from the ileum of control subjects and paired inflamed and non-inflamed ileum of patients with CD (gating strategy: supplemental figure 1A). Although principal component analysis revealed partial clustering of surface marker-based CD4 T cell subsets, there was no complete distinction of all subsets (figure 2A, left; supplemental figure 3A). For example, lamina propria CD4CD8 α T cells only differed from CD69^{high} Trm cells by expression of CD8A. In the epithelium, however, 13 upregulated and 138 downregulated genes were observed in

CD4CD8 α T cells compared to CD69^{high} CD4 Trm cells. None of these genes have clear effector, regulatory nor cytotoxic, functions (supplemental table 1). In mouse epithelium, T-bet and Runx3 induce the intraepithelial CD4 T cell program including CD8 α expression.²⁹ Both T-bet and Runx3 were, however, not differentially expressed in human small intestinal CD4CD8 α T cells in the epithelium compared to the lamina propria, nor compared to CD69^{high} Trm cells or Tregs. CD4CD8 α T cells did differ from Tregs with downregulated *FOXP3*, and downregulation of the canonical Treg markers *IL2RA*, *IKZF2*, *TIGIT* and *TNFRSF18* (supplemental table 1). This is in line with previous data^{15,30} and indicates that CD4CD8 α T cells are clearly different from mouse and human small intestinal FOXP3⁺ Tregs. As expected, the Trm signature was more enriched in CD69^{high} Trm compared to CD69⁻ CD4 T cells within the lamina propria (supplemental figure 3B). Among the 395 upregulated and 31 downregulated genes were many known Trm genes (e.g. *CD69*, *CXCR6*, *IFNG* and *ITGA1*⁴) (supplemental table 1).



< Figure 1. T cell distribution in the human ileum in health and Crohn's disease. (A) Representative imaging mass cytometry images of the distribution of CD4 and regulatory T cells (upper row), Ki-67 (middle row) and Granzyme B (lower row) in control subjects (outer left), non-inflamed (inner left) and inflamed (right) ileum of CD patients. Control subjects $n = 2$, CD $n = 3$. A few examples are highlighted per image. Each column shows the same image, but colored for different targets per row.



< Figure 2. Effector Treg profile in the inflamed epithelium. (A) Unsupervised principal component analysis of all CD4 T cell subsets analyzed by bulk RNA-sequencing colored on subset (left; pink = CD4CD8 $\alpha\alpha$ T cells, green = CD69^{high} Trm cells, blue = CD69⁻ T cells, purple = Tregs), and status (right; pink = CD inflamed, green = CD non-inflamed, blue = control non-inflamed). (B) Gene set enrichment analysis of suppressive¹⁹ (upper left), activated¹⁹ (upper right), tumor-derived tissue Treg¹⁸ (lower left) and conserved human effector Treg²⁰ (lower right) signatures in pairwise comparisons of Tregs derived from non-inflamed and inflamed ileum of CD patients, represented by the normalized enrichment score (NES) and FDR statistical value (FDRq). (C) Selected genes upregulated in Tregs in the inflamed epithelium. TFs, transcription factors.

Moreover, the origin of the samples, control subjects or patients with CD, was not found to fully drive clustering either, irrespective of the presence of inflammation (figure 2A, right; supplemental figure 3A). First, we analyzed the impact of inflammation on the whole CD4 T cell population of combined CD69^{high} Trm cells, CD4CD8 $\alpha\alpha$ T cells and Tregs. Only 1 differentially expressed gene was found when comparing CD4 T cells from paired inflamed and non-inflamed lamina propria of patients with CD. Comparing CD4 T cells from inflamed lamina propria with healthy non-inflamed control subjects resulted in 1030 upregulated and 822 downregulated genes (supplemental table 1). Upregulated genes included *STAT1*, *BATF*, *PRDM1*, *GZMB*, *IL22* and *CCR6*, and associated with processes related to cell activation, cell cycling, and stress. In the epithelium, significant differences in inflamed versus non-inflamed epithelium of patients with CD were found (1009 upregulated and 58 downregulated genes, supplemental table 1). Here, CD4 T cells from the inflamed epithelium showed, among others, increased translation and protein transport, T cell activation and responses to IFN γ , with upregulated genes including ribosomal genes, *CXCR3*, *CCR7*, *TOX2* and *KLF2*.

Even though the relative composition within the CD4 T cell population of the inflamed ileum shifted (supplemental figure 2A,B), only a limited number of transcriptional changes (<10) was found for any of the sorted bulk CD4⁺CD69⁻, CD4⁺CD69^{high}, CD4CD8 $\alpha\alpha$ and Treg subsets derived from inflamed ileum, except for intraepithelial Tregs. Intraepithelial Tregs from inflamed ileum mucosa acquired an effector Treg profile with upregulation of *FOXP3*, *TIGIT* and *TNFRSF1B*, among others (figure 2 B,C, supplemental table 1). Enrichment of gene signatures procured from literature for suppressive, activated, tumor suppressive Tregs and a conserved effector Treg program in inflammation-derived intraepithelial Tregs corroborate these observations (figure 2B).¹⁸⁻²⁰ *FOXP3*, *GATA3*, *BATF*, *RUNX3* and *MAF* were among the upregulated transcription factors (TFs) in Tregs from the inflamed epithelium which have been associated with effector Treg differentiation.^{20,31-33} Both *GATA3* and *RUNX3* are crucial in suppression of inflammation by Tregs.^{32,33} Thus, the most pronounced transcriptional change in CD4 T cell subsets in CD inflammation is the strong effector Treg profile in the epithelial compartment.

Mucosal subcompartment drives the CD4 T cell transcriptomic profile in the ileum.

Clear separation of CD4 T cell subsets was observed based on compartment of residence; the epithelium and lamina propria of the ileum (figure 3A, supplemental table 1). Gene ontology analysis revealed that CD69^{high} Trm cells in the epithelium were enriched for pathways

associated with activation, T cell differentiation and mRNA processing (790 upregulated and 299 downregulated genes for epithelium versus lamina propria) (figure 3B). However, pathways related to activation were upregulated in both lamina propria Tregs and CD4CD8 α T cells (708 and 239 upregulated and 1109 and 734 downregulated genes for epithelium versus lamina propria, respectively). These included cell activation and T cell differentiation for CD4CD8 α T cells, and mRNA processing, stress response and cell cycle regulation for Tregs (figure 3B). The enriched pathways for the different CD4 T cell subsets were predominantly regulated via different genes (21 shared genes in the epithelium and 22 in the lamina propria). In the lamina propria, *TRAF1*, *TRAF4* and *BIRC3* involved in TNF(R) signaling, as well as *IL4R* and *IL2RA* associated with T cell activation and differentiation, were shared among all CD4 T cell subsets.³⁴ In the epithelium genes involved in migration and motility were shared (e.g. *CLIC1*³⁵, *GNAQ*³⁶, *FAM107A*³⁷) (supplemental table 1).

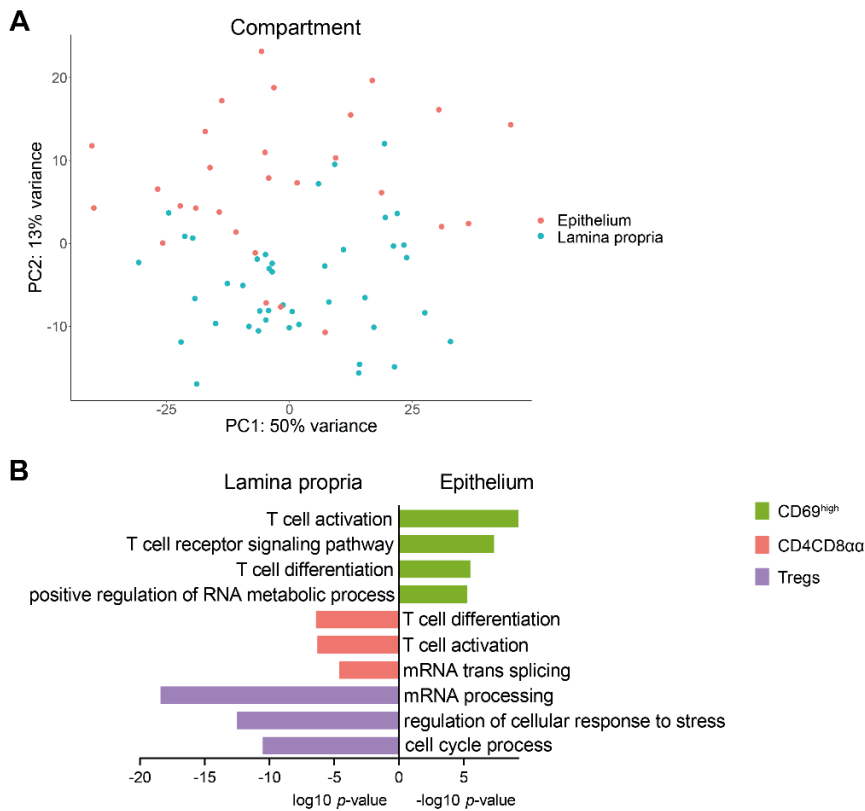


Figure 3. Mucosal subcompartment shapes the transcriptomic profile of CD4 T cells. (A) Unsupervised principal component analysis of all CD4 T cell subsets analyzed by bulk RNA-sequencing colored on compartment of residence (pink = epithelium, blue = lamina propria). (B) Selected biological process terms related to the upregulated genes in the lamina propria for CD69^{high} T_{RM} cells (green), and in the epithelium for CD4CD8 α T cells (pink) and Tregs (purple).

Subsequently, we performed single-cell RNA-sequencing of paired non-inflamed and inflamed ileum-derived CD4 T cells ($CD3^+TCR\gamma\delta^+CD4^+$) from the epithelium and lamina propria of patients with CD to assess potential heterogeneity missed with bulk RNA-sequencing. These data supported our observation that compartment is the primary driver of CD4 T cell clustering (figure 4A-C, gating strategy: supplemental figure 1A). Unsupervised clustering of 1573 cells after quality control revealed five CD4 T cell clusters represented in every patient (figure 4A,D). Cluster 1 (18.6% of all cells) was characterized by *KLF2*, *SELL*, *CCR7*, *TCF7* and *LEF1*, and thus resembled recently migrated/recirculating T cells (figure 4A). This cluster contained both intraepithelial and lamina propria T cells (figure 4E). Similarly, cluster 2 (14.3% of all cells) comprised both lamina propria and intraepithelial cells constituting Tregs (*FOXP3*, *TIGIT*, *CTLA4*, *IKZF2* and *BATF*) (figure 4A,E). Cluster 3 and 4 predominantly comprised lamina propria-derived CD4 T cells (figure 4E). Cluster 3 (26.8% of all cells) seemed to contain a mix of Th1- and Th17-skewed cells identified by *CCL20*, *NFKB1/2*, *TRAF1* and *BHLHE40*, whereas cluster 4 (11.1% of all cells) showed higher expression of heat shock protein family members suggesting that these cells were stressed (figure 4A). The last cluster (cluster 5, 29.2% of all cells) was comprised of intraepithelial CD4 T cells distinguished by expression of innate and/or cytotoxic related genes including *FOS(B)*, *EGR1*, *GZMA*, *JUN* and *IER2* (figure 4A,E, supplemental table 2). CD4CD8 $\alpha\alpha$ T cells mixed with the resident CD4 T cells and not with the Tregs, in line with the bulk RNA-sequencing data (figure 4C). Also, in accordance with the bulk data, inflammation did not result in distinct CD4 T cell profiles. Congruent with the protein data, we did observe a relative increase in CD69^{low} CD4 T cells in all defined clusters in inflammation (figure 1B, 3F). Almost 50% of cluster 1 and 2 cells comprised CD69^{low} T cells, compared to approximately 10-15% for the other clusters. These clusters also showed the highest relative increase of CD69^{low} T cells in inflamed tissue. In summary, bulk and single-cell RNA-sequencing data revealed that the intra-tissue compartmentalization of CD4 T cells is the primary driver of their transcriptomic landscape. During inflammation, the expression profiles of CD4 Trm cells is largely preserved, with a significant influx of CD69^{low} migrating CD4 T cells.

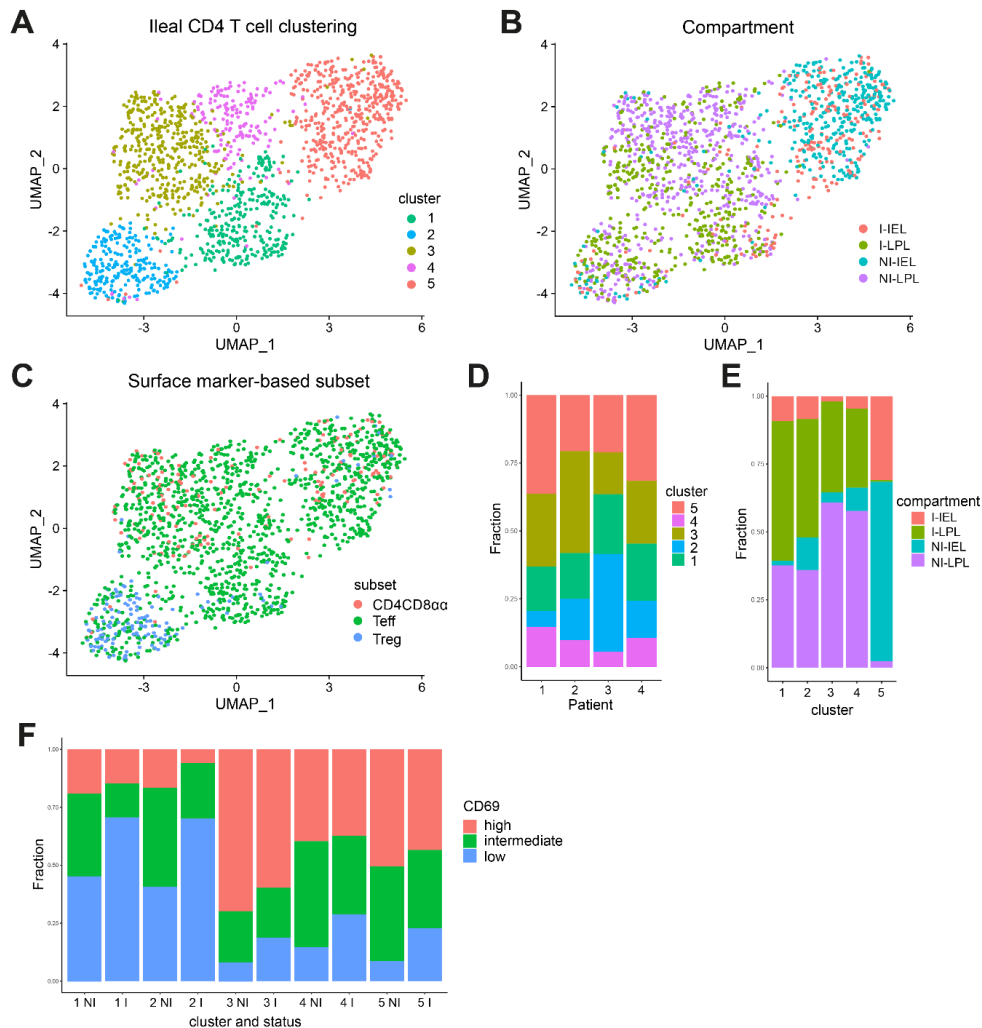


Figure 4. CD4 T cell clusters in the paired non-inflamed and inflamed ileum. (A) Dimensionality reduction of all CD4 T cells ($CD3^+TCR\gamma\delta^+CD4^+$) from the epithelium and lamina propria of four patients with Crohn's disease. Cells are colored based on the assigned cluster. (B) As per A colored on the compartment (IEL = intraepithelial T cell, LPL = lamina propria T cell) and status (I = inflamed, NI = non-inflamed). (C) As per A colored on surface marker-based identification. $CD4CD8\alpha\alpha$ T cell = $CD4^+CD8\alpha^+$ (pink), effector T cell (Teff) = $CD4^+CD127^+CD25^-$ (green), Treg = $CD127^+CD25^+$ (blue). (D) Reproducible composition of the CD4 T cells across the four included patients. y-axis: fraction of cells colored on the cluster as shown in A and separated per patient on the x-axis. (E) Composition of the compartment (epithelium/lamina propria) and status (non-inflamed/inflamed) origins per cluster. y-axis: fraction of cells colored on compartment and separated per cluster as shown in A on the x-axis. (F) Composition of CD69 protein expression among non-inflamed (NI) and inflamed (I) derived CD4 T cells for all clusters, separated by low (negative, blue), intermediate (green) and high (pink) CD69 expression. y-axis: fraction of cells colored on CD69 expression, and separated per cluster, and non-inflamed/inflamed ileum.

The chromatin remodeling genes ARID4B and SATB1 are predicted key regulators of the epithelium compared to lamina propria CD4 T cell compartment.

Since we observed differences in the transcriptional profile of CD4 T cells derived from the lamina propria and epithelium we performed a data-driven network and enrichment analysis (RegEnrich²¹). Herewith, we could identify which key gene regulators, based on TFs and co-factors, were involved in the regulatory network of epithelium compared to lamina propria adaptation of CD4⁺CD69^{high} Trm cells, CD4CD8 α T cells and Tregs combined, irrespective of inflammation. Top predicted regulators were *ARID4B*, *SATB1*, *CREM*, *BAZ1A* and *NFKB1* (all negative, i.e. regulators upregulated in the lamina propria and downregulated in the epithelium) (figure 5A, supplemental table 3). Most regulators were found to be downregulated. Of interest, downregulation of many of the abovementioned regulators are involved in chromatin remodeling and inhibit T cell functioning. The negative regulator ARID4B is known as a master regulator of the phosphatidylinositol-3-kinase (PI3K) pathway related to T cell activation and proliferation.^{38,39} Downstream target genes of the downregulated SATB1 are also involved in T cell effector functions including *TRAF1* and *TRAF4* (TNF receptor-associated factors), *NFKB*, interleukin receptors (e.g. *IL4R*, *IL12RB2*) and *IL2*. Additionally, among the positive regulators were *ELF4*, *TRIM21* and *TRIM27*, all linked to negative regulation of T cell function. *ELF4* has been associated with CD8 T cell quiescence and suppressed proliferation and downregulation of CCR7, CD62L and KLF2 and thereby tissue retention.⁴⁰ *TRIM21* (Ro52) has been linked to negative regulation of pro-inflammatory cytokine production⁴¹ by limiting Th1/Th17 differentiation and thereby suppressing tissue inflammation in an IL23/Th17-dependent manner.^{41,42} Lastly, *TRIM27* does not inhibit Th cell differentiation but negatively impacts CD4 T cell functioning via the PI3K pathway.⁴³ Furthermore, positively regulator-associated genes encompassed *FASLG* and programmed cell death genes, whereas negatively associated downstream genes included cell cycling genes. This suggests a different regulation of proliferation and cell death in these compartments. Altogether, the predicted network of TF regulators involved in adaptation of CD4 T cells to the epithelium compared to the lamina propria showed downregulation of chromatin remodeling, dampening of T cell activation and effector function, as well as regulation of programmed/activation-induced cell death and arrest of cell cycling independent of inflammation. Overall, these data suggest that CD4 T cells in the epithelium have a tightly regulated function and lifespan.

A Transcription factor network of epithelium compared to lamina propria derived CD4 T cells

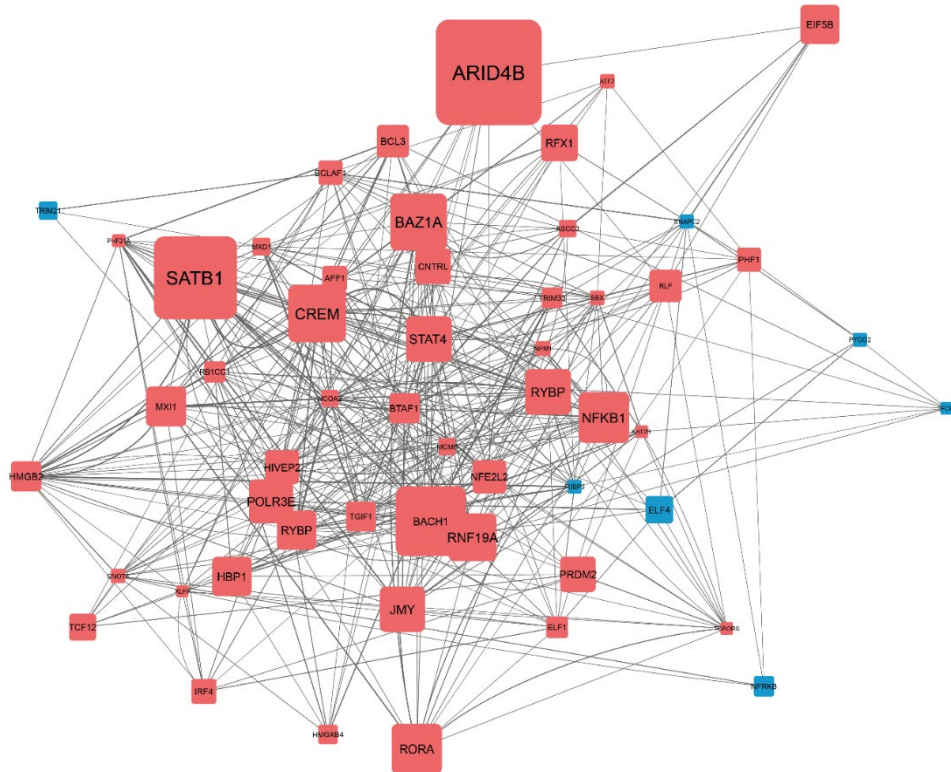


Figure 5. Transcription factor network of epithelium compared to lamina propria derived CD4 T cells. (A) Network inference of key regulators in epithelium compared to lamina propria CD4 T cells on RNA level, based on unsupervised gene regulatory network analysis followed by gene set enrichment analysis of the transcription factors (TFs) and co-factors (pink = upregulation, blue = downregulation). The grey lines indicate connections between regulators (TFs) and their downstream targets (only TFs are shown), the line thickness represents the correlation weight (thicker = higher correlation). Square size indicates $-\log_{10}(p)$ for each comparison, with the p -value derived from differential expression analysis (\log_2 fold change > 0.5 and p -adjusted value < 0.1), text size represents the RegEnrich score; for both, larger indicates higher scores (supplemental table 3).

DISCUSSION

In the present study, we demonstrate that the transcriptional profile of CD4 effector, Trm cells, CD4CD8 α T cells and Tregs is primarily determined by the compartment of residence (epithelium or lamina propria), irrespective of inflammation. The relative composition of the mucosal CD4 T cell population changes in patients with CD with an increase in Tregs. Upon inflammation, Tregs as well as CD4 naive and migrating/infiltrating CD69^{low} T cells further increase, while the number of CD4 Trm cells, CD8 and CD4CD8 α T cells relatively decrease. These changes are most pronounced in the epithelium. Inflammation induces only few transcriptomic changes in lamina propria CD4 Trm cells, Tregs and CD4CD8 α T cells on the bulk and single-cell RNA-sequencing level, indicating that reshaping of CD4 T cell subset

transcriptomes in the inflamed lamina propria of patients with CD is limited. In the inflamed epithelium, however, a considerable upregulation of cell activation, cell cycling and stress response is observed, with Tregs gaining an effector Treg profile. Tregs gaining an effector Treg profile is also seen in tissues in other inflammatory diseases.²⁰ Adaptation of CD4 T cells from the epithelium compared to the lamina propria is driven by chromatin remodeling via *ARID4B* and *SATB1*. The main consequence of adaptation of these cells to the epithelium seems to be a dampening of broad (pro-inflammatory) T cell responses.

Previous studies have shown that T cell subsets derived from the small intestine and colon are transcriptionally different, independent of inflammation.⁴⁴ Additionally, research has indicated that there are less differences between T cell subsets including CD4 and CD8 effector T cells, Tregs and CD4 conventional T cells,^{45,46} and inflamed and non-inflamed gut⁴⁷ than there is between the lamina propria and epithelium.⁴⁵⁻⁴⁷ Our study is the first that explores the effects of both the compartment, epithelium or lamina propria, and presence of inflammation in a spectrum of different CD4 T cell subsets. We conclude that compartment is the primary driver of the transcriptomic profile of a human small intestinal CD4 T cell.

Our data further indicates that the increase in migrating/infiltrating CD69^{low} CD4 T cells constitutes a major change in the local T cell population during inflammation in CD. In recent years, the therapeutic armamentarium of IBD has been extended to the anti-integrin therapy vedolizumab (anti-integrin $\alpha4\beta7$). Sphingosine 1 phosphate (S1P), CCR9 and MAdCAM-1 targeted therapies are also under investigation in clinical trials for IBD.⁴⁸ Based on our data, it might be beneficial to implement lymphocyte trafficking interfering strategies early in the disease to prevent migration/infiltration of these cells. This might also prevent (pathogenic) infiltrating cells to become Trm cells over time.

The transcriptomic differences of CD4 T cells between the epithelium and lamina propria could be due to a preprogrammed destination of T cells or to local factors inducing a compartment-specific profile in the same cell of origin. A recent study in mice showed that T cells receive compartment-specific imprinting for the lamina propria or epithelial compartment in the mesenteric lymph nodes.⁴⁶ However, another study in mice showed that transfer of lamina propria-derived T cells will lead to relocation of these cells to both the lamina propria and epithelium.⁴⁹ Furthermore, overlap in the TCR repertoire for lamina propria and epithelium CD8 Trm cells has been observed,¹⁴ and several studies have shown that T cells adapt to the local microenvironment.^{31,50} It is likely that both lymph node originated compartment-specific imprinting and the local environment contribute to the transcriptomic profile of T cells. Nevertheless, the extensive transcriptomic differences due to compartment of residence emphasizes the importance of considering the lamina propria and epithelium as separate compartments when deciphering the pathogenic mechanisms of chronic mucosal inflammation. This distinct compartmentalization of CD4 T cells also suggests that maintaining and restoring mucosal integrity is of key importance to prevent inappropriate immune responses.

The predicted key regulators of epithelium versus lamina propria CD4 T cell adaptation included TRIM27 involved in limiting Th1/Th17 differentiation.^{41,42} The set of

predicted regulators, among others, could explain the less pronounced Th-cell and more pronounced innate/cytotoxic profile of intraepithelial compared to lamina propria CD4 T cells. Furthermore, both the IMC and bulk RNA-sequencing data indicate that cell cycling/death in the epithelium is tightly controlled, and that local CD4 T cell expansion during inflammatory responses is primarily observed in the lamina propria. Uncontrolled cell death and extensive local expansion in the epithelial layer could potentially disrupt the single-cell layer of epithelial cells and consequently impact mucosal barrier integrity. Altogether, these data indicate a tight regulation of broad, and untargeted, effector function and cell cycling of intraepithelial CD4 T cells. This could potentially be to prevent destructive tissue responses while allowing targeted action via cytotoxicity. That many predicted key regulators are chromatin remodelers suggests that the adaptation to the microenvironment is imprinted in these cells. Future (single-cell) epigenomic/chromatin accessibility sequencing (e.g. ATAC-sequencing) could help to elucidate the specific chromatin alterations that occur, and thus the compartment-specific imprinting that ensues.

Active disease in patients with CD does not result in transcriptional changes in CD4 T cells within the lamina propria. However, compared to the non-inflamed lamina propria of control subjects, cell activation and stress responses were observed. This strongly suggests that in established CD there are changes in the transcriptome of CD4 T cells across the mucosa. Future research should include newly diagnosed patients or prediagnostic samples (with the latter being hard to collect) to assess how CD4 T cells at baseline or before diagnosis are altered. This could be pre-onset changes as shown by presence of an IBD-like microbiome in healthy co-twins at risk of developing IBD,⁵¹ the influence of (previous) administered medication as shown in the blood of IBD patients,⁵² or the effect of previous flares. The fact that CD patients with an ileocecal resection often experience relapses at the anastomosis⁵³ suggests that the gut mucosa of CD patients exhibits (pre-existent) changes, although the occurrence of relapses could also be partly caused by non-immune cell related factors.

Our data indicate that the inflamed epithelium undergoes extensive changes with an upregulation of protein translation and activation of CD4 T cells in patients with CD. The limited transcriptional differences of ileal CD4 Trm cells upon inflammation suggest that infiltrating CD4 T cells might have a pathogenic role. Of note, absence of subset-specific transcriptional changes for CD4 (Trm) cells does not exclude changes on the protein level. For example, our IMC data revealed lamina propria Tregs present in CD4 T cell infiltrates to gain Granzyme B expression and thus cytotoxic effector function which could aid in control of inflammatory responses. Intraepithelial Tregs, however, did adapt by gaining an effector Treg profile. This indicates that the local environment at the epithelial border changes significantly. Tregs are known to suppress pro-inflammatory and/or regulate anti-inflammatory functioning of CD8 T cells, TCR γ δ T cells and innate lymphoid cells,^{54,55} which reside in high abundance at the epithelial border.^{2,3} Additionally, Tregs have direct tissue-specific functions including aiding tissue repair⁵⁶ and/or via interaction with epithelial stem cells⁵⁷ thereby preserving/stimulating mucosal barrier integrity. The significant changes observed in the inflamed epithelium suggest that promoting (effector) Treg differentiation and expansion in

the gut mucosa as therapeutic strategy might be worthwhile. Indeed, a phase 1/2a clinical trial has shown that injection of antigen-specific Tregs in patients with CD resulted in a significant reduction of disease activity.⁵⁸

CD4CD8 α T cells are commonly referred to as cytolytic T cells derived from CD4 T cells that lost ThPOK and gained RUNX3 and T-bet expression, and are primarily found in the (small intestinal) epithelium of mice.^{29,49} Murine small intestinal intraepithelial CD4CD8 α T cells aid in controlling local inflammatory responses via IL-10 and TGF β .^{15,30} Human intestinal CD4CD8 α T cell- studies are limited, with one study showing a potential regulatory role via IL-10, CTLA4, GITR, CD25 and LAG3 in the colonic lamina propria.¹⁶ Our data revealed no difference in the relative presence of ileal CD4CD8 α T cells between the epithelium and lamina propria, or between inflamed and non-inflamed mucosa. Furthermore, downregulation of *ZBTB7B* (encoding ThPOK) was not observed in CD4CD8 α T cells. Our study suggests that CD4CD8 α T cells in the human ileum are (very similar to) Trm cells, and do not express a clear cytotoxic or regulatory transcriptional profile.

In conclusion, our data reveal that there is a CD4 T cell compartment-specific imprinting, with shared key regulators driving the transcriptional network for adaptation to the epithelium compared to the lamina propria. Adaptation to the epithelium seems to result in an overall dampening of effector function and tight regulation of the lifespan. Furthermore, inflammation in patients with CD results in a relative increase of migrating/infiltrating CD69^{low} CD4 T cells, CD4 T cell activation and IFN γ responses as well as a strong effector Treg profile within the epithelium. These data indicate that the lamina propria and epithelium of the human ileum are differentially regulated in both control subjects and CD patients, with a pronounced regulatory role in the inflamed epithelium. Our findings suggest that we should consider both compartments in the therapeutic management of IBD.

METHODS

Participant inclusion

Patients with Crohn's disease were prospectively enrolled at the Department of Gastroenterology and Hepatology, University Medical Center Utrecht and the outpatient clinic of the Rijnstate Crohn and Colitis Centre, Arnhem, The Netherlands. During ileocolonoscopy multiple biopsy specimens were taken for bulk ($n = 4$) and single-cell ($n = 4$) RNA-sequencing of sorted subsets and imaging mass cytometry (IMC; $n = 3$). Non-inflamed biopsies were taken > 2cm of macroscopically visible inflamed ileum. Control subjects for bulk RNA-sequencing ($n = 3$) and IMC ($n = 2$) did not have a diagnosis of IBD and underwent ileocolonoscopy for polyp surveillance and had normal macroscopical ileal mucosa (see table 1 for participant characteristics). Sex was not taken into account when selecting patients due to the sample size which would not allow for correction of the influence of sex on the immune system.

Table 1. Baseline patient characteristics.

	Flow cytometric analysis		IMC		RNA-seq		scRNA-seq
	CD patients (n = 8)	C subjects (n = 5)	CD patients (n = 3)	C subjects (n = 2)	CD patients (n = 4)	C subjects (n = 3)	CD patients (n = 4)
Gender							
Female	2 (25)	4 (80)	2 (66.7)	1 (50)	1 (25)	3 (100)	4 (100)
Male	6 (75)	1 (20)	1 (33.3)	1 (50)	3 (7)	0 (0)	0 (0)
Age, y	39 (29-49)	57 (53-60)	46	36	36 (29-43)	56 (55-58)	44 (30-56)
Treatment at ileocolonoscopy							
None	3 (37.5)	5 (100)	3 (100)	2 (100)	2 (50)	3 (100)	3 (75)
5-ASA	0 (0)	0 (0)	0 (0)	0 (0)	0 (0)	0 (0)	1 (2)
Steroids	1 (12.5)	0 (0)	0 (0)	0 (0)	0 (0)	0 (0)	0 (0)
Thiopurine	2 (25)	0 (0)	0 (0)	0 (0)	1 (25)	0 (0)	0 (0)
Thiopurine + anti-TNF	1 (12.5)	0 (0)	0 (0)	0 (0)	0 (0)	0 (0)	0 (0)
Anti-TNF	1 (12.5)	0 (0)	0 (0)	0 (0)	1 (25)	0 (0)	0 (0)
Anti-IL12/23	0 (0)	0 (0)	0 (0)	0 (0)	0 (0)	0 (0)	0 (0)
SES-CD score		NA		NA		NA	
0-2 inactive	0 (0)		0 (0)		0 (0)		0 (0)
3-6 mild	0 (0)		1 (33.3)		0 (0)		1 (25)
7-15 moderate	2 (25)		1 (33.3)		0 (0)		0 (0)
≥16 severe	0 (0)		3 (33.3)		0 (0)		1 (25)
Rutgeerts score		NA		NA		NA	
i0	1 (12.5)		0 (0)		0 (0)		0 (0)
i1	0 (0)		0 (0)		0 (0)		0 (0)
i2	4 (50)		0 (0)		3 (75)		2 (50)
i3	0 (0)		0 (0)		0 (0)		0 (0)
i4	1 (12.5)		0 (0)		1 (25)		0 (0)
Montreal CD		NA		NA		NA	
Location							
L1: ileal	4 (50)		2 (66.7)		2 (50)		1 (25)
L2: colonic	0 (0)		0 (0)		1 (25)		1 (25)
L3: ileocolonic	4 (50)		1 (33.3)		1 (25)		2 (50)
Behaviour							
B1: nonstricturing, nonpenetrating	5 (62.5)		1 (33.3)		2 (50)		1 (25)
B2: stricturing	2 (25)		2 (66.7)		1 (25)		3 (75)

B3: penetrating	1 (12.5)	0 (0)	1 (25)	0 (0)
Perianal	4 (50)	0 (0)	2 (50)	0 (0)

Values expressed in n (%) or as median with interquartile range. The SES-CD score or the Rutgeerts Score was assessed, dependent on whether it concerned a post-surgical assessment (Rutgeerts score) or not (SES-CD); hence, the total percentage per scoring system does not necessarily add up to 100 percent. CD, Crohn's disease; C, control; IMC, imaging mass cytometry; RNA-seq, RNA-sequencing; sc, single cell; SES- CD, simple endoscopic score for CD.

Enzymatic digestion

Biopsies were collected in HBSS media (Gibco) containing 2% FCS and 0.2% amphotericin B. The intestinal tissue was transferred to HBSS supplemented with 1 mM DTT (Sigma) and placed on a rolling device for 10 min at 4°C. After discarding the supernatant, the intestinal tissue was transferred to HBSS supplemented with 2% FCS and 5 mM EDTA and shaken (2x) at 180 rpm for 30 min at 37°C. The tissue suspension was passed through a 70µm cell strainer (Costar) and constituted the intraepithelial population. To obtain lamina propria T cells, the remaining intestinal biopsies were subsequently incubated for 1 hour at 37°C with 1mg/ml Collagenase IV (Sigma) in RPMI medium (supplemented with 10% FCS, 100 U/ml penicillin-streptomycin and 0.2% Fungizone), then forcefully resuspended through a 19G needle, washed and filtered with 70 µm cell strainer (Costar). The cell suspensions were used for bulk and single-cell RNA-sequencing after sorting different T cell subsets.

Fluorescence-activated Cell Sorting

In preparation of fluorescence-activated cell sorting (FACS) the intestinal cells were incubated with the surface antibodies for 20 minutes in supplemented RPMI (2% FCS, 1% penicillin and streptomycin, 0.2% Fungizone) at 4°C, and subsequently washed in FACS buffer before sorting on a FACSAria™ III (BD) (for gating strategy see supplemental figure 1A). Antibodies used: fixable viability dye eF506 (65-2860-40), anti-human CD3 eF450 (clone OKT3, 48-0037-42; eBioscience), TCRγδ BV510 (clone B1, 331220), CD3 AF700 (clone UCHT1, 300424), CD4 BV785 (clone OKT4, 317442; Biolegend), CD8α APC-Cy7 (clone SK1, 557834), CD127 BV421 (clone HIL-7R-M21, 562436), CD25 PE-Cy7 (clone M-A251, 557741), CD69 PE (clone FN50, 555531; BD Biosciences), CD8α PerCP-Cy5.5 (clone RPA-T8, 301032), CD127 AF647 (clone HCD127, 351318; Biolegend), TCRγδ FITC (clone IMMU510, IM1571U, Beckman Coulter), CD45RA APC-Cy7 (clone HI100, 2120640), CCR7 APC (clone G043H7, 2366070, Sony Biotechnology). Flow data was analyzed using FlowJo v10.

Bulk RNA-sequencing

The sorted cells were thawed for TRIzol (Thermo Fisher Scientific) RNA extraction and stored at -80°C until library preparation. Sequencing libraries were prepared using the Cel-Seq2 Sample Preparation Protocol and sequenced as 75bp paired-end on a NextSeq 500 (Utrecht Sequencing Facility). The reads were demultiplexed and aligned to the human cDNA reference genome (hg38) using BWA (version 0.7.13). Multiple reads mapping to the same gene with the same unique molecular identifier (UMI, 6bp long) were counted as a single read.

Raw counts of splice variants were summed and the raw counts were subsequently transformed employing variance stabilizing transformation. Differential analysis was performed using DESeq2 (Wald's test) with a p-adjusted value < 0.1 considered statistically significant. For visualization purposes the R package DESeq2 was employed. Pathway analysis was performed on the differentially expressed genes as input in Toppfun with standard settings. Gene set enrichment analysis (GSEA¹⁷ v4.0.3), with as input the normalized data (output DESeq2), was used to assess enrichment of gene sets derived from Magnuson *et al.*¹⁸, Guo *et al.*¹⁹ and Mijnheer *et al.*²⁰. One thousand random permutations of the gene sets were used to establish a null distribution of enrichment score against which a normalized enrichment score and FDR-corrected *q* values were calculated. Identification of key-regulators was performed using RegEnrich²¹ v1.0.1 based on the differential gene expression data followed by unsupervised gene regulatory network inference (GENIE3) to construct a network based on the raw gene count data, and GSEA was used for enrichment analysis. Network visualization was performed with Cytoscape²² v3.9.0.

Single-cell RNA-sequencing

Live CD3⁺CD8⁺CD4⁺ cells were sorted (for gating strategy see supplemental figure 1A) into 384-well hard shell plates (Biorad) with 5 μ l of vapor-lock (QIAGEN) containing 100-200 nl of RT primers, dNTPs and synthetic mRNA Spike-Ins and immediately spun down and frozen to -80°C. Cells were prepared for SORT-seq as previously described.²³ Illumina sequencing libraries were then prepared with the TruSeq small RNA primers (Illumina) and sequenced single-end at 75 bp read length with 75,000 reads per cell on a NextSeq500 platform (Illumina). Sequencing reads were mapped against the reference human genome (GRCh38) with BWA.

Quality control was performed in R with *seurat* and cells were dropped when the number of genes was < 150, and/or the percentage of mitochondrial genes was > 35%. Potential doublets were eliminated based on the gene/UMI ratio. Cut-offs were set based on visual inspection of the distribution and preliminary clustering analyses. The raw data expression matrices were subsequently analyzed using *Seurat* (v4²⁴⁻²⁶) following the outline provided by the distributor (<https://satijalab.org/seurat/>). Each dataset was log normalized, variable features were determined using *vst*, and the percent of mitochondrial genes and difference between G1 and G2M phase of the cell-cycle were regressed out. Thereupon, the datasets were merged with *Seurat* and batch-effect correction for patient was performed with *Harmony*.²⁷

For dimensionality reduction first the PC's were calculated (RunPCA) and clustering was performed with UMAP (RunUMAP: 30 dimensions, n.neighbors 20; FindNeighbors: clustering resolution of 0.8). Index sort data was analyzed in FlowJo v10 using the Index sort v3 script (<https://www.flowjo.com/exchange/#/plugin/profile?id=20>). Median Fluorescent Intensity cut-offs were determined based on the gating, and imported as metadata. Subsequent differential gene expression was performed using the MAST test (standard settings, regression for patient) with a p-adjusted value < 0.05 considered statistically significant. Visualization were performed with *seurat*.

Imaging mass cytometry

Intestinal biopsies were fixed in 10% neutral buffered formalin, paraffin-embedded, and two slides containing consecutive 4 μm -thick sections of all samples were prepared. One slide was stained with haematoxylin and eosin (HE) for histological assessment and the second slide was stained for imaging mass cytometry (IMC). IMC combines immunohistochemistry with high-resolution laser ablation of stained tissue sections followed by cytometry by time of flight (CyTOF) mass cytometry enabling imaging of multiple proteins at subcellular resolution.²⁸ All antibodies were conjugated to lanthanide metals (Fluidigm, San Francisco, CA, USA) using the MaxPar antibody labeling kit and protocol (Fluidigm), and eluted in antibody stabilization buffer (Candor Bioscience) for storage.

The slide was baked for 1.5 hours at 60°C, deparaffinized with fresh xylene for 20 minutes and subsequently rehydrated in descending grades of ethanol (100% (10 minutes), 95%, 80%, 70% (5 minutes each). After washing for 5 minutes in milliQ and 10 minutes in PBST (PBS containing 0.1% Tween-20), heat-induced epitope retrieval was conducted in Tris/EDTA (10 mM/1 mM, pH 9.5) for 30 minutes in a 95°C water bath. The slide was allowed to cool to 70°C before washing in PBST for 10 minutes. To decrease non-specific antibody binding, tissue sections were blocked with 3% BSA and Human TruStain FcX (1:100, BioLegend) in PBST for 1 hour at room temperature. The antibody cocktail was prepared by mixing all antibodies at concentrations specific for the assay in PBST+0.5% BSA. After careful removal of the blocking buffer, the slide was incubated overnight at 4°C with the antibody cocktail. Antibodies used: E-cadherin 142Nd (metal tag) (clone 24E10, CST3195BF, Cell Signaling Technology), CD3 170Er (polyclonal, A045229-2, Dako), CD4 156Gd (clone EPR6855, ab181724, Abcam), CD8 α 162Dy (clone C8/144B, 14-0085-82, Thermo Fisher Scientific), FOXP3 155Gd (clone 236A/E7, ab96048, Abcam), Ki-67 168Er (clone B56, 556003, BD Biosciences), Granzyme B 169Tm (clone D6E9W, CST46890BF, Cell Signaling Technology). Following three 5 minutes washes in PBST and rinsing in milliQ the tissue was counterstained with 0.1% toluidine blue for 5 minutes to enable tissue structure visualization under bright field microscopy if desired. Upon washing for 5 minutes in milliQ, the slide was incubated with Ir-intercalator (1:500 in PBST, Fluidigm) for 60 min at room temperature. Finally, the slide was washed in milliQ and air dried for at least for 20 min at room temperature.

Images were acquired at a resolution of 1 μm using a Hyperion Imaging System (Fluidigm). Regions of interest were selected based on the HE slides after which areas with an approximate size of 1,000 x 1,000 μm were ablated and acquired at 200 Hz. Pseudo-colored intensity maps were generated of each mass channel. Composite images were created and analyzed for each sample using Image J (version 1.47), and any changes to the brightness or contrast of a given marker were consistent across all samples.

Statistical analysis

Flow cytometric data was analyzed with a two-tailed Mann-Whitney U or Wilcoxon test with a p-adjusted value < 0.05 considered statistically significant. Data were analyzed with GraphPad

Prism (GraphPad Software version 7.0, La Jolla, CA, USA). Single cell and bulk RNA-sequencing was statistically analyzed as described in the relevant paragraphs.

Data availability statement

The raw count data generated with the bulk and single cell RNA-sequencing are available on <https://github.com/lutterl/CD4-T-cells-ileum>.

Ethics statements

The study protocols (TCBio 17/443, 17/444, 18/522 and NL28761.091.09) were approved by the research ethics committee of the University Medical Center Utrecht (Utrecht, The Netherlands) and the Radboud University Nijmegen Medical Centre (CMO Regio Arnhem-Nijmegen, Nijmegen, The Netherlands), respectively. Written informed consent was obtained from each participating patient before any study-related procedure was performed. The procedures were performed in accordance with the Declaration of Helsinki.

Acknowledgements

The authors thank all participants. They thank Herma Fidler, Fiona van Schaik, Meike Hirdes, Joren ten Hove and Auke Bogte from the department of Gastroenterology and Hepatology, UMC Utrecht for help with collecting patient material, Vincent Meij from the department of Surgery, UMC Utrecht for help with collecting pilot patient material, Michal Mokry, Nico Lansu and Noortje van den Dungen for providing bulk RNA-sequencing services, Single Cell Discoveries for providing single-cell RNA-sequencing services, Domenico Castigliero for help with intestinal tissue slide preparation and Yvonne Vercoulen and Mojtaba Amini for providing imaging mass cytometry services.

REFERENCES

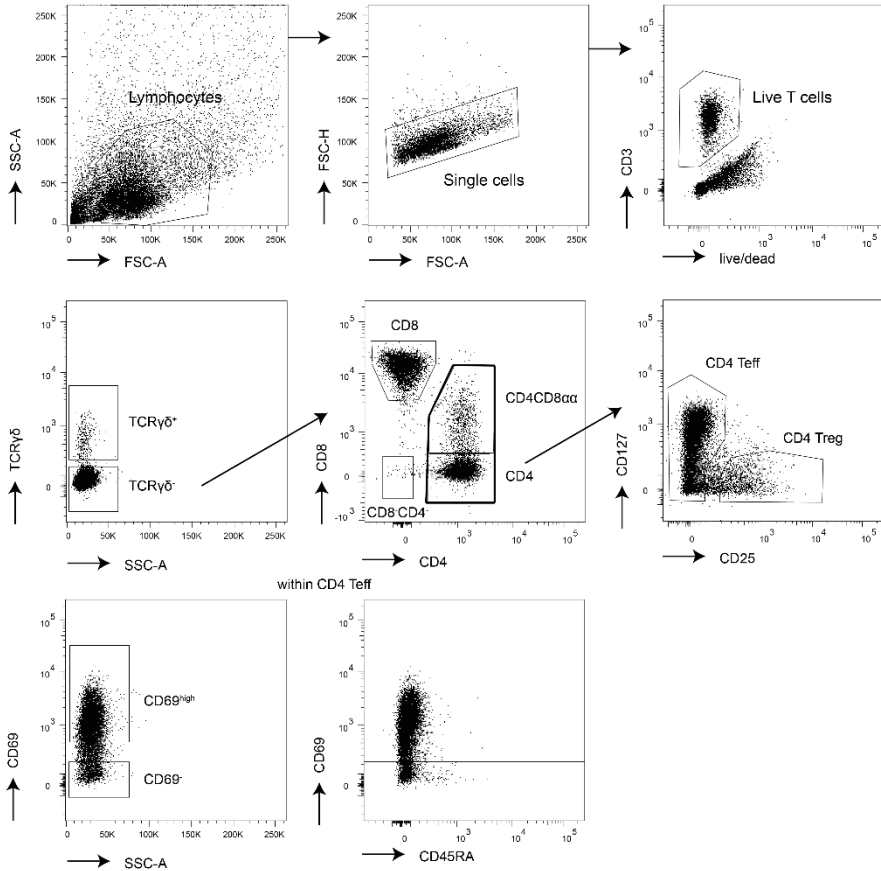
1. Chang, J. T. Pathophysiology of Inflammatory Bowel Diseases. *N. Engl. J. Med.* **383**, 2652–2664 (2020).
2. Mowat, A. M. & Agace, W. W. Regional specialization within the intestinal immune system. *Nat. Rev. Immunol.* **14**, 667–685 (2014).
3. Lutter, L., Hoytema van Konijnenburg, D. P., Brand, E. C., Oldenburg, B. & van Wijk, F. The elusive case of human intraepithelial T cells in gut homeostasis and inflammation. *Nat. Rev. Gastroenterol. Hepatol.* **15**, 637–649 (2018).
4. Kumar, B. V *et al.* Human Tissue-Resident Memory T Cells Are Defined by Core Transcriptional and Functional Signatures in Lymphoid and Mucosal Sites. *Cell Rep.* **20**, 2921–2934 (2017).
5. Fiocchi, C., Battisto, J. R. & Farmer, R. G. Gut mucosal lymphocytes in inflammatory bowel disease: isolation and preliminary functional characterization. *Dig. Dis. Sci.* **24**, 705–717 (1979).
6. Ahn, J. Y. *et al.* Colonic mucosal immune activity in irritable bowel syndrome: Comparison with healthy controls and patients with ulcerative colitis. *Dig. Dis. Sci.* **59**, 1001–1011 (2014).
7. Brown, I., Mino-Kenudson, M., Deshpande, V. & Lauwers, G. Y. Intraepithelial lymphocytosis in architecturally preserved proximal small intestinal mucosa: An increasing diagnostic problem with a wide differential diagnosis. *Archives of Pathology and Laboratory Medicine* vol. 130 1020–1025 (2006).
8. Zundler, S. *et al.* Hobit- and Blimp-1-driven CD4(+) tissue-resident memory T cells control chronic intestinal inflammation. *Nat. Immunol.* **20**, 288–300 (2019).
9. Rubin, S. J. S. *et al.* Mass cytometry reveals systemic and local immune signatures that distinguish inflammatory bowel diseases. *Nat. Commun.* **10**, (2019).
10. Kleinschek, M. A. *et al.* Circulating and gut-resident human Th17 cells express CD161 and promote intestinal inflammation. *J. Exp. Med.* **206**, 525–534 (2009).
11. Hovhannisyan, Z., Treatman, J., Littman, D. R. & Mayer, L. Characterization of interleukin-17-producing regulatory T cells in inflamed intestinal mucosa from patients with inflammatory bowel diseases. *Gastroenterology* **140**, 957–965 (2011).
12. Jaeger, N. *et al.* Single-cell analyses of Crohn's disease tissues reveal intestinal intraepithelial T cells heterogeneity and altered subset distributions. *Nat. Commun.* **12**, 2–13 (2021).
13. Müller, S. *et al.* Activated CD4+ and CD8+ cytotoxic cells are present in increased numbers in the intestinal mucosa from patients with active inflammatory bowel disease. *Am. J. Pathol.* **152**, 261–268 (1998).
14. Bartolomé-Casado, R. *et al.* Resident memory CD8 T cells persist for years in human small intestine. *J. Exp. Med.* **216**, 2412–2426 (2019).
15. Sujino, T. *et al.* Tissue adaptation of regulatory and intraepithelial CD4(+) T cells controls gut inflammation. *Science* **352**, 1581–1586 (2016).
16. Sarrabayrouse, G. *et al.* CD4CD8 $\alpha\alpha$ lymphocytes, a novel human regulatory T cell subset induced by colonic bacteria and deficient in patients with inflammatory bowel disease. *PLoS Biol.* **12**, e1001833 (2014).
17. Subramanian, A. *et al.* Gene set enrichment analysis: a knowledge-based approach for interpreting genome-wide expression profiles. *Proc. Natl. Acad. Sci. U. S. A.* **102**, 15545–50 (2005).
18. Magnuson, A. M. *et al.* Identification and validation of a tumor-infiltrating Treg transcriptional signature conserved across species and tumor types. *Proc. Natl. Acad. Sci. U. S. A.* **115**, E10672–E10681 (2018).
19. Guo, X. *et al.* Global characterization of T cells in non-small-cell lung cancer by single-cell sequencing. *Nat. Med.* **24**, 978–985 (2018).
20. Mijnheer, G. *et al.* Conserved human effector Treg cell transcriptomic and epigenetic signature in arthritic joint inflammation. *Nat. Commun.* **12**, 2710 (2021).
21. Tao, W., Radstake, T. R. D. J. & Pandit, A. RegEnrich: An R package for gene regulator enrichment analysis reveals key role of ETS transcription factor family in interferon signaling. *bioRxiv* 2021.01.24.428029 (2021) doi:10.1101/2021.01.24.428029.
22. Shannon, P. *et al.* Cytoscape: a software environment for integrated models of biomolecular interaction networks. *Genome Res.* **13**, 2498–2504 (2003).
23. Muraro, M. J. *et al.* A Single-Cell Transcriptome Atlas of the Human Pancreas. *Cell Syst.* **3**, 385–394.e3 (2016).
24. Butler, A., Hoffman, P., Smibert, P., Papalexi, E. & Satija, R. Integrating single-cell transcriptomic data across different conditions, technologies, and species. *Nat. Biotechnol.* **36**, 411–420 (2018).

25. Stuart, T. *et al.* Comprehensive Integration of Single-Cell Data. *Cell* **177**, 1888-1902.e21 (2019).
26. Hao, Y. *et al.* Integrated analysis of multimodal single-cell data. *Cell* **184**, 3573-3587.e29 (2021).
27. Korsunsky, I. *et al.* Fast, sensitive and accurate integration of single-cell data with Harmony. *Nat. Methods* **16**, 1289-1296 (2019).
28. Giesen, C. *et al.* Highly multiplexed imaging of tumor tissues with subcellular resolution by mass cytometry. *Nat. Methods* **11**, 417-422 (2014).
29. Reis, B. S., Hoytema van Konijnenburg, D. P., Grivennikov, S. I. & Mucida, D. Transcription factor T-bet regulates intraepithelial lymphocyte functional maturation. *Immunity* **41**, 244-256 (2014).
30. Das, G. *et al.* An important regulatory role for CD4+CD8 alpha alpha T cells in the intestinal epithelial layer in the prevention of inflammatory bowel disease. *Proc. Natl. Acad. Sci. U. S. A.* **100**, 5324-5329 (2003).
31. Liston, A. & Gray, D. H. D. Homeostatic control of regulatory T cell diversity. *Nat. Rev. Immunol.* **14**, 154-65 (2014).
32. Wohlfert, E. A. *et al.* GATA3 controls Foxp3(+) regulatory T cell fate during inflammation in mice. *J. Clin. Invest.* **121**, 4503-4515 (2011).
33. Sugai, M. *et al.* Runx3 Is Required for Full Activation of Regulatory T Cells To Prevent Colitis-Associated Tumor Formation. *J. Immunol.* **186**, 6515 LP - 6520 (2011).
34. Holbrook, J., Lara-Reyna, S., Jarosz-Griffiths, H. & McDermott, M. Tumour necrosis factor signalling in health and disease. *F1000Research* **8**, (2019).
35. Peng, J.-M., Lin, S.-H., Yu, M.-C. & Hsieh, S.-Y. CLIC1 recruits PIP5K1A/C to induce cell-matrix adhesions for tumor metastasis. *J. Clin. Invest.* **131**, (2021).
36. Svensson, L., Stanley, P., Willenbrock, F. & Hogg, N. The Gαq/11 proteins contribute to T lymphocyte migration by promoting turnover of integrin LFA-1 through recycling. *PLoS One* **7**, e38517 (2012).
37. Chetoui, N., El Azreq, M.-A., Boisvert, M., Bergeron, M.-É. & Aoudjit, F. Discoidin domain receptor 1 expression in activated T cells is regulated by the ERK MAP kinase signaling pathway. *J. Cell. Biochem.* **112**, 3666-3674 (2011).
38. Luo, S.-M., Tsai, W.-C., Tsai, C.-K., Chen, Y. & Hueng, D.-Y. ARID4B Knockdown Suppresses PI3K/AKT Signaling and Induces Apoptosis in Human Glioma Cells. *Oncotargets Ther.* **14**, 1843-1855 (2021).
39. Handi, J., Patterson, S. & Levings, M. The Role of the PI3K Signaling Pathway in CD4+ T Cell Differentiation and Function . *Frontiers in Immunology* vol. 3 (2012).
40. Yamada, T., Park, C. S., Mamonkin, M. & Lacorazza, H. D. Transcription factor ELF4 controls the proliferation and homing of CD8+ T cells via the Krüppel-like factors KLF4 and KLF2. *Nat. Immunol.* **10**, 618-626 (2009).
41. Espinosa, A. *et al.* Loss of the lupus autoantigen Ro52/Trim21 induces tissue inflammation and systemic autoimmunity by dysregulating the IL-23-Th17 pathway. *J. Exp. Med.* **206**, 1661-1671 (2009).
42. Zhou, G. *et al.* Tripartite motif-containing (TRIM) 21 negatively regulates intestinal mucosal inflammation through inhibiting T(H)1/T(H)17 cell differentiation in patients with inflammatory bowel diseases. *J. Allergy Clin. Immunol.* **142**, 1218-1228.e12 (2018).
43. Cai, X. *et al.* Tripartite motif containing protein 27 negatively regulates CD4 T cells by ubiquitinating and inhibiting the class II PI3K-C2β. *Proc. Natl. Acad. Sci. U. S. A.* **108**, 20072-20077 (2011).
44. Venkateswaran, S. *et al.* Bowel Location Rather Than Disease Subtype Dominates Transcriptomic Heterogeneity in Pediatric IBD. *Cellular and molecular gastroenterology and hepatology* vol. 6 474-476.e3 (2018).
45. Raine, T., Liu, J. Z., Anderson, C. A., Parkes, M. & Kaser, A. Generation of primary human intestinal T cell transcriptomes reveals differential expression at genetic risk loci for immune-mediated disease. *Gut* **64**, 250-259 (2015).
46. London, M., Bilate, A. M., Castro, T. B. R., Sujino, T. & Mucida, D. Stepwise chromatin and transcriptional acquisition of an intraepithelial lymphocyte program. *Nat. Immunol.* (2021) doi:10.1038/s41590-021-00883-8.
47. Lutter, L. *et al.* Homeostatic Function and Inflammatory Activation of Ileal CD8(+) Tissue-Resident T Cells Is Dependent on Mucosal Location. *Cell. Mol. Gastroenterol. Hepatol.* **12**, 1567-1581 (2021).
48. Al-Bawardy, B., Shivashankar, R. & Proctor, D. D. Novel and Emerging Therapies for Inflammatory Bowel Disease . *Frontiers in Pharmacology* vol. 12 (2021).
49. Mucida, D. *et al.* Transcriptional reprogramming of mature CD4(+) helper T cells generates distinct MHC class II-restricted cytotoxic T lymphocytes. *Nat. Immunol.* **14**, 281-289 (2013).
50. Wienke, J. *et al.* Human Tregs at the materno-fetal interface show site-specific adaptation reminiscent

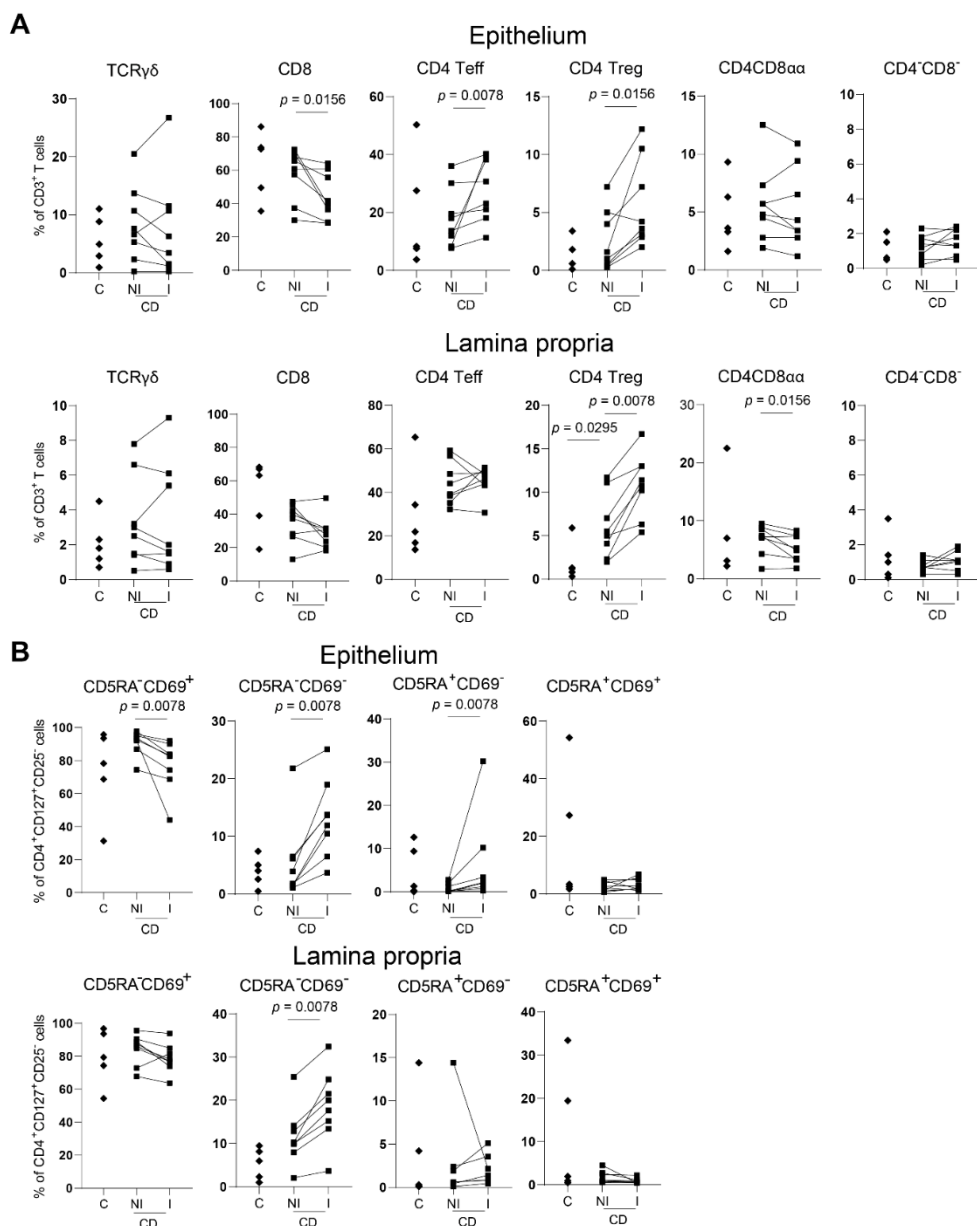
- of tumor Tregs. *JCI insight* **5**, (2020).
51. Brand, E. C. *et al.* Healthy Cotwins Share Gut Microbiome Signatures With Their Inflammatory Bowel Disease Twins and Unrelated Patients. *Gastroenterology* **160**, 1970–1985 (2021).
 52. Kosoy, R. *et al.* Deep Analysis of the Peripheral Immune System in IBD Reveals New Insight in Disease Subtyping and Response to Monotherapy or Combination Therapy. *Cell. Mol. Gastroenterol. Hepatol.* **12**, 599–632 (2021).
 53. Ikeuchi, H. *et al.* Localization of recurrent lesions following ileocolic resection for Crohn’s disease. *BMC Surg.* **21**, 145 (2021).
 54. Meng, X. *et al.* Regulatory T cells in cardiovascular diseases. *Nat. Rev. Cardiol.* **13**, 167–179 (2016).
 55. Park, S.-G. *et al.* T regulatory cells maintain intestinal homeostasis by suppressing $\gamma\delta$ T cells. *Immunity* **33**, 791–803 (2010).
 56. Povoleri, G. A. M. *et al.* Human retinoic acid–regulated CD161 + regulatory T cells support wound repair in intestinal mucosa. *Nat. Immunol.* **19**, 1403–1414 (2018).
 57. Cho, I., Lui, P. P. & Ali, N. Treg regulation of the epithelial stem cell lineage. *J. Immunol. Regen. Med.* **8**, (2020).
 58. Desreumaux, P. *et al.* Safety and efficacy of antigen-specific regulatory T-cell therapy for patients with refractory Crohn’s disease. *Gastroenterology* **143**, 1207-1217.e2 (2012).

SUPPLEMENTARY INFORMATION

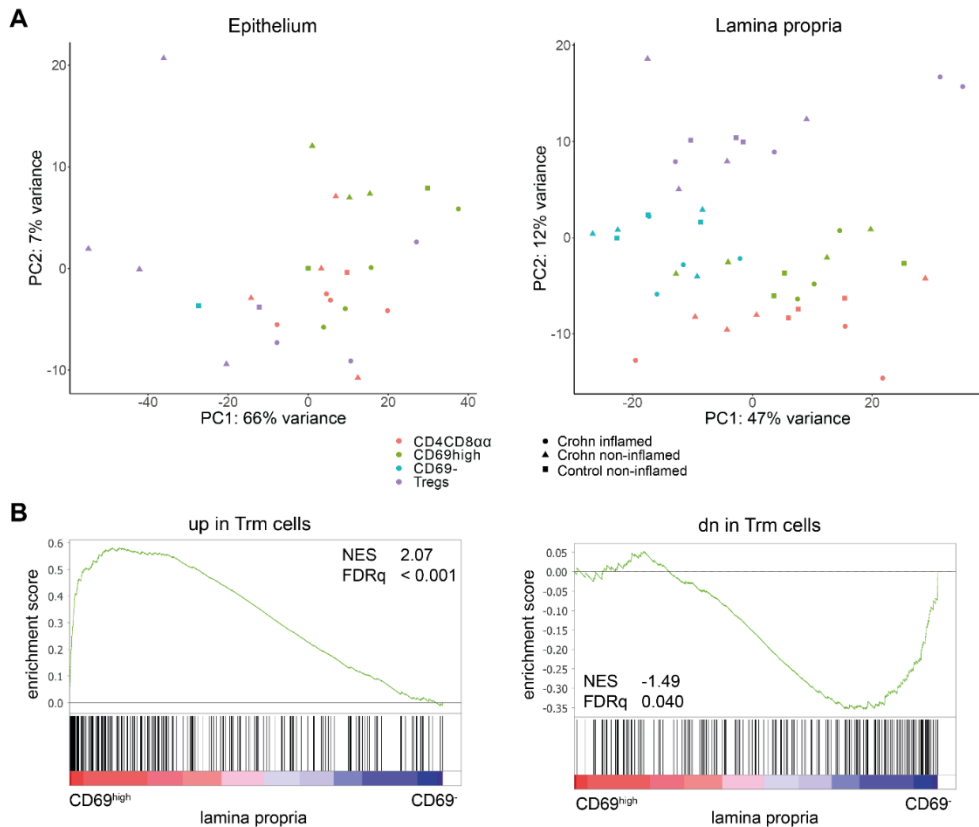
A



Supplemental figure 1. Gating strategy. (A) Gating strategy employed to determine the T cell subset composition, for sorting of CD4⁺CD69^{high}, CD4⁺CD69⁻, CD4⁺ Treg, CD4CD8 $\alpha\alpha$ (CD8 α^+ , vast majority is CD8 $\alpha\alpha$) T cells for bulk RNA-sequencing and CD4⁺ T cells (thick black outline) for single-cell RNA-sequencing, and to determine the CD69/CD45RA composition. TCR, T cell receptor; Teff, T-effector cells; Treg, regulatory T cells.



Supplemental figure 2. T cell composition of the human ileum in health and Crohn's disease. (A) Relative composition of T cell receptor (TCR) $\gamma\delta$, CD8, CD4 effector (Teff, CD127⁺CD25⁻), CD4CD8 $\alpha\alpha$ (CD4⁺CD8 α ⁺), CD4 regulatory T cells (Tregs, CD127^{low}CD25^{high}) and TCR $\gamma\delta$ CD8⁺CD4⁻ cells in the epithelium (upper row) and lamina propria (lower row) of control subjects (C), non-inflamed (NI) and inflamed (I) ileum of Crohn's disease (CD) patients. Lines connect the paired non-inflamed and inflamed datapoints from the patients with CD. Control subjects $n = 5$, CD $n = 8$. (B) Relative composition within CD4 effector T cells of tissue-resident memory (CD45RA⁻CD69⁺), memory (CD45RA⁻CD69⁻), CD4 naive (CD45RA⁺CD69⁻) and recently activated (CD45RA⁺CD69⁺) T cells, similar as to A. Control subjects $n = 5$, CD $n = 8$. Comparisons were performed with a two-tailed Mann Whitney U test for control subject vs non-inflamed CD and Wilcoxon test for paired non-inflamed vs inflamed CD.



Supplemental figure 3. Clustering of CD4 T cell subsets in the epithelium and lamina propria. (A) Unsupervised principal component analysis of all sorted CD4 T cell subsets analyzed by bulk RNA-sequencing, split for epithelium (left) and lamina propria (right), colored on CD4 T cell subset (pink = CD4CD8 $\alpha\alpha$ T cells, green = CD4 CD69^{high} Trm cells, blue = CD4 CD69⁻ T cells, purple = Tregs) and status (circle = CD inflamed ileum, triangle = CD non-inflamed ileum, square = control non-inflamed ileum). (B) Gene set enrichment analysis of a Trm signature⁴ (CD69⁺ vs CD69⁻ T cells) with genes upregulated (left) and downregulated (right) in this signature in pairwise comparisons involving transcriptome data of CD69^{high} and CD69⁻ CD4 T cells derived from non-inflamed ileum of control subjects and non-inflamed and inflamed ileum of patients with CD, represented by the normalized enrichment score (NES) and FDR statistical value (FDRq, multiple hypothesis testing using sample permutation).

Extended Supplementary Data can be found at: <https://github.com/lutterl/PhD-thesis-supplementary-data>.

Chapter 7

Homeostatic function and inflammatory activation of ileal CD8⁺ tissue-resident T cells is dependent on mucosal location

Lisanne Lutter,^{1,2,*} Britt Roosenboom,^{3,*} Eelco C. Brand,^{1,2} José J. ter Linde,^{1,2} Bas Oldenburg,² Ellen G. van Lochem,⁴ Carmen S. Horje Talabur Horjus,^{3,#} Femke van Wijk^{1,#}

*Authors share co-first authorship

#Authors jointly supervised this work

¹Centre for Translational Immunology, University Medical Centre Utrecht, Utrecht, The Netherlands

²Department of Gastroenterology and Hepatology, University Medical Centre Utrecht, Utrecht, The Netherlands

³Department of Gastroenterology and Hepatology, Rijnstate Hospital, Arnhem, The Netherlands

⁴Department of Microbiology and Immunology, Rijnstate Hospital, Arnhem, The Netherlands

Cellular and Molecular Gastroenterology and Hepatology, 2021;12(5):1567-1581

ABSTRACT

Background & Aims: Tissue-resident memory T (Trm) cells, both of the CD4 and CD8 lineage, have been implicated in disease flares in inflammatory bowel disease. However, data are conflicting regarding the profile of human CD8⁺ Trm cells, with studies suggesting both proinflammatory and regulatory functions. It is crucial to understand the functional profile of these cells in the context of (new) therapeutic strategies targeting (trafficking of) gut Trm cells.

Methods: Here, we performed imaging mass cytometry, flow cytometry and RNA-sequencing to compare lamina propria and intraepithelial CD103⁺/CD69⁺CD8⁺ T cells in healthy control subjects and patients with active ileal Crohn's disease.

Results: Our data revealed that lamina propria CD103⁺CD69⁺CD8⁺ T cells have a classical Trm profile with active pathways for regulating cell survival/death and cytokine signaling, whereas intraepithelial CD103⁺CD69⁺CD8⁺ T cells display a tightly regulated innate-like cytotoxic profile. Furthermore, within lamina propria CD8⁺CD103⁻ Trm cells, an Itgb2⁺GzmK⁺KLRG1⁺ population distinct from CD103⁺ CD8⁺ Trm is found. During chronic inflammation, especially intraepithelial CD103⁺CD69⁺CD8⁺ T cells displayed an innate proinflammatory profile with concurrent loss of homeostatic functions.

Conclusions: Altogether, these compartmental and inflammation-induced differences indicate that therapeutic strategies could have a different impact on the same immune cells depending on the local compartment and presence of an inflammatory milieu, and should be taken into account when investigating short- and long-term effects of new gut T cell-targeting drugs.

INTRODUCTION

Inflammatory bowel disease (IBD), comprising Crohn's disease (CD) and ulcerative colitis, is a chronic relapsing-remitting inflammatory disease. To date, there is no cure for IBD; therefore, long-term administration of maintenance therapy is often necessary. Recently, a novel class of drugs has been added to the therapeutic armamentarium for IBD, namely compounds that modulate lymphocyte trafficking such as vedolizumab (anti-integrin $\alpha 4\beta 7$) and natalizumab (anti-integrin $\alpha 4$). Another anti-integrin, etrolizumab (anti-integrin $\beta 7$), is currently in phase III trials.^{1,2} Expression of integrins enables homing of immune cells to tissues, with integrin $\alpha 4\beta 7$ being the primary gut homing receptor.³ Upon localization to the gut the integrin $\beta 7$ monomer can dimerize with integrin αE (CD103). Upregulation of CD103 enables T cells to bind to E-cadherin, expressed by epithelial cells, thereby facilitating their intraepithelial retention.⁴⁻⁶ CD4⁺ T cells are more abundant in the lamina propria, while T cells in the epithelium are primarily of the CD8⁺ lineage.⁴ T cells homed to the lamina propria and epithelium can become tissue-resident memory T (Trm) cells upon expression of the Trm cell markers CD69 and CD103.⁷ Local cues, distinct for the lamina propria and epithelium, might induce further environment-adapted specialization of these Trm cells (CD69⁺CD103^{+/+}).⁸⁻¹⁰

Recently, it has been suggested that lamina propria CD4⁺ and CD8⁺ CD69⁺CD103⁺ Trm might be implicated in disease flares in IBD,¹¹ which implies that targeting these cells in IBD could be beneficial. A proinflammatory profile of colonic CD4⁺CD103⁺ T cells in IBD flares has been observed,^{12,13} but the functional profile of intestinal CD8⁺CD103⁺ T cells is still not completely elucidated.¹⁴⁻¹⁶ Interestingly, in mice adoptive transfer of CD8⁺CD103⁺ T cells reduced the severity of ileitis.¹⁷ Furthermore, we have previously shown that mucosal CD8⁺CD103⁺ T cell percentages in humans decrease by approximately 40% during CD flares compared to healthy control subjects, and normalize upon achieving remission.^{18,19} These findings raise the question whether these cells could have a proinflammatory or regulatory function. To determine compartmental differences and the functional profile of intestinal CD8⁺ Trm cells, we performed flow cytometry, imaging mass cytometry (IMC) and RNA-sequencing on lamina propria and intraepithelial CD103⁺ (and CD103⁻) CD69⁺CD8⁺ T cells in healthy control subjects and patients with active ileal CD.

RESULTS

We determined the localization of ileal CD8⁺CD103⁺ T cells in healthy control subjects and patients with *de novo* CD with imaging mass cytometry. We observed a decrease in percentage of CD103⁺ cells of total CD8⁺ T cells in both the epithelium and lamina propria of CD patients compared to healthy control ileum (Figure 1A). This decrease was most pronounced in the lamina propria with, on average, a 50% reduction in CD103⁺ CD8⁺ T cells compared to a 10% decrease in the epithelium (Figure 1B). Upon presence of inflammation in CD patients, there was an additional 30% decrease in CD103⁺ CD8 T cells in the lamina propria, whereas in the epithelium CD8⁺ T cells remained predominantly CD103⁺ (Figure 1B). Furthermore, there was an absolute decrease in CD8⁺ and consequently CD8⁺CD103⁺ T cells per μm^2 in both the

epithelium and lamina propria of CD patients compared with healthy control subjects (average of 1 CD8⁺ T cell per 1051 μm^2 in human control subjects, per 2249 μm^2 in noninflamed CD patients, and per 2589 μm^2 in inflamed CD patients for the epithelium, and per 839, 1848, and 1957 μm^2 , respectively, for the lamina propria).

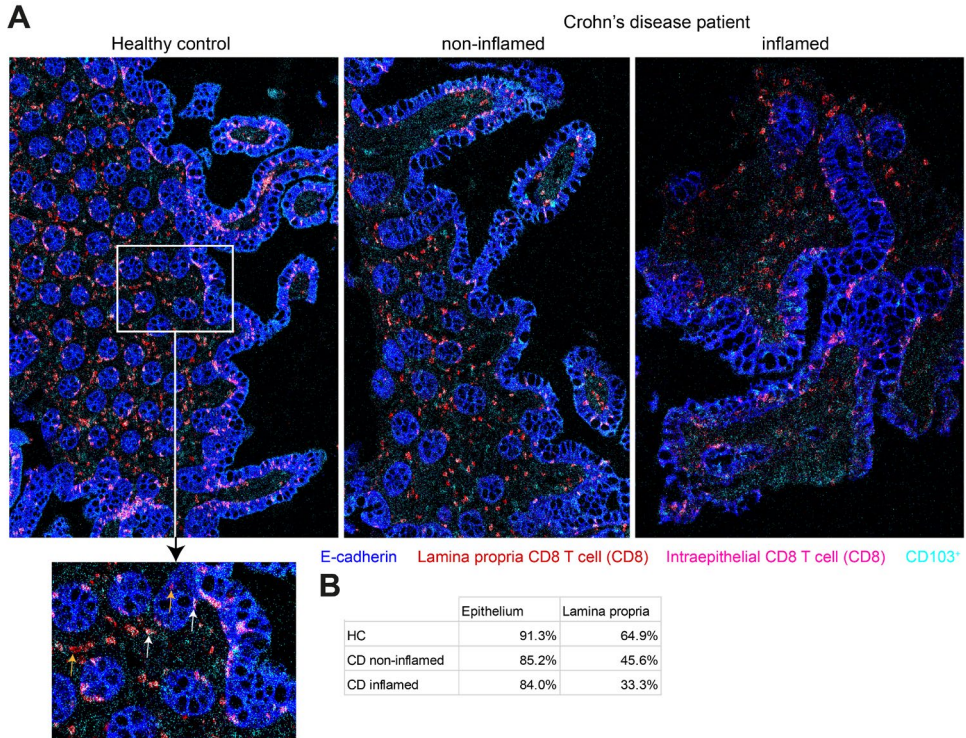


Figure 1. Visualization of CD103⁺ and CD103⁻ CD8⁺ T cells in the human ileum. (A) Representative composite images of imaging mass cytometry performed on human ileum sections showing an overlay of E-cadherin (blue), CD8 (red in lamina propria, pink in epithelium), and CD103 (cyan, colors white in CD8 T cells) for a healthy control (HC) subject (left), noninflamed ileum CD patient (middle), and inflamed ileum of a CD patient (right). The magnified section of the HC subject shows an example of CD103⁺ (white arrows) and CD103⁻ (orange arrows) CD8⁺ T cells within the lamina propria and epithelium. HC subjects: n = 2; CD patients: n = 3 (paired). (B) Quantification of CD103⁺ within CD8⁺ T cells in both the epithelium and lamina propria of the HC, CD noninflamed, and CD inflamed ileum. Every value is an average of 2 (HC subjects and noninflamed CD patients) or 3 (inflamed CD patients) samples measured using imaging mass cytometry. For each of the samples, 2 independent counts were performed.

Flow cytometry analysis of ileal CD8⁺ Trm cells in untreated, *de novo* CD (n = 21) (Figure 2A) showed a negative trend between the proportion of CD8⁺CD69⁺CD103⁺ T cells and the simple endoscopic score for CD of the ileum (Figure 2B). No correlation with other clinical parameters including the Harvey-Bradshaw index, fecal calprotectin or C-reactive protein was found. In addition, we observed a higher proportion of dividing CD8⁺CD69⁺CD103⁺ compared to CD103⁻ T cells in these untreated, *de novo* CD patients (average of 16.4% and 4.5% Ki-67⁺ cells,

respectively) (Figure 2C), indicating that CD8⁺CD69⁺CD103⁺ T cells are activated during inflammation.

To investigate the transcriptional profile of gut Trm cells, we performed RNA-sequencing on flow cytometry-based sorted lamina propria and intraepithelial CD103⁺ (and CD103⁻) CD69⁺CD8⁺ T cells in healthy control subjects and patients with active ileal CD. Unsupervised principal component analysis revealed that samples primarily cluster based on the compartment of residence. This relative compartmentalization was less evident during inflammation and for CD103⁻ T cells (Figure 2D).

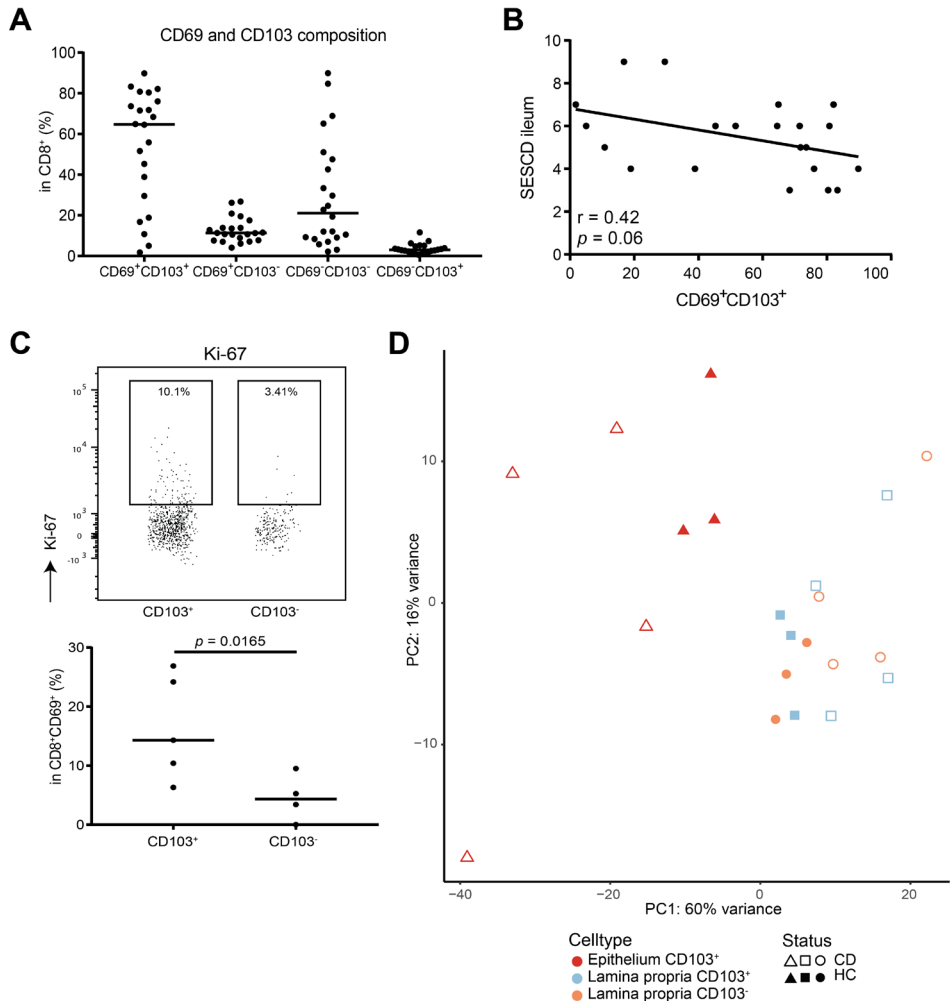


Figure 2. Characterizing human intestinal CD103⁻ and CD103⁺ CD69⁺CD8⁺ T cells. (A) Distribution of CD69⁺/⁻ CD103⁺/⁻ CD3⁺CD8⁺ T-cells within the ileum of patients with active CD (n = 21) at time of endoscopy, characterized by flow cytometry. (B) Scatterplot and fitted linear regression of the simple endoscopic score for CD (SES-CD) for the ileum and the percentage of total mucosal CD8⁺CD69⁺CD103⁺ T cells derived from inflamed ileum of patients with active CD (n = 21), characterized by flow cytometry. Pearson's r and the corresponding P

value are depicted in the graph. (C) Representative gating strategy (upper) and quantification (lower) of Ki-67 in both CD103⁺ and CD103⁻ CD69⁺CD8⁺ T cells in patients with active ileal CD (n = 4). The bar represents the median. Comparison was performed with a paired 2-tailed *t* test. (D) Unsupervised principal component analysis of all CD69⁺CD8⁺ T cell subsets analyzed by RNA-sequencing; CD103⁻ from the lamina propria (orange/circle) and CD103⁺ from the lamina propria (blue/square) and epithelium (red/triangle) from both healthy control (HC) subjects (closed symbols) and CD patients (open symbols). PC, principal component.

Lamina propria CD8⁺CD69⁺CD103⁻ and CD8⁺CD69⁺CD103⁺ T cells have distinct profiles

We first compared the transcriptional profile of CD103⁺ and CD103⁻ CD8⁺ Trm cells (CD69⁺) in the lamina propria. Differential gene expression revealed 22 upregulated and 54 downregulated genes between CD103⁺ and CD103⁻ CD8⁺ Trm cells (false discovery rate [FDR] <0.1) (Supplementary Table 1). These were shared by inflamed (CD) and noninflamed (healthy control) ileum. *KLF2*, *ENC1*, *GZMK*, *KLRG1*, and *S1PR5* genes known to be downregulated in Trm cells⁷ were also downregulated in CD103⁺CD8⁺ T cells compared with CD103⁻CD8⁺ T cells, whereas *EOMES*, a T effector memory-associated transcription factor,²⁰ was upregulated in CD103⁻CD8⁺ T cells (Figure 3A). In line with a more differentiated Trm cell phenotype, CD103⁺ CD8⁺ Trm cells also expressed higher levels of *CD160*, *CD96*, and *KLRC2* (encoding NKG2C) (Figure 3A). On the protein level, a lower expression of integrin β 2 (Itgb2), GzmK, KLRG1 and *EOMES* on CD8⁺CD103⁺ T cells compared to CD8⁺CD103⁻ T cells was confirmed (Figure 3B). These data indicate that CD103⁺ CD8⁺CD69⁺ lamina propria T cells express a less cytotoxic but more pronounced classical Trm cell profile compared with their CD103⁻ counterpart.

Within the CD8⁺CD69⁺CD103⁻ Trm cell compartment, a relatively high heterogeneity was found based on the protein expression data, with <50% Itgb2^{high}, GzmK and KLRG1 expressing cells (Figure 3B). Itgb2^{high} expression was almost mutually exclusive with CD103 expression (Figure 4A), and expression of GzmK and KLRG1 was predominantly confined to the Itgb2^{high} subset (Figure 4B and C). Similarly to CD103⁺ CD8⁺CD69⁺ Trm cells, CD8⁺ Trm cells lacking CD103 and Itgb2^{high} were mostly GzmK and KLRG1 negative (on average 91.8% and 94.2%, respectively; Figure 4C). Additionally, PD-1 expression, often associated with clonal expansion of CD8⁺ T cells,^{21,22} was higher in the Itgb2^{high} compared to CD103⁺ CD8⁺ Trm cells (average of 32.7 vs 14.7%) (Figure 4D). In summary, within CD103⁻ CD8⁺ Trm cells an Itgb2^{high} Trm cell population characterized by GzmK, KLRG1 and PD-1 is found.

The dichotomy between CD103⁺ and CD103⁻ CD8⁺CD69⁺ Trm cells was not found in the epithelial layer. Itgb2^{high} CD8⁺CD69⁺CD103⁻ Trm cells constituted on average 8.9% of epithelial CD8⁺ T cells, and KLRG1⁺ CD8⁺CD69⁺CD103⁻ Trm cells comprised 1.9% of CD8⁺ T cells in the epithelium (Figure 4E).

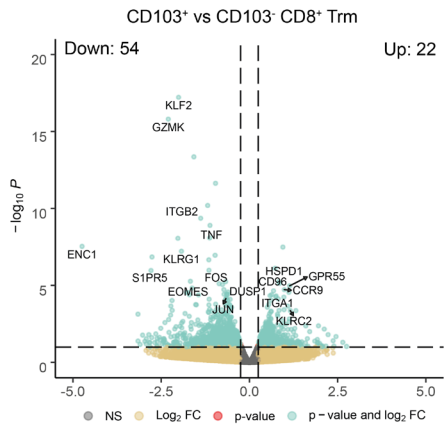
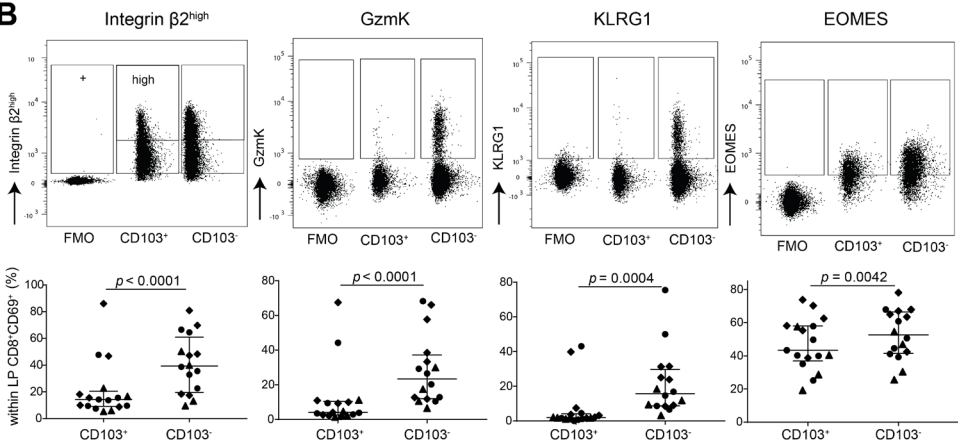
A**B**

Figure 3. Subset defining genes of lamina propria CD8⁺CD69⁺CD103⁻ and CD8⁺CD69⁺CD103⁺ T cells. (A) Volcano plot of the expressed genes, with a nominal P value < 0.99 , comparing lamina propria CD8⁺CD69⁺CD103⁻ to CD8⁺CD69⁺CD103⁺ T cells; selected genes are highlighted. On the x-axis the log₂ fold change (log₂FC) is shown, and on the y-axis the $-\log_{10} P$ value ($-\log_{10} P$). Grey indicates not significantly differentially expressed genes, yellow indicates genes with a log₂FC > 0.25 and $-\log_{10} P > 10 \times 10^{-2.5}$, green indicates genes with a log₂FC > 0.25 and $-\log_{10} P < 10 \times 10^{-2.5}$. (B) Representative flow cytometric dotplots, including Fluorescent Minus One (FMO) control, of Itgb2, GzmK, KLRG1 and EOMES (upper row) and quantification of the respective marker (lower row) comparing lamina propria CD8⁺CD69⁺CD103⁻ and CD103⁺ T cells in healthy control subjects ($n = 6-7$; circles), CD from inflamed (diamonds) and noninflamed (triangles) ileum (paired, $n = 4-6$). Bars represent median and interquartile range. Comparison was performed with a paired 1-tailed t test. NS, not significant.

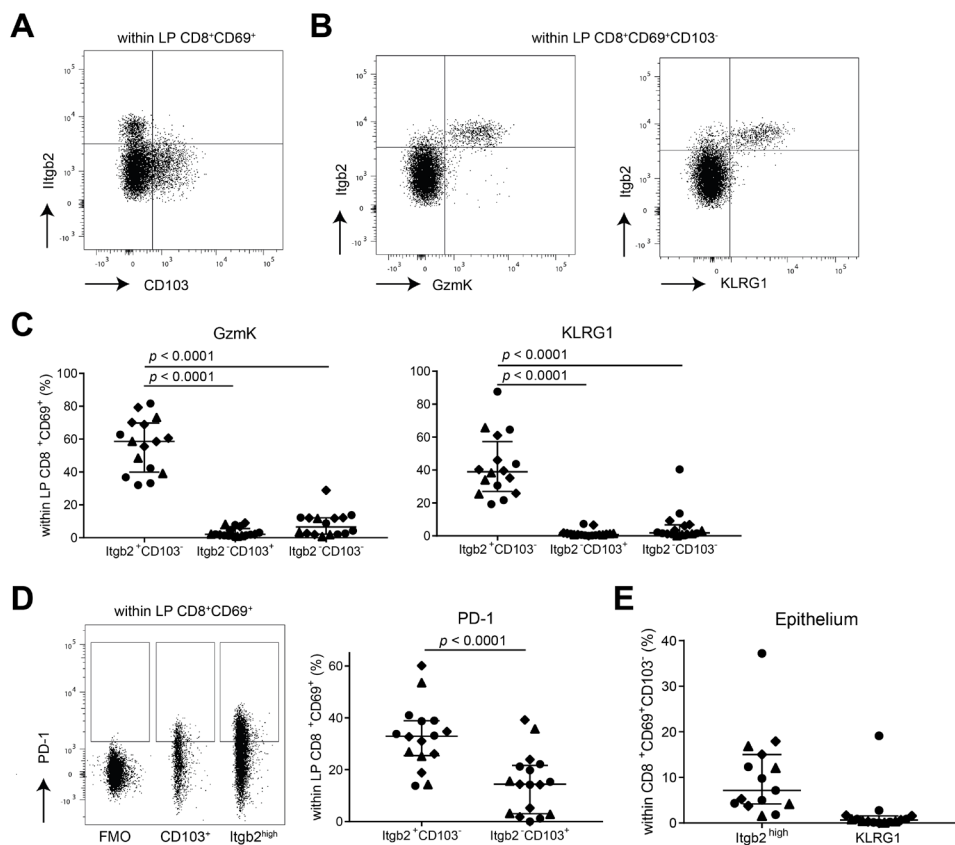


Figure 4. CD8⁺CD69⁺CD103⁺ T cell characterization. (A) Representative flow dotplot of Itgb2^{high} and CD103⁺ expression within lamina propria CD8⁺CD69⁺ T cells. (B) Representative flow dotplot of Itgb2^{high} and GzmK (left) and KLRG1 (right) coexpression within lamina propria CD8⁺CD69⁺CD103⁺ T cells. (C) Quantification of GzmK and KLRG1 within Itgb2⁺CD103⁺, Itgb2^{-/low}CD103⁺, and Itgb2^{-/low}CD103⁻ lamina propria CD8⁺CD69⁺ T cells for healthy control subjects (n = 6-7; circles), CD patients from inflamed (diamonds) and noninflamed (triangles) ileum (paired, n = 4-6). Bars represent median and interquartile range. Comparison was made with a 1-way analysis of variance. (D) Representative flow dotplot including Fluorescence Minus One (FMO) control and quantification of PD-1 within Itgb2^{high}CD103⁺ and Itgb2^{-/low}CD103⁺ lamina propria CD8⁺CD69⁺ T cells. Symbols and n as per panel C. Bars represent median and interquartile range. Comparison was made with a paired 2-tailed *t* test. (E) Quantification of Itgb2^{high} and KLRG1 within epithelial CD8⁺CD69⁺CD103⁺ T cells. Symbols as per panel C. Healthy control subjects: n = 7; CD patients: n = 4. Bars represent median and interquartile range.

The transcriptional profile of ileal CD8⁺CD69⁺CD103⁺ T cells is largely dependent on mucosal localization

Next, we focused on the differences of CD8⁺CD103⁺ Trm cell profiles, based on their spatial distribution. Differential gene expression of intraepithelial compared with lamina propria CD8⁺CD69⁺CD103⁺ T cells revealed 321 upregulated and 413 downregulated genes shared by CD patients and healthy control subjects (FDR < 0.1) (Figure 5A and B; Supplementary Table 1). Subsequent pathway analysis showed enrichment of T cell receptor signaling, cytotoxicity,

and interaction with nonimmune cells in the epithelial compartment (Figure 5B, left panel). In the lamina propria, cytokine signaling and inhibition of apoptosis were enriched (Figure 5B, right panel). In support of the latter, expression of interleukin (IL)-7R, which is essential for T cell homeostasis and long-term survival,^{23,24} was upregulated at both messenger RNA and protein level in lamina propria CD8⁺CD69⁺CD103⁺ T cells (Figure 5D). Furthermore, classical CD8⁺ Trm cell genes, including *RUNX3*, *NR4A2*, *ICOS*, and *LITAF*, showed higher expression in lamina propria CD8⁺CD69⁺CD103⁺ T cells (Figure 5A). The more profound Trm cell profile of lamina propria compared with intraepithelial CD8⁺CD69⁺CD103⁺ T cells was also supported by gene set enrichment analyses for a core Trm cell gene set (Figure 5E).²⁵ However, intraepithelial CD8⁺CD69⁺CD103⁺ T cells did not show enrichment of core effector memory or central memory T cell-related gene sets. We did observe elevated expression of cytotoxic genes such as *NKG7*, *GZMM*, *LTB*, *GZMA*, and killer-immunoglobulin receptors (*KIR2DL4*, *KIR3DL1*, *KIR2DS4*) (Figure 5A) in the epithelial subset. Even though KIRs were elevated on messenger RNA level, no difference for the inhibitory KIRs was observed on protein level, and intraepithelial CD8⁺ T cell KIR expression was low overall (average KIR3DL1 expression of 3.8% in the epithelium). Elevated expression of CD63 was observed in intraepithelial compared with lamina propria CD8⁺CD69⁺CD103⁺ T cells on protein level (Figure 5F), indicative of secretory vesicles containing cytotoxic proteins. Furthermore, CXCR3 was highly expressed on epithelial CD8⁺CD69⁺CD103⁺ T cells (Figure 5G) supporting immunoregulatory interactions with nonlymphoid cells (Figure 5C, left panel), as its ligands are expressed by epithelial cells.²⁶ In addition, the immune checkpoints TIM-3 (*HAVCR2*) and TIGIT were more highly expressed by epithelial CD8⁺CD69⁺CD103⁺ T cells (Figure 5H). In summary, CD8⁺CD69⁺CD103⁺ T cells in the lamina propria show a more classical Trm cell profile and cytokine signaling, whereas in the epithelium a tightly regulated innate-like cytotoxic profile is more pronounced.

Different profiles in healthy control subjects and CD patients

Besides compartmental differences, an inflammatory milieu can influence the transcriptomic and functional profile of tissue T cells. Transcriptional differences between CD103⁺ and CD103⁻ CD8⁺ Trm cells in the lamina propria induced by inflammation were minimal. Only *OASL* and *CCL4* were more highly expressed in CD103⁻ compared with CD103⁺ CD8⁺ Trm cells in inflamed ileum of CD patients. Differences between transcriptional profiles of CD8⁺CD69⁺CD103⁺ T cells between healthy control subjects and active CD patients were mainly found in the epithelium (disease-specific genes: 185 genes in the CD epithelium, 94 genes in the CD lamina propria, and 14 and 42 genes for healthy control subjects, respectively) (Figure 6A; Supplementary Table 1). CD-specific genes included the innate proinflammatory *IER2* and *MIF* for intraepithelial CD8⁺CD69⁺CD103⁺ T cells, and in the lamina propria, *BATF* and *LGALS3*, (encoding Galectin-3), both previously associated as drivers of IBD inflammation (Figure 6B).^{27,28} On the pathway level, there was enrichment of gluconeogenesis in CD patients, whereas in healthy control subjects retinoid (vitamin A) metabolism was enriched in intraepithelial CD8⁺CD69⁺CD103⁺ T cells (Figure 4C). Together this indicates that inflammation in CD patients primarily affects the profile of CD8⁺CD69⁺CD103⁺ T cells in the epithelium.

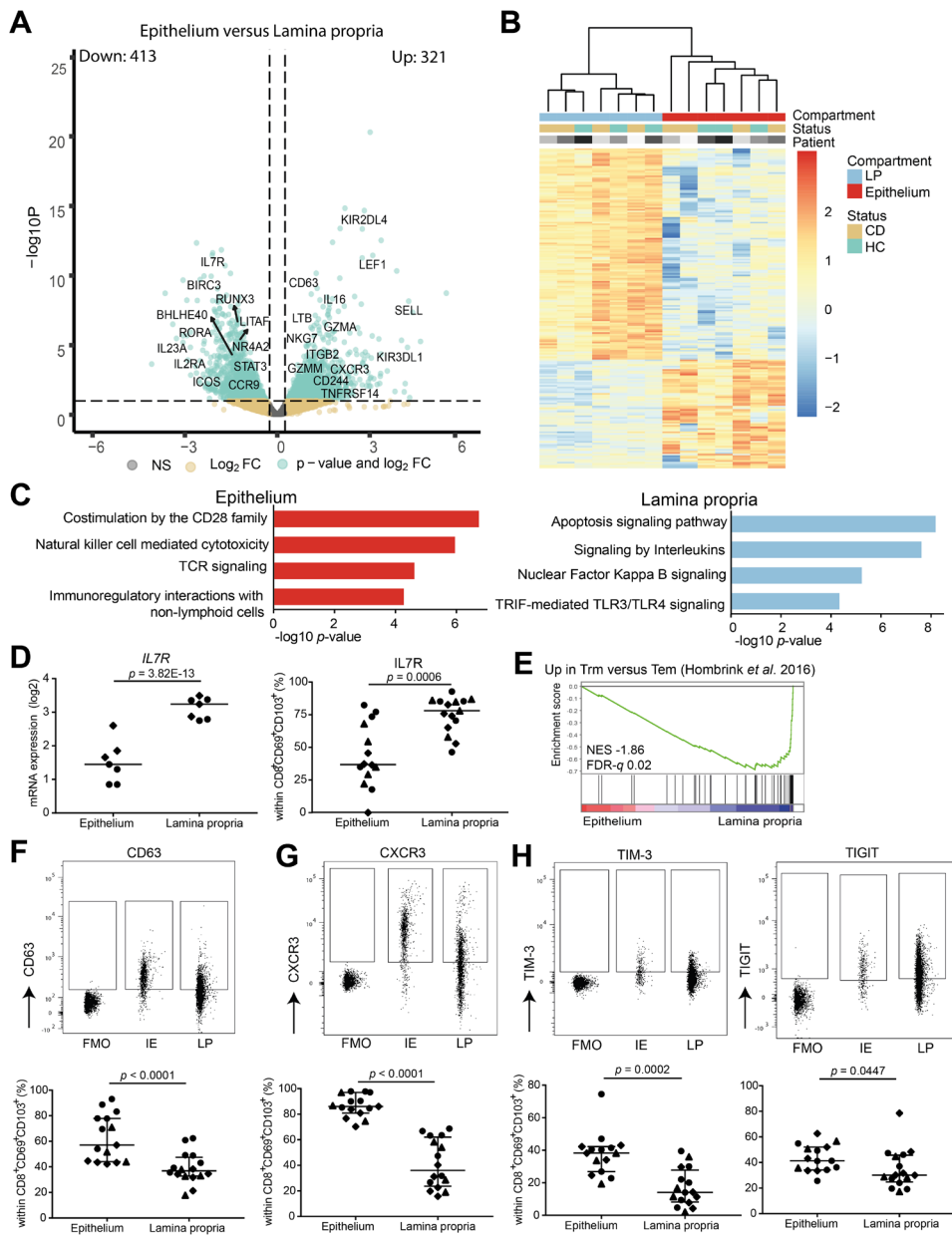


Figure 5. Location shapes the profile of intestinal CD103⁺ CD69⁺ CD8⁺ T cells. (A) Volcano plot of the expressed genes, with a nominal P value < 0.99 , comparing intraepithelial to lamina propria CD8⁺CD69⁺CD103⁺ T cells; selected genes are highlighted. On the x-axis the log₂ fold change (log₂FC) is shown, and on the y-axis the $-\log_{10}$ P value ($-\log_{10}P$) is shown. Grey indicates not significantly differentially expressed genes, yellow indicates genes with a log₂FC > 0.25 and $-\log_{10}P > 10 \times 10^{-2.5}$, green indicates genes with a log₂FC > 0.25 and $-\log_{10}P < 10 \times 10^{-2.5}$. (B) Heatmap of the top 200 differentially expressed genes comparing CD103⁺ intraepithelial and lamina propria

T cells with hierarchical clustering on the columns concerning compartment, status and patient. Rows are z score normalized. (C) Pathway terms related to the 321 genes upregulated in intraepithelial (top) and 413 genes upregulated in lamina propria (bottom) CD8⁺CD69⁺CD103⁺ T cells. (D) Messenger RNA (mRNA) expression (log2 counts; right) and percentage (left) of ileal CD8⁺CD69⁺CD103⁺ T cells expressing IL7R (CD127) in healthy control subjects (n = 3-5; diamonds) and CD patients from inflamed (circles) and noninflamed (triangles) ileum (paired, n = 4-5). Comparison was performed with Wald's statistic and a paired 2-tailed *t* test, respectively. (E) Gene set enrichment analysis of Trm genes in humans (identified by Hombrink et al²⁵) in pairwise comparisons involving intraepithelial and lamina propria CD8⁺CD69⁺CD103⁺ T cells derived from the ileum of healthy adult control subjects and CD patients pooled, represented by the normalized enrichment score and FDR statistical value (FDRq). (F) Representative gating strategy including Fluorescence Minus One (FMO) control (upper panel) and quantification (lower panel) of CD63 in CD8⁺CD69⁺CD103⁺ T cells comparing epithelium (IE) and lamina propria (LP). Bars represent median and interquartile range. Comparison was performed with a paired 1-tailed *t* test. Symbols as per panel D. Healthy control subjects: n = 7, CD patients: n = 3-6. (G) As per panel F but for CXCR3. (H) As per panel F but for TIM-3 (left) and TIGIT (right). Comparison was performed with a paired 2-tailed *t* test.

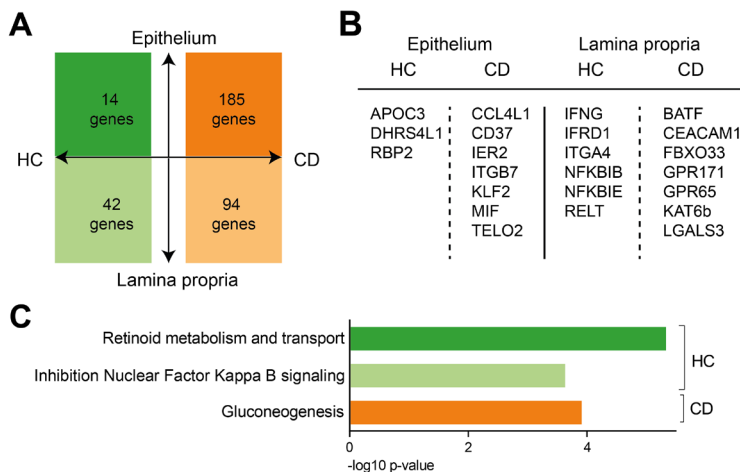


Figure 6. During inflammation, most upregulated genes are found in CD8⁺ Trm from the epithelium. (A) Diagram showing the differentially expressed genes that are specific, ie not differentially expressed in the other disease state, for healthy control (HC) subjects (left) or CD patients (right). The upper part depicts the number of genes that are upregulated and the lower part those that are downregulated in intraepithelial compared with lamina propria CD8⁺CD69⁺CD103⁺ T cells from the ileum. (B) Selection of top genes up- and downregulated as per panel A. (C) Pathway terms related to the genes specific for CD8⁺ T cells from HC subjects or CD patients for both lamina propria and epithelium derived from panel A (colors reflect the colors of panel A).

DISCUSSION

In the present study, we demonstrate that intestinal CD8⁺ Trm cell transcription profiles depend on their mucosal localization. Lamina propria located CD8⁺CD103⁺ T cells have a classical Trm cell profile with active pathways for regulating longevity and cytokine signaling, while intraepithelial CD8⁺CD103⁺ T cells actively sense the external environment as part of the mucosal barrier and display enrichment in natural killer receptors and innate-like markers in line with previous studies in both mice and humans.^{29,30} The changes seen during active inflammation are more pronounced in the intraepithelial CD8⁺CD103⁺ T cell subset, leading to

an innate proinflammatory profile with a concurrent loss of homeostatic functions such as vitamin metabolism. These data support recent observations in ulcerative colitis in which disease-susceptibility loci were mostly enriched in intraepithelial CD8⁺ T cells, especially during active inflammation.⁸ Furthermore, the differences observed between epithelial and lamina propria CD8⁺CD103⁺ Trm cells suggest that potential infiltrating cells from the lamina propria in the epithelial layer also acquire a proinflammatory innate profile. The microenvironment thus has an important role in skewing a cell's phenotype.

We also describe transcriptomic and protein differences between CD103⁻ and CD103⁺ CD8⁺ Trm cells in the lamina propria, which we corroborate and expand upon previous findings in the human intestine.^{9,15,16} The CD8⁺CD103⁻ Trm cell subset in the lamina propria was defined by high *Itgb2* expression further characterized by PD-1, GzmK, KLRG1 and EOMES. A recent study of donor-derived Trm cells after intestinal transplantation also described 2 transcriptionally different CD8⁺ Trm cell subsets, where the CD8⁺CD69⁺CD103⁻ subset characterized by coexpression of *ITGB2* displayed a more cytotoxic profile compared with the CD8⁺CD69⁺CD103⁺ subset.¹⁶ Similar findings were recently reported in a study of ileum samples obtained after ileocecal resection in CD patients demonstrating a statistically significant increase in percentages of CD8⁺CD103⁻KLRG1⁺ Trm cells in inflamed compared with noninflamed ileum and healthy control subjects, with no difference for the CD8⁺CD103⁺ subset.¹⁵ The CD8⁺CD103⁻KLRG1⁺ expressed higher levels of GZMB, whereas CD8⁺CD103⁺ Trm cells expressed higher levels of IL-22, IL-26 and CCL20.¹⁵

Our data show a decrease in CD8⁺ T cells per μm^2 in both the epithelium and lamina propria in inflamed ileum of CD patients compared with paired noninflamed ileum and the ileum of healthy control subjects. Additionally, within CD8⁺CD69⁺ T cells a decrease in CD103⁺ Trm cells and a relative increase of CD103⁻*Itgb2*^{high}KLRG1⁺GzmK⁺ Trm cells was observed in inflamed ileum of CD patients. Recently, Tkachev et al³¹ observed that pathogenic cells in graft-vs-host disease in a simian transplantation model comprise rapidly developed CD8⁺CD69⁺ Trm cells, which were CD103⁻ but expressed *ITGB2*, *CCL4L1*, *CD74* and *CCL3* among others. Another study recently linked appearance and accumulation of a GZMK⁺ CD8⁺ T cell population to an inflammatory phenotype in immune aging. This subset is characterized by both high PD-1 and TIGIT expression, is clonally expanded, and is regulated by EOMES and BATF.²² These data suggest that within the CD103⁻ CD8⁺ Trm cell population in the lamina propria, a CD69⁺CD103⁻*Itgb2*^{high}GzmK⁺KLRG1⁺ Trm cell subset with pathogenic potential is present.

In line with our study, single cell RNA-sequencing of colonic T cells showed presence of multiple CD8⁺ Trm cell clusters, of which a KLRG1⁺EOMES⁺ITGB2⁺ subset is enriched in ulcerative colitis, and the CD103⁺ population in healthy control subjects.³² TCR analysis showed overlap between all CD8⁺ Trm cell clusters except for between these distinct CD8⁺ Trm cell subsets.³² This was similar to findings for KLRG1⁺CD103⁻ and KLRG1⁻CD103⁺ CD8⁺ T cells in ileal transplant material.⁹ These distinct CD8⁺ Trm cell subsets thus seem to originate from different CD8⁺CD69⁺ T cells. CD103⁻ CD8⁺ Trm cells residing in the epithelium and the lamina

propria, however, had similar TCR repertoires,⁹ indicating that they are derived from the same pool.

Lamina propria and epithelial differences, described in the present study, could be partially due to adhesion of CD103 (integrin α E) to E-cadherin, which initiates intracellular signaling to advance effector functions.³³ The receptor E-cadherin is only expressed in the epithelium, so CD103 expression in the lamina propria could be redundant and therefore exert less influence on the function of the cell. Further fine-tuning of the functional profile is most likely induced by local cues.^{4,7} Whether, the severity of inflammation correlates with the magnitude of CD103⁺CD8⁺ T cell changes, both in number and in functional profile, is unknown.

Etolizumab (anti-integrin β 7) has been shown to be promising in phase II and III clinical trials in IBD.^{34,35} In vitro, etolizumab induces internalization of integrin β 7, impairing its adhesion to MADCAM-1, and blocking migration of immune cells to the gut, and has therefore a similar mode of action as the anti-integrin α 4 β 7 antibody vedolizumab.³⁶ Additionally, etolizumab affects the adhesion of integrin α E to E-cadherin resulting in decreasing intraepithelial CD103⁺ cell counts (without distinction for immune cell type)³⁴ and in a reduced accumulation of mainly CD8⁺ and T helper 9 cells.³⁷ Thus, primarily the CD8⁺CD103⁺ T_{RM} cell subset seems to be targeted by etolizumab. The question is whether this is desirable because CD4⁺CD69⁺CD103⁺ and not CD8⁺CD69⁺CD103⁺ T cells have been correlated with disease flares in IBD.¹¹

The fact that higher *ITGAE* (integrin α E/CD103) counts at baseline as reported in the phase II etolizumab trial were related to higher therapeutic response rates does not underline a pathogenic role of the CD8⁺CD103⁺ subset, as this was demonstrated in bulk data³⁴ and thus reflected a combination of dendritic cells, CD4⁺ and/or CD8⁺ T cells. Additionally, post hoc analysis of the latter study showed that patients with high *ITGAE* counts before treatment had milder disease activity with a lower endoscopic disease score at baseline.¹³ This corresponds with our observation that patients with milder disease, defined as a lower simple endoscopic score for CD of the ileum, had higher mucosal levels of CD8⁺CD103⁺ T cells.

Our findings demonstrate the heterogeneity and dual functionality of T_{RM} cell subsets in the intestinal mucosa. Long-term integrin β 7 blockade could have a negative impact on the presence, and thus homeostatic functions, of these CD8⁺CD103⁺ T cells, which clearly warrants further evaluation. For example, CD8⁺ CD103⁺ T cells might contribute to vitamin A metabolism which is essential in maintaining epithelial integrity.³⁸ The suggestion that CD8⁺CD103⁺ T cells in IBD patients in remission regain a regulatory profile¹⁴ should be further studied in a longitudinal cohort. Altogether, these differences indicate that therapeutic strategies could have a different impact on the same immune cells depending on the compartment of residence and presence of an inflammatory milieu, and should be taken into account when investigating short- and long-term effects of new gut T cell-targeting drugs. In conclusion, the transcriptional profile of CD8⁺ T_{RM} cells differs depending on the degree of inflammation and location within the gut.

METHODS

Patient inclusion

Patients with CD, most newly diagnosed, were prospectively enrolled at the outpatient clinic of the Rijnstate Crohn and Colitis Centre (Arnhem, the Netherlands). During ileocolonoscopy multiple biopsy specimens were taken for histopathological analysis, for immunophenotyping by flow cytometry analysis (n = 27), and for RNA-sequencing of sorted subsets and imaging mass cytometry (n = 4). Healthy control subjects (n = 10) underwent ileocolonoscopy for polyp surveillance or iron deficiency. They had normal macroscopical ileal mucosa, which was confirmed by histology (see Table 1 for patient characteristics).

Table 1. Baseline patient characteristics.

	Flow cytometric analysis		RNA-seq		CyTOF	
	CD Patients (n = 27)	HC Subjects (n = 7)	CD Patients (n = 4)	HC Subjects (n = 3)	CD Patients (n = 3)	HC Subjects (n = 2)
Gender						
Female	16 (76.2)	4 (57.1)	3 (75)	2 (66.7)	2 (66.7)	1 (50)
Male	5 (23.8)	3 (42.8)	1 (25)	1 (33.3)	1 (33.3)	1 (50)
Age, y	24 (20-32)	50 (46-60)	49 (30-54)	36	46	36
Smoking status						
Yes	11 (52.4)	0 (0)	2 (50)	2 (66.7)	2 (66.7)	2 (100)
No	7 (33.3)	7 (100)	0 (0)	1 (33.3)	0 (0)	0 (0)
Ceased	3 (14.3)	0 (0)	2 (50)	0 (0)	1 (33.3)	0 (0)
Duration of complaints before ileocolonoscopy, wk	14 (9-23)		4 (1-6)	NA	4	NA
Calprotectin, µg/g	231 (156-487)		120 (51-728)	NA	139	NA
CRP, mg/L	25 (11-62)		9 (4-19)	NA	4	NA
Treatment at ileocolonoscopy						
None	22 (81.4)	7 (100)	4 (100)	3 (100)	3 (100)	2 (100)
5-ASA	0 (0)	0 (0)	0 (0)	0 (0)	0 (0)	0 (0)
Steroids	0 (0)	0 (0)	0 (0)	0 (0)	0 (0)	0 (0)
Thiopurine	1 (4.5)	0 (0)	0 (0)	0 (0)	0 (0)	0 (0)
Mesalamine + thiopurine	0 (0)	0 (0)	0 (0)	0 (0)	0 (0)	0 (0)
Anti-TNF	3 (13.6)	0 (0)	0 (0)	0 (0)	0 (0)	0 (0)
Anti-IL12/23	1 (4.5)	0 (0)	0 (0)	0 (0)	0 (0)	0 (0)

HBI score		NA		NA		NA
<5, remission	2 (7.4)		1 (25)		0 (0)	
5-7 mild disease	12 (44.4)		2 (50)		2 (66.7)	
8-16 moderate disease	9 (33.3)		1 (25)		1 (33.3)	
>16 severe disease	4 (14.8)		0 (0)		0 (0)	
SES-CD score		NA		NA		NA
0-3 inactive disease	0 (0)		0 (0)		0 (0)	
3-7 mild disease	8 (29.6)		1 (25)		1 (33.3)	
7-16 moderate disease	12 (44.4)		2 (50)		1 (33.3)	
≥16 severe disease	7 (25.9)		1 (25)		3 (33.3)	
Montreal CD		NA		NA		NA
Location						
L1: ileal	10 (37)		3 (75)		2 (66.7)	
L2: colonic	0 (0)		0 (0)		0 (0)	
L3: ileocolonic	17 (73)		1 (25)		1 (33.3)	
Behaviour						
B1: nonstricturing, nonpenetrating	23 (85.2)		1 (25)		1 (33.3)	
B2: stricturing	3 (11.1)		3 (75)		2 (66.7)	
B3: penetrating	1 (3.7)		0 (0)		0 (0)	

Values expressed in n (%) or as median with interquartile range. CD, Crohn's disease; CRP, C-reactive protein; HBI, Harvey-Bradshaw index; HC, healthy control; RNA-seq, RNA-sequencing; SES-CD, simple endoscopic score for CD; TNF, tumor necrosis factor.

Mechanical cell isolation

Biopsies for analysis without separation of the lamina propria and epithelium were stored in a phosphate-buffered saline solution at 2-8°C, after which flow cytometric analysis was performed within 8 hours. We carried out mechanical preparation of single cell suspensions. Hereto, specimens were pooled and blended in Hank's Balanced Salt Solution (HBSS) (Gibco, Waltham, MA) supplemented with 1% bovine serum albumin (BSA) using a 70-mm gaze and spatula followed by Ficoll density gradient centrifugation. The homogenate was resuspended, after washing, in 0.5 mL HBSS/1% BSA.

Enzymatic cell isolation

Biopsies collected in HBSS media containing 2% fetal calf serum (FCS) and 0.2% amphotericin B. The intestinal tissue was transferred to HBSS supplemented with 1 mM DTT (Sigma-Aldrich, St Louis, MO) and placed on a rolling device for 10 minutes at 4°C. After discarding the supernatant, the intestinal tissue was transferred to HBSS supplemented with 2% FCS and 5 mM EDTA and shaken (2×) at 180 rpm for 30 minutes at 37°C. The tissue suspension was passed through a 70-µm cell strainer (Costar, Greiner Bio-One, Germany) and constituted the intraepithelial population. To obtain lamina propria T cells, intestinal biopsies were

subsequently incubated for 1 hour at 37°C with 1 mg/ml Collagenase IV (Sigma-Aldrich) in RPMI medium (supplemented with 10% FCS, 100 U/mL penicillin-streptomycin, and 0.2% amphotericin B), then forcefully resuspended through a 19G needle, washed and filtered with 70- μ m cell strainer (Costar). The cell suspensions were used for RNA-sequencing after sorting different T cell subsets.

Imaging mass cytometry

Intestinal biopsies were fixed in 10% neutral buffered formalin, paraffin-embedded, and 2 slides containing consecutive 4- μ m-thick sections of all samples were prepared. One slide was stained with hematoxylin and eosin for histological assessment and the second slide was stained for IMC. IMC combines immunohistochemistry with high-resolution laser ablation of stained tissue sections followed by CyTOF mass cytometry enabling imaging of multiple proteins at subcellular resolution.³⁹ All antibodies were conjugated to lanthanide metals (Fluidigm, San Francisco, CA) using the MaxPar antibody labeling kit and protocol (Fluidigm), and eluted in antibody stabilization buffer (Candor Bioscience, Wangen, Germany) for storage.

The slide was baked for 1.5 hours at 60°C, deparaffinized with fresh xylene for 20 minutes, and subsequently rehydrated in descending grades of ethanol (100% [10 minutes], 95%, 80%, 70% [5 minutes each]). After washing for 5 minutes in Milli-Q and 10 minutes in phosphate-buffered saline containing 0.1% Tween-20 (PBST), heat-induced epitope retrieval was conducted in Tris/EDTA (10 mM/1 mM, pH 9.5) for 30 minutes in a 95°C water bath. The slide was allowed to cool to 70°C before washing in PBST for 10 minutes. To decrease nonspecific antibody binding, tissue sections were blocked with 3% BSA and Human TruStain FcX (1:100, BioLegend, San Diego, CA) in PBST for 1 hour at room temperature. The antibody cocktail was prepared by mixing all antibodies at concentrations specific for the assay in PBST+0.5% BSA. After careful removal of the blocking buffer, the slide was incubated overnight at 4°C with the antibody cocktail. Antibodies used were E-cadherin 142Nd (metal tag) (clone 24E10, CST3195BF, Cell Signaling Technology, Danvers, MA), CD103 153Eu (clone EPR4166(2), ab221210, Abcam, Cambridge, United Kingdom), CD8 α 162Dy (clone C8/144B, 14-0085-82, Thermo Fisher Scientific, Waltham, MA). Following three 5-minute washes in PBST and rinsing in Milli-Q, the tissue was counterstained with 0.1% toluidine blue for 5 minutes to enable tissue structure visualization under bright field microscopy if desired. Upon washing for 5 minutes in Milli-Q, the slide was incubated with Ir-intercalator (1:500 in PBST, Fluidigm) for 60 minutes at room temperature. Finally, the slide was washed in Milli-Q and air dried for at least for 20 minutes at room temperature.

Images were acquired at a resolution of 1 μ m using a Hyperion Imaging System (Fluidigm). Regions of interest were selected based on the hematoxylin and eosin slides after which areas with an approximate size of 1000 \times 1000 μ m were ablated and acquired at 200 Hz. Pseudo-colored intensity maps were generated of each mass channel. Composite images were created and analyzed for each sample using ImageJ (version 1.47; National Institutes of Health, Bethesda, MD), and any changes to the brightness or contrast of a given marker were consistent across all samples.

Flow cytometry

For flow cytometric analysis, the intestinal cells were incubated with surface antibodies for 20 minutes at 4°C. Antibodies used were fixable viability dye eF506 (65-2860-40; eBioscience, San Diego, CA), anti-human CD3 APC-H7 (clone SK7, 560176; BD Biosciences), CD8α PerCP-Cy5.5 (clone SK1, 565310; BD Biosciences), CD8α BV650 (clone UCHT1, 563822; BD Biosciences), CD69 PE (clone L78, 555531; BD Biosciences), CD69 PE-Cy7 (clone FN50, 557745; BD Biosciences), CD103 PE (clone Ber-ACT8, 550260; BD Biosciences), CD103 FITC (clone Ber-ACT8, 550259; BD Biosciences), TIM-3 BV711 (clone 7D3, 565566; BD Biosciences), PD-1 BV711 (clone EH12.1, 564017; BD Biosciences), Itgb2/CD18 FITC (clone TS1/18, 302105; Biolegend), CD3 BV605 (clone UCHT1, 300460; Biolegend), KLRG1 PE-CF594 (clone 14C2A07, 368608; Biolegend), CXCR3 BV605 (clone G025H7, 353728; Biolegend), CD3 AF700 (clone UCHT1, 300424; Biolegend), CD63 FITC (clone H5C6, 353006; Biolegend), CD4 BV785 (clone OKT4, 317442; Biolegend), and TCRγδ BV510 (clone B1, 331220; Biolegend), and TIGIT PerCP-eF710 (clone MBSA43, 46-9500-42; eBioscience). For intracellular staining cells were fixed and permeabilized using eBioscience Fixation and Permeabilization buffers (Invitrogen, Waltham, MA) and stained with intracellular antibodies for 60 minutes at 4°C. Antibodies used were anti-human Ki-67 PE-Cy7 (clone B56, 561283; BD Biosciences), EOMES APC-eF780 (clone WD1928, 47-4877-42; eBioscience), KIR3DL1 BV421 (clone DX9, 312714; Biolegend), Granzyme K PerCP-Cy5.5 (clone GM26E7, 370514; Biolegend), and KIR2DL4 AF700 (clone 181703, FAB2238N-100UG; R&D Systems, Minneapolis, MN). Measurement was performed on a FACSCanto (BD Biosciences) or LSR Fortessa (BD Biosciences) (for gating strategy see Figure 7).

For sorting the intestinal cells were incubated with the surface antibodies for 20 minutes in supplemented RPMI (2% FCS, 1% penicillin and streptomycin, 0.2% amphotericin B) at 4°C, and subsequently washed in fluorescence activated cell sorting buffer before sorting on a FACSaria III (BD Biosciences) (for gating strategy see Figure 7). Antibodies used were fixable viability dye eF506 (65-2860-40; eBioscience), anti-human TCRγδ BV510 (clone B1, 331220; Biolegend), CD3 AF700 (clone UCHT1, 300424; Biolegend), CD4 BV785 (clone OKT4, 317442; Biolegend), CD8α APC-Cy7 (clone SK1, 557834; BD Biosciences), CD127 BV421 (clone HIL-7R-M21, 562436; BD Biosciences), CD25 PE-Cy7 (clone M-A251, 557741; BD Biosciences), CD69 PE (clone FN50, 555531; BD Biosciences), CD103 FITC (clone 2G5, 550259; Beckman Coulter). Flow data was analyzed using FlowJo v10 (TreeStar, Ashland, OR).

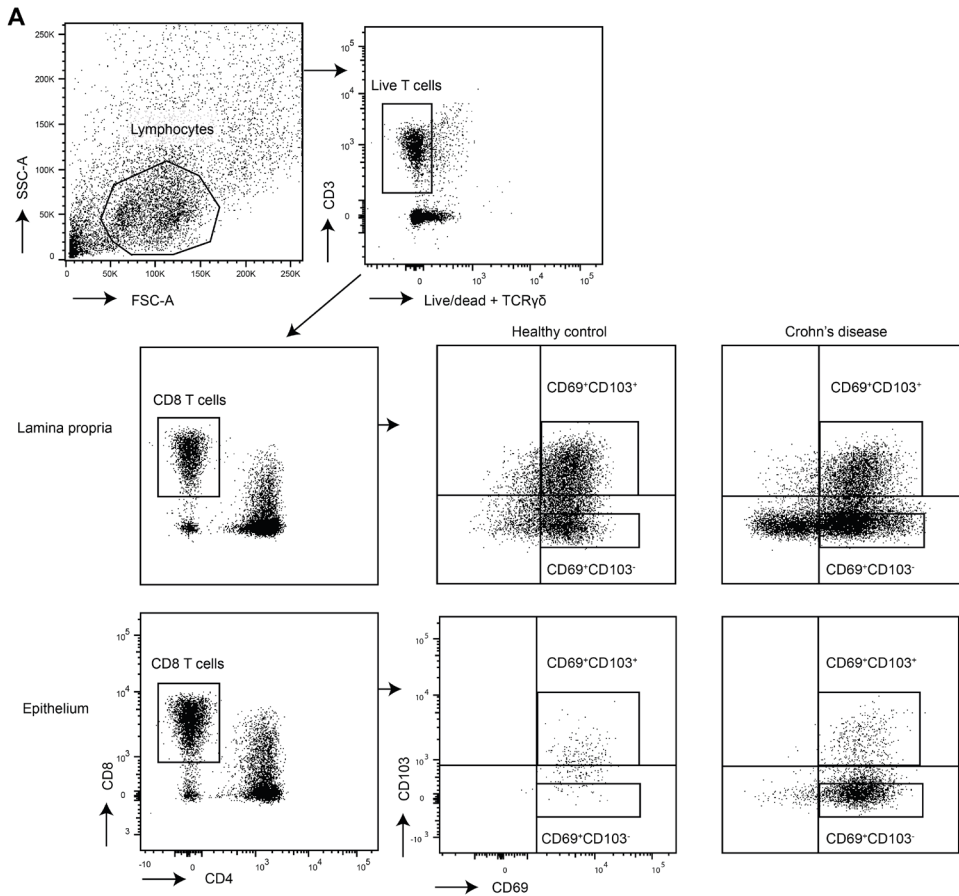


Figure 7. Gating strategy of intestinal CD103⁺ and CD103⁻ CD69⁺CD8⁺ T cells. Gating for fluorescence-activated cell sorting for RNA-sequencing (strict gates) and flow cytometry (quadrant gates).

RNA-sequencing

The sorted cells were thawed for TRIzol (Thermo Fisher Scientific) RNA extraction and stored at -80°C until library preparation. Sequencing libraries were prepared using the Cel-Seq2 Sample Preparation Protocol and sequenced as 75 bp paired-end on a NextSeq 500 (Utrecht Sequencing Facility). The reads were demultiplexed and aligned to the human complementary DNA reference genome (hg38) using BWA (version 0.7.13; <http://bio-bwa.sourceforge.net/>). Multiple reads mapping to the same gene with the same unique molecular identifier (6 bp long) were counted as a single read.

Raw counts of splice variants were summed and the raw counts were subsequently transformed employing variance stabilizing transformation. Ensembl names were converted to HGNC symbol, and if no symbol has been assigned the ensembl reference name was used. Differential analysis was performed using DESeq2 (Wald's test). For visualization purposes the R packages DESeq2, EnhancedVolcano and pheatmap were employed (R Foundation for Statistical Computing, Vienna, Austria). Raw counts were used as input for generating

volcanoplots with the genes colored based on P value and \log_2 fold-change cutoffs, with selected gene symbols shown for the genes with an FDR < 0.1. For heatmaps, transformed counts were z score normalized followed by hierarchical clustering based on samples and genes. Pathway analysis was performed on the differentially expressed genes as input in Topfun with standard settings. Gene set enrichment analysis, with as input the normalized data (output DESeq2), was used to assess enrichment of gene sets derived from the MSigDB C7 database (immunological signatures) and the Trm cell signature for human CD8⁺CD69⁺CD103⁺ T cells as defined by Hombrink et al²⁵. One thousand random permutations of the phenotypic subgroups was used to establish a null distribution of enrichment score against which a normalized enrichment score and FDR-corrected q values were calculated. RNA-sequencing data are available at GEO Accession GSE160925.

Statistical analyses

Flow cytometric data was analyzed with the independent 1-tailed or 2-tailed (paired) t test, or with a 1-way analysis of variance with post hoc Tukey's. For correlation analysis, Spearman's correlation was used. Data were analyzed with SPSS Statistics version 22.0.0.0 (IBM, Armonk, NY) and GraphPad Prism version 7.0 (GraphPad Software, San Diego, CA).

Ethics approval

The study protocol (NL28761.091.09 and TCBio 17/443, 17/444, 18/522) were approved by the research ethics committee of the Radboud University Nijmegen Medical Centre (CMO Regio Arnhem-Nijmegen, Nijmegen, the Netherlands) and the University Medical Center Utrecht, respectively. Written informed consent was obtained from each participating patient before any study-related procedure was performed. The procedures were performed in accordance with the Declaration of Helsinki.

All authors had access to the study data and reviewed and approved the final manuscript.

Acknowledgements

The authors thank Michal Mokry and Nico Lansu for providing RNA-sequencing services, Domenico Castigliego for help with intestinal tissue slide preparation and Yvonne Vercoulen en Mojtaba Amini for providing Imaging Mass Cytometry services.

REFERENCES

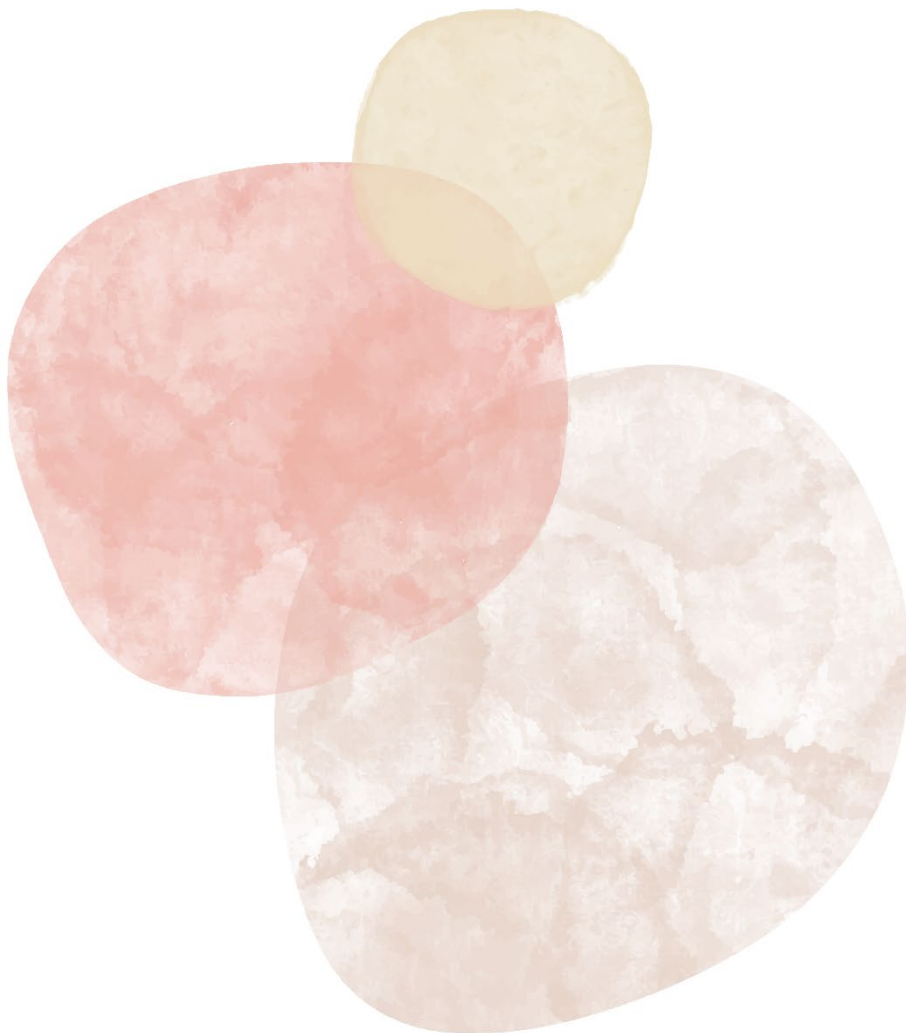
1. Zundler S, Becker E, Schulze L Lou, et al. Immune cell trafficking and retention in inflammatory bowel disease: mechanistic insights and therapeutic advances. *Gut* 2019;68:1688–1700.
2. Sandborn WJ, Vermeire S, Tyrrell H, et al. Etrolizumab for the Treatment of Ulcerative Colitis and Crohn's Disease: An Overview of the Phase 3 Clinical Program. *Adv Ther* 2020;37:3417–3431.
3. Habtezion A, Nguyen LP, Hadeiba H, et al. Leukocyte Trafficking to the Small Intestine and Colon. *Gastroenterology* 2016;150:340–354.
4. Lutter L, Hoytema van Konijnenburg DP, Brand EC, et al. The elusive case of human intraepithelial T cells in gut homeostasis and inflammation. *Nat Rev Gastroenterol Hepatol* 2018;15:637–649.
5. Cepek KL, Shaw SK, Parker CM, et al. Adhesion between epithelial cells and T lymphocytes mediated by E-cadherin and the alpha E beta 7 integrin. *Nature* 1994;372:190–193.
6. Cepek KL, Parker CM, Madara JL, et al. Integrin alpha E beta 7 mediates adhesion of T lymphocytes to epithelial cells. *J Immunol* 1993;150:3459–3470.
7. Kumar B V, Ma W, Miron M, et al. Human Tissue-Resident Memory T Cells Are Defined by Core Transcriptional and Functional Signatures in Lymphoid and Mucosal Sites. *Cell Rep* 2017;20:2921–2934.
8. Corridoni D, Antanaviciute A, Gupta T, et al. *Single-cell atlas of colonic CD8+ T cells in ulcerative colitis*. Springer US; 2020. Available at: <http://dx.doi.org/10.1038/s41591-020-1003-4>.
9. Bartolomé-Casado R, Landsverk OJB, Chauhan SK, et al. Resident memory CD8 T cells persist for years in human small intestine. *J Exp Med* 2019;216:2412–2426. Available at: <https://doi.org/10.1084/jem.20190414>.
10. Mackay LK, Rahimpour A, Ma JZ, et al. The developmental pathway for CD103+CD8+ tissue-resident memory T cells of skin. *Nat Immunol* 2013;14:1294–1301. Available at: <http://dx.doi.org/10.1038/ni.2744>.
11. Zundler S, Becker E, Spocinska M, et al. Hobit- and Blimp-1-driven CD4(+) tissue-resident memory T cells control chronic intestinal inflammation. *Nat Immunol* 2019;20:288–300.
12. Lamb CA, Mansfield JC, Tew GW, et al. alphaEbeta7 Integrin Identifies Subsets of Pro-Inflammatory Colonic CD4+ T Lymphocytes in Ulcerative Colitis. *J Crohns Colitis* 2017;11:610–620.
13. Tew GW, Hackney JA, Gibbons D, et al. Association Between Response to Etrolizumab and Expression of Integrin alphaE and Granzyme A in Colon Biopsies of Patients With Ulcerative Colitis. *Gastroenterology* 2016;150:477–87.e9.
14. Noble A, Durant L, Hoyles L, et al. Deficient Resident Memory T Cell and CD8 T Cell Response to Commensals in Inflammatory Bowel Disease. *J Crohn's Colitis* 2020;14:525–537.
15. Bottois H, Ngollo M, Hammoudi N, et al. KLRG1 and CD103 Expressions Define Distinct Intestinal Tissue-Resident Memory CD8 T Cell Subsets Modulated in Crohn's Disease. *Front Immunol* 2020;11:1–13.
16. FitzPatrick MEB, Provine NM, Garner LC, et al. Human intestinal tissue-resident memory T cells comprise transcriptionally and functionally distinct subsets. *Cell Rep* 2021;34:108661. Available at: <https://doi.org/10.1016/j.celrep.2020.108661>.
17. Ho J, Kurtz CC, Naganuma M, et al. A CD8+/CD103high T cell subset regulates TNF-mediated chronic murine ileitis. *J Immunol* 2008;180:2573–2580.
18. Smids C, Horjus Talabur Horje CS, Drylewicz J, et al. Intestinal T Cell Profiling in Inflammatory Bowel Disease: Linking T Cell Subsets to Disease Activity and Disease Course. *J Crohns Colitis* 2018;12:465–475.
19. Roosenboom B, Wahab PJ, Smids C, et al. Intestinal CD103+CD4+ and CD103+CD8+ T-Cell Subsets in the Gut of Inflammatory Bowel Disease Patients at Diagnosis and During Follow-up. *Inflamm Bowel Dis* 2019;25:1497–1509.
20. Schoettler N, Hrusch CL, Blaine KM, et al. Transcriptional programming and T cell receptor repertoires distinguish human lung and lymph node memory T cells. *Commun Biol* 2019;2:411.
21. Petrelli A, Mijnheer G, Hoytema van Konijnenburg DP, et al. PD-1+CD8+ T cells are clonally expanding effectors in human chronic inflammation. *J Clin Invest* 2018;128:4669–4681.
22. Mogilenko DA, Shpynov O, Andhey PS, et al. Comprehensive Profiling of an Aging Immune System Reveals Clonal GZMK+ CD8+ T Cells as Conserved Hallmark of Inflammaging. *Immunity* 2021;54:99–115.e12. Available at: <https://doi.org/10.1016/j.immuni.2020.11.005>.
23. Carrette F, Surh CD. IL-7 signaling and CD127 receptor regulation in the control of T cell homeostasis.

- Semin Immunol 2012;24:209–217.
24. Kaech S, Tan JT, Wherry EJ, et al. Selective expression of the IL-7R identifies effector CD8 T cells that give rise to long-lived memory cells. *Nat Immunol* 2003;4:1191–1198.
 25. Hombrink P, Helbig C, Backer RA, et al. Programs for the persistence, vigilance and control of human CD8+ lung-resident memory T cells. *Nat Immunol* 2016;17:1467–1478.
 26. Kulkarni N, Pathak M, Lal G. Role of chemokine receptors and intestinal epithelial cells in the mucosal inflammation and tolerance. *J Leukoc Biol* 2017;101:377–394.
 27. Hildner K, Punkenburg E, Abendroth B, et al. Immunopathogenesis of IBD: Batf as a Key Driver of Disease Activity. *Dig Dis* 2016;34 Suppl 1:40–47.
 28. Simovic Markovic B, Nikolic A, Gazdic M, et al. Galectin-3 Plays an Important Pro-inflammatory Role in the Induction Phase of Acute Colitis by Promoting Activation of NLRP3 Inflammasome and Production of IL-1 β in Macrophages. *J Crohn's Colitis* 2016;10:593–606.
 29. Cheroutre H, Lambolez F, Mucida D. The light and dark sides of intestinal intraepithelial lymphocytes. *Nat Rev Immunol* 2011;11:445–456. Available at: <http://www.nature.com/doi/10.1038/nri3007>.
 30. Vandereyken M, James OJ, Swamy M. Mechanisms of activation of innate-like intraepithelial T lymphocytes. *Mucosal Immunol* 2020;13:721–731. Available at: <https://doi.org/10.1038/s41385-020-0294-6>.
 31. Tkachev V, Kaminski J, Lake Potter E, et al. Spatiotemporal single-cell profiling reveals that invasive and tissue-resident memory donor CD8+ T cells drive gastrointestinal acute graft-versus-host disease. *Sci Transl Med* 2021;13.
 32. Boland BS, He Z, Tsai MS, et al. Heterogeneity and clonal relationships of adaptive immune cells in ulcerative colitis revealed by single-cell analyses. *Sci Immunol* 2020;5.
 33. Corgnac S, Boutet M, Kfoury M, et al. The Emerging Role of CD8(+) Tissue Resident Memory T (T(RM)) Cells in Antitumor Immunity: A Unique Functional Contribution of the CD103 Integrin. *Front Immunol* 2018;9:1904.
 34. Vermeire S, O'Byrne S, Keir M, et al. Etrolizumab as induction therapy for ulcerative colitis: a randomised, controlled, phase 2 trial. *Lancet* 2014;384:309–318.
 35. William S, Julian P, Jennifer J, et al. Etrolizumab as Induction Therapy in Moderate to Severe Crohn's Disease: Results From BERGAMOT Cohort 1: P-011. *Off J Am Coll Gastroenterol | ACG* 2018;113. Available at: https://gut.bmj.com/content/67/Suppl_1/A53.1.
 36. Lichnog C, Klabunde S, Becker E, et al. Cellular Mechanisms of Etrolizumab Treatment in Inflammatory Bowel Disease. *Front Pharmacol* 2019;10:39.
 37. Zundler S, Schillinger D, Fischer A, et al. Blockade of alphaEbeta7 integrin suppresses accumulation of CD8+ and Th9 lymphocytes from patients with IBD in the inflamed gut in vivo. *Gut* 2017;66:1936–1948.
 38. Huang Z, Liu Y, Qi G, et al. Role of Vitamin A in the Immune System. *J Clin Med* 2018;7:258.
 39. Giesen C, Wang HAO, Schapiro D, et al. Highly multiplexed imaging of tumor tissues with subcellular resolution by mass cytometry. *Nat Methods* 2014;11:417–422. Available at: <https://doi.org/10.1038/nmeth.2869>.

Extended Supplementary Data can be found at: <https://github.com/lutterl/PhD-thesis-supplementary-data>.

Chapter 8

General discussion



DISCUSSION

This thesis started with describing homeostasis; the ability of our body to maintain a stable internal environment within narrow ranges while adjusting to the changing environment.^{1,2} The immune system is important in the maintenance of homeostasis by continually surveying and responding to challenges with a self-limiting inflammatory response. In this thesis we have further explored the programming and adaptation of T(reg)-cells in humans at tissue sites in both homeostatic and chronic inflammatory conditions, where the inflammatory response is not self-limiting anymore.

The work presented in this thesis focused on how T cells adapt to local microenvironments via programming on the epigenetic, transcriptional and protein level. The primary T cell subsets of focus were regulatory T cells (FOXP3⁺, Tregs; **chapters 2-4 and 6**) and tissue-resident memory T cells (Trm cells; **chapters 6 and 7**). We have shown that adaptation is extensive and tightly regulated in a variety of microenvironments. Among microenvironments shared and site-specific adaptation is observed, and within an environment the transcriptomic profile is primarily driven by the compartment and not the T cell subset or inflammation. Here, the findings will be discussed in the context of recent literature. I will also discuss some of the remaining key questions and give a perspective on chronic tissue inflammation research in humans.

The microenvironment and tissue adaptation

The microenvironment is defined as the immediate small-scale environment consisting of a dynamic population of cellular and non-cellular components including stromal cells, immune cells, neurons, extracellular matrix, cytokines, chemokines and growth factors. These vary between microenvironments, and form a network that helps to maintain homeostasis. In addition to the multidirectional influence of all components in one microenvironment there is also communication with other sites throughout the body. An example hereof is the emerging field that explores the gut-brain axis. There is extensive crosstalk between the gut and brain regulating many homeostatic and non-homeostatic processes. For example, noradrenaline released from neurons can steer the local differentiation of macrophages and T cells.³ The locally residing cells have to adapt to the microenvironment, which is a dynamic process. Adaptation refers to the process of change by which an organism or species becomes better suited to its environment.

The role of the microenvironment

The tissue-specific microenvironment is crucial in shaping the local immune landscape. Moreover, if the immune cell response to a certain component is identical in every organ in our body we would have a problem. For example, sensing a bacterium belonging to the gut microbiota is concerning in the epithelium of the lungs but not in the gut. The microenvironment matters, and it is a key driver of the transcriptional and protein programming of T cells. In **chapter 2, 6 and 7** we showed that the microenvironment is of more influence on the phenotypic and transcriptional profile of a T cell than the surface-marker

based distinction commonly employed in research. This included the surface-marker based CD4⁺CD127⁻CD25⁺ effector cell, CD4⁺CD127⁻CD25⁺ Treg and CD8 T cell subsets. Tregs derived from the synovial fluid environment in patients with juvenile idiopathic arthritis (JIA) are more similar to CD4 non-Tregs in the same environment than they are to Tregs derived from the periphery (**chapter 2**). Even within the same organ there can be a distinct influence of the microenvironment on the programming of immune cells. The transcriptional profile-based clustering of CD4 Trm cells, Tregs and CD4CD8 α T cells on a PCA plot depends mainly on the compartment of residence. Residence in the lamina propria or the epithelium of the ileum defines the transcriptional profile more than the CD4 T cell subset (**chapter 6**). Similar observations were made for CD8 CD103⁺ and CD103⁻ Trm cells (**chapter 7**). Since these compartments are only separated by a 3-10 micron basement membrane it emphasizes the tight regulation of the microenvironment. Distinct adaptation depending on the microenvironment within one organ has also been described in literature. For example, Tregs in the uterus of pregnant women show a discrete profile in the incision (cesarian section) and placental bed sites.⁴

Tissue-specific factors shaping the local immune landscape include both intrinsic factors such as neurons, stromal cells and dendritic cells, but also extrinsic factors like the microbiome, environmental antigens and metabolites present. It was recently shown that structural cells including epithelial cells and fibroblasts have an imprinted tissue-specific adaptation with distinct capabilities for interacting with immune cells. This determines how these structural cells can interact with and skew immune cells.⁵ An example hereof was recently shown in gut-draining lymph nodes in mice. Those draining the proximal gastrointestinal tract had a tolerogenic environment reflected by the tolerogenic transcriptional program of resident stromal cells and migratory dendritic cells. Distal gut-draining lymph nodes formed a more proinflammatory environment. The same antigen presented in these distinct environments resulted in a tolerogenic T cell response in the first, and a proinflammatory T cell response in the latter.⁶ Environment-specific programming of immune cells is also related to the function of an environment itself while in homeostatic conditions. In the gastrointestinal tract there is exposure to food- and microbial-derived antigens that differ along the gastrointestinal tract and have to be tolerated.⁷ Moreover, the epithelium is directly exposed to the outside world whereas the lamina propria receives indirect input from both the inner body and the outside world. The placental bed is another completely different microenvironment which forms the maternal-fetal interface where maternal tolerance for the semi-allograft fetus has to be preserved.⁴ These examples illustrate the importance of the microenvironment when we aim to understand biological processes. However, even though, the microenvironment can induce a distinct phenotype in a cell, a shared core program can be identified as shown for Tregs in **chapter 2** and **4**. Next, I will discuss the adaptation and regulation of Tregs in the tissue microenvironment more in depth.

Tissue adaptation of Tregs

Tregs comprise a subset of CD4 T cells crucial in preserving immune homeostasis by antagonizing immune responses. Mutations in the Treg transcription factor (TF) FOXP3 lead to severe inflammation in both mice and humans.^{8,9} In recent years, potential therapeutic strategies targeting Tregs in both the autoimmune and tumor setting have been explored. In autoimmunity the number and/or functionality of Tregs should be enforced, whereas in the tumor milieu the suppressive capacity of Tregs should be dampened.^{10,11} We should understand local Treg programming, heterogeneity and function to define strategies that will work at the immune-challenged site. In **chapter 2-4** and **6** we have explored this programming and heterogeneity of Tregs in tissue sites. The key findings are summarized in **Figure 1**.

Most importantly, Tregs that migrate from the periphery to a tissue site undergo a set of adaptations. These core adaptations are shared among microenvironments with tissue-specific factors fine-tuning the transcriptional program. This process of adaptation and differentiation is imprinted on the epigenetic level (**chapter 2** and ref ¹²). Upon entrance of a tissue site, Tregs show increased expression of the core Treg profile, differentiate towards effector (e)Tregs and obtain environment-specific markers. In some tissues a dominant T helper (Th) cell skewing is present. For example, in the synovial fluid environment this is reflected by high presence of chemokines and cytokines associated with Th1 cells including IFN γ , TNF α , CXCL9 and CXCL10.¹³ In such a microenvironment Tregs can obtain a co-transcriptional program reflecting the dominant Th type. This does not coincide with gain of Th function or loss of Treg function. The core Treg signature and eTreg differentiation profile actually become more pronounced in non-homeostatic tissues such as an inflammatory or tumor microenvironment. Treg polarization has been observed in a variety of microenvironments. Both in inflammatory conditions as we observed in the synovial fluid (**chapter 2-3**), but also in homeostatic conditions such as in visceral adipose Tregs characterized by co-transcription of PPAR γ .¹⁴ This polarization allows for Treg survival and function in those microenvironments.¹⁵ Interestingly, the Tregs residing at the epithelial barrier of the ileum in patients with Crohn's disease gained an eTreg profile but did not express a specific co-transcriptional program (**chapter 6**). Crohn's disease is associated with a more dominant Th1/Th17 profile.¹⁶ However, most data has been derived from the bulk mucosa or lamina propria alone. The epithelium and lamina propria form two distinct compartments with the epithelium primarily seeded with CD8 and not CD4 T cells (**chapter 5-7**). It might therefore be that there is no specific Th-skewing in the epithelium, but only in the lamina propria. Indeed, most intraepithelial T cells have an innate-like cytotoxic 'activated-yet-resting' phenotype enabling rapid but tightly regulated responses to preserve barrier integrity (**chapter 5-7**). Moreover, it is unknown if a CD8 T cell dominant environment induces a specific co-transcriptional program in Tregs. To understand Treg adaptation in the epithelium of the gut this should be explored.

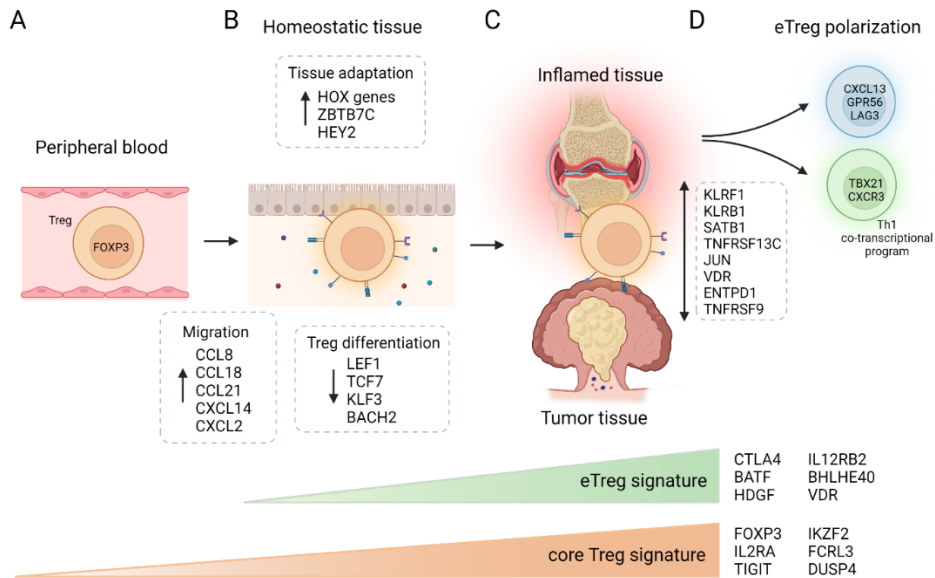


Figure 1. Overview of Treg tissue adaptation and programming. Shown are key changes and markers involved in the adaptation and differentiation of a Treg upon migration from the peripheral blood to tissue under homeostatic conditions and inflammatory/tumor conditions. (A) Tregs in the peripheral blood circulate throughout the body until the cognate antigen is encountered. They are characterized by a core Treg signature with FOXP3 as the primary transcription factor (TF). (B) Upon migration of Tregs from the periphery to a homeostatic tissue site several adaptations occur. Tregs upregulate a variety of chemokines and chemokine receptors that aid migration, attract other (immune) cells and promotes Treg differentiation. In addition, Tregs adapt to the tissue and effector (e)Treg differentiation is initiated for which several TFs such as LEF1 and TCF7 are downregulated, and effector markers including CTLA4 and BATF are upregulated (chapters 2 and 4). (C) Tregs in an inflammatory or tumor microenvironment show a further strengthening of the core Treg and eTreg signatures. Much of the Treg transcriptional program is shared between these environments, but some divergence in markers preferentially expressed in an inflammatory or tumor environment is present (chapters 2 and 4). (D) Tregs present in an inflammatory microenvironment can further polarize following separate differentiation trajectories. For example, in Th1-polarized environments co-expression of a core Treg and Th1 transcriptional program can be observed. These polarized eTregs maintain their Treg function reflected by an immunosuppressive capacity and they do not obtain functions related to the Th co-transcriptional program (chapters 2 and 3). Created with Biorender.com.

Treg programming by transcription factors

Adaptation to the microenvironment is regulated by a network of genes. The DNA in every cell has the code for about 20,000-40,000 protein-coding genes.¹⁷ Of these protein-coding genes an estimated 1600 genes code for TFs. TFs are the proteins that enable transcription of DNA to RNA, which can then be translated to protein; they regulate gene transcription. Depending on the cell type the same TF can regulate different genes, and depending on the cofactor the influence can be an inhibitory or activating role in gene transcription (reviewed in ref¹⁸). In a nutshell, changes in one TF will not tell us the whole story. This underscores the importance of elucidating the programs that define regulatory TF networks to help further understand the transcriptional programming of cells and within settings that orchestrate adaptation. In

chapter 2 we investigated which genes form the core transcriptional program of the eTreg program in the synovial fluid environment of patients with JIA. Key TFs downregulated in eTregs were *TCF7*, *LEF1*, *JUN* and *SPEN*, while upregulated key TFs included *ENO1*, *THRAP3* and *VDR*. This network of TFs regulating eTreg differentiation was also reflected in eTregs derived from patients with rheumatoid arthritis patients and the skin, breast and colorectal cancer (CRC) environment. BATF another TF that was highly upregulated in these eTregs and has previously been associated with the establishment of Tregs in tissue and their differentiation.^{12,19,20} We indeed also identified BATF as key regulator of Treg tissue adaptation and eTreg differentiation upon analysis of the shared transcriptional program of eTregs in a variety of tissues (**chapter 4**). That BATF was increased in synovial fluid-derived Tregs but not a predicted key regulator of eTreg differentiation in the synovial fluid environment is likely due to tissue-specific factors. The composition of the liquid synovial fluid is different than that of solid organs such as the skin and intestines resulting in a different network of cells receiving and providing signals.

BHLHE40 was one of the predicted TFs of eTreg differentiation and CXCL13⁺ polarized Tregs (**chapter 2-4**). BHLHE40 is also known as DEC1, Sharp2, Stra13 and Bhlhe2. Environmental stimuli such as hypoxia and growth factors as well as TCR stimulation regulate BHLHE40 expression. BHLHE40 controls the cell cycle, apoptosis and cytokine production.^{21,22} In CD4 effector T cells BHLHE40 induces proinflammatory GM-CSF and prevents anti-inflammatory IL-10 expression, which protects mice from experimental autoimmune encephalomyelitis.²² In contrast, old mice that do not express BHLHE40 develop lymphoproliferative disorders.^{23,24} BHLHE40 is not required for Treg lineage commitment but for the long-term maintenance of Tregs. BHLHE40 interacts with RUNX1 and together bind the locus for IL2RA. Expression of CD25 (encoded by IL2RA) is required for the long-term maintenance of Tregs.²⁴ Indeed, in **chapter 3** we showed that the TF network regulating the transcriptional program of CXCL13⁺ polarized Tregs included both BHLHE40 and RUNX1. This example demonstrates how one TF can have pleiotropic roles with the function depending on the cell subset and the TFs and other genes it interacts with.

Immune-cell mirroring and CXCL13 in chronic inflammation

In addition to tissue adaptation, another relevant observation is the shared expression of CXCL13 and inhibitory immune checkpoints, most notably PD-1 and LAG3, among T cell subsets (Tregs, CD4 and CD8 lineage) in diverse inflammatory microenvironments including synovial fluid and lung, colon and skin tumors (**chapter 2 and 3**).³⁴⁻⁴¹ Thus, part of the immune cells present in chronic inflammatory environments seem to mirror each other. Other genes commonly expressed by these cells include *CCL5*, *GPLY* and *HAVCR2* (**chapter 3** and refs ^{34,37,38}). These genes are often associated with terminally differentiated exhausted T cells. However, these cells retained their function and proliferative capacity (**chapter 3**), and there is no consensus yet on whether exhausted cells show a lack of effector function or a change in effector function.⁴² CXCL13⁺ Tregs were suppressive in the synovial fluid environment of patients with JIA (**chapter 3**), and CXCL13⁺ CD8 T cells were tumor-reactive in cancerous tissue

in melanoma patients.³⁴ Furthermore, these cells constitute a distinct subset with a separate developmental trajectory and clonal TCR-repertoire, and are only observed in effector sites. A small minority of peripheral-derived Tregs expressed CXCL13 on mRNA level (**chapter 4**) but not on the protein level (**chapter 3**). Concurrent with the expression of CXCL13 was the upregulation of several inhibitory immune checkpoints with foremost PD-1 and LAG3 (**chapter 2-4** and refs³⁴⁻⁴¹). Inhibitory immune checkpoints prevent aberrant responses of the immune system and avoid tissue damage. They are upregulated on T cells upon activation and regulate the immune response by limiting proliferation and cytokine production among others.⁴³ Expression of inhibitory immune checkpoints can result from prolonged antigen stimulation and has been associated with T cell exhaustion.^{44,45} However, the type of inhibitory immune checkpoint(s) expressed seems to be mostly dependent on the activation signal and the differentiation route of a cell. The expression of inhibitory immune checkpoints does not identify dysfunctional cells. Moreover, inhibitory immune checkpoint can also be observed in the absence of prolonged antigen stimulation.⁴⁶ It has been hypothesized that T cells that are highly activated express inhibitory immune checkpoints to also make them more susceptible for negative regulation.

The role of CXCL13⁺ T cells in chronic inflammation

CXCL13, is also known as B-cell attracting chemokine 1 (BCA-1) or B-lymphocyte chemoattractant (BLC). CXCL13 attracts cells expressing CXCR5, the only known receptor for CXCL13, enabling the formation and function of lymphoid structures. A multitude of cells express CXCL13 including stromal cells, B cells, fibroblasts and T follicular helper cells (Tfh cells, CD4 lineage). Lymphoid structures are present throughout the body; in secondary lymph nodes, in the tonsils, peyer's patches in the small intestine and colonic patches in the colon. Inflammatory conditions can lead to the formation of lymphoid aggregates which are less organized or organized ectopic (tertiary) lymphoid structures (ELS). Tfh cells in lymphoid structure drive B cell expansion and maturation. They are characterized by expression of BCL6, CXCR5, PD-1, MAF, ICOS and CXCL13. Studies have shown that Th1, Th2 and Th17 cells can differentiate into Tfh-like cells.⁴⁷ Tfh-like cells can also provide B cell help when they express Tfh cell characteristic markers such as CXCL13 and IL21.^{48,49} In addition, lymphoid structures harbor T follicular regulatory (Tfr) cells that can suppress the germinal center response by interacting with both Tfh and B cells. Tfr cells are also characterized by BCL6 and CXCR5 expression, but, whereas they maintain FOXP3 expression, CD25 is downregulated.⁵⁰ Less is known about follicular CD8 T cells that express BCL6, CXCR5, PD-1, ICOS and CD40L. These cells maintain cytotoxic capacity,⁵¹ and have been identified in lymphoid follicles both during homeostasis and inflammatory responses.⁵¹⁻⁵³

Interestingly, we and others have observed the presence of CXCL13⁺ T cells that do not express the key follicular TF BCL6, nor express CXCR5 or CCR7 required for lymphoid follicle entrance. These cells also express inhibitory receptors other than PD-1 such as LAG3 which not associated with follicular cells (**chapter 3**). One of these T cell subsets concern CD4 T cells expressing PD-1, IL21, CXCL13, MAF and ICOS. These T peripheral helper (Tph) cells are

not found in lymphoid tissue but are present in chronically inflamed environments. Nevertheless, both Tph cells can induce B cell differentiation.^{54,55} A recent study revealed the presence of CD4 T cells with this same phenotype in patients with celiac disease where they comprised 0.3-1.5% of the intestinal CD4 T cells. Most of the gluten tetramer-binding T cells in untreated celiac disease exhibit this phenotype, and this phenotype even becomes more prevalent upon a gluten challenge in patients who have been on a gluten-free diet.⁵⁶ In tumor tissue of patients with melanoma the present CXCL13⁺ CD8 T cells were tumor-reactive.³⁴ CXCL13⁺ Tregs in the synovial fluid of JIA patients bear a clonal repertoire (**chapter 3**) but their specificity is, as of yet, unknown. A link with B cell help was not made in either of these studies. Tregs that have lost FOXP3 expression and gained proinflammatory cytokine production potential (exTregs) are found in inflamed tissue environments.⁵⁷ Combined with a self-biased TCR repertoire enables Tregs to acquire a pathogenic phenotype. However, the CXCL13⁺ Tregs still expressed high levels of FOXP3 and had no cytokine producing capacity (**chapter 3**). Therefore, there are no indications these Tregs are at risk of becoming exTregs and thereby pathogenic. Even though this CXCL13-related phenotype seems to be expressed in a small percentage of cells, due to their potential beneficial and pathogenic roles exploring the TCR repertoire and shared TCR-sequence patterns to help decipher the cognate antigen is of interest.

Rheumatoid arthritis, JIA, celiac disease, Crohn's disease and tumors are associated with the formation of ELS. Development of ELS occurs in the context of chronic inflammation but the signals initiating ELS formation are unclear. In 20-40% of all people with a chronic inflammatory disease ELS development is observed.^{47,56,58} On the one hand, CXCL13⁺ Tregs might play a role in ELS formation via CXCL13 among others. On the other hand, the Treg phenotype we have observed could reflect the adaptation of Tfh/Tph co-transcriptional program enabling local survival and function of those Tregs. This would be in keeping with a co-transcriptional program being acquired in Th1- or Th2-polarized inflammatory settings or even in adipose tissue Tregs.¹⁵ Even though the TF BCL6 is not expressed by these Tregs, the Tfh cell-associated TF MAF is (**chapter 3**). In Th1-skewed inflammatory environments, the differentiation of a CD4 T cell towards a Th1 or Tfh fate occurs parallel, and fate seems to be determined based on the cytokines that steer downstream TF signaling with the T cell.^{59,60} Moreover, Th1 and Tfh cells seem to share a transitional stage in their differentiation, which is Tfh-like.⁶⁰ The detection of CXCL13⁺ Tregs, therefore, could also represent a transitional stage towards a Th1 dual program. The separate developmental trajectories as observed between CXCL13⁺ and Th1-polarized synovial fluid Tregs in **chapter 3** make this explanation less plausible. In summary, in chronic inflammation a percentage of T cells can bear a B cell helping phenotype without expressing typical follicular markers and inhibitory immune checkpoints. These cells are clonally expanded, and are functioning despite their seemingly exhausted phenotype for which both pathogenic and beneficial roles described. Several recent studies have suggested that these CXCL13⁺ T cells can serve as biomarkers for therapeutic responses⁶¹ or CXCL13-related targeting as therapy itself,⁶² which remains to be fully explored.

CXCL13 expression in Tregs

Expression of CXCL13 by FOXP3⁺ Tregs is counterintuitive since IL-2 limiting conditions promote CXCL13 expression,^{63,64} and Tregs rely on IL-2 for maintenance and proliferation.⁶⁵ However, IL-2 limiting conditions, similar to TGFβ rich conditions, are not driving CXCL13 expression but increase its expression. In CD4 effector T cells the absence of TGFβ rich and/or IL-2 limiting conditions, still resulted in about 10% of the cells expressing CXCL13. This was a less strong induction and only occurred when the TF SOX4 involved in CXCL13 expression was turned on.⁶⁴ TCR stimulation and presence of proinflammatory cytokines including type I interferons can also induce CXCL13 expression.⁶⁶ Remaining questions to be addressed include how CXCL13 expression is regulated specifically in FOXP3⁺ Tregs. TFs for which the binding sites are in the promotor of CXCL13 include POU2F1, PPARγ1, PPARγ2, IRF7A, RORA1 and HIF1A.^{67,68} Both RoRα and HIF1α are crucial TFs for Treg survival and functioning under inflammatory conditions. This was shown for RoRα in the skin during allergic reactions,⁶⁹ and for HIF1α in colitis models⁷⁰. These two therefore form credible options for regulating CXCL13 expression in Tregs in a chronic inflammatory environment. Whether this phenotype is a transitional stage towards a Th1-polarized transcriptional program or not, is steered by local antigens, and is related to acquiring a B cell helper function, remains to be established. Acquiring a B cell help function seems improbable since Tregs are known for their suppressive properties of immune cells including B cells, and Th1-polarized Tregs also do not gain Th1-functions.

Tissue-resident memory T cells

In the past 10-15 years, the study of Trm cells has been an emerging field. The first discovery of Trm cells in the early 2000's was in mice and focused on the CD8⁺ lineage.^{71,72} By now, tissue residency has also been shown for CD4 T cells although less is known about their programming and function. Trm cells are described as memory T cells that are non-recirculating but take up permanent residence in tissues. Additionally, due to their memory phenotype they can respond rapidly to a local challenge without the need for recruitment of peripheral T cells.⁷³⁻⁷⁵ Common surface markers to distinguish these cells from other memory T cells, i.e. T central memory (Tcm) and T effector memory (Tem) cells, are CD69⁺, CD103⁺ (integrin αE), CD62L⁻ and CCR7⁻ (see **chapter 1**).^{71,72,76-78} The transcriptional program of Trm cells further separates them from Tcm/Tem cells. The TFs driving this program are still being elucidated in humans, but include HOBIT, BLIMP1, NOTCH, AHR and RUNX3.^{75,79-82} Open questions regarding Trm cells are the extent of heterogeneity and plasticity present within the Trm cell compartment. Moreover, to what extent the functional profile of a Trm cell is dependent on the microenvironment, and thus changes depending on homeostatic or non-homeostatic tissue conditions, has to be addressed. This is crucial to explore if and when targeting Trm cells in disease is of interest. It also is unclear whether a Trm cell in humans can take up permanent residence in the tissue, or at some point will recirculate. We explored Trm cells in **chapters 6** and **7**. The key findings are summarized in **Figure 2**.

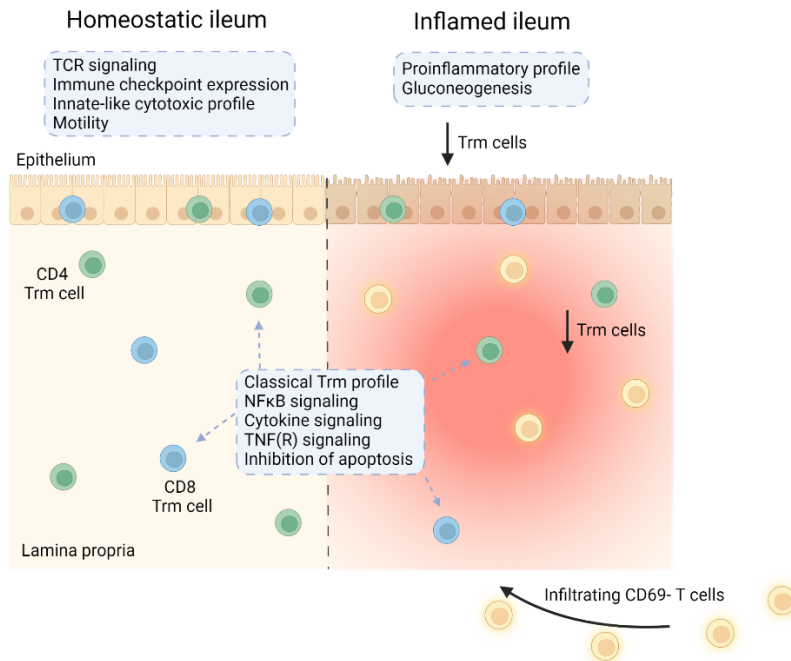


Figure 2. Tissue-resident memory T cells in the intestinal mucosa. The key processes and profiles regarding tissue-resident memory T (Trm) cell adaptation in both the epithelium and lamina propria of the intestinal mucosa are shown. This concerns Trm cell adaptation in the homeostatic mucosa, as well as the changes that occur upon the presence of inflammation. Shared processes and profiles between CD4 and CD8 Trm cells are shown. Inflammation in the lamina propria does not induce considerable differences in the transcriptional profile of Trm cells, whereas it does in the epithelium.

Definition of a Trm cell

In recent years, our knowledge on Trm cells has expanded. Studies in both mice and humans have suggested that Trm cells can recirculate.^{83–85} Upon recirculation, small intestinal CD8 Trm cells lose expression of CD69 and CD103, but retain epigenetic imprinting of their Trm cell profile. These cells regain their Trm cell markers upon relocalization.⁸³ A similar process has been observed in skin Trm cells in a murine model⁸⁴ and in humans.^{85,86} The potential to recirculate poses the question what those cells drive to recirculate. The migration of a naïve T cell from the periphery to a tissue site is initiated by antigen-driven stimulatory signals by an antigen-presenting cell in a lymph node. Thereupon, the naïve T cell can differentiate into an effector T cell and home to, and expand in the tissue site where action is required (the expansion phase). Subsequently, the vast majority of effector cells will go into apoptosis (the contraction phase) and some will become memory T cells (the memory phase).^{87,88} This process is characterized by downregulation of CCR7, CD62L and sphingosine 1-phosphate receptor 1 (S1PR1).^{71,72,76–78,89} This ensures retention of a Trm cell in the tissue. Subsequent upregulation of CD49a (integrin $\alpha 1$) or CD103 (integrin αE) further facilitates long-term persistence in tissues by binding collagen fibers or E-cadherin on epithelial cells,

respectively.^{90,91} The reversed route has been less well explored with unknown signals initiating tissue egress, although S1P1-linked egress is possible upon CD69 downregulation. CD69 upregulation occurs in response to inflammatory stimuli such as IFN α/β , TNF α and TCR activation.⁹²⁻⁹⁴ The mechanism of CD69 downregulation upon restimulation with the pathogenic stimulus resulting in tissue egress of Trm cells remains elusive.⁸³ Since recirculation also appears to occur in steady-state,⁸⁶ egress probably does not only occur upon re-recognition of the cognate antigen. In **chapter 6** we performed single cell RNA-sequencing of ileal CD4 T cells. Within the defined clusters we observed that CD4 T cells derived from the inflamed ileum showed a relative higher proportion of cells that were CD69^{low/intermediate} and not CD69^{high}. The clustering together indicates that these cells have a similar profile. An explanation is that these CD69^{low/intermediate} are, at least in part, recirculating Trm cells, that have reacquired the transcriptional program but not yet the Trm surface markers. They could also be differentiating from effector T cells towards a full Trm cell profile, which is a gradual process.⁹⁵ Another explanation could be that these cells are infiltrating T cells, however, there were no or minimal transcriptional differences observed between these CD69^{low/intermediate} and CD69^{high} CD4 T cells. It is well known that Trm cells (CD69⁺) differ from Tcm and Tem cells (CD69⁻) on the transcriptional level. However, these data were based on comparisons made between CD69⁻ Tcm/Tem cells populations derived from secondary lymphoid tissue (i.e. tissue-draining lymph nodes and spleen) and CD69⁺ Trm cells from barrier tissue sites (i.e. lung, gut and skin).^{79,96} These are distinct environments. Whereas secondary lymphoid organs are geared for immune activation and regulation, barrier tissue sites are where they function. This could have driven the observed differences in the transcriptional program, and highlights the need for intra-tissue comparison of CD69⁻ Tem/Tcm and CD69⁺ Trm subsets. Bulk RNA-sequencing did reveal differences between intestinal CD69⁻ and CD69⁺ CD4 T cells. Considering the single cell RNA-sequencing data this is driven by the portion of CD69⁻ cells that have recently migrated (CCR7⁺, **chapter 6**). Single cell DNA methylation studies could help distinguish the state and fate of these cells. This may help identify which cell subset, e.g. infiltrating or resident T cells, drives and/or reinforces reoccurring inflammation.

Moreover, within the CD69⁺CD103⁻ subset of the CD8 Trm cell population in the small intestine of patients with Crohn's disease we observed a cytotoxic phenotype. This phenotype has been associated with a pathogenic potential in both IBD and acute graft-versus-host disease, but was detected in the intestinal mucosa irrespective of the presence of inflammation (**chapter 7** and refs⁹⁷⁻¹⁰⁰). It seems improbable that their presence can be explained by prolonged exposure to inflammatory signals since these cells are found in the setting of both acute and chronic inflammation. Even though these cells expressed CD69 they also expressed KLRG1. KLRG1 expression, often concurrent with low CD127 (IL7R) expression (**chapter 7**), is associated with terminal differentiation of Tem cells and/or short-lived effector cells,¹⁰¹⁻¹⁰³ but not with Trm cells. This could indicate that these CD69⁺CD103⁻KLRG1⁺ cells are Trm cells that have lost their plasticity and are terminally differentiated. It can also indicate that these CD69⁺ CD8 T cells are not Trm cells. Together with the minimal transcriptional differences between CD69^{low} and CD69⁺ CD4 T cells within a cluster in patients with Crohn's

disease, this suggests that CD69 is not an infallible Trm cell marker, especially in the setting of chronic inflammation. These data illustrate the advances in the field, but also capture the continuum on which T cells seem to reside. Caution should be taken when translating findings from study to study.

Unconventional Trm cells

In barrier tissues such as the intestinal mucosa, TCR $\alpha\beta^+$ cells that express both CD4 and the homodimer CD8 $\alpha\alpha$ are found. Most knowledge on these cells is derived from mouse models where they are found to reside abundantly, and predominantly, in the epithelial layer of the intestines.^{104,105} CD4CD8 $\alpha\alpha$ T cells have been defined as cytotoxic CD4 T cells that lost expression of the TF ThPOK while gaining Runx3 expression which is a CD8 T cell-associated TF.¹⁰⁶ As shown in **chapter 6**, lamina propria-derived CD4CD8 $\alpha\alpha$ T cells in the human ileal lamina propria are transcriptionally identical to CD4 Trm cells except for expression of CD8A. TCR $\alpha\beta^+$ CD8 $\alpha\alpha$ (CD4 $^+$ and CD8 β^+) can also be found in the skin. Here, they were shown to be the largest resident T cell population arising after Herpes virus infection, with CD8 $\alpha\beta$ T cells mostly disappearing quickly post-infection. CD8 $\alpha\alpha$ T cells rapidly responded to reactivation of the Herpes virus resulting in subclinical reactivation and containment of tissue damage.¹⁰⁷ Co-expression of CD8 $\alpha\alpha$ can act as repressor of TCR-mediated cell activation, and could therefore be a self-regulating mechanism of CD4 T cells carrying a TCR with high antigen affinity. These cells might therefore play an important role in maintaining immunological tolerance (reviewed in **chapter 5**). Future studies comparing the TCR-repertoire of CD4 Trm cells and CD4CD8 $\alpha\alpha$ T cells can help to elucidate the role of these cells in the intestine. Intraepithelial CD4CD8 $\alpha\alpha$ T cells did differ from CD4 Trm cells in the human ileum. However, none of the differentially expressed genes included the TFs driving the core Trm cell program, except for AhR which was actually more highly expressed in CD4CD8 $\alpha\alpha$ T cells (**chapter 6**). These data underline that translation from mice to humans is not infallible. Whereas CD4CD8 $\alpha\alpha$ T cells in mice are considered cytotoxic CD4 T cells in the epithelial layer, in the human intestinal mucosa they seem to be CD4 Trm cells.

Dual role of Trm cells in disease

Recurrent inflammation at the same anatomical location in chronic inflammatory diseases such as psoriasis and IBD suggests a potential pathogenic role for Trm cells. Indeed, in psoriasis the presence of psoriasis-associated IL17A and IL22 cytokine-producing Trm cells in the well-demarcated lesional skin has been shown. Blockade of these cells can prevent development of psoriatic lesions in mice.^{108,109} Generation of protective Trm cells upon viral skin infection which seed throughout the skin and upon re-infection can counter the pathogen themselves have also been observed.^{73,110} Similarly, in **chapter 6** we observed a relative decrease of intraepithelial CD4 Trm cells and no significant changes in the transcriptomic profile of CD4 Trm cells in patients with active Crohn's disease (i.e. inflamed ileum). We did observe an extensive influx of incoming/infiltrating CD4 T cells. Furthermore, in **chapter 7** we detected a decrease in CD8CD013 $^+$ Trm cell number. Another study reported an increase in gut

CD103⁺ cells, without distinction for cell-type, in IBD patients, which was found to be correlated with disease activity.⁸¹ There seem to be potential functional differences for the same surface-marker based subset found in different environments. Intraepithelial but not lamina propria CD69⁺CD103⁺ CD8 Trm cells showed an innate proinflammatory profile during inflammation in patients with Crohn's disease (**chapter 7**). These data illustrate that a Trm cell can be both pathogenic and protective. These dual potential roles of Trm cells are probably due to heterogeneity within the Trm cell compartment, duration of disease and compartment of residence such as the epithelium versus the lamina propria of the intestinal tract. Furthermore, the type of inflammation; pathogen-induced or self-antigen-induced inflammation, progressive or relapsing-remitting inflammation, or even bystander cell activation might also be of importance as suggested by the skin Trm cell data.^{73,108-110} Several studies have shown heterogeneity within the Trm cell compartment such as quiescent versus cytokine-producing Trm cells⁹⁶, and polyfunctional versus granzyme-dominant Trm cells (**chapter 7** and refs^{99,111}). Future studies will have to further explore the heterogeneity within the Trm cell population, and assess potential protective and pathogenic Trm cell subsets in chronic inflammatory diseases.

In recent years our comprehension of T cell type, state and fate has increased considerably. It was recently shown that the classification of CD4 T cells in naïve, effector memory, central memory and terminally differentiated subsets by means of CD45RA, CD27, CCR7 and CD62L does not reflect the subsequent functional stages of these cells. Killer-like receptors and GPR56 better define this functional differentiation process.¹¹² These data are derived from peripheral blood T cells in homeostatic conditions and indicate that differentiation occurs in a continuum, with a lineage (often) not forming distinct subsets. Moreover, we and others have shown that the microenvironment is paramount for the transcriptomic and phenotypic profile of a cell (**chapters 2-7**). For example, the priming of T cells by dendritic cells and the level and duration of inflammation can steer a CD8 T cell towards a KLRG1⁺ or KLRG1⁻ phenotype.¹¹³ Timepoint of sampling is another factor of importance in the program detected in a cell. For example, Trm cells acquire their phenotype gradually.⁹⁵ Classification of cells has implications for our understanding of pathogenic mechanisms and therapeutic approaches. These data demonstrate that the classification of cells becomes more refined which will hopefully aid in the development of more precise targets in therapeutic strategies.

Treatment of chronic inflammatory diseases

The data presented in this thesis mostly explored the programming of T cells in a chronic inflammatory environment. Even though there was no specific focus on therapy, findings presented in this thesis might help guide the therapeutic management of chronic inflammation-related diseases. First, we have shown and discussed that Tregs can adapt to local inflammatory environments by attaining an additional transcriptional and protein program defined by the Th-polarized environment present (**chapters 2-4**). For example, in the more Th1/17-skewed environment of the synovial fluid of patients with JIA, Tregs adapt by obtaining CXCR3 expression similar to Th1 and Th17 cells (**chapter 2**). CXCR3-blocking

antibodies inhibited CXCR3-related migration in *in vitro* cell line experiments and *in vivo* mouse model studies, which was accompanied by a relative reduction of Th1, Th17 and Th22 cells. This resulted in increased Treg percentages, reduced proinflammatory cytokine expression and in reduced disease severity scores.^{114–116} What has to be addressed here is whether these strategies also affect the functioning of Tregs with a Th1 co-transcriptional program, which thus express CXCR3. Especially for the timeframe between initiation of therapy and resolution of inflammation where the environment might still be Th1-dominant, blocking CXCR3 on Tregs could interfere with their survival and immunosuppressive function in this phase.

Second, the data presented in **chapters 2-7** show that location matters. T cells adapt to the local environment and this adaptation can be very distinct even among closely related microenvironments (**chapter 6** and **7**, reviewed in **chapter 5**). This concerns both a distinct distribution of immune cells, as well as a distinct profile of the same cell subset in closely related compartments. For example, CD4 Trm cells in the epithelium compared to the lamina propria were enriched for pathways associated with TCR activation, T cell differentiation and mRNA processing (**chapter 6**). Disruption of compartmentalization is commonly observed in inflammation, and could impact resolution of the inflammatory response if cells normally residing in one compartment are found in another compartment without proper adaptation of their transcriptional and phenotypic program. This might result in aberrant immune activation and impede tissue repair. In recent years, the treatment of IBD has shifted from minimizing clinical symptoms to minimizing disease activity as early and completely as possible. Mucosal healing, defined as a normal macroscopic aspect of the mucosa during ileocolonoscopy, is one of the main treatment goals.¹¹⁷ Complete mucosal healing translates to a favorable prognosis in the long-term compared to partial mucosal healing.¹¹⁸ Recently, histological remission has also been included in the definition of mucosal healing. There are several available indexes to score histological remission which include cell density and cell type in the lamina propria and epithelium, crypt architecture irregularities and mucin depletion.¹¹⁹ Whether taking compartmentalization of the intestinal mucosa into consideration for the definition of histological healing improves the long-term outcome of patients with IBD remains to be addressed. Identifying one or a few T cell markers that define proper compartmentalization within the mucosal compartment that can also be assessed by histology might prove difficult. In both active Crohn's disease and ulcerative colitis the basement membrane is disrupted facilitating immune cell infiltration. The basement membrane seems to recover upon remission, although it is unclear if all constituents of the basement membrane normalize.^{120–122} It would, therefore, be of interest to assess if the integrity (quantity and continuity) of the basement membrane, separating the lamina propria and epithelium, can function as surrogate marker for intact mucosal compartmentalization. This only concerns mucosal localization and restoration. Patients with Crohn's disease can have a fistulizing or stenosing phenotype as well. Fistulizing Crohn's disease is characterized by epithelial to mesenchymal transition with penetration of epithelial cells into the mucosa.¹²³ Stenosing of the intestines in Crohn's disease is due to remodeling of the extracellular matrix and fibrosis formation, which can be observed in the submucosa and subserosa.¹²⁴ A step

further than mucosal healing would thus be transmural healing. Data regarding the importance of compartmentalization within the mucosa and the influence of immune cells on stenosing and fistulizing disease suggest that it would be worthwhile to explore transmural healing as treatment goal in Crohn's disease.

Third, CD8 Trm cells in the inflamed epithelium gain a proinflammatory profile (**chapter 7**). It therefore seems valuable to target these cells during active disease. For example with etrolizumab targeting integrin- $\beta 7$ which is highly expressed on intraepithelial lymphocytes. Integrin- $\beta 7$ is part of the integrin- $\alpha E\beta 7$ dimer of which the αE monomer binds E-cadherin on epithelial cells, enabling intraepithelial retention of these T cells (reviewed in **chapter 5**). The average lifespan of human memory T cells is estimated to be 164 and 157 days for CD4 and CD8 memory T cells, respectively.^{125,126} How this translates to human Trm cells is unknown, but if similar, this could mean a gradual decrease of intraepithelial integrin- $\beta 7^+$ Trm cells upon long-term treatment with anti-trafficking agents such as etrolizumab. On the one hand, long-term anti-trafficking therapy could reduce relapses by limiting immune cell influx, and establishment of potential pathogenic Trm cell clones. On the other hand, this could impair homeostatic functioning of the mucosal barrier including immunosurveillance in the epithelial layer and subsequently elicit an inflammatory response. Pathogenic Trm cell clones might even reside in peripheral sites after recirculation from the tissue. Return upon cessation of anti-trafficking therapy might result in a new flare of the disease if the cognate antigen is encountered. Moreover, patients with colonic IBD have an increased risk of developing colitis-associated dysplasia and CRC.^{127,128} CRC cells can express E-cadherin,¹²⁹ and the interaction of integrin- $\alpha E\beta 7^+$ CD8 tumor-infiltrating T cells and E-cadherin expressed on tumor cells allows for tumor lysis. Blocking this interaction greatly reduces T cell-mediated tumor lysis.¹³⁰ This is another potential long-term risk to be taken into account, which indicates that the therapeutic management should include the assessment of these risks per patient based on disease history, lifestyle and genetic factors among others. In addition, our data has indicated that the increase in infiltrating T cells constitutes a major change during inflammation in Crohn's disease (**chapter 5**). These data also support the targeting of immune cell trafficking to tissue sites, but without targeting beneficial resident cells. Examples of potential targets include GPR15 for T cells trafficking to the colon and CCR9 for the small intestine.^{7,131} Also preventing tissue trafficking are Sphingosine 1 phosphate (S1P) and MAdCAM-1 targeted therapies that are under investigation in clinical trials for IBD.¹³² If immune cell trafficking would be targeted early in the disease course this could potentially prevent the establishment of pathogenic T cell clones in tissue sites.

Fourth, targeting non-immune components of the mucosa in patients with IBD could provide an alternative approach that avoids the use of long-term immunosuppression with its related potential adverse effects. A pronounced inflammation at presentation hallmarks IBD, RA and other chronic inflammatory conditions. However, there are other factors contributing to the pathogenesis and relapsing-remitting inflammation as well. Fecal microbiota transplantation has been shown to benefit a subset of patients with ulcerative colitis. This results in a decrease in the proinflammatory phenotype of local immune cells, a decrease in

proinflammatory markers, and an increase in anti-inflammatory markers.¹³³ In Muntjewerff et al., 2021 (see list of publications) we explored the role of CST in the intestines of both mice and humans. CST-knockout mice experienced impaired gut permeability, a dysbiosis similar to IBD patients, decreased tight and adherens junction expression, and infiltration of immune cells in the lamina propria among others (**Figure 3**). This was all reversed upon suppletion with CST. Suppletion with CST can impact mucosal integrity with normalization of the local immune system as well. CST is an endogenous peptide and would therefore be an attractive therapeutic agent in the treatment of intestinal inflammation. CST has been tested in rats (not CST-knockout) incorporated in reperfusion therapy which can be employed to restore blood flow after acute myocardial infarction. Addition of CST showed a cardioprotective effect with a reduction of the infarct size and reduced oxidative stress in heart cells.^{134,135} This demonstrated that the suppletion with exogenous CST in an animal model not experiencing a genetic deficiency/absence of CST can be employed as a therapeutic approach.

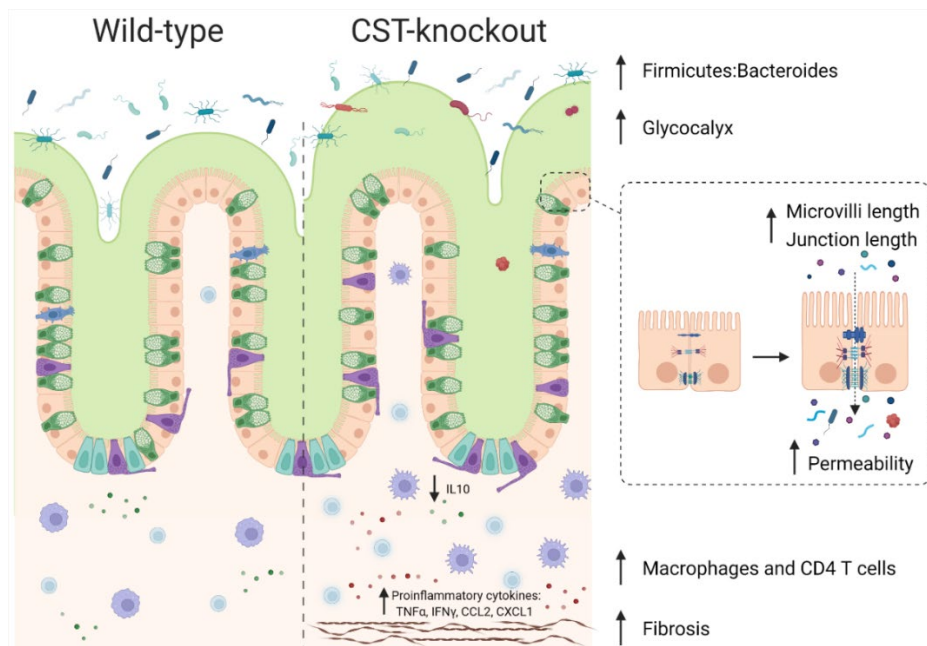


Figure 3. Intestinal morphology and function in catestatin-knockout mice. Comparison of the intestinal morphology and function of wild-type mice (left) with catestatin (CST)-knockout mice (right). In CST- knockout mice only the 63 nucleotides encoding CST have been deleted from the pro-hormone chromogranin A. Created with Biorender.com.

From mice to humans

Traditionally, most immunological studies have been performed in mouse models. It is known that mice models come short when translating findings to the human setting. There have been efforts to better recapitulate the situation and responses observed in humans in animal models. In the late nineties the first humanized mouse models were developed in which (part

of) the humane immune system is transferred.¹³⁶⁻¹³⁸ In addition, in recent years the use of wildlings which are descendants of C57Bl/6 mice born to wild mice have been used in animal studies. These mice have a more experienced immune phenotype with antigen-experienced T cells in tissues as also observed in humans.^{139,140} However, differences in the immune system, lifespan and antigen-exposure of mice and humans will remain present. An example that became apparent in **chapter 6** is the discrepancy between intestinal CD4CD8 $\alpha\alpha$ T cells in mice and humans. In mice these cells are predominantly found in the epithelium and in humans in the lamina propria. Moreover, in mice a lineage re-commitment from CD4 effector to CD4CD8 $\alpha\alpha$ T cells is regulated by loss of the CD4 TF ThPOK (ZBTB7B) and gain of the CD8-related TF RUNX3 resulting in cytotoxic CD4 T cells.¹⁰⁶ We did not observe a difference in ThPOK expression or gain of RUNX3 expression compared to CD4 effector T cells. The CD4CD8 $\alpha\alpha$ T cells in the lamina propria actually did not differ from CD4 effector T cells on transcriptional level except for *CD8A*. On the protein level these CD4CD8 $\alpha\alpha$ T cells could still diverge from CD4 effector T cells in the lamina propria, but these data do indicate a difference between mice and humans. Also in **chapter 2** we observed remarkable differences between mice and human eTregs. In mice KLRG1 is a key marker to identify eTregs, whereas in humans it is absent in eTregs in the synovial fluid environment. IL12RB2 was a key marker of eTregs in humans but not in mice. In mice the impaired expression of IL-12R β 2 actually prevented Tregs from fully differentiating towards Th1 cells.¹⁴¹ Potential differences due to the microenvironment could be of influence. However, in **chapter 4** we consistently observed absence of KLRG1 in eTregs, while IL12RB2 was as marker for eTregs irrespective of the tissue type and homeostatic, inflammatory or tumor tissue setting. It was previously also shown that Treg lineage-specific elements are not conserved between mice and humans.¹⁴² These data show that findings in mice cannot be directly or fully translated to the human settings. Animal studies do allow for a thorough exploration of concepts that cannot (yet) be studied in humans. The concepts that T cells can reside in tissues, and that Tregs adapt to tissue sites by gaining an effector profile are derived from mice models. In conclusion, mice models can contribute and even lead to breakthroughs in our understanding of homeostatic and pathological mechanisms in humans. However, to implement the gained conceptual knowledge from animal studies we also first need to fill the gap of knowledge that exists regarding human tissue immunology. The advances in new technologies such as in situ sequencing allow us to explore more questions in the human setting. Research in humans, however, does come with its own challenges.

Challenges in chronic tissue inflammation research in humans

Murine models often rely on a single inbred strain of similar age and sex, with little to no variation in their exposome and microbiome. In contrast, among humans there is considerable genetic variability, a plethora of environmental factors including diet and viruses as well as variation in age and sex resulting in more heterogeneous study populations. Here, I will discuss three challenges in human immunology research, also with respect to the chapters presented in this thesis.

Sex

In most published studies, the majority of included control subjects and patients are male.^{143,144} Several studies indicate that the immune responses and disease susceptibility differs between males and females.¹⁴⁵ In general, autoimmune diseases affect females more often than males with 8 out of 10 people diagnosed with an autoimmune disease being female.^{143,146-150} This has been reported both in JIA with a female to male ratio of 3-6.6:1,¹⁴⁶ and in Crohn's disease with a ratio of 1.1-1.8.8:1.¹⁴⁸ Disease presentation also differs with males suffering more often from a more severe disease course^{143,146,150} and males with Crohn's disease having an overall higher prevalence of extra-intestinal manifestations.^{149,150} This can partly be ascribed to hormonal differences between females and males. The sex steroids estrogen, testosterone and progesterone have direct and indirect immunomodulatory effects.^{143,151,152} For example, data indicate that females show a more profound T cell activation post-vaccination,¹⁵³ and females with rheumatoid arthritis (but also other autoimmune diseases) who are pregnant often experience less disease activity under the high estrogen and progesterone levels present in the 3rd trimester.¹⁴³ However, even in children before the onset of puberty a sex-related bias is detected.¹⁴⁶ This indicates that non-hormonal factors related to the sex chromosomal composition (X/Y) might be involved as well. The X-chromosome contains the transcription sites of a diverse set of genes related to the immune system including FOXP3.^{151,152} The X-chromosome is also linked to some genetic susceptibility loci for Crohn's disease such as the toll-like receptor 8 (TLR8).¹⁵² It also harbors about 10% of the known microRNA's (miRNA) in humans¹⁵⁴ which can modulate gene expression in immune cells.^{154,155}

In this thesis we did not select our patients or control subjects based on sex or gender, nor did we disaggregate the data by sex or gender since we did not have sufficient participant numbers to stratify by sex. Moreover, in **chapter 2, 3, 6** and **7** we actually regressed out the influence of patient variability in the transcriptomic data, and therefore also potential sex-related differences. In Muntjewerff et al., 2021 we were able to determine the absence of a potential correlation between the peptides CgA and CST and the sex of the included subjects. We did, however, use a simple linear regression instead of a multivariate analysis. In a simple linear regression we cannot account for the influence of sex while accounting for the influence of other confounding factors such as age. The variation induced by sex differences is approximately 2-3% for the global immune cell composition in the blood.¹⁵⁶ How this translates to tissue sites is unknown, but the expression of an estimated 3000 genes are sex-biased in tissues.¹⁵⁷ Furthermore, sex steroids can influence intestinal microbiome composition and diversity in mice.^{158,159} We know that there is extensive interaction between the microbiome and the gut immune system, most notably in IBD (reviewed in **chapter 5**).^{160,161} In healthy individuals, gut lamina propria-resident CD4 T cells showed increased activation and turnover with a more Th17-skewed profile, and an increased presence of FOXP3⁺ Tregs in females compared to males. Upregulated genes and pathways in CD4 T cells derived from females included PI3K/AKT signaling, STAT3 signaling and integrin signaling all related to immune activation.¹⁶² The PI3K pathway, associated with T cell activation and proliferation, is

negatively regulated in CD4 T(rm) cells from the epithelium compared to the lamina propria (**chapter 6**). The hypothesis is that the resulting dampening of intraepithelial lymphocyte activation helps prevent excessive immune responses. That pathways involved in maintenance of homeostasis at the mucosal barrier are to some extent sex-biased might be linked to the difference between males and females in Crohn's disease susceptibility or disease course.

Circadian rhythm

Nearly all life forms follow a circadian rhythm; a cycle of roughly 24 hours. In 1729, it was first recorded that plants following a rhythm of opening and closing their leaves. Not until 1984 it was realized that these observed rhythms were endogenously regulated on the transcriptional level.¹⁶³ Experiments performed with animal studies often follow a preplanned approach with set times. This results in the study of cells and/or processes at similar timepoints for every (repeat) experiment. Research with human-derived material, however, is often dependent on the agenda of the subject and the hospital/setting where material will be acquired. The consequence is that the time of sampling varies throughout the day which could result in differences due to the circadian rhythm of the body. CgA and CST levels correlated with disease activity in patients with IBD. We did observe variability of plasma and fecal CgA and CST levels in controls and patients with IBD (Muntjewerff et al., 2021, see list of publications). A circadian clock controls the secretion of CgA with the highest levels in the morning, a second lower, peak in the afternoon and constant relatively low levels during the rest of the day.¹⁶⁴⁻¹⁶⁶ Whether CST secretion is subject to a circadian rhythm as well is presently unknown, but it seems likely because it is a splicing product of CgA. At least for one of the known enzymes involved in CgA to CST processing, cathepsin L, a similar circadian rhythm as for CgA was observed.¹⁶⁷ Sampling at different timepoints might therefore have impacted the results. Moreover, the circadian rhythm is crucial in intestinal tissue homeostasis with a disruption in the genes regulating circadian rhythm resulting in intestinal inflammation.^{168,169} Colonic permeability also follows a circadian rhythm with a peak in permeability around 10:00 and 18:00,¹⁷⁰ which is just after the daily peaks in CgA levels. In CST-knockout mice an increased intestinal permeability was observed that could be reversed with CST supplementation (Muntjewerff et al., 2021). Patients with active IBD also experience an increased intestinal permeability.^{171,172} CST levels are elevated in patients with IBD, and relative to CgA more during remission than in active disease (Muntjewerff et al., 2021). This could indicate an increased processing of CgA to CST, which may serve as protective mechanism to prevent potential relapse-eliciting intestinal permeability, among which during the circadian-related increased intestinal permeability.

What is healthy?

In this thesis we have mostly focused on exploring processes that are altered in patients with a chronic inflammatory disease. Control subjects were included as well, but we do not have a thorough understanding of the normal ranges of the immunological parameters studied. Control subjects were not suffering from chronic inflammatory conditions, and were excluded

if they used corticosteroids in the previous 3 months or anti-integrin biologicals in the past two years (**chapter 6** and **7**).¹⁷³ These criteria, however, do not completely exclude the presence of any current or past disease, which could have affected immune memory and consequently immune cell constitution and immunodynamics at tissue sites. Most control subjects visited our university medical center, implying symptoms and/or an extensive medical history. There is still little data at present on what a healthy tissue immune system in humans constitutes. For example, below are two imaging mass cytometry figures of control subjects' ileum (**Figure 4**). Both did not have a medical history and underwent ileocolonoscopy for a colon check-up for non-inflammatory reasons (e.g. polyp surveillance, iron deficiency) (**chapter 6** and **7**). Histological examination did not show active nor chronic inflammation in either (left: female, 39 years of age; right male, 33 years of age). The images show a striking different pattern of T cell distribution, with a much denser CD4 and CD8 T cell-seeded lamina propria compartment on the right as compared to the left. Findings based on one immune system component is insufficient to define whether a person's immune system is within the normal range or not.¹⁷⁴ Thus, both these images might show a tissue immune system within the normal range even though the visual aspect differs considerably.

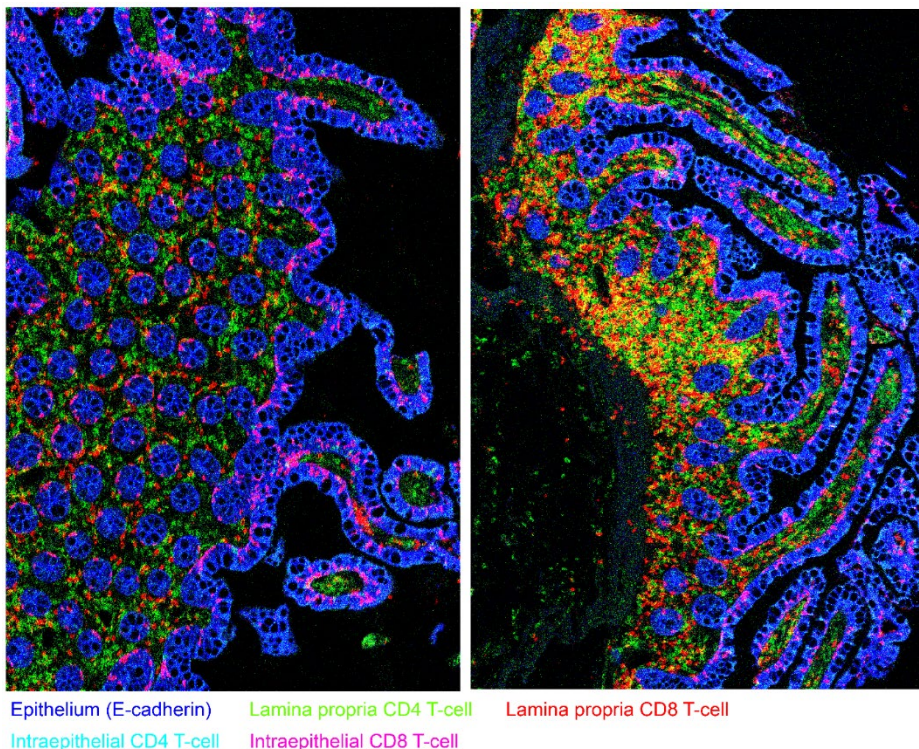


Figure 4. Imaging mass cytometry of the non-inflamed ileum of two control subjects. The density of cells, both CD4 and CD8 T cells, in the lamina propria is different between both ileal sections. Both sections are derived from control subjects without any (known) disease, and no active or chronic inflammation was present (nor

within the year following this ileocolonoscopy). This suggests that healthy tissue exists along a spectrum; a spectrum that still has to be explored when it comes to visual techniques.

Mapping of the blood immune system in healthy individuals has been performed more extensively.¹⁷⁴⁻¹⁷⁹ These studies indicate that the healthy blood immune system is stable over time, irrespective of challenges to the immune system, and forms a continuum among healthy individuals. Separate groups among healthy individuals could not be defined based on any factor specifically. This continuum is most likely due to a mixture of intrinsic and environmental factors that vary among humans. In tissues there is much more interaction with the external environment, especially in barrier tissues such as in the intestines, lungs and skin. How do the findings in the peripheral blood translate to the tissue immune system? The observations indicate that for tissue immunity we should look at the total architecture and functioning to be able to assess immunological homeostasis and disruption hereof. There are several efforts focusing on the spatial distribution of tissue immune cells. Extensive pathology databases providing huge sample sizes could aid in understanding the homeostatic immune system. However, tissue of controls not visiting the hospital with a complaint or a diagnosis, nor being a family member which might pose problems when genetics underlie a disease is limited. Initiatives such as the Human Cell Atlas project to map all (healthy) human cells,^{180,181} or that of the Donna Farber laboratory (Department of Microbiology and Immunology at Columbia University Irving Medical Center) where human tissue of deceased donors is received will also help to determine the homeostatic immune architecture of a tissue. Resection material such as skin and attached fat can also be acquired relatively easily of donors upon breast reduction or abdominoplasty. However, resected skin and fat from abdominoplasties due to weight loss of the donor might show remodeling due to external forces and low grade chronic inflammation owing to metabolic/hormonal abnormalities as a consequence of obesity. Exploring the normal range in tissue immune system architecture and function will help us understand where and how it goes wrong in (chronic) tissue inflammation.

Conclusion

In conclusion, T cells in tissue microenvironments are highly adaptable, with local cues driving differentiation, functioning and maintenance of these T cells. This adaptation is tightly regulated within a microenvironment. However, striking overlap in transcriptional and phenotypical programming can be observed, especially in non-homeostatic conditions such as inflammation. Understanding the local immunodynamics in homeostatic and inflammatory conditions, and the interplay with other physiological systems will improve our understanding of the tissue immune system as well as aid therapeutic approaches in diseases.

REFERENCES

1. Silverthorn, D. U. *Human physiology: an integrated approach*. (Pearson International Edition).
2. Richet, C. R. *Dictionnaire de physiologie*. vol. 4 (1900).
3. Powell, N., Walker, M. M. & Talley, N. J. The mucosal immune system: master regulator of bidirectional gut–brain communications. *Nat. Rev. Gastroenterol. Hepatol.* **14**, 143–159 (2017).
4. Wienke, J. *et al.* Human Tregs at the materno-fetal interface show site-specific adaptation reminiscent of tumor Tregs. *JCI insight* **5**, e137926 (2020).
5. Krausgruber, T. *et al.* Structural cells are key regulators of organ-specific immune responses. *Nature* **583**, 296–302 (2020).
6. Esterházy, D. *et al.* Compartmentalized gut lymph node drainage dictates adaptive immune responses. *Nature* **569**, 126–130 (2019).
7. Mowat, A. M. & Agace, W. W. Regional specialization within the intestinal immune system. *Nat. Rev. Immunol.* **14**, 667–685 (2014).
8. Brunkow, M. E. *et al.* Disruption of a new forkhead/winged-helix protein, scurfy, results in the fatal lymphoproliferative disorder of the scurfy mouse. *Nat. Genet.* **27**, 68–73 (2001).
9. Ochs, H. D. *et al.* The immune dysregulation, polyendocrinopathy, enteropathy, X-linked syndrome (IPEX) is caused by mutations of FOXP3. *Nat. Genet.* **27**, 20–21 (2001).
10. Raffin, C., Vo, L. T. & Bluestone, J. A. T(reg) cell-based therapies: challenges and perspectives. *Nat. Rev. Immunol.* **20**, 158–172 (2020).
11. Li, C., Jiang, P., Wei, S., Xu, X. & Wang, J. Regulatory T cells in tumor microenvironment: new mechanisms, potential therapeutic strategies and future prospects. *Mol. Cancer* **19**, 116 (2020).
12. Delacher, M. *et al.* Genome-wide DNA-methylation landscape defines specialization of regulatory T cells in tissues. *Nat. Immunol.* **18**, 1160–1172 (2017).
13. Annunziato, F., Cosmi, L., Liotta, F., Maggi, E. & Romagnani, S. Human Th1 dichotomy: origin, phenotype and biologic activities. *Immunology* **144**, 343–351 (2014).
14. Feuerer, M. *et al.* Lean, but not obese, fat is enriched for a unique population of regulatory T cells that affect metabolic parameters. *Nat. Med.* **15**, 930–939 (2009).
15. Liston, A. & Gray, D. H. D. Homeostatic control of regulatory T cell diversity. *Nat. Rev. Immunol.* **14**, 154–65 (2014).
16. Brand, S. Crohn's disease: Th1, Th17 or both? The change of a paradigm: new immunological and genetic insights implicate Th17 cells in the pathogenesis of Crohn's disease. *Gut* **58**, 1152–1167 (2009).
17. Lander, E. S. *et al.* Initial sequencing and analysis of the human genome. *Nature* **409**, 860–921 (2001).
18. Lambert, S. A. *et al.* The Human Transcription Factors. *Cell* **172**, 650–665 (2018).
19. Miragaia, R. J. *et al.* Single-Cell Transcriptomics of Regulatory T Cells Reveals Trajectories of Tissue Adaptation. *Immunity* **50**, 493–504.e7 (2019).
20. Hayatsu, N. *et al.* Analyses of a Mutant Foxp3 Allele Reveal BATF as a Critical Transcription Factor in the Differentiation and Accumulation of Tissue Regulatory T Cells. *Immunity* **47**, 268–283.e9 (2017).
21. Miyazaki, K. *et al.* Identification of Functional Hypoxia Response Elements in the Promoter Region of the DEC1 and DEC2 Genes. *J. Biol. Chem.* **277**, 47014–47021 (2002).
22. Lin, C.-C. *et al.* Bhlhe40 controls cytokine production by T cells and is essential for pathogenicity in autoimmune neuroinflammation. *Nat. Commun.* **5**, 3551 (2014).
23. Sun, H., Lu, B., Li, R. Q., Flavell, R. A. & Taneja, R. Defective T cell activation and autoimmune disorder in Stra13-deficient mice. *Nat. Immunol.* **2**, 1040–1047 (2001).
24. Miyazaki, K. *et al.* The role of the basic helix-loop-helix transcription factor Dec1 in the regulatory T cells. *J. Immunol.* **185**, 7330–7339 (2010).
25. Muntjewerff, E. M., Christoffersson, G., Mahata, S. K. & van den Bogaart, G. Putative regulation of macrophage-mediated inflammation by catenatin. *Trends Immunol.* **43**, 41–50 (2022).
26. Mahata, S. K. & Corti, A. Chromogranin A and its fragments in cardiovascular, immunometabolic, and

- cancer regulation. *Ann. N. Y. Acad. Sci.* **1455**, 34–58 (2019).
27. Zissimopoulos, A. *et al.* Chromogranin A as a biomarker of disease activity and biologic therapy in inflammatory bowel disease: a prospective observational study. *Scand. J. Gastroenterol.* **49**, 942–949 (2014).
 28. Sciola, V. *et al.* Plasma chromogranin a in patients with inflammatory bowel disease. *Inflamm. Bowel Dis.* **15**, 867–871 (2009).
 29. Wagner, M. *et al.* Increased fecal levels of chromogranin A, chromogranin B, and secretoneurin in collagenous colitis. *Inflammation* **36**, 855–861 (2013).
 30. Zivkovic, P. M. *et al.* Serum Catestatin Levels and Arterial Stiffness Parameters Are Increased in Patients with Inflammatory Bowel Disease. *J. Clin. Med.* **9**, 628 (2020).
 31. Packey, C. D. & Sartor, R. B. Commensal bacteria, traditional and opportunistic pathogens, dysbiosis and bacterial killing in inflammatory bowel diseases. *Curr. Opin. Infect. Dis.* **22**, 292–301 (2009).
 32. González-Dávila, P. *et al.* Catestatin selects for colonization of antimicrobial-resistant gut bacterial communities. *ISME J.* **16**, 1873–1882 (2022).
 33. Muntjewerff, E. M. *et al.* The anti-inflammatory peptide Catestatin blocks chemotaxis. *J. Leukoc. Biol.* **112**, 273–278 (2021).
 34. Li, H. *et al.* Dysfunctional CD8 T Cells Form a Proliferative, Dynamically Regulated Compartment within Human Melanoma. *Cell* **176**, 775–789.e18 (2019).
 35. Zhang, L. *et al.* Lineage tracking reveals dynamic relationships of T cells in colorectal cancer. *Nature* **564**, 268–272 (2018).
 36. Rao, D. A. T cells that help B cells in chronically inflamed tissues. *Front. Immunol.* **9**, 1924 (2018).
 37. van der Leun, A. M., Thommen, D. S. & Schumacher, T. N. CD8(+) T cell states in human cancer: insights from single-cell analysis. *Nat. Rev. Cancer* **20**, 218–232 (2020).
 38. Maschmeyer, P. *et al.* Antigen-driven PD-1⁺TOX⁺BHLHE40⁺ and PD-1⁺TOX⁺EOMES⁺ T lymphocytes regulate juvenile idiopathic arthritis in situ. *Eur. J. Immunol.* **4**, 915–929 (2021).
 39. Workel, H. H. *et al.* A Transcriptionally Distinct CXCL13⁺CD103⁺CD8⁺ T-cell Population Is Associated with B-cell Recruitment and Neoantigen Load in Human Cancer. *Cancer Immunol. Res.* **7**, 784–796 (2019).
 40. Tomohiro, A. *et al.* Single-cell profiling reveals the importance of CXCL13/CXCR5 axis biology in lymphocyte-rich classic Hodgkin lymphoma. *Proc. Natl. Acad. Sci.* **118**, e2105822118 (2021).
 41. Kobayashi, S. *et al.* A distinct human CD4⁺ T cell subset that secretes CXCL13 in rheumatoid synovium. *Arthritis Rheum.* **65**, 3063–3072 (2013).
 42. Blank, C. U. *et al.* Defining ‘T cell exhaustion’. *Nat. Rev. Immunol.* **19**, 665–674 (2019).
 43. Rotte, A., Jin, J. Y. & Lemaire, V. Mechanistic overview of immune checkpoints to support the rational design of their combinations in cancer immunotherapy. *Ann. Oncol.* **29**, 71–83 (2018).
 44. Lamarche, C. *et al.* Repeated stimulation or tonic-signaling chimeric antigen receptors drive regulatory T cell exhaustion. *bioRxiv* 2020.06.27.175158 (2020).
 45. Blackburn, S. D. *et al.* Coregulation of CD8⁺ T cell exhaustion by multiple inhibitory receptors during chronic viral infection. *Nat. Immunol.* **10**, 29–37 (2009).
 46. Legat, A., Speiser, D. E., Pircher, H., Zehn, D. & Fuentes Marraco, S. A. Inhibitory Receptor Expression Depends More Dominantly on Differentiation and Activation than ‘Exhaustion’ of Human CD8 T Cells. *Front. Immunol.* **4**, 455 (2013).
 47. Pitzalis, C., Jones, G. W., Bombardieri, M. & Jones, S. A. Ectopic lymphoid-like structures in infection, cancer and autoimmunity. *Nat. Rev. Immunol.* **14**, 447–462 (2014).
 48. Manzo, A. *et al.* Mature antigen-experienced T helper cells synthesize and secrete the B cell chemoattractant CXCL13 in the inflammatory environment of the rheumatoid joint. *Arthritis Rheum.* **58**, 3377–3387 (2008).
 49. Odegard, J. M. *et al.* ICOS-dependent extrafollicular helper T cells elicit IgG production via IL-21 in systemic autoimmunity. *J. Exp. Med.* **205**, 2873–2886 (2008).

50. Lu, Y. & Craft, J. T. Follicular Regulatory Cells: Choreographers of Productive Germinal Center Responses. *Frontiers in Immunology* **12**, 679909 (2021).
51. Perdomo-Celis, F., Taborda, N. A. & Rugeles, M. T. Follicular CD8+ T Cells: Origin, Function and Importance during HIV Infection. *Frontiers in Immunology* **8**, 1241 (2017).
52. Brask, S. *et al.* Quantification of CD8-positive lymphocytes in lymph node follicles from HIV-infected male homosexuals and controls. *Acta Pathol. Microbiol. Immunol. Scand. Sect. A, Pathol.* **95**, 155–157 (1987).
53. Quigley, M. F., Gonzalez, V. D., Granath, A., Andersson, J. & Sandberg, J. K. CXCR5⁺ CCR7⁻ CD8 T cells are early effector memory cells that infiltrate tonsil B cell follicles. *Eur. J. Immunol.* **37**, 3352–3362 (2007).
54. Rao, D. A. *et al.* Pathologically expanded peripheral T helper cell subset drives B cells in rheumatoid arthritis. *Nature* **542**, 110–114 (2017).
55. Rao, D. A. The rise of peripheral T helper cells in autoimmune disease. *Nat. Rev. Rheumatol.* **15**, 453–454 (2019).
56. Christophersen, A. *et al.* Distinct phenotype of CD4⁺ T cells driving celiac disease identified in multiple autoimmune conditions. *Nat. Med.* **25**, 734–737 (2019).
57. Zhou, X. *et al.* Instability of the transcription factor Foxp3 leads to the generation of pathogenic memory T cells in vivo. *Nat. Immunol.* **10**, 1000–1007 (2009).
58. Drayton, D. L., Liao, S., Mounzer, R. H. & Ruddle, N. H. Lymphoid organ development: from ontogeny to neogenesis. *Nat. Immunol.* **7**, 344–353 (2006).
59. Nakayamada, S. *et al.* Early Th1 cell differentiation is marked by a Tfh cell-like transition. *Immunity* **35**, 919–931 (2011).
60. Lönnberg, T. *et al.* Single-cell RNA-seq and computational analysis using temporal mixture modelling resolves Th1/Tfh fate bifurcation in malaria. *Sci. Immunol.* **2**, eaal2192 (2017).
61. Bechman, K., Dalrymple, A., Southey-Bassols, C., Cope, A. P. & Galloway, J. B. A systematic review of CXCL13 as a biomarker of disease and treatment response in rheumatoid arthritis. *BMC Rheumatol.* **4**, 70 (2020).
62. Klimatcheva, E. *et al.* CXCL13 antibody for the treatment of autoimmune disorders. *BMC Immunol.* **16**, 6 (2015).
63. Kobayashi, S. *et al.* TGF- β induces the differentiation of human CXCL13-producing CD4⁺ T cells. *Eur. J. Immunol.* **46**, 360–371 (2016).
64. Yoshitomi, H. *et al.* Human Sox4 facilitates the development of CXCL13-producing helper T cells in inflammatory environments. *Nat. Commun.* **9**, 1–10 (2018).
65. Mijnheer, G. *et al.* Conserved human effector Treg cell transcriptomic and epigenetic signature in arthritic joint inflammation. *Nat. Commun.* **12**, 2710 (2021).
66. Kobayashi, S. *et al.* TGF- β induces the differentiation of human CXCL13-producing CD4⁺ T cells. *Eur. J. Immunol.* **46**, 360–371 (2016).
67. CXCL13 gene. <https://www.genecards.org/cgi-bin/carddisp.pl?gene=CXCL13>.
68. Méndez-Maldonado, K. *et al.* Hypoxia inducible transcription factor (HIF-1) regulates CXCL13 expression: Clinical implications in pediatric non-Hodgkin's lymphoma. *Boletín Médico del Hosp. Infant. México English Ed.* **71**, 25–35 (2014).
69. Malhotra, N. *et al.* ROR α -expressing T regulatory cells restrain allergic skin inflammation. *Sci. Immunol.* **3**, eaao6923 (2018).
70. T., C. E. *et al.* Hypoxia-inducible factor-1 alpha-dependent induction of FoxP3 drives regulatory T-cell abundance and function during inflammatory hypoxia of the mucosa. *Proc. Natl. Acad. Sci.* **109**, E2784–E2793 (2012).
71. Masopust, D. Preferential Localization of Effector Memory Cells in Nonlymphoid Tissue. *Science* **291**, 2413–2417 (2001).
72. Hogan, R. J. *et al.* Activated antigen-specific CD8+ T cells persist in the lungs following recovery from

- respiratory virus infections. *J. Immunol.* **166**, 1813–1822 (2001).
73. Jiang, X. *et al.* Skin infection generates non-migratory memory CD8⁺ T(RM) cells providing global skin immunity. *Nature* **483**, 227–231 (2012).
 74. Clark, R. A. Resident memory T cells in human health and disease. *Sci. Transl. Med.* **7**, 269rv1–269rv1 (2015).
 75. Park, C. O. & Kupper, T. S. The emerging role of resident memory T cells in protective immunity and inflammatory disease. *Nat. Med.* **21**, 688–697 (2015).
 76. Clark, R. A. *et al.* Skin effector memory T cells do not recirculate and provide immune protection in alemtuzumab-treated CTCL patients. *Sci. Transl. Med.* **4**, 117ra7 (2012).
 77. Sathaliyawala, T. *et al.* Distribution and Compartmentalization of Human Circulating and Tissue-Resident Memory T Cell Subsets. *Immunity* **38**, 187–197 (2013).
 78. Teijaro, J. R. *et al.* Cutting Edge: Tissue-Retentive Lung Memory CD4⁺ T Cells Mediate Optimal Protection to Respiratory Virus Infection. *J. Immunol.* **187**, 5510–5514 (2011).
 79. Mackay, L. K. *et al.* The developmental pathway for CD103⁺CD8⁺ tissue-resident memory T cells of skin. *Nat. Immunol.* **14**, 1294–1301 (2013).
 80. Mackay, L. K. *et al.* Hobit and Blimp1 instruct a universal transcriptional program of tissue residency in lymphocytes. *Science* **352**, 459–463 (2016).
 81. Zundler, S. *et al.* Hobit- and Blimp-1-driven CD4⁺ tissue-resident memory T cells control chronic intestinal inflammation. *Nat. Immunol.* **20**, 288–300 (2019).
 82. Kumar, B. V *et al.* Human Tissue-Resident Memory T Cells Are Defined by Core Transcriptional and Functional Signatures in Lymphoid and Mucosal Sites. *Cell Rep.* **20**, 2921–2934 (2017).
 83. Fonseca, R. *et al.* Developmental plasticity allows outside-in immune responses by resident memory T cells. *Nat. Immunol.* **21**, 412–421 (2020).
 84. Bromley, S. K., Thomas, S. Y. & Luster, A. D. Chemokine receptor CCR7 guides T cell exit from peripheral tissues and entry into afferent lymphatics. *Nat. Immunol.* **6**, 895–901 (2005).
 85. de Almeida, P. G. *et al.* Human skin-resident host T cells can persist long term after allogeneic stem cell transplantation and maintain recirculation potential. *Sci. Immunol.* **7**, eabe2634 (2022).
 86. Klicznik, M. M. *et al.* Human CD4⁺CD103⁺ cutaneous resident memory T cells are found in the circulation of healthy individuals. *Sci. Immunol.* **4**, eaav8995 (2019).
 87. Murphy, K. & Weaver, C. *Janeway's Immunobiology*. (Garland Science, 2016).
 88. Sallusto, F., Lenig, D., Förster, R., Lipp, M. & Lanzavecchia, A. Two subsets of memory T lymphocytes with distinct homing potentials and effector functions. *Nature* **401**, 708–712 (1999).
 89. Skon, C. N. *et al.* Transcriptional downregulation of S1pr1 is required for the establishment of resident memory CD8⁺ T cells. *Nat. Immunol.* **14**, 1285–1293 (2013).
 90. Cheuk, S. *et al.* CD49a Expression Defines Tissue-Resident CD8⁺ T Cells Poised for Cytotoxic Function in Human Skin. *Immunity* **46**, 287–300 (2017).
 91. Reilly, E. C. *et al.* T(RM) integrins CD103 and CD49a differentially support adherence and motility after resolution of influenza virus infection. *Proc. Natl. Acad. Sci. U. S. A.* **117**, 12306–12314 (2020).
 92. Shiow, L. R. *et al.* CD69 acts downstream of interferon- α/β to inhibit S1P1 and lymphocyte egress from lymphoid organs. *Nature* **440**, 540–544 (2006).
 93. Lin, S. J., Chao, H. C. & Kuo, M. L. The effect of interleukin-12 and interleukin-15 on CD69 expression of T-lymphocytes and natural killer cells from umbilical cord blood. *Biol. Neonate* **78**, 181–185 (2000).
 94. Rutella, S. *et al.* Induction of CD69 antigen on normal CD4⁺ and CD8⁺ lymphocyte subsets and its relationship with the phenotype of responding T-cells. *Cytometry* **38**, 95–101 (1999).
 95. Bartolomé-Casado, R. *et al.* CD4⁺ T cells persist for years in the human small intestine and display a T(H)1 cytokine profile. *Mucosal Immunol.* **14**, 402–410 (2021).
 96. Kumar, B. V *et al.* Functional heterogeneity of human tissue-resident memory T cells based on dye efflux capacities *JCI insight* **3**, e123568 (2018).
 97. Bartolomé-Casado, R. *et al.* Resident memory CD8 T cells persist for years in human small intestine. *J.*

- Exp. Med.* **216**, 2412–2426 (2019).
98. Bottois, H. *et al.* KLRG1 and CD103 Expressions Define Distinct Intestinal Tissue-Resident Memory CD8 T Cell Subsets Modulated in Crohn's Disease. *Front. Immunol.* **11**, 1–13 (2020).
99. FitzPatrick, M. E. B. *et al.* Human intestinal tissue-resident memory T cells comprise transcriptionally and functionally distinct subsets. *Cell Rep.* **34**, 108661 (2021).
100. Tkachev, V. *et al.* Spatiotemporal single-cell profiling reveals that invasive and tissue-resident memory donor CD8+ T cells drive gastrointestinal acute graft-versus-host disease. *Sci. Transl. Med.* **13**, (2021).
101. Kaech, S. *et al.* Selective expression of the IL-7R identifies effector CD8 T cells that give rise to long-lived memory cells. *Nat. Immunol.* **4**, 1191–1198 (2003).
102. Sarkar, S. *et al.* Functional and genomic profiling of effector CD8 T cell subsets with distinct memory fates. *J. Exp. Med.* **205**, 625–640 (2008).
103. Justin, M. J. *et al.* Delineation of a molecularly distinct terminally differentiated memory CD8 T cell population. *Proc. Natl. Acad. Sci.* **117**, 25667–25678 (2020).
104. Guy-Grand, D., Malassis-Seris, M., Briottet, C. & Vassalli, P. Cytotoxic differentiation of mouse gut thymodependent and independent intraepithelial T lymphocytes is induced locally. Correlation between functional assays, presence of perforin and granzyme transcripts, and cytoplasmic granules. *J. Exp. Med.* **173**, 1549–1552 (1991).
105. Sasahara, T., Tamauchi, H., Ikewaki, N. & Kubota, K. Unique properties of a cytotoxic CD4+CD8+ intraepithelial T-cell line established from the mouse intestinal epithelium. *Microbiol. Immunol.* **38**, 191–199 (1994).
106. Mucida, D. *et al.* Transcriptional reprogramming of mature CD4+ helper T cells generates distinct MHC class II-restricted cytotoxic T lymphocytes. *Nat. Immunol.* **14**, 281–289 (2013).
107. Zhu, J. *et al.* Immune surveillance by CD8 α^+ skin-resident T cells in human herpes virus infection. *Nature* **497**, 494–497 (2013).
108. Cheuk, S. *et al.* Epidermal Th22 and Tc17 cells form a localized disease memory in clinically healed psoriasis. *J. Immunol.* **192**, 3111–3120 (2014).
109. Boyman, O. *et al.* Spontaneous Development of Psoriasis in a New Animal Model Shows an Essential Role for Resident T Cells and Tumor Necrosis Factor- α . *J. Exp. Med.* **199**, 731–736 (2004).
110. Liu, L. *et al.* Epidermal injury and infection during poxvirus immunization is crucial for the generation of highly protective T cell-mediated immunity. *Nat. Med.* **16**, 224–227 (2010).
111. Lutter, L. *et al.* Homeostatic Function and Inflammatory Activation of Ileal CD8+ Tissue-Resident T Cells Is Dependent on Mucosal Location. *Cell. Mol. Gastroenterol. Hepatol.* **12**, 1567–1581 (2021).
112. Truong, K. L. *et al.* Killer-like receptors and GPR56 progressive expression defines cytokine production of human CD4+ memory T cells. *Nat. Commun.* **10**, 1–15 (2019).
113. Joshi, N. S. *et al.* Inflammation directs memory precursor and short-lived effector CD8(+) T cell fates via the graded expression of T-bet transcription factor. *Immunity* **27**, 281–295 (2007).
114. Jenh, C.-H. *et al.* A selective and potent CXCR3 antagonist SCH 546738 attenuates the development of autoimmune diseases and delays graft rejection. *BMC Immunol.* **13**, 2 (2012).
115. Kim, B. *et al.* JN-2, a C-X-C motif chemokine receptor 3 antagonist, ameliorates arthritis progression in an animal model. *Eur. J. Pharmacol.* **823**, 1–10 (2018).
116. Bakheet, S. A. *et al.* CXCR3 antagonist AMG487 suppresses rheumatoid arthritis pathogenesis and progression by shifting the Th17/Treg cell balance. *Cell. Signal.* **64**, 109395 (2019).
117. Hindryckx, P. *et al.* Clinical trials in luminal Crohn's disease: a historical perspective. *J. Crohns. Colitis* **8**, 1339–1350 (2014).
118. Yzet, C. *et al.* Complete Endoscopic Healing Associated With Better Outcomes Than Partial Endoscopic Healing in Patients With Crohn's Disease. *Clin. Gastroenterol. Hepatol. Off. Clin. Pract. J. Am. Gastroenterol. Assoc.* **18**, 2256–2261 (2020).
119. Vespa, E. *et al.* Histological Scores in Patients with Inflammatory Bowel Diseases: The State of the Art. *Journal of Clinical Medicine* vol. 11 (2022).

120. Schmehl, K., Florian, S., Jacobasch, G., Salomon, A. & Körber, J. Deficiency of epithelial basement membrane laminin in ulcerative colitis affected human colonic mucosa. *Int. J. Colorectal Dis.* **15**, 39–48 (2000).
121. Bouatrouss, Y., Herring-Gillam, F. E., Gosselin, J., Poisson, J. & Beaulieu, J. F. Altered Expression of Laminins in Crohn's Disease Small Intestinal Mucosa. *Am. J. Pathol.* **156**, 45–50 (2000).
122. Shimshoni, E. *et al.* Distinct extracellular-matrix remodeling events precede symptoms of inflammation. *Matrix Biol.* **96**, 47–68 (2021).
123. Panés, J. & Rimola, J. Perianal fistulizing Crohn's disease: pathogenesis, diagnosis and therapy. *Nat. Rev. Gastroenterol. Hepatol.* **14**, 652–664 (2017).
124. Zidar, N. *et al.* Pathology of Fibrosis in Crohn's Disease-Contribution to Understanding Its Pathogenesis. *Frontiers in Medicine* vol. 7 (2020).
125. Westera, L. *et al.* Closing the gap between T-cell life span estimates from stable isotope-labeling studies in mice and humans. *Blood* **122**, 2205–2212 (2013).
126. Borghans, J. A. M., Tesselaar, K. & de Boer, R. J. Current best estimates for the average lifespans of mouse and human leukocytes: reviewing two decades of deuterium-labeling experiments. *Immunol. Rev.* **285**, 233–248 (2018).
127. Jess, T. *et al.* Survival and cause specific mortality in patients with inflammatory bowel disease: a long term outcome study in Olmsted County, Minnesota, 1940-2004. *Gut* **55**, 1248–1254 (2006).
128. Lutgens, M. W. M. D. *et al.* Declining risk of colorectal cancer in inflammatory bowel disease: an updated meta-analysis of population-based cohort studies. *Inflamm. Bowel Dis.* **19**, 789–799 (2013).
129. Dorudi, S., Sheffield, J. P., Poulosom, R., Northover, J. M. & Hart, I. R. E-cadherin expression in colorectal cancer. An immunocytochemical and in situ hybridization study. *Am. J. Pathol.* **142**, 981–986 (1993).
130. Le Floc'h, A. *et al.* Alpha E beta 7 integrin interaction with E-cadherin promotes antitumor CTL activity by triggering lytic granule polarization and exocytosis. *J. Exp. Med.* **204**, 559–570 (2007).
131. Habtezion, A., Nguyen, L. P., Hadeiba, H. & Butcher, E. C. Leukocyte Trafficking to the Small Intestine and Colon. *Gastroenterology* **150**, 340–354 (2016).
132. Al-Bawardy, B., Shivashankar, R. & Proctor, D. D. Novel and Emerging Therapies for Inflammatory Bowel Disease. *Frontiers in Pharmacology* **12**, 651415 (2021).
133. Tan, P., Li, X., Shen, J. & Feng, Q. Fecal Microbiota Transplantation for the Treatment of Inflammatory Bowel Disease: An Update. *Frontiers in Pharmacology* **11**, 574533 (2020).
134. Perrelli, M. G. *et al.* Catestatin reduces myocardial ischaemia/reperfusion injury: involvement of PI3K/Akt, PKCs, mitochondrial KATP channels and ROS signalling. *Pflugers Arch.* **465**, 1031–1040 (2013).
135. Bassino, E. *et al.* Catestatin exerts direct protective effects on rat cardiomyocytes undergoing ischemia/reperfusion by stimulating PI3K-Akt-GSK3 β pathway and preserving mitochondrial membrane potential. *PLoS One* **10**, e0119790 (2015).
136. Kamel-Reid, S. & Dick, J. E. Engraftment of immune-deficient mice with human hematopoietic stem cells. *Science* **242**, 1706–1709 (1988).
137. McCune, J. M. *et al.* The SCID-hu mouse: murine model for the analysis of human hematolymphoid differentiation and function. *Science* **241**, 1632–1639 (1988).
138. Mosier, D. E., Gulizia, R. J., Baird, S. M. & Wilson, D. B. Transfer of a functional human immune system to mice with severe combined immunodeficiency. *Nature* **335**, 256–259 (1988).
139. Masopust, D., Sivula, C. P. & Jameson, S. C. Of Mice, Dirty Mice, and Men: Using Mice To Understand Human Immunology. *J. Immunol.* **199**, 383–388 (2017).
140. Hamilton, S. E. *et al.* New Insights into the Immune System Using Dirty Mice. *J. Immunol.* **205**, 3–11 (2020).
141. Koch, M. A. *et al.* T-bet⁺ Treg Cells Undergo Abortive Th1 Cell Differentiation due to Impaired Expression of IL-12 Receptor β 2. *Immunity* **37**, 501–510 (2012).
142. Arvey, A. *et al.* Inflammation-induced repression of chromatin bound by the transcription factor Foxp3

- in regulatory T cells. *Nat. Immunol.* **15**, 580–587 (2014).
143. Whitacre, C. C. Sex differences in autoimmune disease. *Nat. Immunol.* **2**, 777–780 (2001).
 144. Heidari, S., Babor, T. F., De Castro, P., Tort, S. & Curno, M. Sex and Gender Equity in Research: rationale for the SAGER guidelines and recommended use. *Res. Integr. Peer Rev.* **1**, 2 (2016).
 145. Klein, S. L. & Flanagan, K. L. Sex differences in immune responses. *Nat. Rev. Immunol.* **16**, 626–638 (2016).
 146. Cattalini, M., Soliani, M., Caparello, M. C. & Cimaz, R. Sex Differences in Pediatric Rheumatology. *Clin. Rev. Allergy Immunol.* **56**, 293–307 (2019).
 147. Greuter, T., Manser, C., Pittet, V., Vavricka, S. R. & Biedermann, L. Gender Differences in Inflammatory Bowel Disease. *Digestion* **101**, 98–104 (2020).
 148. Brant, S. R. & Nguyen, G. C. Is there a gender difference in the prevalence of Crohn's disease or ulcerative colitis? *Inflamm. Bowel Dis.* **14**, 2–3 (2008).
 149. Severs, M. *et al.* Sex-Related Differences in Patients With Inflammatory Bowel Disease: Results of 2 Prospective Cohort Studies. *Inflamm. Bowel Dis.* **24**, 1298–1306 (2018).
 150. Rustgi, S. D., Kayal, M. & Shah, S. C. Sex-based differences in inflammatory bowel diseases: a review. *Therap. Adv. Gastroenterol.* **13**, 1756284820915043 (2020).
 151. Fish, E. N. The X-files in immunity: sex-based differences predispose immune responses. *Nat. Rev. Immunol.* **8**, 737–744 (2008).
 152. Kaminsky, Z., Wang, S. & Petronis, A. Complex disease, gender and epigenetics. *Ann. Med.* **38**, 530–544 (2006).
 153. Furman, D. *et al.* Systems analysis of sex differences reveals an immunosuppressive role for testosterone in the response to influenza vaccination. *Proc. Natl. Acad. Sci. U. S. A.* **111**, 869–874 (2014).
 154. Pinheiro, I., Dejager, L. & Libert, C. X-chromosome-located microRNAs in immunity: might they explain male/female differences? *Bioessays* **33**, 791–802 (2011).
 155. Rodríguez-Galán, A., Fernández-Messina, L. & Sánchez-Madrid, F. Control of Immunoregulatory Molecules by miRNAs in T Cell Activation. *Front. Immunol.* **9**, 2148 (2018).
 156. Lakshmikanth, T. *et al.* Human Immune System Variation during 1 Year. *Cell Rep.* **32**, 107923 (2020).
 157. Sahin, N. *et al.* Conservation, acquisition, and functional impact of sex-biased gene expression in mammals. *Science*. **365**, eaaw7317 (2019).
 158. Markle, J. G. M. *et al.* Sex differences in the gut microbiome drive hormone-dependent regulation of autoimmunity. *Science* **339**, 1084–1088 (2013).
 159. Org, E. *et al.* Sex differences and hormonal effects on gut microbiota composition in mice. *Gut Microbes* **7**, 313–322 (2016).
 160. Hoytema van Konijnenburg, D. P. *et al.* Intestinal epithelial and intraepithelial T cell crosstalk mediates a dynamic response to infection. *Cell* **171**, 783–794.e13 (2017).
 161. Belkaid, Y. & Hand, T. W. Role of the microbiota in immunity and inflammation. *Cell* **157**, 121–141 (2014).
 162. Sankaran-Walters, S. *et al.* Sex differences matter in the gut: effect on mucosal immune activation and inflammation. *Biol. Sex Differ.* **4**, 10 (2013).
 163. Huang, R.-C. The discoveries of molecular mechanisms for the circadian rhythm: The 2017 Nobel Prize in Physiology or Medicine. *Biomedical journal* **41**, 5–8 (2018).
 164. Giampaolo, B., Angelica, M. & Antonio, S. Chromogranin 'A' in normal subjects, essential hypertensives and adrenalectomized patients. *Clin. Endocrinol. (Oxf)*. **57**, 41–50 (2002).
 165. Den, R., Toda, M., Nagasawa, S., Kitamura, K. & Morimoto, K. Circadian rhythm of human salivary chromogranin A. *Biomed. Res.* **28**, 57–60 (2007).
 166. Hong, R. H., Yang, Y. J., Kim, S. Y., Lee, W. Y. & Hong, Y. P. Determination of appropriate sampling time for job stress assessment: the salivary chromogranin A and cortisol in adult females. *J. Prev. Med. Public Health* **42**, 231–236 (2009).
 167. Cimerman, N., Brguljan, P. M., Krašovec, M., Šuškovič, S. & Kos, J. Circadian characteristics of

- cathepsins B, H, L, and stefins A and B, potential markers for disease, in normal sera. *Clin. Chim. Acta* **282**, 211–218 (1999).
168. Pagel, R. *et al.* Circadian rhythm disruption impairs tissue homeostasis and exacerbates chronic inflammation in the intestine. *FASEB J.* **31**, 4707–4719 (2017).
169. Summa, K. C. *et al.* Disruption of the Circadian Clock in Mice Increases Intestinal Permeability and Promotes Alcohol-Induced Hepatic Pathology and Inflammation. *PLoS One* **8**, e67102 (2013).
170. Kyoko, O. *et al.* Expressions of tight junction proteins Occludin and Claudin-1 are under the circadian control in the mouse large intestine: implications in intestinal permeability and susceptibility to colitis. *PLoS One* **9**, e98016 (2014).
171. D’Incà, R. *et al.* Intestinal permeability test as a predictor of clinical course in Crohn’s disease. *Am. J. Gastroenterol.* **94**, 2956–2960 (1999).
172. Arnott, I. D., Kingstone, K. & Ghosh, S. Abnormal intestinal permeability predicts relapse in inactive Crohn disease. *Scand. J. Gastroenterol.* **35**, 1163–1169 (2000).
173. Kosoy, R. *et al.* Deep Analysis of the Peripheral Immune System in IBD Reveals New Insight in Disease Subtyping and Response to Monotherapy or Combination Therapy. *Cell. Mol. Gastroenterol. Hepatol.* **12**, 599–632 (2021).
174. Carr, E. J. *et al.* The cellular composition of the human immune system is shaped by age and cohabitation. *Nat. Immunol.* **17**, 461–468 (2016).
175. Brodin, P. *et al.* Variation in the Human Immune System Is Largely Driven by Non-Heritable Influences. *Cell* **160**, 37–47 (2015).
176. J., K. K. *et al.* Continuous immunotypes describe human immune variation and predict diverse responses. *Proc. Natl. Acad. Sci.* **114**, E6097–E6106 (2017).
177. Orrù, V. *et al.* Genetic variants regulating immune cell levels in health and disease. *Cell* **155**, 242–256 (2013).
178. Tsang, J. S. *et al.* Global analyses of human immune variation reveal baseline predictors of postvaccination responses. *Cell* **157**, 499–513 (2014).
179. Liefferinckx, C. *et al.* New approach to determine the healthy immune variations by combining clustering methods. *Sci. Rep.* **11**, 8917 (2021).
180. Regev, A. *et al.* The Human Cell Atlas White Paper. *arXiv* (2018).
181. Regev, A. *et al.* The human cell atlas. *Elife* **6**, e27041 (2017).

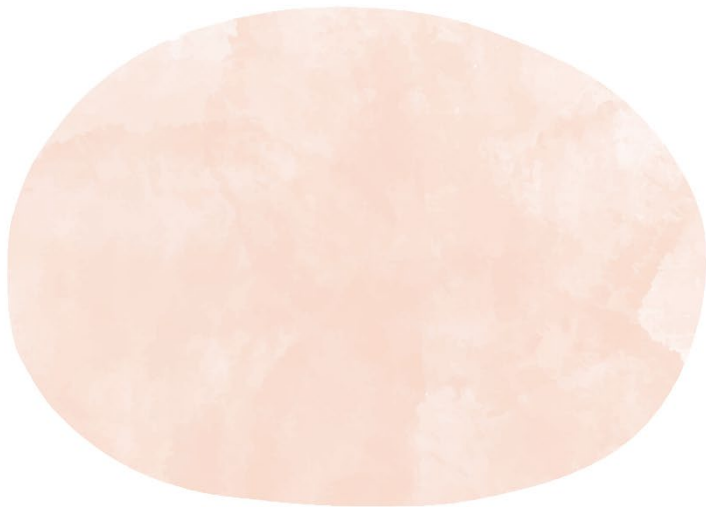
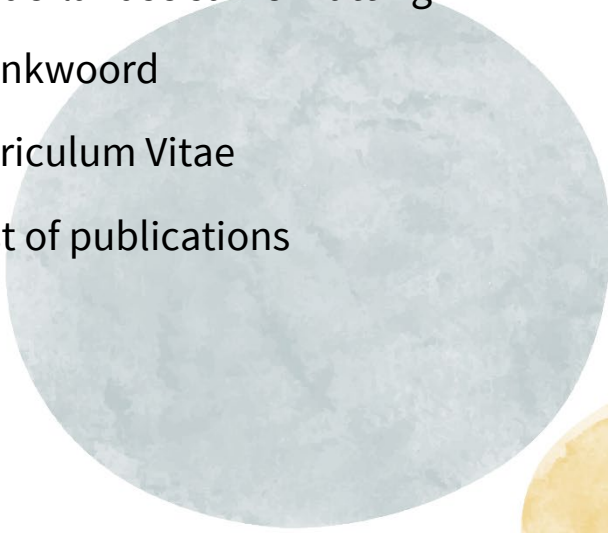
Addendum

Nederlandse samenvatting

Dankwoord

Curriculum Vitae

List of publications



NEDERLANDSE SAMENVATTING

Dit proefschrift verkent de programmering en aanpassing van afweercellen in weefsels tijdens chronische ontsteking. In de samenvatting hieronder worden deze begrippen toegelicht en de inhoud van het proefschrift besproken.

Het afweersysteem

Ons lichaam wordt constant blootgesteld aan factoren die het lichaam prikkelen zoals eten, medicijnen, bacteriën, virussen, crème, microplastics en fysieke schade. De moleculen die gepresenteerd worden aan het afweersysteem noemen we antigenen. Presentatie van antigenen kan een reactie van het afweersysteem (immuunsysteem) opwekken om het lichaam te beschermen. Activatie van het immuunsysteem resulteert in een ontsteking (inflammatie). Ontsteking is een fysiologische respons en veelal zelflimiterend zodra hetgeen wat de activatie opgewekt heeft is opgeruimd. Het lichaam onderhoudt zo homeostase; een nauw gereguleerde stabiele interne omgeving. Een belangrijk cel type welke onderdeel is van het immuunsysteem zijn de T cellen. Deze zijn grofweg op te delen in de CD8 cytotoxische, CD4 helper en CD4 regulatoire cellen. CD8 cytotoxische T cellen hebben het vermogen om geïnfecteerde cellen te doden. CD4 helper T cellen zijn helpers die andere cellen kunnen reguleren, maar ook zelf een rol hebben in de immuunrespons. CD4 regulatoire T cellen (Tregs) staan bekend om hun vermogen om een immuunrespons te onderdrukken.

Chronische ontsteking

De afstemming tussen T cellen in hun respons is van belang in het behoud van, of terugkeer naar, homeostase. Soms stopt een immuunrespons echter niet vanzelf en dan spreken we van chronische ontsteking zoals gezien wordt in juveniele idiopathische artritis (JIA) en de ziekte van Crohn. JIA staat ook bekend als jeugdreuma, waarbij ontstekingen in de gewrichten plaatsvinden. Kinderen met jeugdreuma hebben een lagere kwaliteit van leven dan gemiddeld met pijn, vermoeidheid, psychosociale klachten en op lange termijn mogelijk schade aan gewrichten wat de groei kan belemmeren. De ziekte van Crohn is een aandoening waarbij er sprake is van telkens terugkerende ontsteking welke in het hele maagdarmkanaal kan ontstaan. Soms komen ontstekingen ook buiten het maagdarmkanaal voor, dan spreken we van extra-intestinale manifestaties. Van de mensen met de ziekte van Crohn heeft uiteindelijk 80% een operatie nodig om een deel van de aangedane darm weg te halen. Chronische ontstekingsziekten kunnen dus veel impact op het leven hebben. De behandeling van chronische ontstekingsziekten richt zich veelal op onderdrukking van het immuunsysteem. De mechanistische data waarop de behandelingen gebaseerd zijn komt voornamelijk uit studies met muismodellen. Het immuunsysteem van muizen en mensen is niet identiek. Hoe in mensen chronische ontstekingsreacties in verschillende weefsels gereguleerd worden, en welke rollen de verschillende ontstekingscellen hebben is nog niet voldoende duidelijk. Ondanks het grote aanbod aan behandelingsmogelijkheden houden veel mensen met een chronische ontstekingsziekte klachten, of verliezen ze de respons op een behandeling. Er is

meer kennis nodig over de lokale programmering en rol van het immuunsysteem om het mechanisme achter chronische ontsteking en de behandeling hiervan beter te leren begrijpen.

De eerste drie hoofdstukken van dit proefschrift richten zich op de programmering en adaptatie van Tregs in weefsel. T cellen komen overal in het lichaam voor. Het overgrote deel van de T cellen is te vinden in weefsel waar ze een rol in chronische ontsteking kunnen hebben. Het betrof Tregs uit ontstekingsvocht in **hoofdstuk 2** en **3**. In **hoofdstuk 4** hebben we dit uitgebreid naar Tregs in verscheidene weefsels tijdens homeostase, chronische ontsteking en in tumorweefsel.

In **hoofdstuk 2** hebben we de programmering van Tregs in het synoviaal vocht van patiënten met juveniele idiopathische artritis onderzocht. Dit onderzoek hebben we gedaan op eiwitniveau, transcriptieel niveau (RNA-sequencing) en epigenetisch niveau (ChIP-sequencing). We hebben gekeken welke delen van het DNA, de genetische code, actief zijn en kunnen leiden tot het maken van een eiwit. Het DNA is namelijk in nagenoeg alle cellen van het lichaam hetzelfde, maar per type cel verschilt het welke delen van het DNA afgeschreven kunnen worden. DNA wordt afgeschreven naar RNA waar uiteindelijk eiwit van gemaakt kan worden. Deze eiwitten bepalen hoe een cel zich gedraagt en welke functies de cel heeft. Wij hebben ontdekt dat Tregs uit het synoviaal vocht anders geprogrammeerd zijn dan Tregs uit het bloed. Tregs uit het synoviaal vocht zijn meer gespecialiseerd wat zich uit in het tot expressie brengen van bepaalde effector moleculen zoals CTLA4, PD1 en ICOS. Hiermee kunnen deze Tregs hun immunosuppressieve functie uitvoeren. Het profiel wat ze krijgen noemen we een effector Treg profiel. Daarnaast passen Tregs zich aan hun lokale ontstekingsomgeving aan door markers tot expressie te brengen van het dominante CD4 helper T cel profiel. In dit geval Tbet, CXCR3 en IL12 β 2. De hypothese is dat deze aanpassing Tregs helpt om in de ontstekingsomgeving te overleven en te functioneren. Onze data hebben we vergeleken met data verkregen over Tregs aanwezig in verschillende type tumoren in mensen. Daarmee hebben we een profiel ontdekt dat uniek lijkt te zijn voor Tregs in een menselijke ontstekingsomgeving gericht op specialisatie van de cellen. Tevens zijn er enkele verschillen tussen de Tregs geïnduceerd door de lokale omgeving.

In **hoofdstuk 3** hebben we de programmering van de Tregs in synoviaal vocht verder uitgediept. Hiervoor hebben we gebruik gemaakt van single cell RNA-sequencing zodat we per cel het profiel kunnen bestuderen. Met behulp van deze techniek vonden we vier verschillende Treg clusters in synoviaal vocht. Eén deel van deze Tregs bracht markers tot expressie die indiceerden dat deze Tregs recent naar het synoviaal vocht gemigreerd waren. Tevens waren er twee geactiveerde Treg clusters die een klassiek effector Treg profiel tot expressie brachten, maar waarvan het ene cluster een dominanter onderdrukkend en het ander een dominanter cytotoxisch profiel had. Tenslotte was er een cluster gedefinieerd door GPR56⁺, CD161⁺ en CXCL13⁺. Bioinformatische analyse wijst erop dat differentiatie van Tregs vanuit het migrerende Treg cluster richting de klassieke effector Tregs of richting de GPR56⁺CD161⁺CXCL13⁺ Tregs verloopt. Dit wordt ondersteund door analyses van het TCR repertoire. De TCR is de receptor van T cellen die bepalen welke antigenen herkend wordt.

GPR56⁺CD161⁺CXCL13⁺ Tregs zijn nog niet eerder geïdentificeerd. Fenotypische analyses wijzen erop dat deze cellen functioneren als Tregs, ondanks dat ze markers tot expressie brengen die veelal met verminderde dan wel afwezige oorspronkelijke functie van de betreffende cel worden geassocieerd (exhaustion). In de literatuur worden T cellen die een vergelijkbaar fenotype als deze Tregs tot expressie brengen in verband gebracht met chronische ontsteking. Dit wijst mogelijk op een belangrijke rol voor deze cellen in chronische ontsteking. Tenslotte vonden we dat BATF een belangrijke transcriptiefactor is voor effector Treg differentiatie. Transcriptiefactoren zijn eiwitten die binden aan de promotoren van genen zodat ze worden afgeschreven. BHLHE40 is een transcriptiefactor die het profiel van GPR56⁺CD161⁺CXCL13⁺ Tregs lijkt te sturen, en JAZF1 van klassieke effector Tregs.

In **hoofdstuk 4** hebben we gebruik gemaakt van publiekelijk beschikbare Treg datasets. Na integratie van de datasets hebben we gekeken welke genen worden afgeschreven bij de overgang van bloed naar weefsel, en vervolgens naar chronische ontsteking en de tumor omgeving. HOX genen lijken bepalend voor de eerste aanpassing van Tregs aan weefsel. Aangekomen in weefsel zien we dat Tregs ook meerdere genen tot expressie brengen die interactie met, en invloed op, de lokale omgeving uitoefenen. Vervolgens krijgen de Tregs een geactiveerd profiel en worden het effector Tregs zoals ook beschreven in hoofdstuk 2 en 3. Dit effector profiel komt nog sterker tot expressie in chronisch ontstoken weefsel en de tumor omgeving. BATF is een transcriptiefactor die belangrijk lijkt voor de aanpassing van Tregs aan weefsel zodra ze uit het bloed migreren, ongeacht het type weefsel. Verder zien we dat FOXP3, HDGF en NR3C2 belangrijke transcriptiefactoren zijn voor de aanpassing van Tregs aan de chronisch ontstoken en/of de tumor omgeving. Onderscheidend tussen Tregs uit deze twee niet-homeostatische omgevingen is de expressie van chemokines en chemokine receptoren. Deze zorgen onder andere voor het aantrekken van andere cellen naar weefsel, en het bewegen van de Tregs zelf naar en door weefsel. Dat deze deels verschillend tot expressie komen in chronisch ontstoken weefsel en de tumor omgeving wijst erop dat dit mogelijke aangrijpingspunten voor therapie kunnen vormen.

Vervolgens hebben we ingezoomd op het immuunsysteem van de darmen. In de darmen worden miljarden bacteriën en voedselantigenen gescheiden van het lichaam door een enkele epitheliale cellaag. Het is een van de locaties waar het immuunsysteem vrijwel direct in contact komt met de buitenwereld. Het is van cruciaal belang dat het intestinale (mucosale) immuunsysteem in de darm kan reageren op bedreigingen zonder schade aan het epitheel te veroorzaken. Dit mucosale immuunsysteem bestaat onder andere uit de grootste populatie T immuun cellen in het menselijk lichaam; er bevinden zich meer T cellen in de darm dan in de rest van het lichaam bij elkaar. Er wordt gedacht dat deze mucosale T cellen een belangrijke rol spelen in (chronische) inflammatie in het maag-darmstelsel, maar er is zeer weinig bekend over de eigenschappen en functies van deze specifieke intestinale immuun cellen, met name in de mens.

Allereerst bespreken we in **hoofdstuk 5** dat de aanpassing van T cellen aan de omgeving heel specifiek kan zijn. We hebben de specifieke rol van T cellen die verblijven in de

epitheliale laag van de mucosa van de darmen in mensen samengevat. In onder andere de ziekte van Crohn, coeliakie en colorectaal carcinoom zien we dat de respons van T cellen in het epitheel en in de lamina propria verschilt. De lamina propria ligt onder het epitheel en vormt samen met het epitheel de mucosa. Deze twee lagen van de mucosa worden alleen gescheiden door een dun basaal membraan van 7 μm , dit is vergelijkbaar met de diameter van een enkele T cel. De verschillende respons op uitlokkende factoren van de cellen in deze lagen wijst erop dat de cellen in het epitheel en de lamina propria een andere rol hebben. Door in te gaan op het specifieke profiel en de rollen van de cellen aanwezig in het epitheel willen we inzicht geven in het belang van het beschouwen van het epitheel en de lamina propria als aparte compartimenten.

In **hoofdstuk 6** en **7** laten we de verschillen tussen verscheidene T cel subsets gelegen in het epitheel en de lamina propria van de menselijke darm zien. Hiervoor hebben we met behulp van enzymen het epitheel van de lamina propria gescheiden. In **hoofdstuk 6** kijken we naar de CD4 T cellen in mensen zonder ziekte van het maagdkanaal en mensen met de ziekte van Crohn. Net als in de voorgaande hoofdstukken hebben we ook hier op zowel eiwitniveau als op RNA-niveau gekeken. Tijdens ontsteking zien we een toename van Tregs en migrerende/infiltrerende CD4 T cellen. Als we de verschillende CD4 T cel types samen groeperen dan zien we een overkoepelende respons in het epitheel. Er is activatie van de T cellen, een verhoogde IFN γ respons wat onder andere de ontstekingsrespons stimuleert, en Tregs krijgen een effector profiel. In de lamina propria zien we echter weinig verschillen op RNA-niveau. Het lijkt erop dat chromatine remodelers zoals ARID4B en SATB1 een belangrijke rol spelen in het verkrijgen van het T cel profiel in het epitheel. Chromatine bestaat uit DNA en eiwitten in de kern van een cel. Chromatine remodelers kunnen de structuur van het chromatine aanpassen zodat genen meer of minder afleesbaar worden, en zodoende het profiel van een cel veranderen. De algemene invloed van deze chromatine remodelers in CD4 T cellen die zich vestigen in het epitheel lijken het onderdrukken van brede (pro-ontsteking) responsen en een strakke regulatie van de levensduur te zijn.

In **hoofdstuk 7** kijken we naar de CD8 T cellen in beide mucosale compartimenten. We hebben hier specifiek gekeken naar de CD8 T cellen waarvan gedacht wordt dat ze lang/permanent in het weefsel verblijven. Deze cellen worden gekarakteriseerd door CD69 en deels ook CD103 expressie op hun celmembraan. Allereerst zagen we in de CD8 T cel populatie in de lamina propria die CD69, maar geen CD103, tot expressie brengt een Itgb2⁺GzmK⁺KLRG1⁺ cluster. In de literatuur wordt dit profiel aan een meer cytotoxisch en mogelijk pathogeen profiel gerelateerd wordt. De CD8 T cellen in de lamina propria van de darmen die zowel CD69 als CD103 tot expressie brengen hebben een klassiek tissue-resident memory T (Trm, weefsel verblijvend) profiel. Kenmerkend hierbij is actieve regulatie van overleving en celdood, en cytokine signalering. In het epitheel wordt deze dichotomie niet gezien. De meeste intra-epitheliale CD8 T cellen zijn zowel CD69 als CD103 positief en hebben een meer aangeboren cytotoxisch profiel. Tijdens chronische ontsteking verkrijgen de cellen in het epitheel een meer aangeboren pro-ontstekingsprofiel met ogenschijnlijk verlies van homeostatische functies. Zowel in **hoofdstuk 6** als **hoofdstuk 7** zien we met name veranderingen in de T cellen in het

epitheel tijdens ontsteking. Beide hoofdstukken laten zien dat het van toegevoegde waarde zou zijn als de verschillen tussen het epitheel en de lamina propria, en de verschillen geïnduceerd door ontsteking worden meegenomen in het bepalen van de beste behandelingsstrategie. Zeker als we kijken naar de lange termijn effecten van therapieën die het afweersysteem onderdrukken.

Samenvattend heeft het onderzoek in dit proefschrift nieuwe inzichten gegeven over hoe verscheidene T cellen geprogrammeerd zijn en zich aanpassen aan de lokale omgeving in chronische ontstekingsziekten in mensen. We laten zien dat de aanpassing van T cellen aan de omgeving zeer bepalend voor het profiel is, en strak wordt gereguleerd. De kern van de aanpassing aan weefsel wordt gedeeld tussen T cellen ongeacht het type weefsel en de staat van het weefsel, en hier bovenop zien we aanpassing specifiek voor de omgeving. Het profiel van T cellen in weefsels wordt dus met name gedreven door het compartiment en niet door het type T cel of ontsteking. Met het onderzoek hebben we nieuwe mechanismen ontdekt over hoe dit deel van het menselijk immuunsysteem werkt tijdens chronische ontsteking en wat omgeving specifieke aanpassingen zijn. Dit geeft aanknopingspunten voor verder onderzoek om chronische ontstekingsziekten en de behandeling hiervan beter te begrijpen en aan te pakken.

DANKWOORD

Niks in dit proefschrift was tot stand gekomen zonder de hulp van velen op werk en daarbuiten. Het was soms net een wildwaterbaan maar ik heb genoten de afgelopen jaren, en ben door veel mensen geïnspireerd geraakt.

Lieve **Femke**, wat een geluk dat er ruimte was om bij jou een PhD traject vorm te kunnen geven. Als mens en als baas had ik mij geen betere supervisor kunnen voorstellen. Vaak liep ik binnen voor een korte vraag maar liep ik pas een uur later weer weg. Altijd met nieuwe ideeën (soms voor vakantie of een boek), inzichten en steevast een glimlach. Je bent heel goed in het zien van de kern en het geven van richting, wat heel fijn is als je zelf diep onder de analyses bent begraven en alles interessant is. Het is mooi om te zien hoe je een visie hebt en hier vol voor gaat, en daarbij helemaal jezelf blijft. Nog fijner is dat je dit ook doorgeeft aan je groep, en mij de vrijheid hebt gegeven om veel nieuwe dingen te leren. Gelukkig is onze samenwerking nog niet afgelopen en komen er volgens mij nog veel mooie dingen aan!

Beste **Bas**, voor mij ben je een groot voorbeeld in het combineren van de kliniek, onderwijs en onderzoek. Ik heb er bewondering voor hoe je alle ballen hoog weet te houden en ondertussen jezelf bekend weet te maken met hele nieuwe onderzoeksgebieden. Ik ben heel blij dat we samen in het chromogranine A/catestatine project zijn gestapt. Je weet als geen ander de juiste vragen te stellen om weer een stap verder te komen en je nieuwsgierigheid is aanstekelijk. De gesprekken over ‘wat na mijn PhD’ waren erg fijn en hebben mij geholpen om voor mij de beste keuze te kunnen maken.

Dear **Hilde**, you opened my eyes to the deep waters of mucosal immunology and made me determined of wanting to do a PhD in the field. The first few weeks of my internship in your lab were mind blowing. I felt like I had to learn a new language to be able to follow everyone and I'm happy you helped me grasp the basics. The depth of immunological knowledge and drive in your lab was amazing. Thank you for the experience.

Onderdeel zijn van de van Wijk groep, dan tref je het met je collega's. **David**, wat een geluk dat ik mijn thesis onder jouw begeleiding mocht schrijven en zo uiteindelijk mijn PhD in ben gerold. Heel veel succes met het opstarten van je eigen groep. **Eveline**, ik ben blij dat ik in je laatste maanden bij de stamceltransplantatie studie kon aanhaken en de lijn vervolgens door mocht zetten. **Judith**, het was heel fijn om af en toe samen te sparren of gewoon even frustraties te uiten. **Gerdien**, ik ben blij dat je mij je SF Treg project toevertrouwde. Het was voor mij een sprong in het diepe maar we hebben er een mooi stuk van gemaakt. **Anoushka**, I'm very happy you'll continue the SF Treg project. I cannot imagine more capable and kinder hands in which to leave the project. **José**, dank voor het samenwerken aan de darmprojecten. Jouw geduld en precisie heeft de imaging mass cytometry mogelijk gemaakt. **Elise**, ik trof het enorm met jou als stagestudent en ik ben heel blij dat je nu je PhD in de groep doet. Het is fijn om met vol vertrouwen projecten in jouw handen achter te laten. **Lek**, your perseverance with

processing the countless of breastmilk samples was admirable and I'm happy you survived all of the talking in the office with us. Lieve **Eelco**, ik ben ontzettend blij dat ik vlak na jou in het lab kwam en dat we samen op hebben kunnen trekken. Of het nou een zomerschool in Leuven, avonden (nachten) van het opwerken en sorten van biopten, mijn ontelbare telefoontjes en mailtjes om analysevraagstukken te bespreken, of de vrijdagmiddag sessies om even frustraties te uiten waren (als ik al klaar was, maar jij juist eindelijk tijd voor het labwerk had). Je hebt zeker je sporen achter gelaten want volgens mij ben je verantwoordelijk voor alle titels van de stukken in dit proefschrift. Ik ben heel blij dat je straks naast me staat! Lieve **Marlot**, waardevol als analist, nog waardevoller als vriendin! De afgelopen jaren heb je alle hoogte- en dieptepunten van het begin tot het einde van mijn PhD met mij meegemaakt. Een ongelofelijk avontuur. Het was zo makkelijk om even naar beneden te lopen om bij te kunnen kletsen, en die momenten mis ik zeker wel. Samen met Eelco kan ik mij geen beter persoon bedenken om straks naast mij te staan! Het is bijzonder om te zien hoe de groep gegroeid is over de jaren. **Arjan, Jorg, Saskia, Mick, Leonie, Irena, Hidde, Theo, Roselie, Coco, Victor, Jonas** heel veel dank en heel veel succes met jullie onderzoeken!

Het CTI is groter dan de van Wijk groep en ik heb veel mensen te bedanken waarvan er vast een paar hier niet genoemd zijn, dus dank! **Saskia, Mareille** en **Anne-Marie**, dank dat jullie altijd klaar stonden voor al mijn vragen (en noodtoestanden op het einde). **Pien** en **Jeroen**, als jullie mij de beginselen van het sorten niet hadden aangeleerd was er weinig tot stand gekomen van het proefschrift. **Michel**, ik ben blij dat je het gat van Pien en Jeroen opgevuld hebt. Dank voor jullie hulp. **Michal, Noortje** and **Nico**, thank you for processing all the RNA-seq samples and Michal, thank you for replying every time I came back to you with another question about the data. **Jorg** (van Loosdregt), je energie is aanstekelijk en ik ben heel blij dat we samen hebben kunnen werken aan het JIA project. **Bas** (Vastert), het zit hem in de naam want ook jij bent voor mij een voorbeeld in het combineren van je passie voor de kliniek en het onderzoek. Dank dat je altijd bereid was om te helpen met het verkrijgen van patiëntmateriaal. **Rianne**, de hoeveelheid qPCRs die je erdoorheen gewerkt hebt voor het SF project was bewonderingswaardig. Dank voor je hulp! **Julia**, thank you for being my roommate and for introducing me to the heart and brain comics. **Lotte**, je zorgde voor een goed begin van mijn PhD want in de eerste maand konden we samen op congres in Italië. **Fran**, succes met de nieuwe avonturen die gaan komen. **Doron, Helen, Arthur**, dank dat ik een kleine bijdrage mocht leveren aan jullie onderzoek.

Naast het CTI was ik ook een appendix van de MDL afdeling, dank dat ik mocht aanhaken. Lieve **Joren, Hans-Paul, Remi, Maartje, Anouk W., Anouk O., Charlotte, Krijn, Janine, Cas, Ilse, Kim** en **Lisa**, ondanks dat ik niet bij jullie op de kamer zat voelde ik mij altijd onderdeel van de groep. De arts-onderzoeker weekendjes en de wintersport avonturen waren geweldig. **Hans-Paul**, hopelijk volgen er volgend jaar weer fietstochten. Ik in zone 'ik ga kapot' terwijl jij drie lagen nodig hebt om warm te blijven...altijd genieten. Zeker als je voor een zonnebril een tocht van > 250 km maakt. **Anouk W.**, ik heb bewondering voor je organisatorische talent. Hoe je alle

lopende lijnen en gigantische hoeveelheden materiaal van de IBD surveillance studie netjes op een rijtje had...ik doe het je niet na. Succes met de laatste loodjes! **Remi**, het was mooi om te zien hoe je het ene na het andere stuk wist te publiceren zonder dat je glimlach (volgens mij) ooit verdween. **Herma**, het vertrouwen wat de patiënten van de stamceltransplantatie studie hadden in jou was mooi om te zien. Je bent voor mij een arts die je naast je wilt hebben als je langdurig ziek bent! **Nofel**, dank dat ik mocht bijdragen aan stamceltransplantatie project voor patiënten met de ziekte van Crohn. **Ada** en **Miriam**, dank voor het inplannen van alle meetings en hulp bij alle vragen aan de MDL kant. Alle andere MDL artsen, verpleegkundig specialisten en verpleegkundigen op de endoscopie, dank voor jullie hulp.

Dit boekje is tot stand gekomen door meerdere samenwerkingen. **Yvonne**, dank je wel voor je hulp met de imaging mass cytometry experimenten. **Carmen**, **Britt** en **Ellen**, het begon met een verzoek voor materiaal en het groeide uit tot een mooie samenwerking. **Carmen**, jouw enthousiasme voor onderzoek is aanstekelijk! Ik hoop dat ik tijdens mijn carrière diezelfde nieuwsgierigheid zal behouden. **Britt**, ik heb geen idee hoe jij het allemaal voor elkaar weet te boxen. Ik heb er bewondering voor en ik ben blij dat we hebben kunnen samen werken. **Mir-Farzin** and **Patrick**, I enjoyed the exchange of ideas which ended up in working together on two projects. Patrick, your drive and interest in science is admirable. **Geert**, **Sushil**, and **Elke**, completely unexplored terrain for me but I loved diving into the world of chromogranin A and catestatin. This is a storyline we'll hear off more in the future! **Suzanne**, zonder jou hadden we niet naar chromogranine A en castestatine in IBS patiënten kunnen kijken. Dank voor alle moeite. **Karin** and **Celia**, even though I was in the final stages of my PhD with time pressure to finish the projects you both jumped in to help us. Thank you.

Over de jaren heb ik vele mensen gebeld om te vragen om wat lichaamsmateriaal af te staan voor onderzoek. Het is geweldig om te beseffen hoeveel mensen hiertoe bereid zijn. Dank voor jullie bijdrage!

Saskia, wat een route hebben we afgelegd. Van biomedische wetenschappen in Amsterdam tot aan Tanzania voor ons keuzecoschap. Ik denk nog vaak aan Tanzania terug. Alle soms toch wel bizarre ervaringen in en buiten het ziekenhuis, het eten (pindakaas is weer terug van weggeweest), de safari en de wandeltocht door de Usambara bergen. Ik ben blij dat ik die ervaringen met jou heb kunnen delen.

Elke, onze ontmoeting begon natuurlijk niet als samenwerking maar op een onbewoond eiland (bijna dan). Ik ben heel blij dat je over alles net zo enthousiast ben als ik, en altijd in bent voor nieuwe dingen. Of het nou hiken op een onbewoond eiland of leren borstcrawl is. Er zijn heel veel mooie dingen om op terug te kijken. Hopelijk mogen er nog veel avonturen volgen.

Mariona, even after not seeing each other for two years due to corona it felt exactly the same as before when I visited. I admire your grinding attitude and always being able to persevere. The bike rides in the morning before work were awesome and left me energized (and hungry) the whole day. Sadly no one else is willing to bike with me at those crazy hours... I love your excitement for the outdoors and Peru is an adventure I will never forget. I hope there are many hikes, waves to surf, delicious (Spanish) food and just fun times in the future.

Elena and Carina, you go together as my two favorite Germans (since there is no competition). I love how we're all different but work so well together. Elena, I enjoy the discussions we can have about anything, literally. Your ability to view a topic from multiple perspectives is stimulating and it doesn't matter if we agree or not, sharing thoughts with you is always fun. Carina, you're the most caring and giving person I know. You'll never let someone go hungry, are always there for other people, and your excitement about bees is infectious. You both have made my PhD time a hundred times better. From all the conversations in the office, your tolerance of me talking to my computer, seeing our own vegetables grow in our garden, delicious dinners, game nights, book club, being my designated corona family during the first lockdown and many other things. It's very weird suddenly not seeing both of you almost every day. I promise to never plan a hike again, but will happily join on any adventure you'll feel like.

Desirée, ik kan onze ontmoeting als kersverse stage studenten aan het KIT nog goed herinneren. Ik had geen idee dat het tot zo'n vriendschap uit zou groeien, maar gelukkig houden we het nog met elkaar uit voor sushi dates, om te fietsen of gewoon om te kletsen. Er is zoveel veranderd de afgelopen jaren en ik ben blij dat we samen de hoogte- en dieptepunten hebben doorgemaakt.

Saskia, Reynold en Escher, het is heel fijn om mensen te kennen die niet zelf diep in het onderzoek zitten om weer even met beide voeten op de grond te gezet te worden. Bedankt voor alle weekenden dat het gewoon even spelen in de (speel)tuin, thuis dansen, gekke bekken trekken en eten was. Hopelijk volgen er nog veel van dit soort momenten!

Ilske en Elja, ik heb meer nodig dan een klein stukje tekst om uit te drukken hoe dankbaar ik ben voor jullie. Jullie kennen al mijn gekke trekjes en het is een heel fijn en veilig gevoel om te weten dat jullie er zijn. Vroeger zaten we niet altijd op één lijn maar het heeft mooie verhalen opgeleverd voor tijdens het eten, tot wanhoop van Pascal... IIs, soms heb ik het gevoel dat ons brein op dezelfde manier werkt en dat jij als geen ander mijn hersenspinsels kunt volgen. Als ik het niet kan verwoorden kan jij het wel voor mij. El, waar zou ik zijn zonder onze jaarlijkse adrenaline rush in een pretpark, het delen van sport en onze wekelijkse bel-uurtjes terwijl we allebei geen bellers zijn. Wat een geluk dat ik jullie heb! **Hans en Pascal**, wat fijn dat jullie het nog met Ilske en Elja uithouden. Op nog naar nog meer spelletjesavonden tot vreugde van Hans en het herkauwen van herinneringen tot vreugde van Pascal.

Lieve **Papa** en **mama**, bedankt voor alle steun, jullie luisterend oor, bemoedigende woorden en het voor mij klaar staan. Het was heel fijn om mijn eigen keuzes te kunnen maken met de wetenschap dat welk pad het uiteindelijk ook zou zijn geworden jullie mij erin zouden steunen. Niemand die deze route vroeger zou hebben voorspeld voor mij. Misschien hebben de fluorescerende epjes en bacteriën op het lab als kind wel het eerste vuurtje in mijn nieuwsgierigheid aangewakkerd. Dank dat jullie altijd mijn dromen hebben ondersteund!

CURRICULUM VITAE

Lisanne Lutter was born on July 26th 1990 in Haarlem, the Netherlands. In 2008 she completed secondary education at College Hageveld in Heemstede, followed by the James Boswell Institute in Utrecht to obtain a Nature and Health profile. In 2009, Lisanne started her study Biomedical Sciences at the University of Amsterdam where she received her Bachelor's degree *cum honore* and *cum laude*, discovering her interest in immunology. Subsequently, she began



her medical training in the 4-year competitive Master's program Selective Utrecht Medical Master (SUMMA) to become a clinician-scientist, combing a medical degree with research training. Lisanne carried out her research internship in the laboratory of Hilde Cheroutre at La Jolla Institute in San Diego, the United States of America. Here she discovered the intriguing world of T cell regulation at the mucosal border of the intestinal tract.

After obtaining her medical degree in 2017 she started her PhD under supervision of Prof. dr. Femke van Wijk and Prof. dr. Bas Oldenburg on T cell regulation and adaptation of which the work is presented in this thesis. This research was performed at the Center for Translational Immunology and the department of Gastroenterology and Hepatology at the University Medical Center Utrecht. During her PhD she completed the University Teaching Qualification (Basis Kwalificatie Onderwijs), was an invited speaker at the Antwerp TCR meeting in 2018, and received a travel award for her oral presentation at the 2nd Human & Translational Immunology Conference in 2020, the research award for outstanding oral abstract, the Clinical Immunology trainee award and the FOCIS Center for Excellence award for the FOCIS of 2021.

In July 2022 Lisanne started her residency in Pathology at the Amsterdam University Medical Center, the Netherlands.

LIST OF PUBLICATIONS

Included in this thesis

Lutter L, van der Wal M, Brand EC, Maschmeyer P, Vastert B, Mashreghi MF, van Loosdregt J, van Wijk F. Human regulatory T-cells locally differentiate and are functionally heterogeneous within the inflamed arthritic joint. *Clinical and Translational Immunology* **11**, e1420 (2022).

Lutter L*, Roosenboom B*, Brand EC, ter Linde JJ, Oldenburg B, van Lochem EG, Horjus Talabur Horje CS*, van Wijk F*. Homeostatic function and inflammatory activation of ileal CD8⁺ tissue-resident T cells is dependent on mucosal location. *Cellular and Molecular Gastroenterology and Hepatology* **12**, 1567-1581 (2021).

Lutter L*, Mijnheer G*, Mokry M, van der Wal M, Fleskens V, Scholman R, Pandit A, Tao W, Wekking M, Vervoort S, Roberts C, Petrelli A, Peeters JGC, Knijff M, de Roock S, Vastert S, Taams LS, van Loosdregt J, van Wijk F. Conserved human effector Treg signature is reflected in transcriptomic and epigenetic landscape. *Nature Communications* **12**, 2710 (2021).

Lutter L, Hoytema van Konijnenburg DP, Brand EC, Oldenburg B, van Wijk F. The elusive case of human intraepithelial T cells in gut homeostasis and inflammation. *Nature Reviews Gastroenterology & Hepatology* **15**, 637-649 (2018).

Not included in this thesis

Muntjewerff, EM, **Lutter, L**, Nicolassen, MJT, and van den Bogaart, G. The Hormone Chromogranin A Balances Gut Wall Function. Available at: <https://thefairjournal.com/2021/07/06/chromogranin/>.

Muntjewerff EM*, Tang K*, **Lutter L**, Christoffersson G, Nicolassen MJT, Gao H, Katkar GD, Das S, ter Beest M, Ying W, Ghosh P, El Aidy S, Oldenburg B, van den Bogaart G, Mahata SK. Chromogranin A regulates gut permeability via the antagonistic actions of its proteolytic peptides. *Acta Physiologica* **30**, e13655 (2021).

Maschmeyer P, Heinz GA*, Skopnik CM*, **Lutter L**, Mazzoni A, Heinrich F, von Stuckrad SL, Wirth LE, Tran CL, Riedel R, Lehmann K, Sakwa I, Cimaz R, Giudici F, Mall MA, Enghard P, Vastert B, Chang H, Durek P, Annunziato F, van Wijk F, Radbruch A, Kallinich T, Mashreghi M. Antigen-driven PD-1⁺TOX⁺BHLHE40⁺ and PD-1⁺TOX⁺EOMES⁺ T lymphocytes regulate juvenile idiopathic arthritis in situ. *European Journal Immunology* **51**, 915-929 (2021).

von Richthofen HJ, Gollnast D, van Capel TMM, Giovannone B, Westerlaken GHA, **Lutter L**, Oldenburg B, Hijnen D, van der Vlist M, de Jong EC, Meyaard L. Signal Inhibitory Receptor on Leukocytes-1 is highly expressed on lung monocytes, but absent on mononuclear phagocytes in skin and colon. *Cellular Immunology* **357**, 104199 (2020).

Lutter L*, Spierings J*, van Rhijn-Brouwer FCC, van Laar JM, van Wijk F. Resetting the T Cell Compartment in Autoimmune Diseases With Autologous Hematopoietic Stem Cell Transplantation: An Update. *Frontiers in Immunology* **9**, 767 (2018).

*Shared authorship

